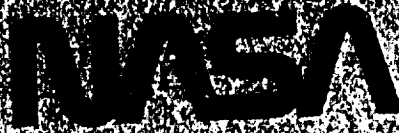


P 470

NASA-CR-175078



SMALL ENGINE COMPONENT TECHNOLOGY (SECT) STUDY FINAL REPORT

by
M. Early, R. Dawson, P. Zeiner, M. Turk, and K. Bonn

BARRETT TURBINE ENGINE COMPANY
A DIVISION OF THE BARRETT CORPORATION

LIBRARY COPY

SEP 25 1986

LEY RESEARCH CENTER
LIBRARY, NASA
HAMPTON, VIRGINIA

Date for general release March 31, 1991

prepared for
NATIONAL AERONAUTICS AND SPACE ADMINISTRATION
LEWIS RESEARCH CENTER
and
U.S. ARMY AVIATION RESEARCH AND TECHNOLOGY ACTIVITY
PROPULSION DIRECTORATE
NASA LEWIS RESEARCH CENTER
NAS3-24544

ORIGINAL PAGE IS
OF POOR QUALITY

N91-24205

Unclas
0019840

63
#2/07

(NASA-CR-175078) SMALL ENGINE COMPONENT
TECHNOLOGY (SECT) FINAL REPORT (Garrett
Turbine Engine Co.) 470 p
CSCL 215

1. Report No. NASA CR-175078 AVSCOM TR-86-C-11		2. Government Accession No.		3. Recipient's Catalog No.	
4. Title and Subtitle SMALL ENGINE COMPONENT TECHNOLOGY (SECT) PROGRAM FINAL REPORT TECHNICAL VOLUME				5. Report Date March, 1986	
				6. Performing Organization Code	
7. Author(s) M. EARLY, R. DAWSON, P. ZEINER, M. TURK, K. BENN				8. Performing Organization Report No. 21-5776-2A	
9. Performing Organization Name and Address GARRETT TURBINE ENGINE COMPANY 111 S. 34 ST. PHOENIX, AZ 85010				10. Work Unit No.	
				11. Contract or Grant No. NAS3-24544	
12. Sponsoring Agency Name and Address NATIONAL AERONAUTICS AND SPACE ADMINISTRATION NASA-LEWIS RESEARCH CENTER 21000 BROOKPARK ROAD, CLEVELAND, OHIO 44135				13. Type of Report and Period Covered CONTRACTOR REPORT	
				14. Sponsoring Agency Code 535-05-01 1L161101AH45	
15. Supplementary Notes PROJECT MANAGER, MICHAEL R. VANCO NASA LEWIS RESEARCH CENTER CLEVELAND, OH 44135					
16. Abstract A study of small gas turbine engines was conducted to identify high payoff technologies for year-2000 engines and to define companion technology plans. The study addressed engines in the 186 to 746 KW (250 to 1000 shp) or equivalent thrust range for rotorcraft, commuter (turboprop), cruise missile (turbojet), and APU applications. The results of this study show that aggressive advancement of high payoff technologies can produce significant benefits, including reduced SFC, weight, and cost for year-2000 engines. Mission studies for these engines show potential fuel burn reductions of 22 to 71 percent. These engine benefits translate into reductions in rotorcraft and commuter aircraft direct operating costs (DOC) of 7 to 11 percent, and in APU-related DOCs of 37 to 47 percent. The study further shows that cruise missile range can be increased by as much as 200 percent (320 percent with slurry fuels) for a year-2000 missile-turbojet system compared to a current rocket-powered system. The high payoff technologies were identified and the benefits were quantified. Based on this, technology plans were defined for each of the four engine applications as recommended guidelines for further NASA research and technology efforts to establish technology readiness by year 2000.					
17. Key Words (Suggested by Author(s)) ENGINE COMPONENT TECHNOLOGIES ROTORCRAFT COMMUTER AIRCRAFT CRUISE MISSILE ENGINES APU				18. Distribution Statement [REDACTED]	
19. Security Classif. (of this report) UNCLASSIFIED		20. Security Classif. (of this page) UNCLASSIFIED		21. No. of Pages 437	
				22. Price*	

FOREWORD

The authors acknowledge the contributions of G.S. Hoppin III and Dr. W. W. Waterman, whose efforts enhanced the technology definitions and plans in the study.

PRECEDING PAGE BLANK NOT FILMED

111

PRECEDING PAGE BLANK NOT FILMED

TABLE OF CONTENTS

	<u>Page</u>
SUMMARY	1
1.0 INTRODUCTION	5
2.0 ROTORCRAFT ENGINES	9
2.1 Task I - Selection of Evaluation Procedures and Assumptions	9
2.1.1 Reference Rotorcraft	9
2.1.2 Reference Mission for Rotorcraft	13
2.1.3 Reference Engine for Rotorcraft	15
2.1.4 Environmental Constraints	22
2.1.5 Economic Model for Rotorcraft	25
2.1.6 Trade Factors for Rotorcraft	27
2.2 Task II - Engine Configuration and Cycle Evaluation	28
2.2.1 Technology Projections	30
2.2.2 Cycle/Engine Studies	47
2.2.3 Cycle/Engine Selection	62
2.3 Task III - System Performance Evaluation	66
2.3.1 Engine/Cycle Refinements	66
2.3.2 Mission/Economic Analysis	68
2.4 Task IV - Small Engine Component Technology Plan	71
2.4.1 Technology Identification/Benefits	71
2.4.2 Technology Plan	79
2.5 Summary	171
3.0 COMMUTER TURBOPROP ENGINES	175
3.1 Task I - Selection of Evaluation Procedures and Assumptions	175
3.1.1 Reference Aircraft for Commuter	175
3.1.2 Reference Mission for Commuter	177
3.1.3 Reference Engine for Commuter	182
3.1.4 Environmental Constraints	188
3.1.5 Economic Model for Commuters	191
3.1.6 Trade Factors for Commuters	201

PRECEDING PAGE BLANK NOT FILMED

TABLE OF CONTENTS

	<u>Page</u>
3.2 Task II - Engine Configuration and Cycle Evaluation	204
3.2.1 Technology Projections	204
3.2.2 Cycle/Engine Studies	205
3.2.3 Cycle/Engine Selection	232
3.3 Task III - System Performance Evaluation	235
3.3.1 Engine/Cycle Refinements	235
3.3.2 Mission/Economic Analysis	237
3.4 Task IV - Small Engine Component Technology Plan	237
3.4.1 Technology Identification/Benefits	241
3.4.2 Technology Plan	242
3.5 Summary	245
4.0 SUPERSONIC CRUISE MISSILE ENGINES	247
4.1 Task I - Selection of Evaluation Procedures and Assumptions	247
4.1.1 Reference Missiles	247
4.1.2 Reference Engines	250
4.1.3 Reference Mission	261
4.1.4 Economic Model	264
4.1.5 Environmental Constraints	265
4.1.6 Trade Factors	267
4.2 Task II - Engine Configuration and Cycle Evaluation	268
4.2.1 Technology Projections	269
4.2.2 Engine Cycle/Configuration Study	277
4.2.3 Cycle/Configuration Selection	288
4.3 Task III - System Performance Evaluation	288
4.3.1 Engine/Cycle Refinements	291
4.3.2 Mission Analysis	295

TABLE OF CONTENTS

	<u>Page</u>
4.4 Task IV - Small Engine Component Technology (SECT) Plan for Missile Application	297
4.4.1 Advanced Technology Identification and Benefits	297
4.4.2 Technology Plan	304
4.5 Summary	358
5.0 AUXILIARY POWER UNITS	361
5.1 Task I - Selection of Evaluation Procedures and Assumptions	361
5.1.1 Reference Aircraft	361
5.1.2 Reference Duty Cycle	362
5.1.3 Reference APU	364
5.1.4 Environmental Constraints	366
5.1.5 Economic Model	369
5.1.6 Trade Factors	371
5.2 Engine Configuration and Cycle Evaluation	372
5.2.1 Technology Projections, APU	373
5.2.2 APU Cycle/Configuration Studies	379
5.2.3 Cycle/Engine Selection	390
5.3 Task III System Performance Evaluation	394
5.3.1 Duty Cycle Analysis	394
5.4 Small Engine Component Technology Plan	398
5.4.1 Advanced Technology Benefits	398
5.4.2 Technology Plan	403
5.5 Summary	428
6.0 CONCLUSIONS	431
6.1 Technology Benefits	431
6.2 Technology Identification	433
REFERENCES	437
APPENDIX A - LIST OF SYMBOLS	439
DISTRIBUTION LIST	444

LIST OF FIGURES

<u>Figure</u>	<u>Title</u>	<u>Page</u>
1	SECT Reference Rotorcraft	11
2	Operating Profile of Typical Rotorcraft	14
3	SECT Rotorcraft Mission	16
4	Rotorcraft Reference Engine Configuration	17
5A	Rotorcraft Engine Cost	23
5B	Rotorcraft DOC Breakdown - Reference Engine	29
6	Aluminum Metal Temperature Limit	32
7	Comparison of Turbine Material Strengths	36
8	Compressor Performance Projections	37
9	Combustor Technology Projections	39
10	HP Turbine Performance Projections	40
11	LP Turbine Performance Projections	41
12	Typical Plate-Fin Counterflow Recuperator Configuration	43
13	Ceramic Recuperator Manufacturing Process	45
14	GTEC Empirical Study Approach	46
15	GTEC Engine Weight Estimate Approach	48
16A	Idealized Cycle Study Results with Constant Efficiencies	50
16B	Cycle Study Results With Mechanical Limits	50
17	Simple-Cycle Study Configurations and Options	51
18	Rotorcraft Simple-Cycle Performance Results - Metallic Turbines	52
19	Rotorcraft Simple-Cycle Performance Results - Ceramic Turbines	54

LIST OF FIGURES (Contd)

<u>Figure</u>	<u>Title</u>	<u>Page</u>
20	Projected Engine Size, Weight, and Cost Improvements With Advanced Metallics and Ceramics	55
21	DOC Comparison of Advanced Metallic and Ceramic Engines	57
22	Simple-Cycle Performance With An Axial-Centrifugal Compressor Metallic Turbine	58
23	DOC Impact of Advanced Axial-Centrifugal Compressor Versus Two-Stage Centrifugal Compressor - Metallic Turbines	59
24	Simple Cycle Performance With a Two-Stage (Cooled) Metallic HP Turbine	60
25	DOC Impact of Metallic Two-Stage HP Turbine Versus a Single-Stage Metallic Turbine	61
26	Performance Impact of Downscaling, Simple Cycle - Metallic Turbines	63
27	Performance of Recuperated Cycles for Rotorcraft Application	64
28	Projected Engine and DOC Improvements for Recuperated Engines	65
29	Task II to Task III Engine Performance Changes	67
30	Off-Design Performance Comparison for Rotorcraft Engines (Installed Performance)	69
31	Projected Reductions in Rotorcraft Parameters	70
32	Projected Reductions in Rotorcraft DOC for Simple Cycle Versus Recuperated Engines	72
33	Helicopter DOC Results For Simple Cycle and Recuperated Engines	73

LIST OF FIGURES (Contd)

<u>Figure</u>	<u>Title</u>	<u>Page</u>
34	Technical Approach for Estimating Technology Benefits	75
35	Projected DOC Benefits (Percent) for Isolated Technologies	77
36	Comparison of Projected DOC Benefits (Percent) for Recuperated Versus Simple-Cycle Engines	78
37	Ceramics Technology Schedule	80
38	AGT101 Power Plant	82
39	Recuperator Technology Schedule	93
40	Test Modules of Increasing Complexity	95
41	Ceramic Recuperator Program Schedule	96
42	Conceptual Ceramic Duct Design for Recuperator Core	99
43	Ceramic/Metallic Duct Attachment	103
44	Material Technology Schedule for Turbine Metallics	112
45	Turbine Technology Schedule	120
46	Combustor Technology Schedule	129
47	Compressor Technology Schedule	134
48	L2F Measuring System	138
49	Material Technology Advancement Schedule for "Cold-Section" Parts	146
50	Engine Systems Technology Schedule	158
51	GTEC Experience and Projections for Seal Capabilities	159
52	Rayleigh Pad Seal Operation	161

LIST OF FIGURES (Contd)

<u>Figure</u>	<u>Title</u>	<u>Page</u>
53	Mechanical, Pneumatic, and Self-Acting Forces on a Rayleigh Pad Seal	162
54	Typical Brush Seal	167
55	Rotorcraft Mission Analysis Results	172
56	Standup Cabin for Reference Commuter	176
57	SECT Reference Commuter Aircraft	178
58	Present Commuter Aircraft Stage Lengths	179
59	Survey Results of Present Airfield Altitudes	179
60	Commuter Reference Mission	183
61	Commuter Reference Engine Configuration	184
62A	Reference Engine Costs Based on Mean Market Sell Price	189
62B	Commuter DOC Breakdown - Reference Engine	203
63	Regenerator Technology Projections Based on AGT101 Experience	206
64	Commuter Recuperated-Cycle Study Configurations and Options	207
65	Recuperated-Cycle Performance Results for Commuter Application	209
66	Impact of Recuperator Pressure Drop on Performance	211
67	Impact of Recuperator Effectiveness and Pressure Drop on Weight and Size	212
68	Weight Comparison of Recuperator Types	214
69	Recuperated Engine Weight Trend As a Function of Specific Power	215

LIST OF FIGURES (Contd)

<u>Figure</u>	<u>Title</u>	<u>Page</u>
70	Recuperated Engine Cost Trend As a Function of Specific Power	216
71	Impact of Effectiveness and Pressure Drop On Recuperator Cost	217
72	Reduction in Commuter DOC As a Function of SFC and Specific Power	219
73	Reduction in Commuter DOC As a Function of Recuperator Effectiveness and Pressure Drop	220
74	Compressor Configuration Effects on Commuter Engine Performance	221
75	DOC Comparison for Different Compressor Configurations	222
76	Performance Comparison of Ceramic Versus Advanced Metallic Turbines	224
77	Performance Comparison of Ceramic Versus Carbon-Carbon Turbines	225
78	DOC Comparison of Ceramic Versus Advanced Metallic and Carbon-Carbon Turbines	226
79	Regenerated Cycle Performance Results for Commuter Application	228
80	Impact of Regenerator Leakage on Performance	229
81	Impact of Regenerator Effectiveness and Leakage On Size and Weight	230
82	Impact of Regenerator Effectiveness and Leakage on DOC	231
83	Simple Cycle for Commuter Selected from Rotorcraft Study	233
84	DOC Comparison of Recuperated, Regenerated, and Simple Cycles	234

LIST OF FIGURES (Contd)

<u>Figure</u>	<u>Title</u>	<u>Page</u>
85	Part-Power Performance Comparison for the Commuter Application	238
86	Projected Reductions in Commuter Parameters, Recuperated Engine Mission Results	239
87	Commuter DOC Results for Recuperated Engines	240
88	Technical Approach for Estimating Technology Benefits	243
89	Projected DOC Benefits (Percent) for Isolated Technologies	244
90	Commuter Mission Analysis Results	246
91	Reference Missile Configuration with Rocket Propulsion System	249
92	Reference Missile Configuration with Turbojet Propulsion System	251
93	Reference Turbojet Engine Configuration and Data Summary	255
94	Missile Thrust and Drag	257
95	Several Missile Scenarios for the Future	262
96	Representative Reference Mission	263
97	Advanced Compressor High-Temperature Material Requirements	270
98	Axial Compressor Performance Projections	273
99	Cruise Missile Combustor Technology Projections	275
100	Cruise Missile HP Turbine Projections	276
101	Missile Cycle/Configuration Study Engine Options	279
102	Engines Sized by Minimum Acceleration Condition	280

LIST OF FIGURES (Contd)

<u>Figure</u>	<u>Title</u>	<u>Page</u>
103	Missile Cycle Study Results	282
104	Compressor Inlet and Exit Corrected Flow Variation	283
105	Axial and Axial-Centrifugal Compressor Diameter Comparison	285
106	Compressor Axial Blade Height Limits	286
107	Missile Engine Weight, Size, and Cost Trends	287
108	Missile Engine Range and Cost/Range Trends	289
109	Selected Missile Engine	290
110	Impact of Compressor Size Change	293
111	Impact of Turbine Size and Loading Change	294
112	Performance Comparison of Reference and Year-2000 Turbojet Engines	296
113	Missile Range and Cost Per Range Comparison of Reference and Year-2000 Turbojet Engines	298
114	Comparison of Technology Benefits to Missile System	301
115	Benefits of Additional Technologies	302
116	Missile Range Comparison	303
117	Materials Technology Schedule	305
118	Combustor Technology Schedule	312
119	Significant Increases in Cruise Missile Range are Possible with High-Energy Fuels	318
120	Boron-Slurry Element Combustor Test Rig	320
121	GTEC Pure Airblast Nozzle	322

LIST OF FIGURES (Contd)

<u>Figure</u>	<u>Title</u>	<u>Page</u>
122	Volumetric LHV Advantage Results in Range Improvement Potential	323
123	Axial Compressor Technology Program Schedules	325
124	Turbine Technology Schedules	338
125	"Inserted" Blade Concept	343
126	Proposed "Spiral" Weave	344
127	System Technology Schedule	345
128	Proposed Fuel Pump/PMG Module	352
129	Cruise Missile Mission Analysis Results	359
130	Cross Section of Reference APU Without the Gearbox	365
131	Projected Centrifugal Compressor Efficiency	374
132	Projected Centrifugal Compressor Efficiencies	376
133	Projected Efficiency for High-Pressure Axial Turbine Stage	377
134	Projected Efficiency for Low-Pressure Axial Turbine Stage	378
135	Projected Radial Inflow Turbine Efficiency in Year 2000	380
136	Projected Annular Combustor Performance in Year 2000	381
137	APU Cycles Investigated in the SECT Study	382
138	APU Simple Cycles Using Axial Turbine Wheels	384
139	APU Cycle Performance Results	385
140	AGT101 Regenerated Engine Cross Section	387

LIST OF FIGURES (Contd)

<u>Figure</u>	<u>Title</u>	<u>Page</u>
141	Projected Performance for APU Based on Scaled AGT101	388
142	APU Cost Comparison	389
143	APU Weight Comparison	391
144	APU DOC Comparison	392
145	Reduction in DOC for Selected APU Cycles	397
146	DOC Benefits from APU Technologies	399
147	APU Technology Benefit Comparison in DOC Per Hour	400
148	Ceramics Technology Schedule	404
149	APU Radial Turbine Technology Schedule	410
150	APU Compressor Technology Schedule	418
151	Systems Technology Scheme for APU	423
152	GTEC Self-Acting Foil Journal Bearing Concept With Backing Spring	425
153	APU Mission Analysis Results	429

LIST OF TABLES

<u>Table</u>	<u>Title</u>	<u>Page</u>
I	Projected DOC Reductions for Rotorcraft, Commuter, and APU Engines	2
II	Projected Mission Benefits for Year-2000 Cruise Missile Engines	3
III	High-Payoff Technology Categories	4
1	Rotorcraft Component Weight Savings	10
2	Critical Sizing Condition	10
3	SECT Reference Rotorcraft Data	12
4	Materials for Rotorcraft Reference Engine	18
5	Rotorcraft Reference Engine Design Point Data	20
6	Rotorcraft Reference Engine Design Data	21
7	Modular Weight Breakdown	22
8	Rotorcraft Vehicle Partitions	26
9	Basis for DOC Computations	26
10	Rotorcraft Trade Factors	28
11	Year-2000 "Cold" Material Projections	31
12	Projected Properties for Hot-End Materials	34
13	Recuperator Technology Projections	44
14	Commuter Reference Engine Design Point Data	186
15	Commuter Reference Engine Sea Level Data	187
16	Modular Weight Breakdown	188
17	Commuter Vehicle Partitions	192
18	Aircraft Parameters for the Economic Model	192
19	Commuter Owner/Operator Costs	196

LIST OF TABLES (Contd)

<u>Table</u>	<u>Title</u>	<u>Page</u>
20	Commuter Trade Factors	202
21	Performance Refinements from Task II	236
22	Turbojet-Powered Missile Weights	250
23	Turbojet-Powered Missile Aerodynamics	252
24	Reference Turbojet Component Materials	254
25	Reference (Turbojet) Engine - Design Point Data	258
26	Reference (Turbojet) Engine - Max Power Cruise Data	259
27	Reference (Turbojet) Engine - SLS, Uninstalled Data	260
28	Economic Model for the Cruise Missile	266
29	Missile Trade Factors (Constant Missile Volume)	268
30	Additional Material Technologies for Cruise Missile Engine	272
31	Task III Missile Engine Performance Refinements	292
32	Evaluation of Slurry Fuels for LRCM HF-3	324
33	Operational APU Duty Cycle	363
34	Reference Engine Design-Point Performance - Sea-Level, Static, ISA, Max, Uninstalled	367
35	Reference Engine Off-Design Performance - Sea-Level, Static, ISA, Uninstalled	368
36	APU Trade Factors	372
37	SECT Simple-Cycle APU Design Point Performance - Sea-Level Static, ISA, Max, Uninstalled	393
38	SECT Regenerated APU Design Point Performance - Sea-Level, Static, ISA, Max, Uninstalled	395

SMALL ENGINE
COMPONENT TECHNOLOGY
(SECT) PROGRAM
FINAL REPORT

SUMMARY

Small Engine Component Technology (SECT) studies are the first step in a new NASA initiative to improve the domestic technology base for year-2000 small gas turbine engines in the 186 to 746 kW (250 to 1000 shp) or equivalent thrust range. The studies address four engine applications, including rotorcraft, commuter (turboprop), cruise missile (turbojet), and auxiliary power unit (APU). The objectives of the studies are to identify high payoff technologies for year-2000 engines and to provide companion technology plans for guiding future government research and technology efforts.

GTEC has conducted this SECT study for all four engine applications of interest. The study approach, methodology, and results are documented in this final report. The study approach is outlined as follows:

- o Year-2000 aircraft and missions as well as performance and configuration data for current-technology engines were defined. Based on this, reference cost and cruise missile range data were estimated. Trade factors were computed to assess benefits of technology changes to the engines.
- o Technology projections to year 2000 were made. Based on these projections, cycle studies were made to define and conceptualize year-2000 engines.

- o The year-2000 engines were evaluated for the aircraft and missions defined for this study.
- o Engine performance and aircraft cost/missile range data were compared for the year 2000 versus current technology engines. High payoff technologies were identified and benefits were quantified. Based on this, technology plans were defined for each of the four engines of this study.

The results of this study show that an aggressive small engine component technology program of high-payoff technologies can produce significant benefits for year-2000 engines. These benefits, as expressed in reductions in fuel burn and aircraft direct operating costs (DOC), are summarized in Table I for the rotorcraft, commuter, and APU engines.

TABLE I. PROJECTED DOC REDUCTIONS FOR ROTORCRAFT, COMMUTER, AND APU ENGINES

Application	Cycle	Reduction In Fuel Burn (Percent)	DOC Reduction	
			Low Fuel Price* (Percent)	High Fuel Price** (Percent)
Rotorcraft	Simple Recuperated	21.9	7.0	8.7
		41.6	7.4	11.4
Commuter	Recuperated	35.0	5.7	11.1
APU	Simple Regenerated	43.2	36.7	38.3
		70.8	39.0	47.0
*Low fuel price assumed for this study was \$0.264/liter (\$1/gal) **High fuel price assumed for this study was \$0.528/liter (\$2/gal)				

Study results further show that dramatic mission benefits can be realized for the reduced volume engines as projected for year-2000 cruise missiles. These benefits are summarized in terms of missile range and cost/range (Table II) for three missile engine combinations that were defined for this study, and for the separate effects of slurry fuels.

TABLE II. PROJECTED MISSION BENEFITS FOR YEAR-2000 CRUISE MISSILE ENGINES

Missile/Engine	Δ Engine Volume (Percent)	Δ Range (Percent)	Δ Cost/ Kilometer (nm) (Percent)
Current Missile (Rocket Powered)	-	-56	+126
Current Missile (Near-Term Turbojet, 1989 Technology)	Reference 373 cm ³ (6111 in ³)	Reference 126 km (68 nm)	Reference \$3970/km (\$7353/nm)
Advanced Missile (Year-2000 Turbojet)	-41	+32	-27
Advanced Missile (Year-2000 Turbojet plus Slurry Fuels)	-41	+84	-

The high payoff technologies were identified and are categorized in Table III for the four engine applications of this study. Discrete technology programs were defined for high payoff technologies in these categories. Overall technology plans were defined for each engine application as recommended guidelines for future research and technology efforts to establish technology readiness by the year 2000.

TABLE III. HIGH-PAYOFF TECHNOLOGIES

	Application*
Ceramics	R, C, A
Carbon-Carbon (coated)	M
Heat Recovery Devices	
Recuperators	R, C
Regenerators	A
Turbine Metallics	R, C
"Cold" Materials (for cold parts)	R, C, M, A
Turbine Performance	
Axial	R, C, M
Radial	A
Combustor Technologies	
Reverse-flow	R, C, A
Through-flow	M
Compressor Performance	
Centrifugal	R, C, A
Axial	M
System Technologies	
Seals and Lubricants	R, C, A
Advanced Thrust Nozzles	M
Advanced (High Temperature) Accessories	M
Ceramic Bearings	M
Foil Journal Bearing	A

*R = Rotorcraft, C = Commuter, M = Cruise Missile, A = APU

SMALL ENGINE
COMPONENT TECHNOLOGY
(SECT) PROGRAM
FINAL REPORT

1.0 INTRODUCTION

NASA has identified the need for a small engine component technology initiative, based on a widely known performance disparity between large and small gas turbine engines. Small gas turbine engine performance in the 186 to 746 kW (250 to 1000 shp) size range is significantly lower than that of large engines. This is primarily because the component efficiencies of small engines are lower than those of large engines; analytical design and manufacturing techniques of large engines are not directly transferable to small engines.

Foreign competition in the small engine market is growing and the U.S. percentage share of this market has been steadily decreasing. NASA Lewis Research Center and U.S. Army Aviation Research and Activity Center - Propulsion Directorate have addressed this problem with the initiation of the Small Engine Component Technology (SECT) Studies. The scope of this program has been defined to include small gas turbine engines for rotorcraft, commuter aircraft, tactical cruise missiles, and auxiliary power units (APU).

The purpose of this effort is to provide technology plans for guiding future research and technology efforts. The program addresses the technology requirements as envisioned for small turbine engines of 186 to 746 kW (250 to 1000 shp) suitable for use in commercial or military rotorcraft, commuter aircraft, tactical cruise missiles, and auxiliary power units (APU). Parallel studies were conducted for these applications to identify high-

payoff technologies for year-2000 engines and to establish technology plans for guiding future NASA-sponsored research and technology efforts to establish technology readiness by year 2000. The studies documented in this report are in the following sections:

- 2.0 Rotorcraft Engines
- 3.0 Commuter Turboshaft Engines
- 4.0 Cruise Missile Turbojet Engines
- 5.0 Auxiliary Power Units

The SECT study consists of four major tasks, which are described in the following paragraphs:

Task I - Selection of Evaluation Procedures and Assumptions

Year-2000 aircraft and missions were defined, along with current technology engines (reference engines), for baseline data. Environmental constraints were projected to assess the potential impact on year-2000 engines, and economic models were defined to facilitate evaluation of aircraft operating costs. Trade factors were computed for primary engine features to allow for quantifying beneficial engine changes that might result from technology advancements to the year 2000. These studies are reported in paragraphs 2.1, 3.1, 4.1, and 5.1 for the respective engines.

Task II - Engine Configuration and Cycle Evaluation

Technology projections and engine cycle and configuration studies were made to conceptualize year-2000 engine performance levels, weights, envelopes, and costs. Results were compared to the reference engines, and trade factors were applied to quantify potential gains. Promising engine candidates were selected for

further evaluation. These studies are reported in paragraphs 2.2, 3.2, 4.2, and 5.2 for the respective engines.

Task III - System Performance Evaluation

Operating costs of aircraft with selected year-2000 engines were computed and compared to data for the reference engines. These studies are reported in paragraphs 2.3, 3.3, 4.3, and 5.3 for the respective engines.

Task IV - Small Engine Component Technology Plan

Technology advances as projected for year-2000 engines were isolated, and benefits for each were quantified in terms of aircraft/missile operating costs. High-payoff technologies were identified and technology plans were defined for each of the four engine applications of this study. These studies are reported in paragraphs 2.4, 3.4, 4.4, and 5.4 for the respective engines.

2.0 ROTORCRAFT ENGINES

This section presents Garrett's SECT study approach, methodology, and results as established for the rotorcraft engines as envisioned for the year 2000. The section is organized into four major tasks as conducted and described in paragraph 1.2 of this report.

2.1 Task I - Selection of Evaluation Procedures and Assumptions

The following paragraphs present the study results for the reference rotorcraft, mission, engine, projected environmental constraints, economic model, and the trade factors.

2.1.1 Reference Rotorcraft

A reference rotorcraft was configured and sized for this study using NASA computer program HESCOMP. (Reference 1)

The configured aircraft, which is a derivative of the Sikorsky S76 Mark II rotorcraft, represents a year-2000 reference aircraft. Major technology projections, including weight reductions in the airframe and associated subsystems, figure-of-merit improvements in the main rotor, and improved aerodynamics, were applied to the S76. Additionally, the reference engines as defined for this study in paragraph 2.1.3 were incorporated into the reference rotorcraft.

The technology factors applied to the weight predictions represent the component weight savings as shown in Table 1.

The combination of fixed engine power and rotorcraft system takeoff performance requirements act to determine the rotorcraft takeoff gross weight. The critical sizing condition is as shown in Table 2.

PRECEDING PAGE BLANK NOT FILMED

The combination of fixed engine power and rotorcraft system takeoff performance requirements act to determine the rotorcraft takeoff gross weight. The critical sizing condition is as shown in Table 2.

TABLE 1. ROTORCRAFT COMPONENT WEIGHT SAVINGS

Component	Weight Savings (percent)	
Main rotor blades	1	
Main rotor hub	30	
Main rotor drive system	11	
Horizontal tail	40	
Tail rotor blades	20	
Fuselage	25	
Landing gear	13	
Main rotor controls	8	
Rotor systems controls	70	
Cockpit controls	60	
	S76	SECT Rotorcraft
Figure-of-merit, main rotor NOTE: Figure-of-merit = induced power/total power	0.75	0.78
Gross weight/effective flat plate area	4101 kg/m ² (840 lb/ft ²)	3750 kg/m ² (768 lb/ft ²)

TABLE 2. CRITICAL SIZING CONDITION.

Pressure altitude	1219 m (4000 ft)
Outside air temperature	35C (95F)
Intermediate rated power (IRP)	95 percent
Rate of climb	152 m/min (500 ft/min)
Thrust-to-weight ratio	1.03

The characteristics of the resultant sized vehicle that meet this takeoff criteria and the reference mission are shown in

ORIGINAL PAGE IS
OF POOR QUALITY



SIKORSKY S76 MARK II ROTORCRAFT

- TWIN ENGINE 746 KW (1000 SHP EACH)
- WEIGHTS (INCLUDING PILOT WEIGHT OF 95.3 KG (210 LB))
 - EMPTY — 1985 KG (4375 LB)
 - FUEL — 591 KG (1303 LB)
 - PAYLOAD — 1667 KG (3676 LB)
 - TOGW — 4338 KG (9564 LB)

TECHNOLOGY ADVANCEMENTS

- WEIGHT REDUCTIONS IN AIRFRAME AND SUBSYSTEMS (~ 18 PERCENT)
- AERODYNAMIC IMPROVEMENTS IN MAIN ROTOR
- REDUCED DRAG
- 1985 SECT REFERENCE ENGINES
INSTALLED WEIGHT = 336.6 KG (742 LB)
(BOTH ENGINES)

TECHNOLOGY
ADVANCEMENTS
(RESIZED)



YEAR-2000 SECT ROTORCRAFT

65-281-53

Figure 1. SECT Reference Rotorcraft.

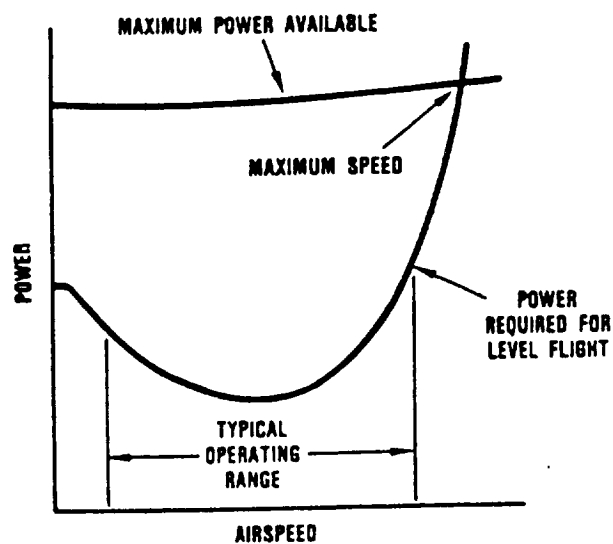
TABLE 3. SECT REFERENCE ROTORCRAFT DATA

HESCOMP Summary			
Rotors		Main Rotor	Tail Rotor
Diameter, m (ft)		12.93 (42.41)	2.44 (8.00)
No. of Blades		4	4
Solidity		0.075	0.172
Ct/Sigma		0.080	0.070
Disk Loading, kg/m ² (lb/ft ²)		33.05 (6.77)	56.05 (11.28)
Tip Speed, m/s (ft/sec)		213.4 (700)	213.4 (700)
Drive System Rating, kW (shp)		1342.8 (1800)	149.2 (200)
Weight, kg (lb)		244.72 (540)	53.63 (118)
Propulsion (Primary Uninstalled)			
Number of Engines		2	
Power Per Engine, kW (shp)		746 (1000)	
Weight Per Engine, kg (lb)		137 (303)	
Dimensions		Vertical Tail	Horizontal Tail
Area, m ² (ft ²)		1.93 (20.8)	2.00 (21.5)
Aspect Ratio		2.04	4.35
Taper Ratio		0.48	0.50
Span, m (ft)		1.98 (6.5)	2.96 (9.7)
Fuselage Length, m (ft)		12.98 (42.6)	
Overall Length, m (ft)		16.31 (53)	
Fuselage Width, m (ft)		2.13 (7)	
Weights, kg (lb)			
Propulsion	905.6 (1997)	Payload	1667.4 (3676)
Empty	1984.1 (4374)	Structure	618.6 (1364)
Fuel	591.4 (1303)	Gross	4337.9 (9564)
Aerodynamics			
Flat Plate Area, m ² (ft ²)		1.15 (12.3)	
Mean Skin Friction, Coefficient		0.1683	
Wetted Area, m ² (ft ²)		68.1 (733)	

2.1.2 Reference Mission For Rotorcraft

Both military and civil helicopter missions were considered for the SECT rotorcraft application. A survey of the civil and military markets included the three following typical mission types:

- o Heavy lift missions are typified by moving heavy loads short distances. The engine can be expected to go from idle to full power and back in less than a minute. This mission has a large number of transient cycles and is the most demanding on the mechanical design of the engine because the severe transients in speed and temperature have an adverse effect on engine life.
- o Inspection/surveillance/scout missions are characterized by long periods of operation at low flight speeds, the speed being established by the observer's ability to visually inspect objects from the air. As illustrated in Figure 2, the power required for level flight of a generic rotorcraft during such missions is substantially less than the power available. The engine can be expected to be operating well below full-power rating during most of this type of mission. This emphasizes the importance of engine part-power fuel economy for rotorcraft engines.
- o Ferry missions are characterized by long periods spent at a cruise setting. This mission is similar to the inspection/surveillance/scout mission except that the power level is somewhat higher. Low specific fuel consumption at these higher power levels is of major importance for the ferry mission.



65-281-29

Figure 2. Operating Profile of Typical Rotorcraft.

On the basis of recommendations by helicopter manufacturers, NASA-Ames, and Garrett project personnel, a mission was defined that is representative of some military and civil ferry applications, including TV coverage. The selected reference mission consists of five cruise legs separated by periods of hover at each destination point. The mission, along with mission data, is depicted in Figure 3.

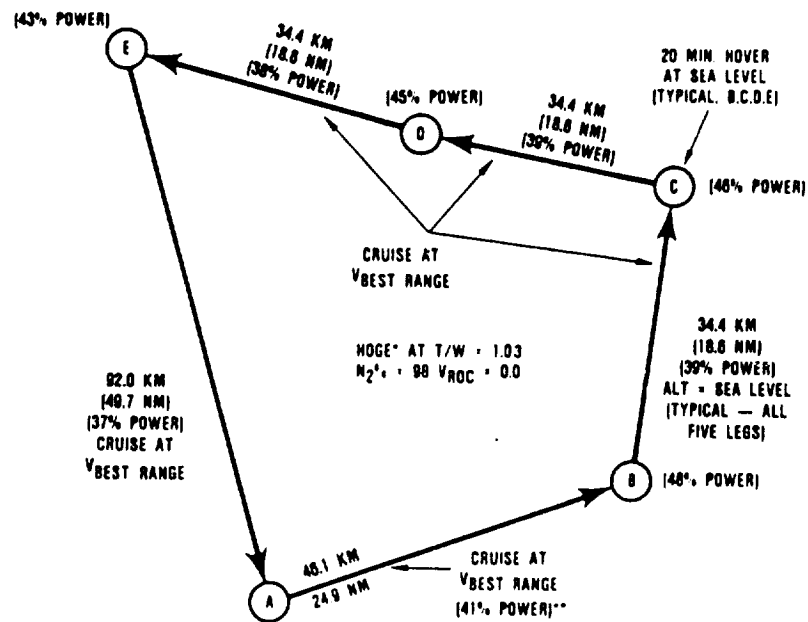
2.1.3 Reference Engine For Rotorcraft

Engines under development at GTEC were surveyed and evaluated to establish the reference engine for the rotorcraft application. The performance and operating parameters of these engines were adjusted to define the reference engine and to represent 1985 engine-demonstrated levels of component technology.

Configuration - The reference engine is shown schematically in Figure 4. The engine is a two-spool design that uses a two-stage centrifugal compressor driven by a two-stage axial turbine. A reverse-flow annular combustor placed around a high-pressure (HP) turbine results in a compact HP spool. The low-pressure (LP) spool consists of a two-stage axial power turbine with a front drive arrangement. The engine also has an inlet particle separator (IPS) with a mechanical blower system.

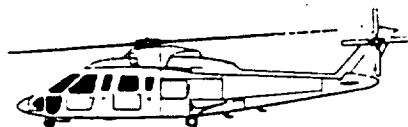
Materials - The materials used in the reference aircraft engine are based on present Garrett technology as reflected in 1985 engine-demonstrated components. The materials for the major components, as selected for the reference engine, are as listed in Table 4.

Performance - The reference engine performance is based on existing engine components as adjusted to represent 1985 engine-demonstrated levels. These components have been scaled as necessary



*HOVER OUT OF GROUND EFFECT

**PERCENTAGE OF SLS T/O RATING 746 KW (1000 SHP)



65-281-51

MISSION LENGTH: 241 KM (130.4 NM)

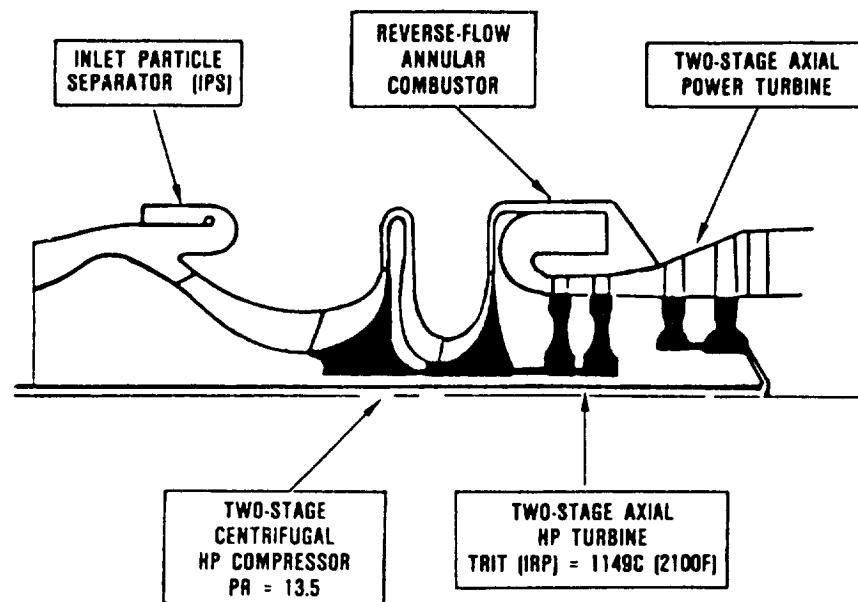
MISSION TIMES:

HOVER — 1 HOUR, 20 MINUTES

CRUISE — 59 MINUTES

BLOCK — 2 HOURS, 19 MINUTES

Figure 3. SECT Rotorcraft Mission.



65-281-33

Figure 4. Rotorcraft Reference Engine Configuration.

TABLE 4. MATERIALS FOR ROTORCRAFT REFERENCE ENGINE

<u>Accessory Gearbox Cases</u>		: Aluminum
<u>Compressor</u>		
Stage 1	Impeller	: Titanium 6-4
	Diffuser	: INCO 718 6-2-4-2
Stage 2	Impeller	: Titanium
	Diffuser	: INCO 718
<u>Combustor</u>		: HS 188
<u>HP Turbine</u>		
Stage 1	Stator	- MAR-M 247 DS - Cooled
	Blade	- MAR-M 247 DS - Cooled
	Disk	- Waspaloy B
Stage 2	Stator	- MAR-M 247 Equiaxed - Uncooled
	Blade	- MAR-M 247 DS - Uncooled
	Disk	- Waspaloy B
<u>LP Turbine</u>		
Stage 1	Stator	- MAR-M 247 Equiaxed
	Blade	- MAR-M 247 Equiaxed
	Disk	- Superwaspaloy
Stage 2	Stator	- MAR-M 247 Equiaxed
	Blade	- MAR-M 247 Equiaxed
	Disk	- Superwaspaloy
<u>Shafts</u>	INCO 718	

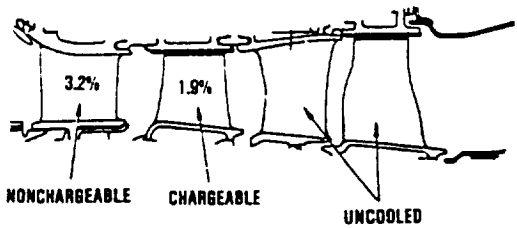
to meet the power output of 746 kW (1000 shp). The resulting engine and component performances are summarized in Tables 5 and 6.

The reference engine achieves 746 kW (1000 shp) at the sea level, static, ISA condition at a turbine rotor inlet temperature of 1149C (2100F). At this condition, the compressor inlet corrected flow is 3.037 kg/s (6.696 lbs/sec) and the reference HP turbine cooling flow is 6.8 percent. The engine achieves a specific fuel consumption (SFC) of 0.285 (kg/hr)/kW (0.468 (lb/hr)/hp). The two-stage centrifugal compressor has a 13.5:1 pressure ratio with an adiabatic efficiency of 78.7 percent. The HP and LP turbines have efficiencies of 87.0 percent and 88.5 percent, respectively. Shaft power output is transmitted at 2408 rad/s (23,000 rpm).

At a cruise condition (37 percent power) the reference engine achieves an SFC of 0.381 (0.627), or 34 percent higher than at the design point. Turbine inlet temperature decreases from 1149 to 853C (2100 to 1567F) and compressor inlet corrected flow decreases from 3.037 to 2.173 kg/s (6.696 to 4.796 lb/sec), respectively.

Weight - The reference engine weight, including the IPS and engine accessories, has been computed to be 138 kg (303 lb), as shown in Table 7. This weight was generated with the WATE-S computer program originally established by GTEC for NASA. (Reference 2) The program inputs for this computation included cycle information, materials definition, and measured and calculated weights for the IPS, engine controls, and accessories. This same computer program and reference engine weights for IPS, controls, and accessories were also used for follow-on computations for year-2000 engine weight estimates to achieve comparable weight data. Engine size estimates are an overall length of 40.4 inches and a maximum diameter of 14.4 inches.

TABLE 5. ROTORCRAFT REFERENCE ENGINE DESIGN POINT DATA

Design Point Performance-Sea Level, Static, ISA, IRP, Uninstalled With No Production Margins	
Overall Engine Performance	Component Performance
Engine Rating, kW (shp)	746 (1000)
SFC (kg/hr)/kW, (lb/hp)/hr	0.285 (0.468)
Turbine Inlet Temperature	
o HP Turbine, C (F)	1149 (2100)
o LP Turbine, C (F)	769 (1416)
Overall Cycle PR	13.37
Inlet $W\sqrt{\theta}/\delta$, kg/s (lb/sec)	3.604 (7.941)
Compressor Inlet $W\sqrt{\theta}/\delta$, kg/s (lb/sec)	3.037 (6.696)
N _{LP} , rad/s (rpm)	2408 (23,000)
N _{HP} , rad/s (rpm)	4679 (44,690)
Fuel LHV, kJ/kg (Btu/lb)	42,798 (18,400)
TOTAL CHARGEABLE COOLING FLOW = 8.8%	
 <p>32% 1.9% NONCHARGEABLE CHARGEABLE UNCOOLED</p>	
<u>IPS</u>	
o $W\sqrt{\theta}/\delta$, kg/s (lb/sec)	0.62 (1.36)
o Bypass Flow	
o Extraction, kW (shp)	5.5 (7.4)
o $\Delta P/P$, %	3.6
<u>HP Compressor</u>	
<u>Stage 1</u>	
o PR	4.73
o η_{AD} , %	81.8
o η_{Poly} , %	85.3
<u>Stage 2</u>	
o PR	2.85
o η_{AD} , %	81.6
o η_{Poly} , %	84.0
<u>Overall</u>	
o PR	13.5
o η_{AD} , %	78.7
o η_{Poly} , %	84.7
o Exit $W\sqrt{\theta}/\delta$, kg/s (lb/sec)	0.32 (0.69)
<u>Combustor</u>	
o η , %	99.98
o $\Delta P/F$, %	4
<u>HP Turbine</u>	
o $W\sqrt{\theta}/\delta$, kg/s (lb/sec)	0.50 (1.10)
o η_{AD} , %	87.0
o Cooling Flow, %	6.8
o Interturbine, % ($\Delta P/P$)	1.4
<u>LP Turbine</u>	
o $W\sqrt{\theta}/\delta$, kg/s (lb/sec)	1.95 (4.30)
o η_{AD} , %	88.5
o LPT-NOZ P/P, %	2.5

*Stator and blade cooling flows are shown. The second-stage stator and blades are uncooled. The balance of the cooling flows (4.9%) are used for disk and firtree cooling.

TABLE 6. ROTORCRAFT REFERENCE ENGINE DESIGN DATA

Cruise Performance-Sea Level, Static, ISA, 37% Power, Uninstalled With No Production Margins.			
Overall Engine Performance		Component Performance	
Engine Rating, kg (shp)	276 (370)	<u>IPS</u>	
SFC, (kg/hr)/kW (lb/hp)/hr	0.381 (0.627)	o $W\sqrt{\theta}/\delta$, kg/s (lb/sec)	0.529 (1.167)
Turbine Inlet Temperature		o Bypass Flow	
o HP Turbine, C (F)	853 (1567)	o Extraction, kW (shp)	4.0 (5.3)
o LP Turbine, C (F)	553 (1028)	o $\Delta P/P$, %	2.73
Overall Cycle PR	8.50	<u>HP Compressor</u>	
Inlet $W\sqrt{\theta}/\delta$, kg/s (lb/sec)	2.678 (5.904)	<u>Stage 1</u>	
Compressor Inlet $W\sqrt{\theta}/\delta$, kg/s (lb/sec)	2.173 (4.791)	o PR	3.66
N_{LP} , rad/s (rpm)	2408 (23,000)	o η_{AD} , %	83.3
N_{HP} , rad/s (rpm)	4679 (38,501)	o η_{Poly} , %	86.0
Fuel LHV, kJ/kg (Btu/lb)	42,798 (18,400)	<u>Stage 2</u>	
		o PR	2.34
		o η_{AD} , %	82.7
		o η_{Poly} , %	84.5
		<u>Overall</u>	
		o PR	8.55
		o η_{AD} , %	80.7
		o η_{Poly} , %	85.4
		o Exit $W\sqrt{\theta}/\delta$, kg/s (lb/sec)	0.33 (0.73)
		<u>Combustor</u>	
		o η , %	99.97
		o $\Delta P/P$, %	4.39
		<u>HP Turbine</u>	
		o $W\sqrt{\theta}/\delta$, kg/s (lb/sec)	0.457 (1.096)
		o η_{AD} , %	86.1
		o Cooling Flow, %	6.8
		o Interturbine, % ($\Delta P/P$)	1.3
		<u>LP Turbine</u>	
		o $W\sqrt{\theta}/\delta$, kg/s (lb/sec)	1.859 (4.098)
		o η_{AD} , %	88.6
		o LPT-NOZ $\Delta P/P$, %	1.13

TABLE 7. MODULAR WEIGHT BREAKDOWN

<u>Module</u>	<u>Weight (lb)</u>
IPS	31.5
Compressor	33.6
Combustor	51.3
HP Turbine	34.5
LP Turbine	72.7
Controls and Accessories	<u>79.6</u>
TOTAL	303.2

Cost - The reference engine cost was estimated at \$185,000 (1985 dollars). This cost is based on a mean sell price for turboshaft engines in this size class, as shown in Figure 5A. The sell price range is based on a GTEC market survey of presently available turboshaft engines in the 447 to 895 kW (600 to 1200 shp) range.

2.1.4 Environmental Constraints

Environmental constraints for the year 2000 were projected for rotorcraft engines based on a review of existing regulations and projections. Two major areas, noise and emissions, were addressed to establish year-2000 guidelines as based on the following sources:

Noise

Federal Aviation Administration (FAA)
 International Civil Aviation Organization (ICAO)
 Committee on Aircraft Noise (CAN)
 Aerospace Industries Association (AIA)
 General Aircraft Manufacturer's Association (GAMA)

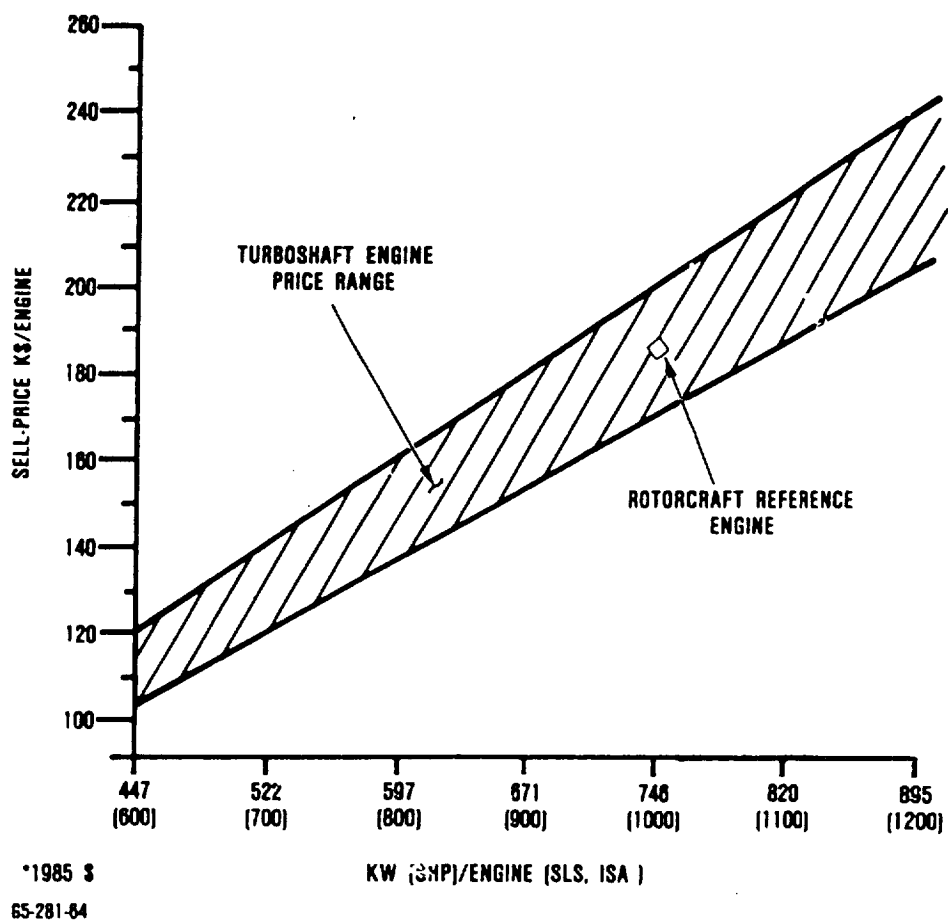


Figure 5A. Rotorcraft Engine Cost.

Emissions

U.S. Air Force AFR 19-1 (1979)

International Civil Aviation Organization (ICAO) (1982)

Environmental Protection Agency (EPA) (1984)

Governmental noise limits and standards for helicopters remain in the infancy stage. The FAA proposed a set of noise limits for helicopters several years ago, but the proposed regulation was withdrawn because of significant inadequacies. The FAA currently is working on the subject and should develop a new helicopter noise proposal in the next few years. Significant FAA funds have been spent on the development of a helicopter noise data base and standard measurement procedures. ICAO has published a noise standard for helicopters, which includes limits for takeoff, approach, and overflight conditions. In May, 1983, the ICAO CAN/7 delegates voted to recommend a 3 dB increase in the noise limits; however, the member states have not yet approved the change.

Research in helicopter noise, which will continue for the next 20 years, will concentrate on the reduction of rotor noise. The technology funding for the reduction of helicopter gas turbine engine noise will be somewhat limited unless the associated environmental impact becomes a greater concern to the various governments. Overall, no great increases in the stringency of the existing standards are expected. The exceptions would be rules imposed by local governments without federal intervention.

The 3 dB relaxation in stringency proposed at CAN/7 should disappear by the year 2000, and the resulting noise limits should be similar to those currently adopted. Therefore, the Garrett SECT study has used the existing ICAO Annex 16 Chapter 8 noise standards for helicopters.

Emission levels likely to be required by the year 2000 for a 746 kW (1000 shp) size class turboshaft are as follows:

- o Smoke levels - below the level of visibility, smoke number (SN) = 50
- o Gaseous emissions - unregulated for civil engines

2.1.5 Economic Model for Rotorcraft

This paragraph presents the economic modeling used for the rotorcraft engines of this study. The model in the NASA Helicopter Synthesis computer program, HESCOMP, was employed and rotorcraft partitions were defined as presented in Table 8.

Direct operating costs (DOC), calculated by the HESCOMP program, were based on study assumptions and fixed/variable costs shown in Table 9, including the fuel prices selected for this study.* The low and high fuel prices selected bracket the expected year-2000 fuel costs and are stated in 1985 dollars.

All cost estimates were calculated internally within HESCOMP. This cost estimate subroutine is thoroughly documented in reference 3.

Engine costs were estimated for each engine separately. Costs for the reference engine were based on estimated market sell prices for 1985, as described in paragraph 2.1.3. Costs for advanced technology, year-2000 engines were based on cost factors as applied to the reference engine cost for parts/components

*Low fuel price: \$0.264/liter (\$1/gal)
High fuel price: \$0.528/liter (\$2/gal)

TABLE 8. ROTORCRAFT VEHICLE PARTITIONS

Component	Costs
Airframe minus nacelle	Variable
Nacelle	Variable
Payload	Fixed
Mission	Fixed
Fuel Tankage	Variable
TOGW Limit	Variable
Rotor	Fixed
Fuel Load	Variable
Engine	Variable
Engine Cost	Variable

TABLE 9. BASIS FOR DOC COMPUTATIONS

Assumptions		Fixed Costs	Variable Costs
Number of Engines (Excluding Spares)	3000	Load Interest Rate	Engine Aircraft
Spares	4 percent	Imputed Interest Rate	Fuel*
Potential Aircraft	1500	Depreciation Schedule	Airframe Maintenance
Annual Use	2500 hr	Insurance Schedule	Engine Maintenance
Service Life	7 years	Tax Rate	Crew Expenses
Takeoff Gross Weight (Structural Limit)	4338 kg (9564 lb)	Crew Wages	
Payload	1667 kg (3676 lb)	Hanger Rent	
		Miscellaneous	
*Based on \$0.264 and \$0.528/liter (\$1 and \$2/gal)			

replaced by new technologies. These costs adjustments included a projected 15 percent cost reduction by year 2000 for current technology parts.

The DOC model used in this study resides within the HESCOMP program. Within this code, the following constant values were used:

Pilot salary, \$30,000/year

Copilot salary, \$20,000/year

Oil consumption rate, 0.061 kg/hr (0.135 lb/hr) per engine

Factor for nonrevenue flight (1.03)

All costs for this study are expressed in 1985 dollars.

2.1.6 Trade Factors for Rotorcraft

This section presents trade factors based on the reference mission, aircraft, and engine for the rotorcraft engine application as computed for Task II evaluation.

The trade factors relate rotorcraft owner-operator costs to changes in engine parameters. They are based on the SECT reference rotorcraft (year 2000) and mission (year 2000), and on the SECT reference engine (year 1995). The trade factors were computed with the HESCOMP computer program, in accordance with the selected economic model discussed in paragraph 2.1.5.

The trade factors that constitute differentials for the listed parameters are presented in Table 10 for the fuel prices selected for this study. The values shown are DOC changes in trip cost for each one percent change in the given parameter. The DOC/trip is \$1,378 for the low fuel price, and \$1,560 for the high fuel price, as shown in the reference engine DOC breakdown

TABLE 10. ROTORCRAFT TRADE FACTORS

	\$0.264/liter (\$1/gal)	\$0.528/liter (\$2/gal)
Δ DOC/1% Δ engine SFC	\$3.07	\$5.25
Δ DOC/1% Δ engine weight	\$0.41	\$0.56
Δ DOC/1% Δ engine diameter	\$0.05	\$0.05
Δ DOC/1% Δ engine length	\$0.04	\$0.05
Δ DOC/1% Δ engine cost	\$0.92	\$0.92

in Figure 5B. The DOC breakdown indicates that a number of factors contribute to aircraft DOC. Of these factors, the majority are only indirectly influenced by the propulsion system. One exception is fuel cost, which is directly influenced by engine SFC. As shown, this engine-sensitive portion of DOC constitutes only 10 to 25 percent of the total, depending on the fuel price.

These factors, as computed by the HESCOMP program, include the synergistic effects on the engine and rotorcraft system for engine changes. As such, the Δ DOC values reflect the effect of the nominal engine changes (i.e., engine SFC) and attendant changes to the rotorcraft system (fuel weight, tankage size, power required, etc.) that result for the reference mission.

2.2 Task II - Engine Configuration and Cycle Evaluation

The cycle/configuration studies for the rotorcraft application parametrically considered a range of potential combinations in terms of turbine rotor inlet temperature (TRIT), cycle pressure ratio (CPR), component types, materials and associated efficiencies, cooling flows, pressure drops, and leakages as projected for year-2000 capabilities. From the range of engines considered, a final engine selection for Task III evaluation was

ORIGINAL PAGE IS
OF POOR QUALITY

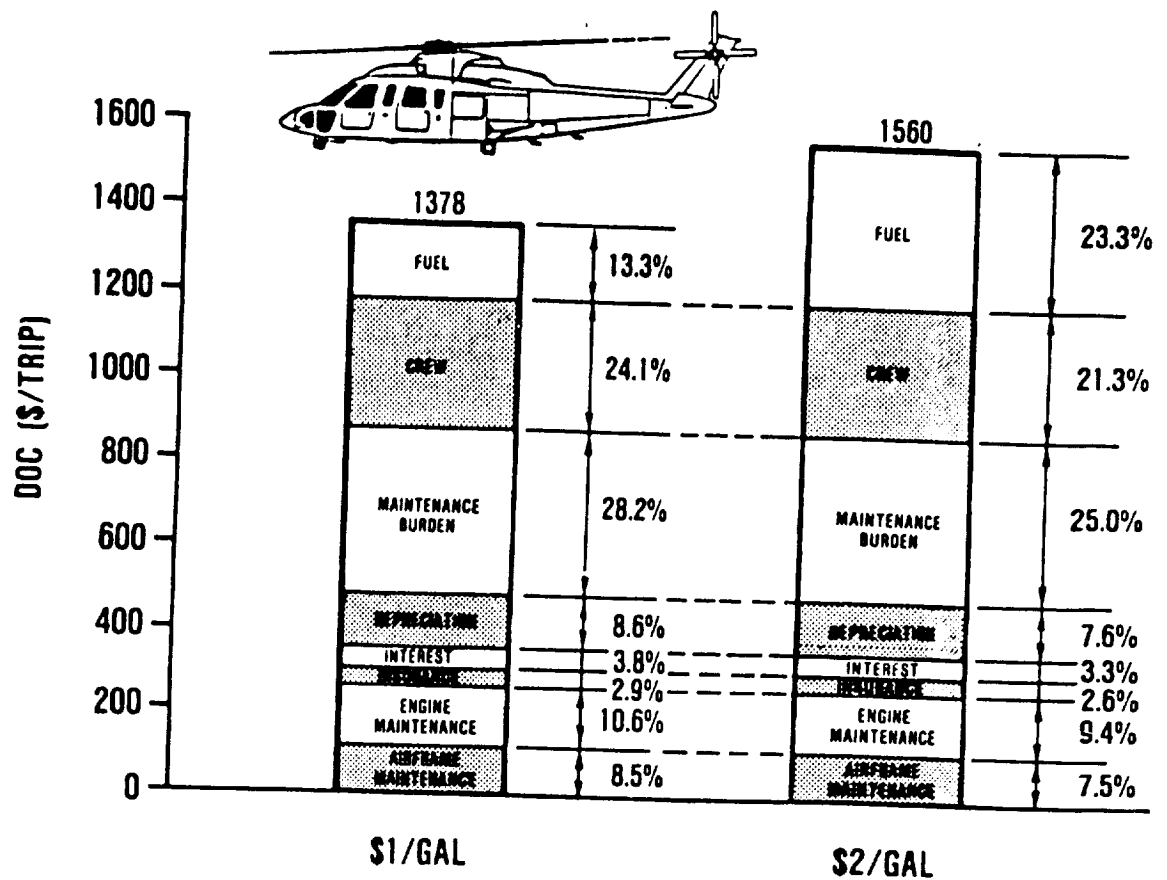


Figure 5B. Rotorcraft DOC Breakdown - Reference Engine.

made on the basis of payoff in aircraft direct operating cost (DOC). The DOC improvements were estimated through the trade factors (established in Task I), which relate changes to DOC in terms of changes in engine performance (SFC), weight, diameter, length, and cost (changes are relative to the 1985 reference engine). Size, weight, and cost were quantified for each engine of interest.

2.2.1 Technology Projections

The initial task in configuring potential rotorcraft engines for the year 2000 was to establish the expected level of technology in that time frame. Inherent in these projections is the assumption that the technologies will be available by the year 2000. Technologies have been identified in three major areas: materials, aerodynamics/thermodynamics, and mechanical improvements. These technologies impact the cycle study in terms of efficiency levels, turbine inlet temperature limits, and cooling flow requirements, as well as turbine stage count and hub speed limits.

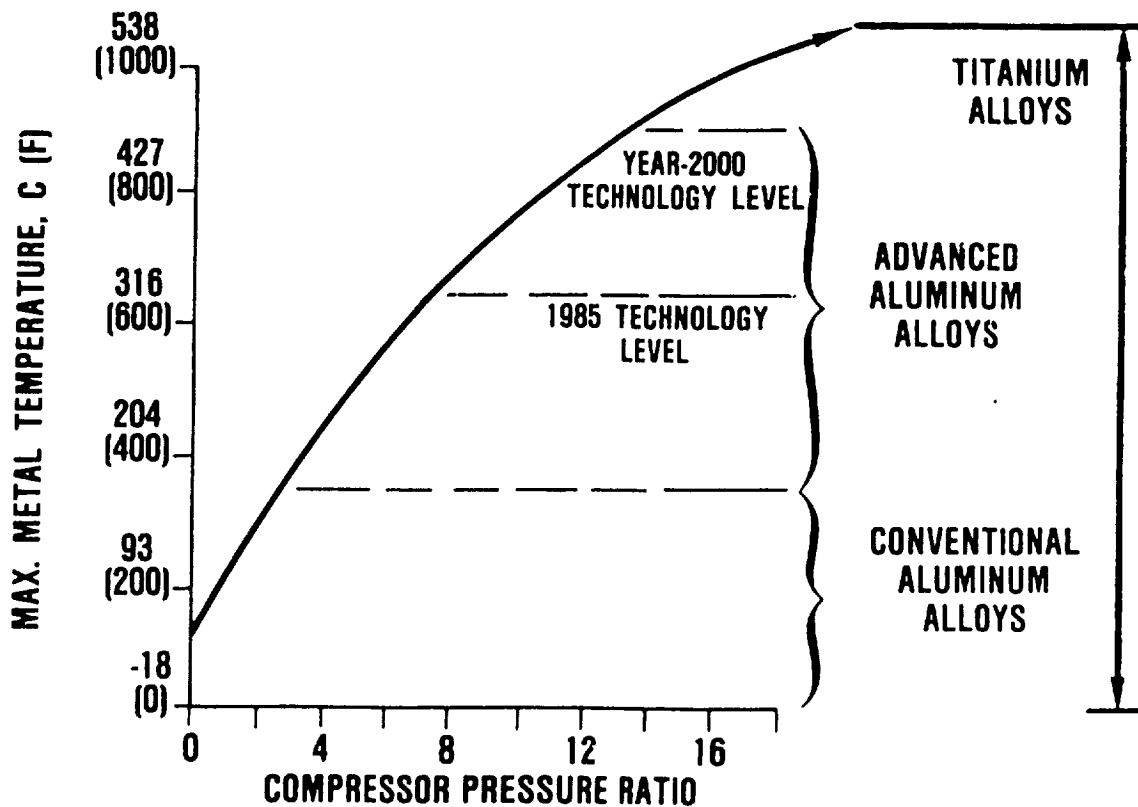
2.2.1.1 Materials

Both hot- and cold-end material technologies have been identified for future engines. For the cold end, four key materials have been considered for the rotorcraft application, as shown on Table 11. These materials primarily allow reduction in engine weight and cost.

For the compressor, two materials offer the potential of reduced cost: high-temperature powder metallurgy aluminum alloys and cast titanium alloys. Powder metallurgy aluminum can potentially reduce cost and weight relative to materials presently used. As shown in Figure 6, material temperatures between

TABLE 11. YEAR-2000 "COLD" MATERIAL PROJECTIONS

	High-Temperature Powder Metallurgy Aluminum Alloy	Cast Titanium Alloy	Polymeric Composites	Titanium Metal Matrix Composite
Application	Vanes, Blades, Rotors	Vanes, Blades, Rotors	Gearboxes	Shafts
Density, kg/cm ³ (lb/in ³)	0.003 (0.11)	0.004 (0.16)	0.002 (0.07)	0.001 (0.05)
Temperature Limit, C (F)	454 (850)	538 (1000)	260 (500)	482 (900)
Strength, MPa (ksi)	552 (80) at 24C (75F) 20.7 (30) at 454C (850F)	1100 (160) at 24C (75F) 34.5 (50) at 538C (100F)	345 (50) at 24C (75F)	689 (100) at 482C (900F)
Cost Factor*	0.7	0.8	0.9 - 1.2	3
Weight Factor*	0.6	1	0.7	0.5
*1.0 is 1985 metallic engine part				



- OBJECTIVE
 - EXTEND USE OF ALUMINUM ALLOYS
- PAYOFFS
 - REDUCED WEIGHT
 - REDUCED INERTIA
 - LOWER COST

65-281-7

Figure 6. Aluminum Metal Temperature Limit.

454 and 482C (850 and 900F) will be possible by the year 2000, allowing application of aluminum for higher compressor pressure engines. Present aluminum alloys have been successfully tested to over 316C (600F).

Cast titanium alloys offer the possibility of 20 percent cost reductions through the elimination of expensive machining operations. Other materials of interest are polymeric composites for gearboxes and metal matrix composites for shafts. Polymeric composites are predicted to reduce weight by as much as 30 percent relative to present aluminum gearboxes. Metal matrix composites for shafting are expected to be a required technology for year-2000 turboshaft engines in this small size class. The 50 percent reduction in weight, combined with favorable high-temperature strength, achieve the critical speed margins needed for the high spool speeds and small bore sizes of future engines.

In addition, four key hot-end materials have been identified, as shown in Table 12. These include two metallics: super single crystal for turbine blades and vanes, and Ni_3Al for turbine disks. Projections for two nonmetallics (ceramics coated and carbon-carbon) were also made for turbines, combustors, and transition liners.

Super single crystal increases the temperature capability of present single-crystal materials by approximately 56C (100F). Super single crystal allows higher stress and loading levels and, for a cooled turbine, could reduce cooling flow requirements at a given temperature.

Nickel aluminide (Ni_3Al) offers the potential of an improved strength-to-weight ratio by reducing weight approximately 15 percent relative to present alloy materials. This leads to higher turbine hub speed capabilities, resulting in reduced turbine stage count and/or aerodynamic loading.

TABLE 12. PROJECTED PROPERTIES FOR HOT-END MATERIALS

Application	Metallics			Nonmetallics	
	Super SC	Ni3Al	Ceramics	Carbon-Carbon	
	Blades/ Vanes	Disks	Vanes, blades, rotors, combustors, transition liners, recuperators	Vanes, blades, rotors, combustors, transition liners	
Density, kg/cm3 (lb/in3)	0.009 (0.31)	0.007 (0.27)	0.003 (0.12)	0.002 (0.065)	
Material Temperature Limit, C (F)	1093 (2000)	760 (1400)	1538 (2800)	2205 (4000)	
Strength kN/cm2 (ksi)	17.2 (25) at 1093C (2000F)	89.6 (130) at 760C (1400F)	27.6 (40) at 1538C (2800F)	51.7 (75) at 2205C (4000F)	
Cost Factor*	3	1	1	2	
Weight Factor*	1	0.85	0.4	0.3	

*1.0 is cost factor for 1985 metallic engine part.

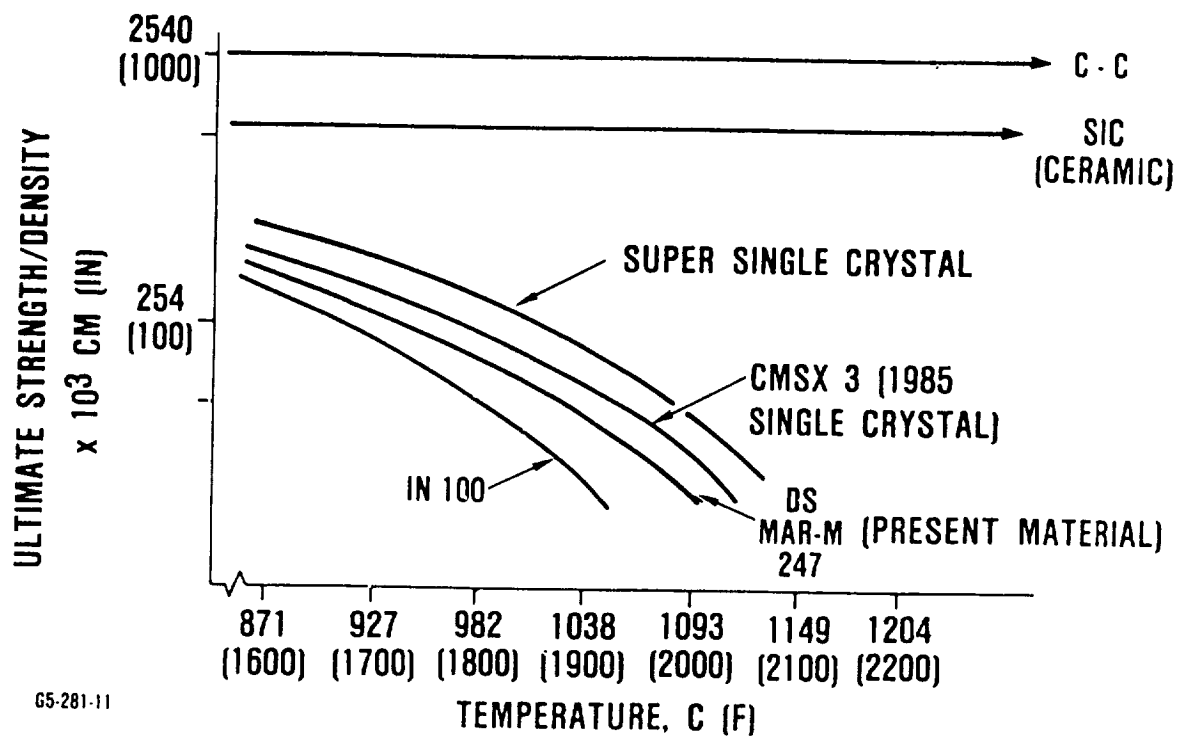
The nonmetallics can greatly increase strength at temperature, as shown in Figure 7, and also increase turbine material temperature capabilities. Both materials also reduce component weights significantly, relative to present metallics. The key improvement is the increased temperature capability that will allow higher turbine inlet temperatures without cooled turbine blading. For ceramics, the maximum material temperature limit is projected to be 1538C (2800F). Assuming a favorable combustor pattern factor ($PF \leq 0.12$, as estimated for year 2000), engine cycle temperatures up to 1427C (2600F) are projected.

Carbon-carbon has even greater temperature potential, up to 2205C (4000F), with suitable coatings. Coated carbon-carbon was included in this technology projection for completeness and clarity and is an important consideration for (unmanned) cruise missile engines as discussed in Section 4.0 of this report. However, GTEC projections show a low probability of achieving technological readiness by year 2000 for this material system for long-life engines installed in manned aircraft. Therefore, coated carbon-carbon was eliminated as a further candidate for the SECT rotorcraft engine studies.

2.2.1.2 Aerodynamics

Improvements in aerodynamic performance in terms of increased component efficiencies, reduced losses, and higher aerodynamic loading capabilities are predicted for compressors, combustors, and turbines by the year 2000.

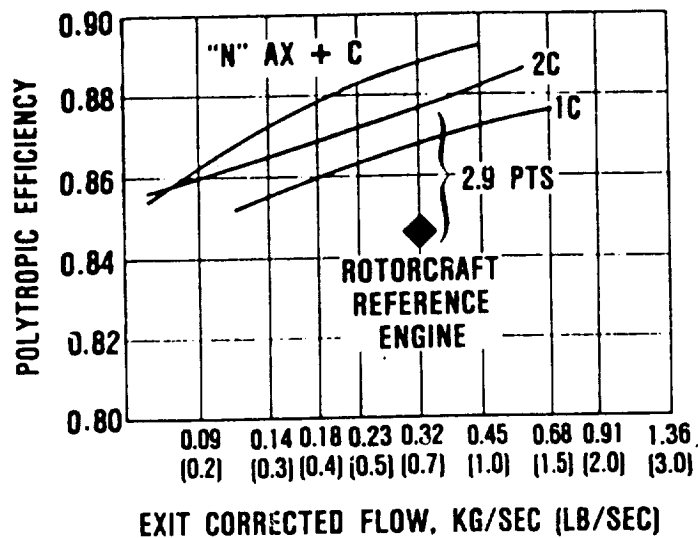
Three compressor configurations were considered for the rotorcraft application: single-stage centrifugal, two-stage centrifugal, and axial-centrifugal. The year-2000 efficiency predictions (polytropic), shown in Figure 8, are based on configuration as well as size and pressure ratio and are presented in terms of exit corrected flow.



GS-281-11

Figure 7. Comparison of Turbine Material Strengths.

ROTORCRAFT/COMMUTER COMPRESSOR PERFORMANCE



- REASONABLE STAGE LOADING
 - AXIAL FIRST STAGE P/P = 1.65
 - EQUAL WORK SPLIT FOR 2 CENTRIFUGAL
- 3 PERCENT CLEARANCE/BLADE TIP WIDTH
- 0.3 EXIT MACH NUMBER

EFFICIENCY IMPROVEMENTS (PERCENT OF TOTAL)

- DEVELOPMENT OF 3-D VISCOUS ANALYTICAL CODES AND NONINTRUSIVE MEASUREMENT TECHNIQUES TO SUPPORT ANALYTICAL DEVELOPMENT (60%)
- IMPROVED CLEARANCE CONTROL (20%)
- REDUCE DIFFUSER VANE INLET LOSSES WITH 3-D DIFFUSERS (10%)
- REDUCE IMPELLER SHOCK AND SECONDARY LOSSES (10%)

OTHER IMPROVEMENTS

- DEVELOP HIGHER LOADED VANE DIFFUSERS (LOWER WEIGHT)

65-281-5

Figure 8. Compressor Performance Projections.

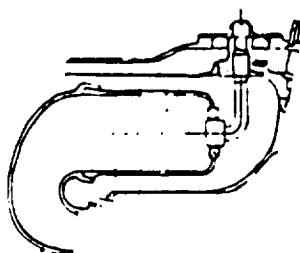
Relative to the reference rotorcraft compressor, a 2.9 point improvement in polytropic efficiency is foreseen (approximately four points improvement in adiabatic efficiency) for a two-stage centrifugal compressor. This improvement in efficiency is primarily attributed to the anticipated development of 3-D viscous analytical codes. Additional payoffs are seen from improved clearance control, reduced diffuser vane inlet losses, and reduced impeller shock and secondary losses.

Improvements in combustor performance are expected in several areas. As shown in Figure 9, combustor pattern factors will be reduced to the 0.10 to 0.13 range. Additionally, diffuser technology will be improved to maintain present pressure drop levels at increased inlet Mach numbers. Year-2000 combustors will also have higher heat release rates, reduced size, and improved durability.

The HP turbine performance projections are based on flow size and stage mean work coefficient for a two-stage axial configuration, as shown in Figure 10. Inclusion of the work coefficient, which is a function of mean blade speed, brings rotational speed and dimensional aspects into the cycle analysis. For the HP turbine, a two-point improvement is predicted relative to the uncooled reference turbine. The efficiency improvements are from projected reductions in vane/blade interaction losses, and rotor tip losses.

The LP turbine performance projections are similarly presented in Figure 11. A 2.9-point efficiency improvement is predicted for LP turbines relative to the reference configuration. The projected improvements are due primarily to minimizing vane/blade interaction losses, and rotor tip clearance losses.

ROTORCRAFT/COMMUTER (R/C)

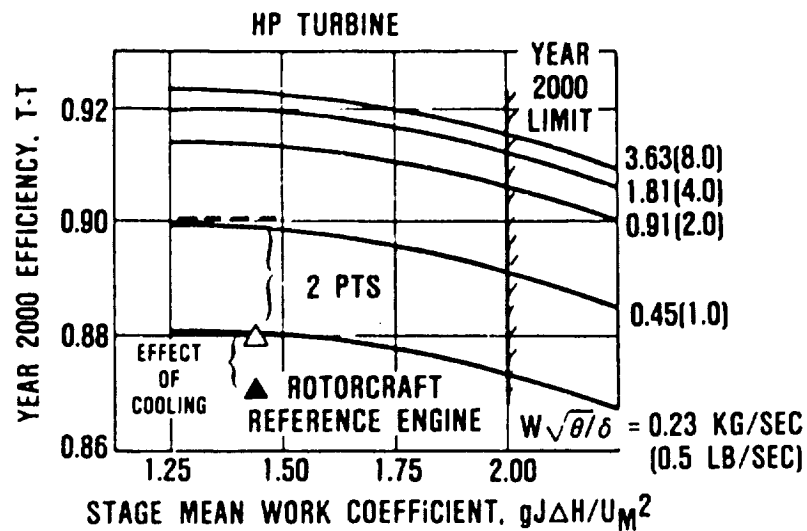


PARAMETER \ ENGINE	REFERENCE ENGINES R/C	YEAR 2000 ROTORCRAFT/ COMMUTER
COMPRESSOR EXIT M_N	0.15/0.4	0.3
COMBUSTOR $\Delta P/P$	4.0%	4.0%
COMBUSTOR η	0.998	0.998
PATTERN FACTOR	0.15-0.20	0.10-0.13

- CYCLE PARAMETERS ($\Delta P/P$, η) REMAIN THE SAME
- IMPROVED DIFFUSER TECHNOLOGY FOR INCREASED COMPRESSOR EXIT MACH NUMBER
- ADDITIONAL TECHNOLOGY IMPROVEMENTS
 - REDUCED PATTERN FACTOR
 - HIGHER HEAT RELEASE RATE
 - REDUCED SIZE
 - INCREASED DURABILITY

65-281-36

Figure 9. Combustor Technology Projections.



- NO FAB CONSTRAINTS
- UNSHROUDED BLADE
- 2 PERCENT TIP CLEARANCE
- UNCOOLED
- TWO-STAGE AXIAL

EFFICIENCY IMPROVEMENT PROJECTIONS

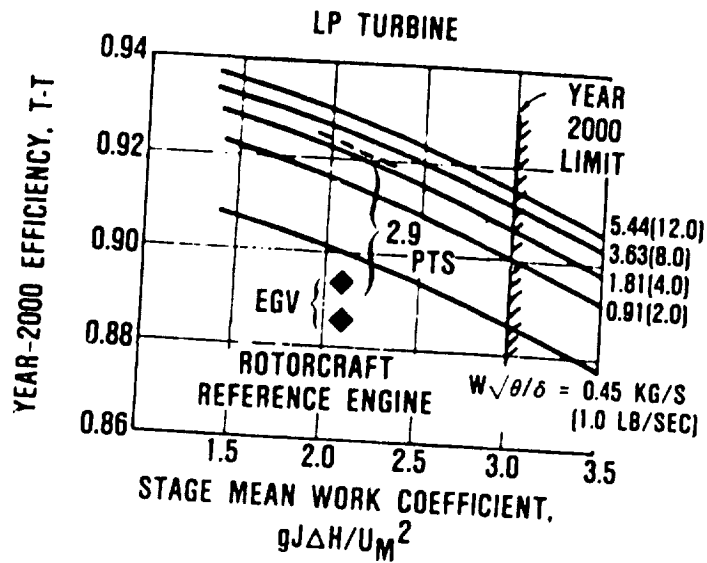
- REDUCED ROTOR TIP LOSSES (55%)
- MINIMIZE VANE
BLADE INTERACTION LOSSES (45%)

OTHER IMPROVEMENTS

- DESIGN TECHNIQUES FOR IMPROVED
PERFORMANCE/LIFE/COST TRADES

GS-281-2

Figure 10. HP Turbine Performance Projections.



- NO FAB CONSTRAINTS
- SHROUDED BLADE
- 1 PERCENT TIP CLEARANCE
- UNCOOLED
- TWO-STAGE AXIAL

EFFICIENCY IMPROVEMENT PROJECTIONS

- MINIMIZE VANE/BLADE INTERACTION LOSSES

OTHER IMPROVEMENTS

- DESIGN TECHNIQUES FOR IMPROVED PERFORMANCE/LIFE/COST TRADES

65-281-9

Figure 11. LP Turbine Performance Projections.

2.2.1.3 Recuperator

Improvements in recuperator technology will come in two areas, materials and processes. Of particular interest in this study was the counterflow platefin recuperator design. A typical cross section is depicted in Figure 12.

Material improvements are expected in both metallics and nonmetallics. As shown in Table 13, a nitride-dispersion-strengthened 300 stainless steel has the potential for increasing recuperator operating temperatures from a present limit of 816C (1500F) to between 982C (1800F) and 1093C (2000F).

Ceramics could further increase the temperature limit above 1437C (2600F). Furthermore, the 3 to 1 density advantage of ceramics is predicted to reduce overall recuperator weight by approximately 50 percent. At present, only experimental heat exchanger modules have been evaluated with ceramics, but by the year 2000, ceramic heat exchangers are predicted to be operational. One key to making ceramics operational is improving the manufacturing process, as schematically shown in Figure 13.

2.2.1.4 Mechanical Technology

After material and aerodynamic capabilities had been established, mechanical limits were set. As shown in Figure 14, GTEC uses established empirical correlations to set the mechanical inputs for the cycle evaluation. Considered in the cycle study were turbine hub speed limits, turbine blade AN^2 limits, as well as TRIT constraints and cooling flow requirements. These were set based on materials and mechanical technologies as projected for the year 2000.

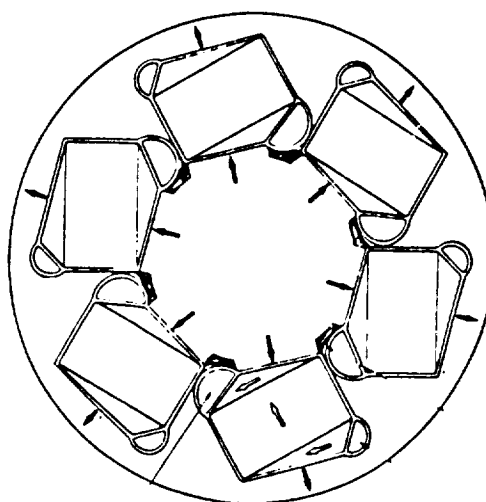
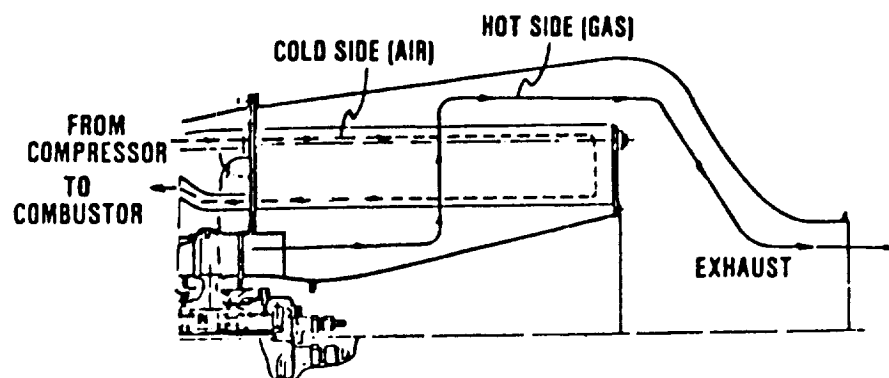


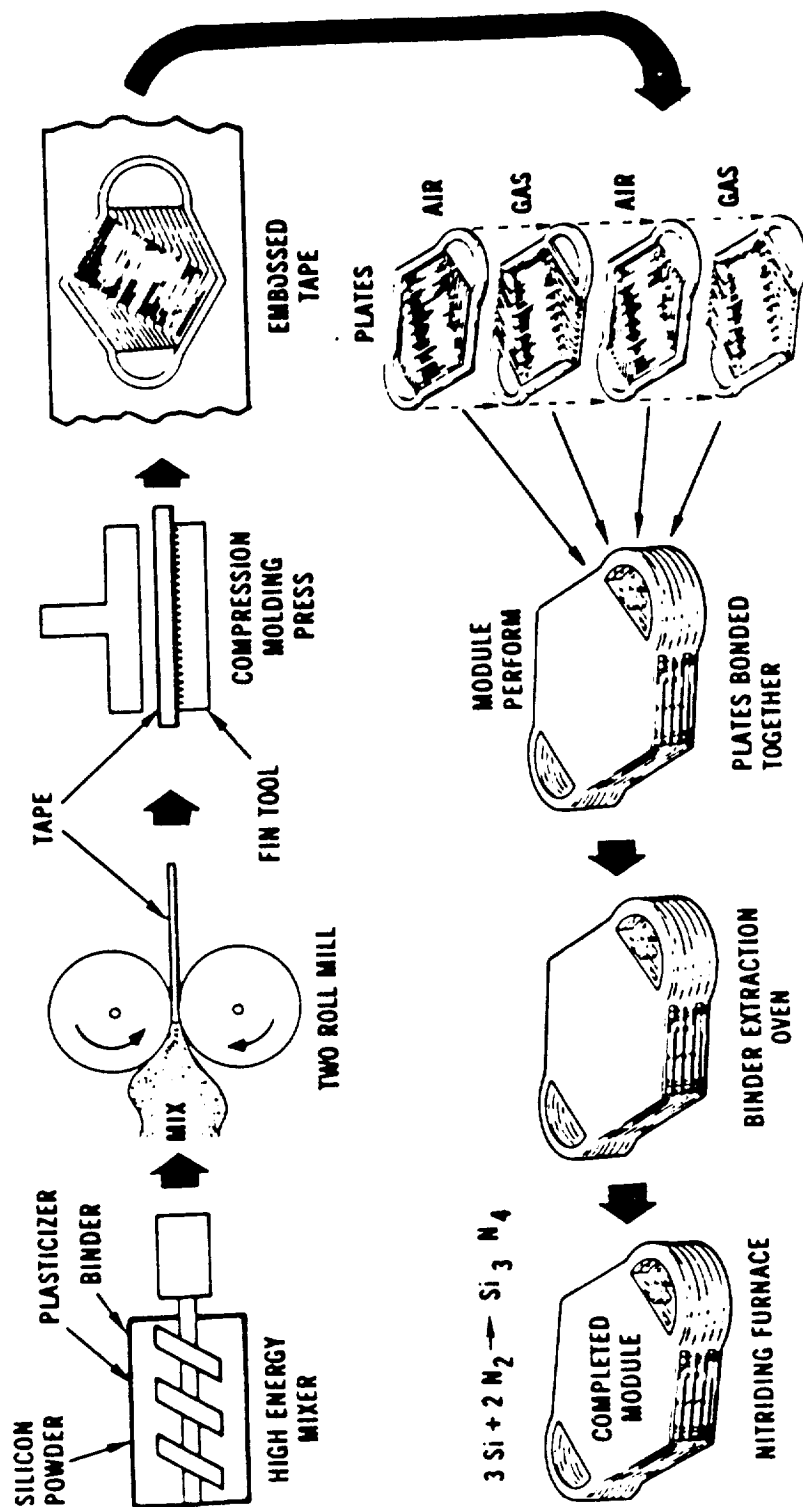
PLATE-FIN CROSS SECTION

65-281-38

Figure 12. Typical Plate-Fin Counterflow Recuperator Configuration.

TABLE 13. RECUPERATOR TECHNOLOGY PROJECTIONS.

Metals	
1985	Year 2000
Chromium-molybdenum steel	Nitride-dispersion-strengthened 300 stainless steel
Fin Density:	Fin Density:
37 fins per 2.54 cm (1 in.)	37 fins per 2.54 cm (1 in.)
Maximum Temperature is 816C (1500F) for short times	Maximum temperature is 982C (1800F) to 1093C (2000F)
Ceramics	
1985	Year 2000
Experimental plate-fin HXs	Operational plate-fin units
Plain Fins:	Offset Fins:
30 fins per 2.54cm (1 in.)	35 fins per 2.54cm (1 in.)
0.04cm (0.015 in.) thickness	0.03cm (0.010 in.) thickness
	Maximum temperature is 1427C (2600F) to 1538C (2800F)



GS-281-37

Figure 13. Ceramic Recuperator Manufacturing Process.

ASSUMPTIONS

- MATERIALS
- LIFE REQUIREMENTS
- CYCLE/CONFIGURATION
- AERO LIMITS

GTEC
EMPIRICAL
CORRELATIONS



MECHANICAL INPUT TO CYCLE*

- TURBINE HUB SPEED LIMITS
366-488 M/SEC (1200-1600 FT/SEC)
- AN^2 LIMITS 33.3-77.4
(5.0×10^{10} TO 12×10^{10})
- TRIT LIMITS**
- COOLING FLOW
REQUIREMENTS

65-281-39

*LIMITS DEPENDENT ON MATERIALS, CONFIGURATION, AND APPLICATION

**1427C (2600F) FOR UNCOOLED CERAMIC TURBINE BLADES
2204C (4000F) FOR CARBON-CARBON TURBINE BLADES

Figure 14. GTEC Empirical Study Approach.

2.2.1.5 Cost, Weight, and Size Estimates

To complete the input required for estimating aircraft DOC (with trade factors) cost, weight, and size estimates were required for each engine of interest.

The cost estimates for the candidate engines of this study were based on the reference engine cost and on a buildup of component costs as estimated by GTEC manufacturing. Each engine cost was therefore estimated separately, based on technologies employed, number and type of components, TRIT, and flow size. The costs are projected to year 2000 but are expressed in year-1935 dollars. The cost adjustments include a projected 15 percent cost reduction for parts/components manufactured in the year 2000.

Engine size and weight were estimated with the WATE-S (Weight Analysis of Turbine Engine - Small) computer program. (Reference 2) As depicted on Figure 15, the WATE program uses various mechanical, aerodynamic, material, and cycle inputs to calculate stresses, and size components to establish a power section size and weight buildup. For SECT, the accessory gearbox, accessories, recuperator, regenerator, and associated ducting were estimated manually (based on historical data) to get a total engine size and weight.

2.2.2 Cycle/Engine Studies

Traditionally, the typical parametric cycle study examines a range of key cycle variables such as turbine inlet temperature and compressor pressure ratio. Moreover, a number of simplifying assumptions are typically made, such as maintaining constant compressor polytropic efficiency and turbine adiabatic efficiency (without consideration of stage counts) as well as basing turbine

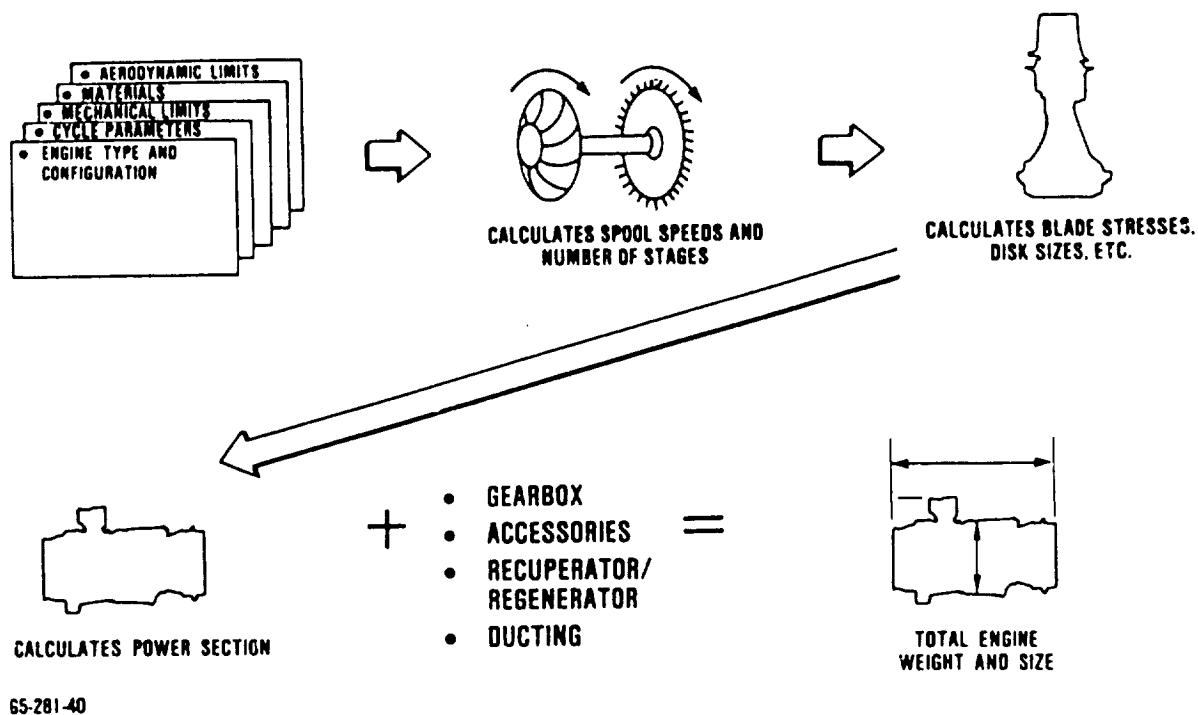


Figure 15. GTEC Engine Weight Estimate Approach.

cooling flow on TRIT only. These and other idealized assumptions result in smooth and well behaved performance trends as shown in Figure 16A.

Not addressed in an idealized study, however, are the effects on efficiency of compressor and turbine stage counts, materials/mechanical constraints, spool speeds, and accurate cooling flows based on the number of cooled stages and on cooling air temperatures and TRIT levels. Consideration of these mechanical limitations in the cycle study fragments the results into a number of distinct families such as shown in Figure 16B. Relative to the idealized cycle study, incorporating such mechanical limitations eliminates many unrealistic cycles/engine configurations from the cycle results.

2.2.2.1 Simple-Cycle Study

Primarily simple (conventional) cycles were investigated for the rotorcraft application. A variety of engine configurations, as shown in Figure 17, were considered. Both two-stage centrifugal and axial centrifugal compressors were evaluated, as were ceramic and advanced metallic turbines. Turbine rotor inlet temperatures ranging from 1204C (2200F) to 1538C (2800F), and cycle pressure ratios from 16 to 26 were considered.

A data plot of SFC versus specific power is displayed in Figure 18. The plot shows a cycle result, for an engine configured with a two-stage centrifugal compressor and advanced metallics in the axial HP and LP turbines. HP and LP turbine stage count and blade or vane materials are identified. The curves are fragmented, as expected, into several engine families with different turbine stage counts and cooling flow requirements. SFCs up to 15 percent lower than the reference engine result for this

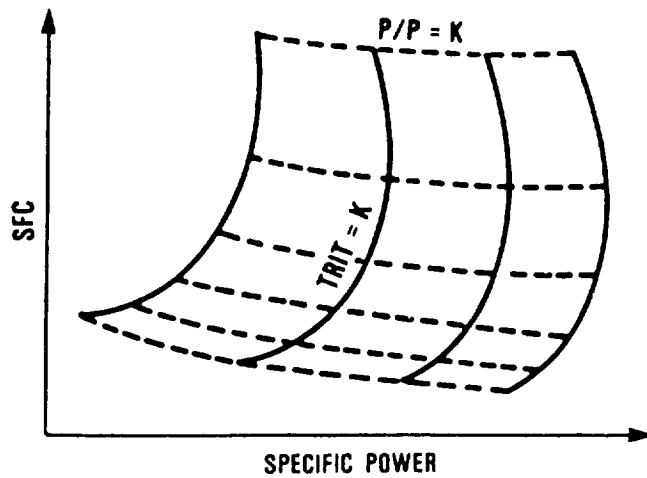
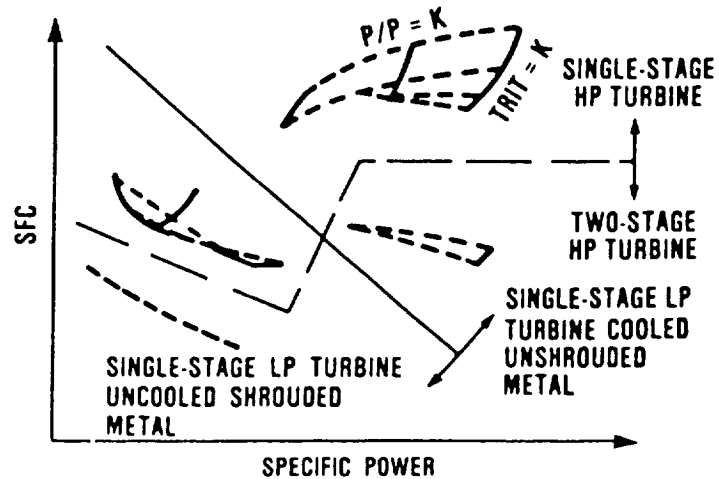


Figure 16A. Idealized Cycle Study Results with Constant Efficiencies.



65-281-41

Figure 16B. Cycle Study Results With Mechanical Limits.

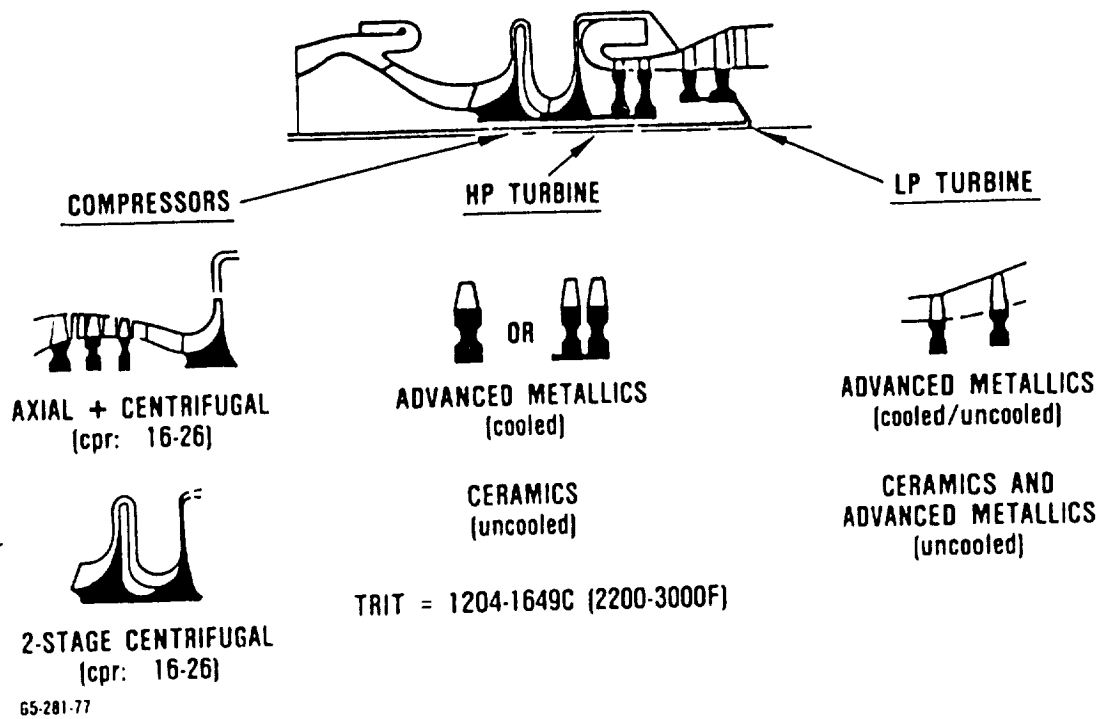
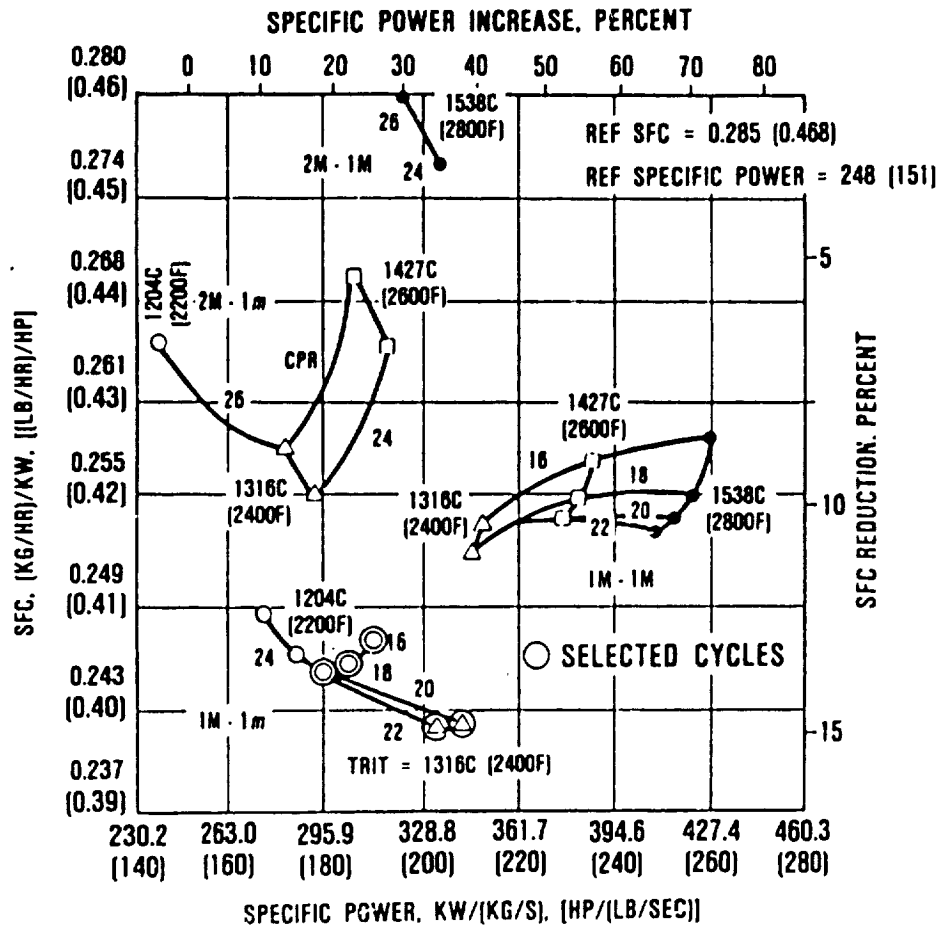
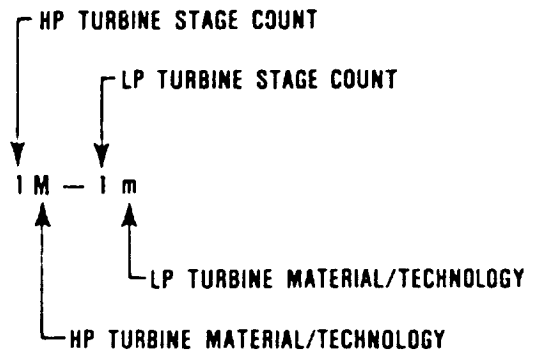


Figure 17. Simple-Cycle Study Configurations and Options.



- CONFIGURATION**
- 746KW (1000 SHP)
 - COMPRESSOR: TWO-STAGE CENTRIFUGAL
 - HP TURBINE: MINIMUM STAGE COUNT
 - LP TURBINE: MINIMUM STAGE COUNT
 - ADVANCED METALLIC TURBINES
(M = COOLED, m = UNCOOLED)



65-281-100

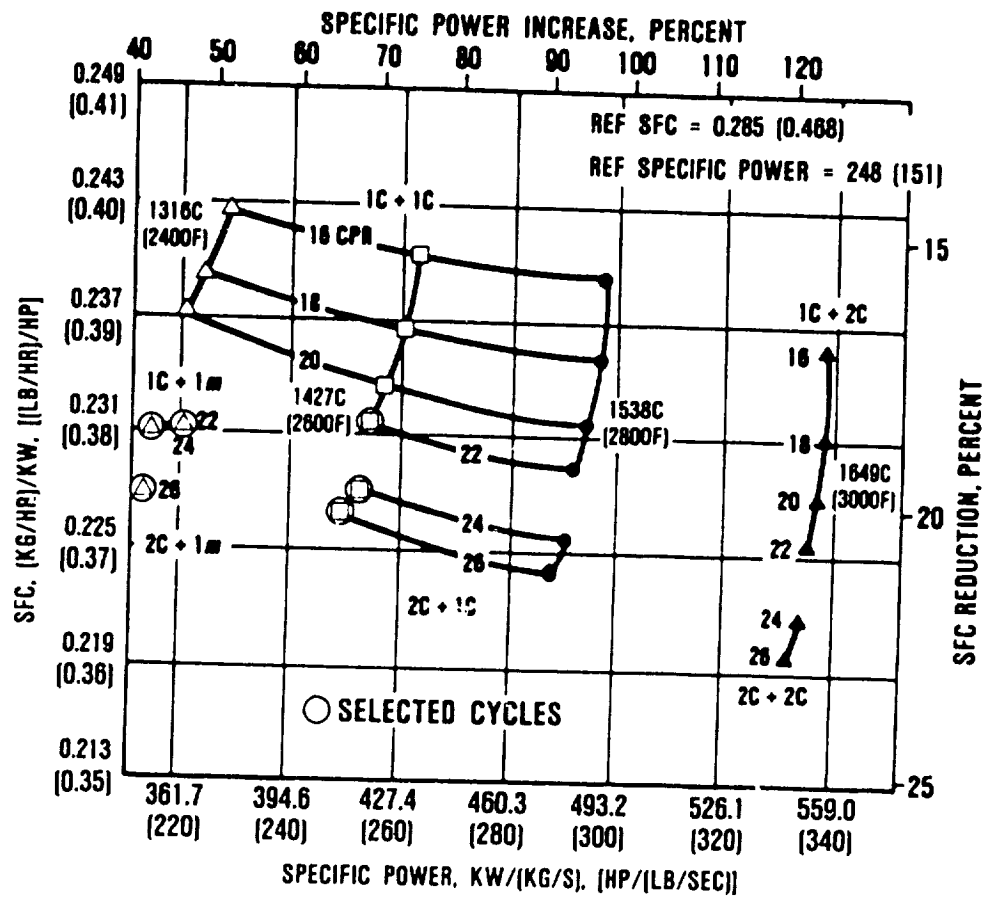
Figure 18. Rotorcraft Simple-Cycle Performance Results - Metallic Turbines.

case. Several candidate engines, as indicated, were selected for further evaluation in terms of weight, size, cost, and DOC estimates.

Of the technologies studied, the use of ceramics for blades and vanes has the largest performance impact. Replacement of the advanced metallics allows turbine cooling to be eliminated, resulting in an SFC improvement of over 20 percent relative to the reference engine, as shown in Figure 19. The cycles shown are all uncooled, however, based on the material temperature limit of ceramics, some cooling would be required above inlet temperatures of 1427C (2600F). The cycles selected for further evaluation have therefore been limited to 1427C (2600F), as indicated.

Size, weight, and cost were estimated for each of the engines from the selected advanced metallic and ceramic turbine cycles. The resulting values are presented in terms of deltas relative to the reference engine, as shown on Figure 20. As indicated, the ceramic turbines achieve superior results relative to advanced metallics in terms of all four parameters, weight, length, diameter, and cost. One of the more promising cycles uses ceramics at a TRIT of 1427C (2600F) and a 22:1 pressure ratio. With this configuration, weight is reduced by 50.3 kg (111 lb) (-36.6 percent) relative to the reference engine. Diameter is reduced by 13.2 cm (5.2 in.) (-36.1 percent), length by 44.2 cm (17.4 in.) (-43.1 percent), and cost by \$34,200 (-18.4 percent).

The payoffs for improvements in size, weight, and cost were evaluated in terms of their respective impacts on mission performance by DOC. The DOCs were estimated by trade factors shown in Task I, derived from the reference engine as "flown" on the year-2000 reference mission and rotorcraft. Both high and low fuel prices, as defined in paragraph 2.1.5, were used.



- HP TURBINE: CERAMICS (C)
MINIMUM STAGE COUNT
- LP TURBINE: CERAMICS (C)
AND ADVANCED METALLICS
(M, UNCOOLED)
- 746 KW (1000 SHP)
- COMPRESSOR: TWO-STAGE
CENTRIFUGAL

65-281-101

Figure 19. Rotorcraft Simple-Cycle Performance Results - Ceramic Turbines.

ORIGINAL PAGE IS
OF POOR QUALITY

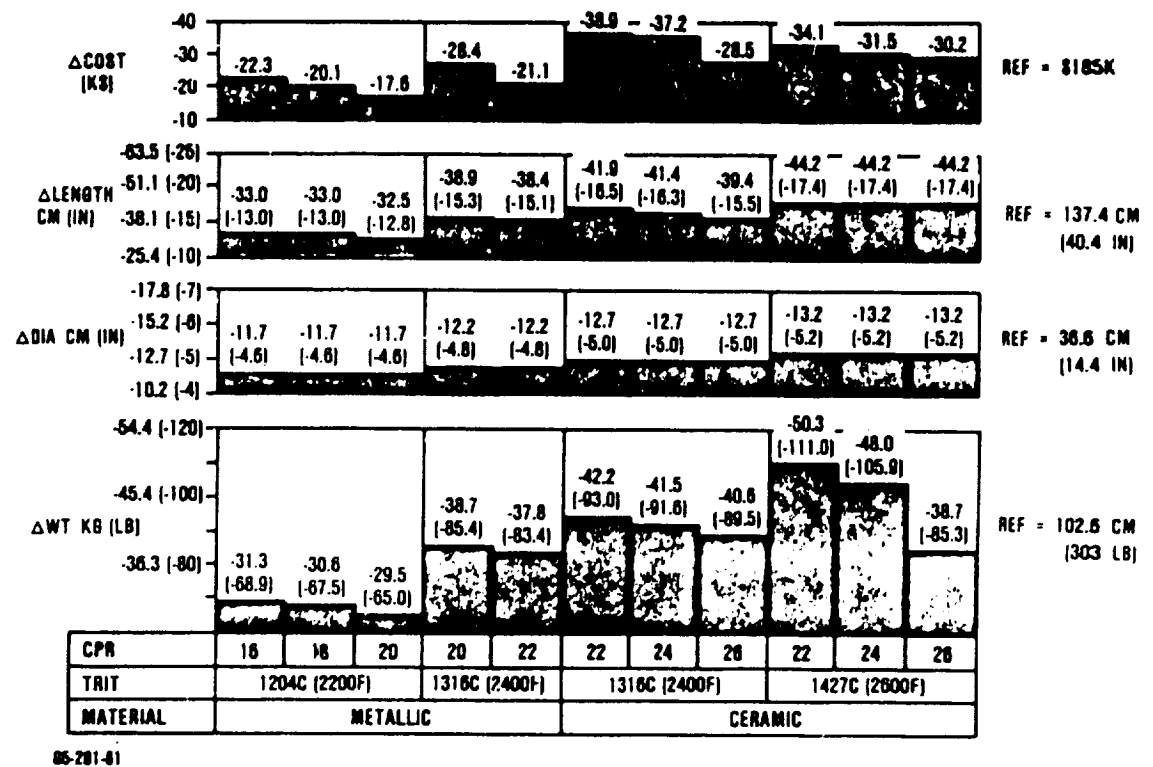


Figure 20. Projected Engine Size, Weight, and Cost Improvements With Advanced Metallics and Ceramics.

Figure 21 presents the resulting DOC values for the selected cycles in terms of deltas relative to the reference engine. Again, the ceramic engines are superior to those with advanced metallic turbines. The ceramic engine, at a TRIT of 1427C (2600F) and a PR of 24:1, has the highest reduction in DOC. Although increasing the pressure ratio from 22:1 to 24:1 has additional DOC payoffs, this cycle requires an additional HP turbine stage which would increase maintenance costs (not accounted for during Task II). Based on these DOC results, the ceramic engine with a TRIT of 1427C (2600F) and a PR of 22:1 was selected for further evaluation.

Other cycle/configuration trades considered were 1) replacing the two-stage centrifugal compressor with an axial-centrifugal, and 2) replacing single cooled HP turbines with two lightly loaded stages.

The axial-centrifugal compressor showed a slight performance advantage, 1.5 percent in SFC (Figure 22), compared to the two-stage centrifugal configuration (Figure 18). However, in terms of DOC, little or no improvement is projected beyond the engines with two-stage centrifugals, as shown in Figure 23. The SFC advantage of the axial centrifugal is offset by the greater size and cost of this configuration.

The two-stage HP turbine also shows no performance benefit. The additional cooling flow required for the second stage results in a reduction in overall engine performance, as shown on Figure 24 (compare to Figure 18). Engine weight, size, cost, and DOC are as presented in Figure 25, clearly showing the advantage of the single stage HP turbine, particularly in terms of DOC.

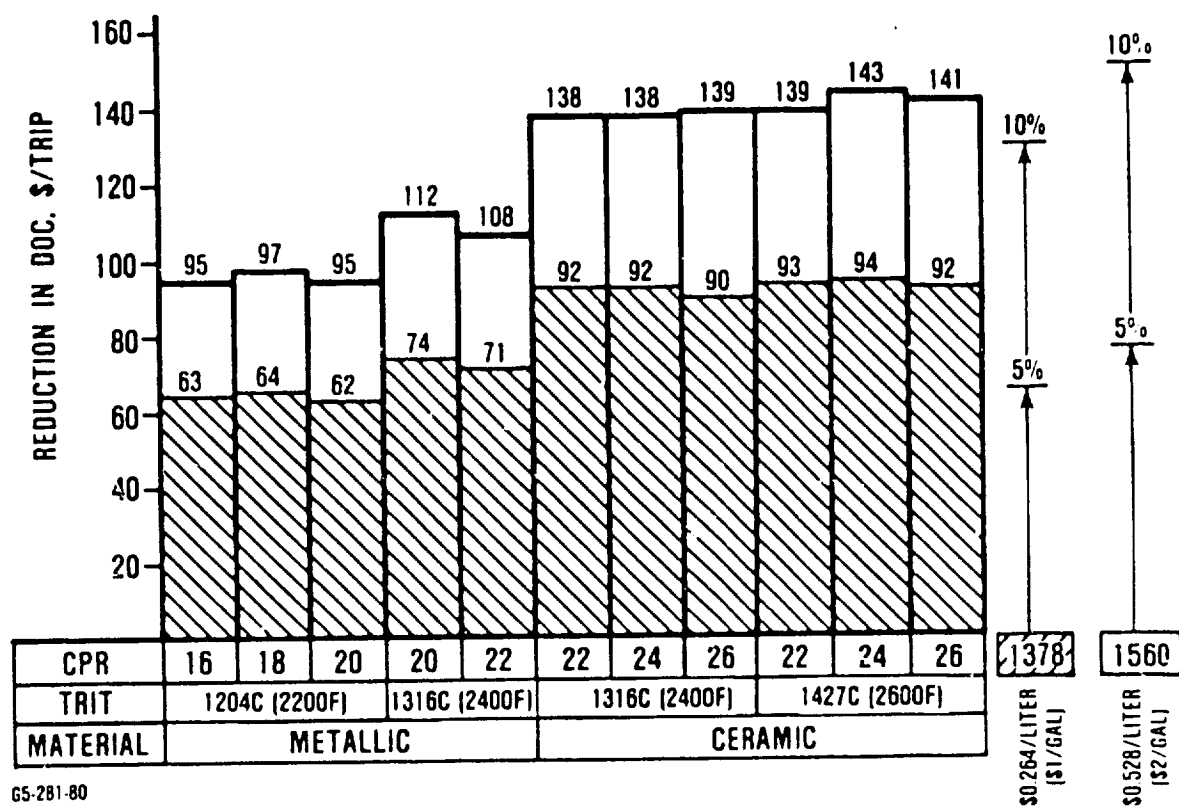


Figure 21. DOC Comparison of Advanced Metallic and Ceramic Engines.

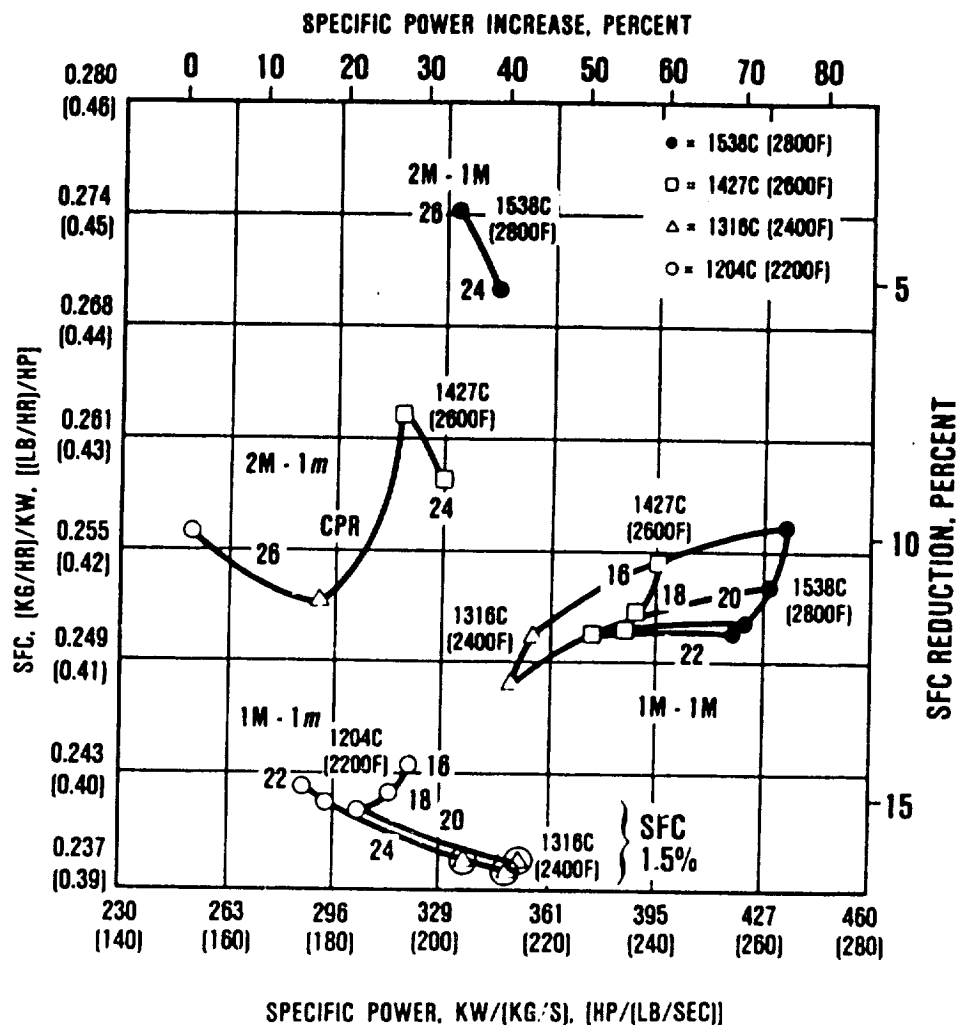


Figure 22. Simple Cycle Performance With an Axial-Centrifugal Compressor and Metallic Turbine.

ORIGINAL PAGE IS
POOR QUALITY

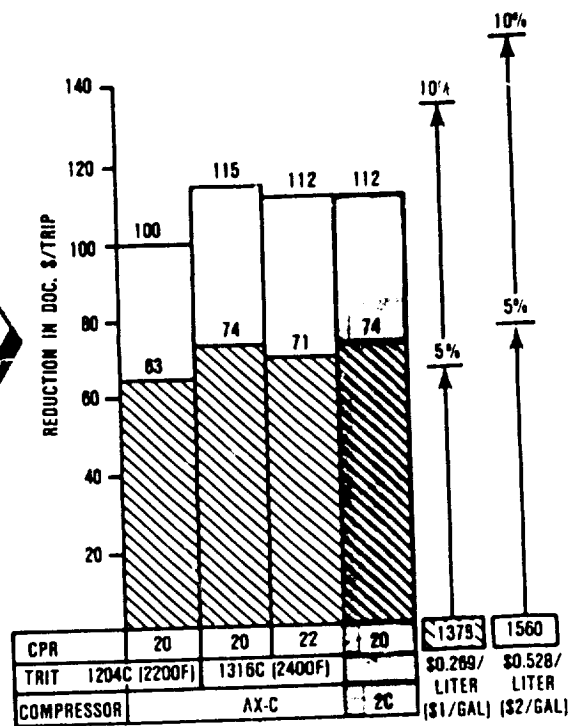
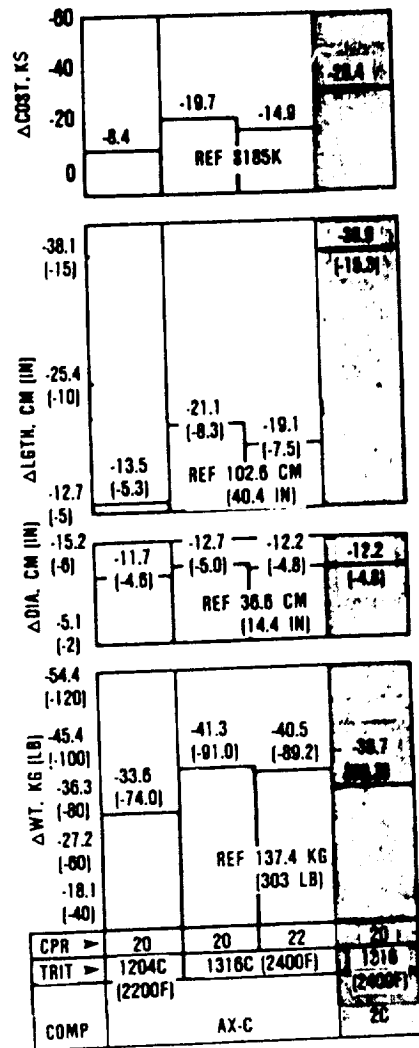
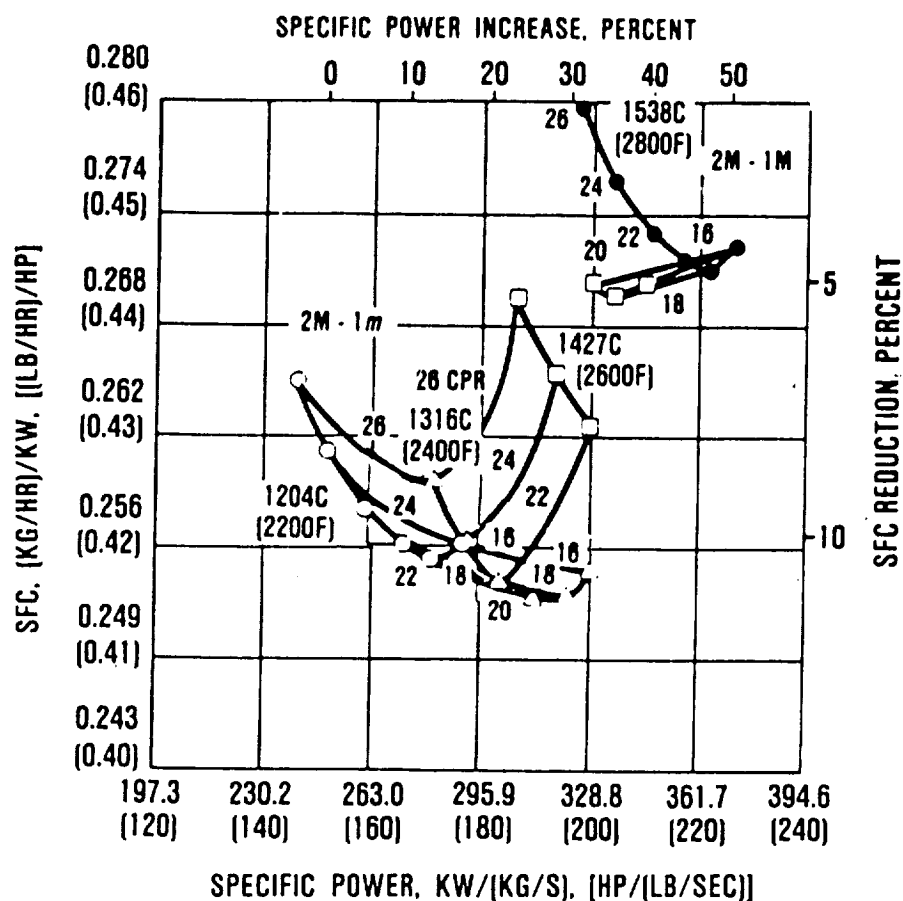


Figure 23. DOC Impact of Advanced Axial-Centrifugal Compressor Versus Two-Stage Centrifugal Compressor - Metallic Turbines.



- 746 KW (1000 SHP)
- COMPRESSOR: TWO-STAGE CENTRIFUGAL
- HP TURBINE: ADVANCED METALLICS TWO STAGE
- LP TURBINE: ADVANCED METALLICS
- = 1204C (2200F)
- △ = 1316C (2400F)
- = 1427C (2600F)
- = 1538C (2800F)

65-281-102

Figure 24. Simple-Cycle Performance with a Two-Stage (Cooled) Metallic HP Turbine.

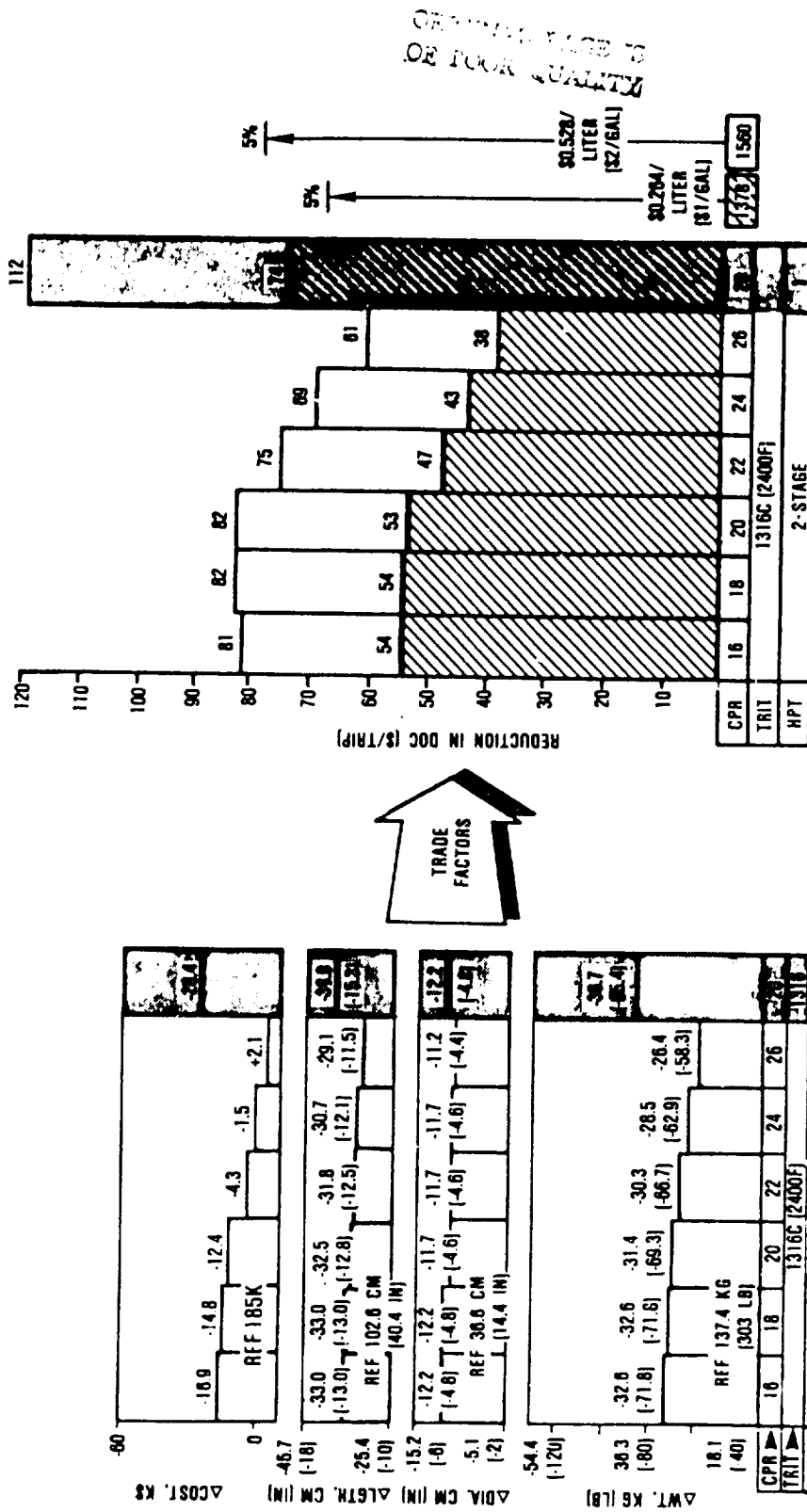


Figure 25. DOC Impact of Metallic Two-Stage HP Turbine Versus a Single-Stage Metallic Turbine.

The impact of size, or scaling, was also examined. A 373 kW (500 shp) engine was investigated with the baseline configuration to determine the performance impact. Comparing the downscaled engines (Figure 26) to the baseline (Figure 18), SFCs are increased by approximately 5 percent at the lower flow size because of a reduction in component efficiencies. For example, at a pressure ratio of 20:1 and a TRIT of 2400F, SFC is 0.417 at the lower flow size, compared to 0.398 at the higher flow size.

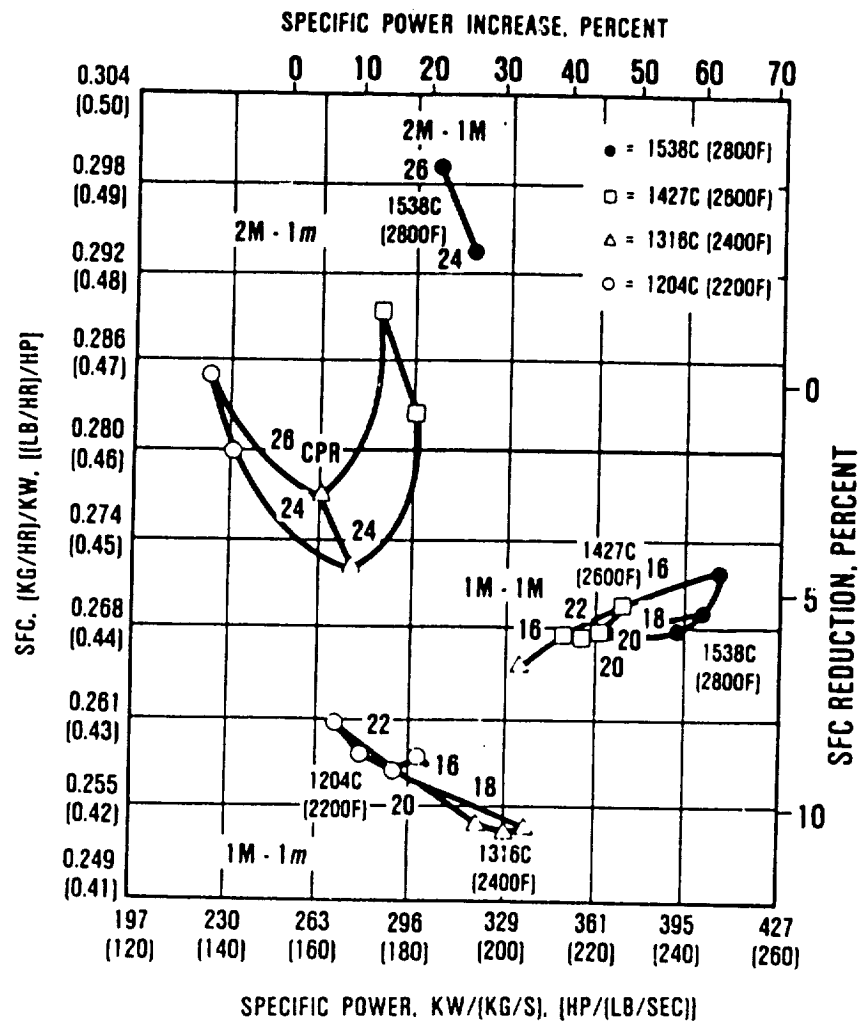
2.2.2.2 Recuperated Cycles Study

In addition to the conventional simple-cycle engines, a number of recuperated cycles were evaluated for the rotorcraft application as well. The cycles were selected based on results from the commuter cycle studies discussed in paragraph 3.2. The resulting performance, presented in Figure 27, shows a significant reduction in SFC (up to 27 percent relative to the reference), with an effectiveness of 0.7. Higher levels of effectiveness would further reduce SFC. The cycles shown use a variable LP turbine to take advantage of improved part-power performance (particularly critical for the rotorcraft mission) by maintaining a high temperature delta across the recuperator. Weight, size, cost, and DOC improvements are presented in Figure 28.

2.2.2.3 Cycle/Engine Selection

Based on the DOC results two cycles, a conventional simple cycle and a cycle using recuperation, were selected for further evaluation in Task III.

The simple-cycle engine is configured with a two-stage centrifugal compressor with a pressure ratio of 22. The compressor is driven by a single-stage uncooled ceramic axial HP turbine. The LP (power) turbine consists of two uncooled stages, and is



● 373 KW (500 SHP)

○ COMPRESSOR: TWO-STAGE CENTRIFUGAL

○ HP TURBINE: ADVANCED METALLICS
 MINIMUM STAGE COUNT

○ LP TURBINE: ADVANCED METALLICS

DOWNSCALING REDUCES SFC BY APPROXIMATELY 5%.

G5-281-87

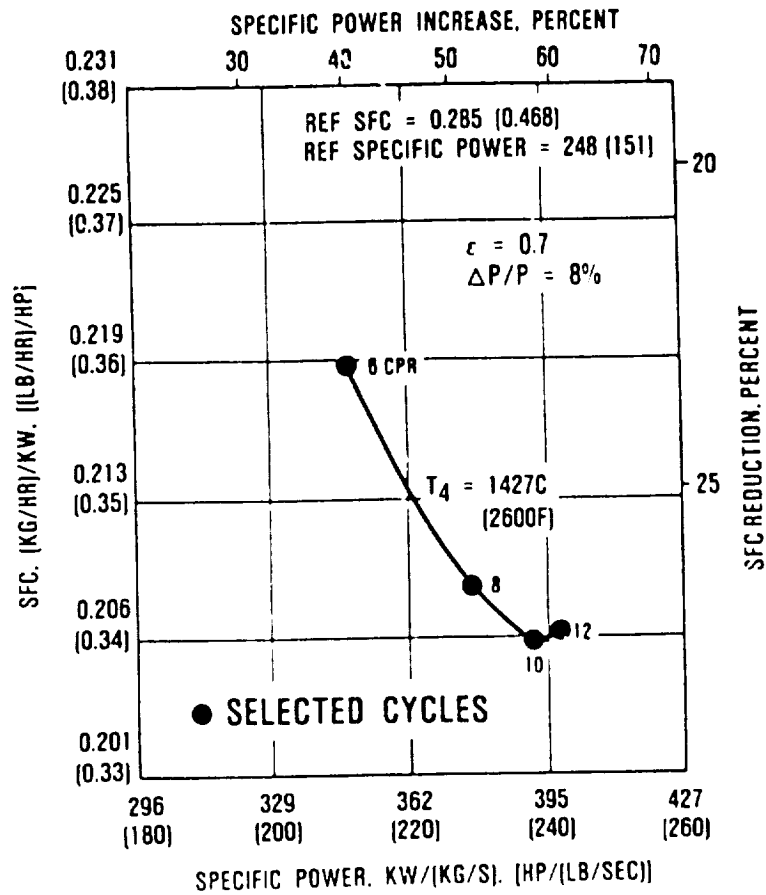
Figure 26. Performance Impact of Downscaling, Simple Cycle - Metallic Turbines.

CONFIGURATION

(HEAT RECOVERY CYCLE)

746 KW (1000 SHP)

- COMPRESSOR: ONE-STAGE CENTRIFUGAL
- HP TURBINE: CERAMIC ONE STAGE
- LP TURBINE: CERAMIC VARIABLE GEOMETRY THREE-STAGE



65-281-96

Figure 27. Performance of Recuperated Cycles for Rotorcraft Application.

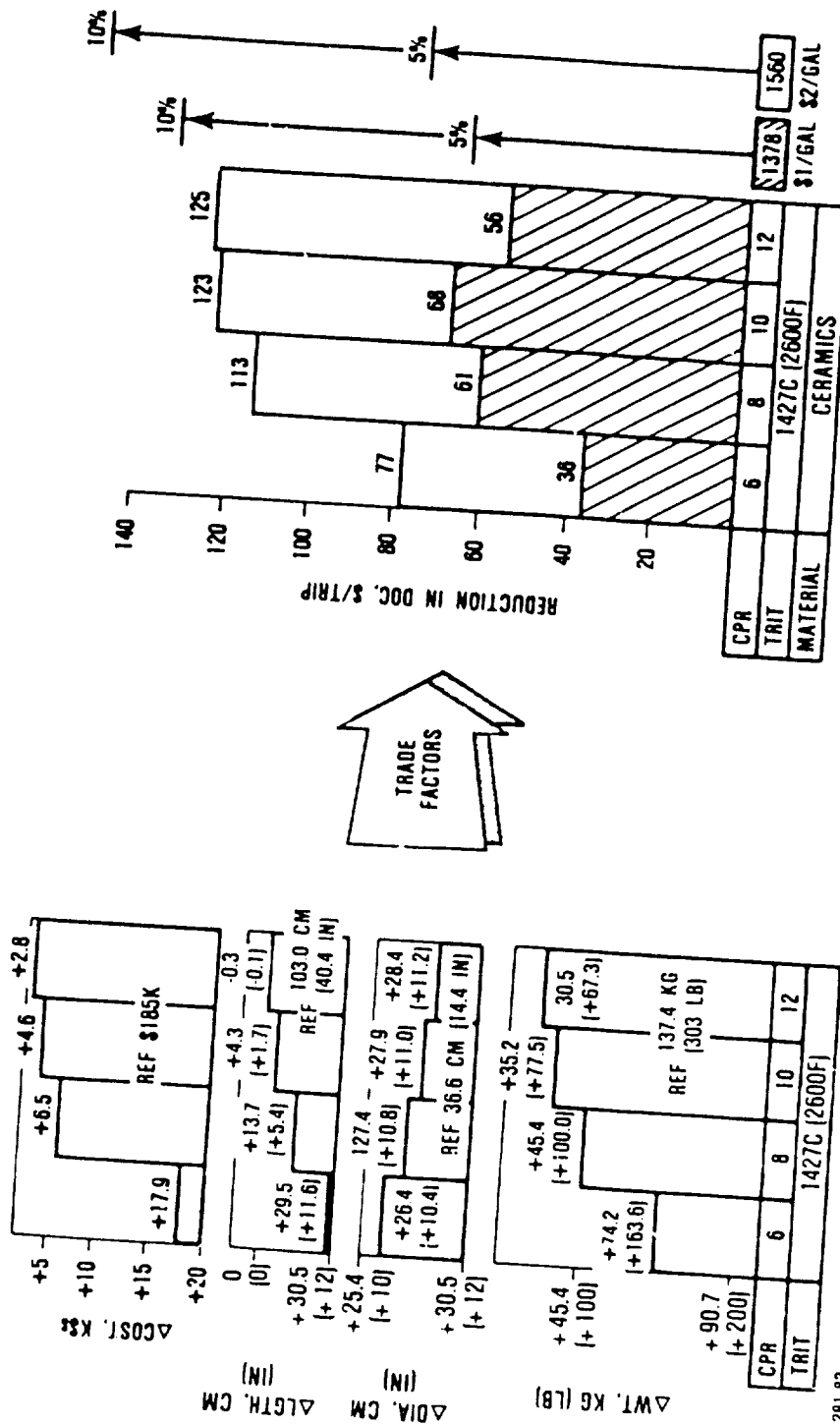


Figure 28. Projected Engine and DOC Improvements for Recuperated Engines.

ceramic as necessary to remain uncooled. HP TRIT was set at 1427C (2600F).

Based on DOC considerations in Figure 28, the heat recovery cycle was selected with an uncooled ceramic turbine at 1427C (2600F) TRIT. The single-stage turbine drives a single-stage centrifugal compressor with a pressure ratio of 10. A multistage variable uncooled power turbine is incorporated for better part-power fuel consumption, which will be ceramic as necessary. The fixed-boundary recuperator has an effectiveness of 0.8 with an 8 percent pressure drop (based on the results of the commuter study, section 3.2.3).



2.3 Task III - System Performance Evaluation

In Task III, the two engines selected from Task II were evaluated in terms of their impact on overall aircraft system performance. A detailed mission analysis was conducted (using the HESCOMP model) for both aircraft/engine systems requiring an extensive matrix of off-design performance. Finally, the selected engines were evaluated in detail with the HESCOMP economic model to determine aircraft direct operating costs (DOC).

Prior to the system performance evaluations, both selected configurations were further refined by the typical GTEC preliminary design process.

2.3.1 Engine/Cycle Refinements

Several minor engine refinements were made to the year-2000 engines selected in Task II. These refinements were made following a more detailed design analysis of each engine component. The identified refinements and the resulting performance effects are summarized in Figure 29. For the simple-cycle, size, weight,

PARAMETERS					COMMENTS
	TASK II	TASK III	TASK II	TASK III	
SFC. (KG/HR)/KW. (LB/HR)/HP	0.232 (0.381)	0.225 (0.369)	0.195 (0.321)	0.194 (0.319)	COST AND WEIGHT RECUPERATOR COST/WEIGHT REASSESSED. 101.2 KG (223 LB)*** SELL PRICE AND RECUPERATOR COSTS REASSESSED
SPECIFIC POWER. KW/(KG/S). (HP/(LB/SEC))	417.9 (254.2)	430.1 (261.6)	384.7 (234.0)	385.7 (234.6)	
WEIGHT. KG (LB)	87.1 (192.0)	88.6 (195.3)	230.5 (430.0)	180.9 (398.8)***	
LENGTH. CM (IN)	58.4 (23.0)	58.9 (23.2)	106.9 (42.1)	96.0 (37.8)	
DIAMETER. CM (IN)	23.4 (9.2)	23.4 (9.2)	68.8 (27.1)	64.5 (25.4)	
COST. K\$	143.0	143.6	177.1	193.0	
COMPRESSOR					TASK III η_s PER GTEC PRELIMINARY DESIGN PROGRAM
$W\sqrt{\theta/\delta}$ INLET KG/S (LB/SEC)	1.80 (3.97)	1.75 (3.86)	1.94 (4.27)	1.95 (4.31)	
$W\sqrt{\theta/\delta}$ EXIT KG/S (LB/SEC)	0.129 (0.284)	0.125 (0.276)	0.270 (0.595)	0.272 (0.600)	
PR	22	22	10	10	
η_{AD}	0.802	0.801	0.818	0.818	
η_{POLY}	0.866	0.865	0.866	0.866	
COMBUSTOR					*SINGLE STAGE **ADDITION OF $\Delta H/\theta$ LIMIT FORCED 2-STAGE LPT IN TASK III
TRIT. C (F)	1427 (2600)	1427 (2600)	1427 (2600)	1427 (2600)	
$\Delta P/P$. PERCENT	4	4	5	5	
HP TURBINE					
$W\sqrt{\theta/\delta}$ KG/S (LB/SEC)	0.204 (0.450)	0.198 (0.437)	0.489 (1.078)	0.493 (1.066)	
$\Delta H/U^2$	1.91	1.89	1.25	1.32	
η	0.870	0.866	0.904	0.893	
N (RPM)	67,487	68,937	63,482	60,994	
LP TURBINE					
$W\sqrt{\theta/\delta}$ KG/S (LB/SEC)	0.760 (1.676)	0.751 (1.656)	1.092 (2.407)	1.300 (2.426)	
$\Delta H/U^2$	2.44	1.37	1.78	1.73	
η	0.861*	0.910**	0.863	0.874	
N (RPM)	43,477	44,977	34,890	34,627	

G5 281 99

Figure 29. Task II to Task III Engine Performance Changes.

and cost remained relatively unchanged. SFC and specific power, however, improved by 3.1 percent and 2.9 percent respectively, primarily due to an increase in LP turbine efficiency. LP turbine efficiency was improved nearly 5 points by the addition of a second stage. This stage addition was necessary because the turbine corrected work ($\Delta H/\theta$) exceeded the limit as projected for the year 2000.

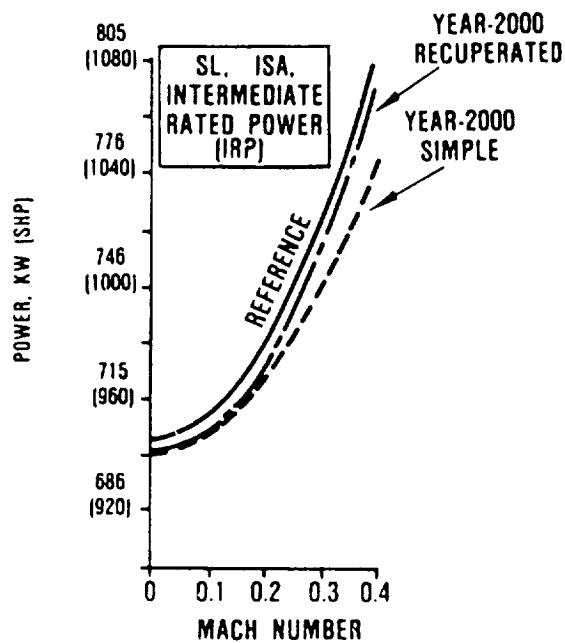
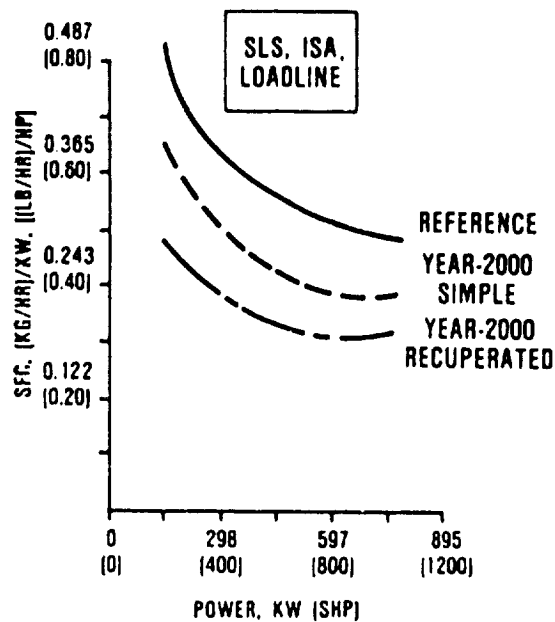
For the recuperated cycle, engine performance changed only slightly, but weight, size, and cost estimates were revised. The changes in size, weight, and cost are primarily due to a reassessment of the recuperator design and cost estimates, resulting in a size and weight reduction of 6 to 10 percent and a cost increase of 9 percent. These refinements were analyzed and found to have no effect on the optimum cycle selection.

2.3.2 Mission/Economic Analysis

The mission and economic analyses for the rotorcraft application were conducted with the reference mission and aircraft using the HESCOMP mission/economic model, all as defined in Task I.

To support the mission analysis, a matrix of off-design performance conditions and power settings were generated. A comparison of sea-level, static load lines (Figure 30) indicates that the recuperated engine has superior part-power SFC to both the advanced simple cycle and the reference engine. A Mach number lapse rate comparison as presented in Figure 30, shows little difference between the three engines.

The resulting mission performance is summarized in Figure 31. As shown, the key change is the reduction in fuel burn, 21.9



65-281-94

Figure 30. Off-Design Performance Comparison for Rotorcraft Engines (Installed Performance).

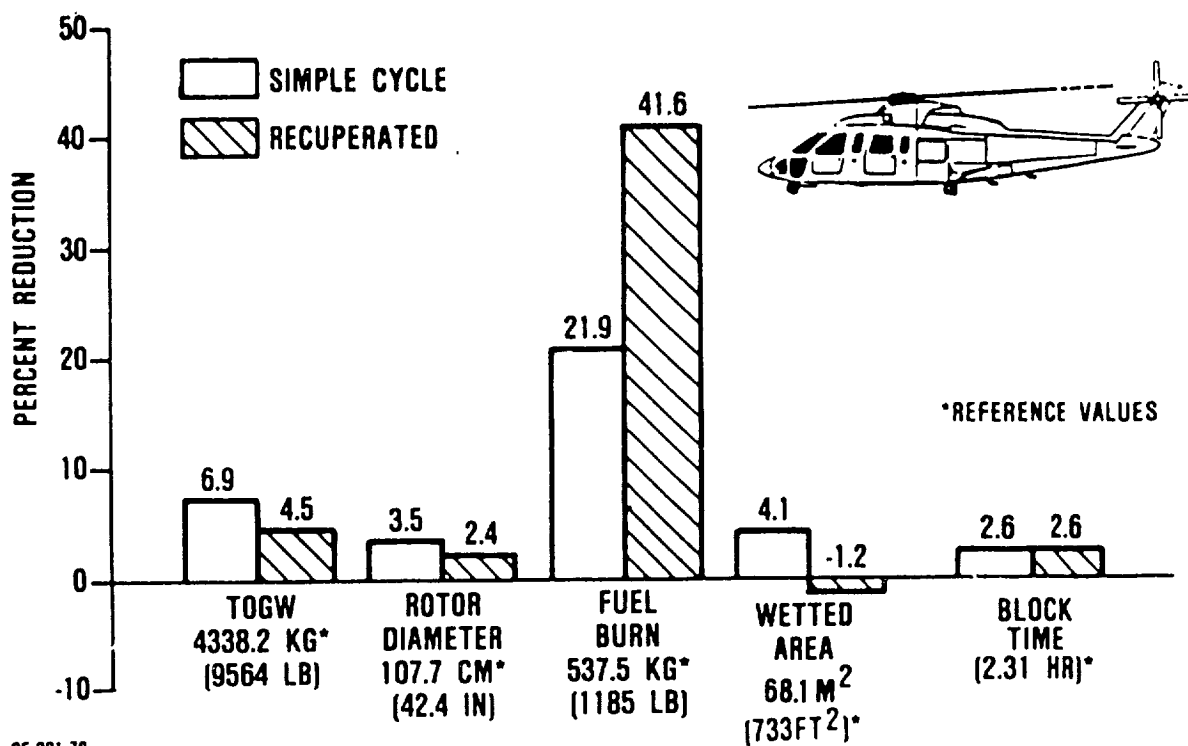


Figure 31. Projected Reductions in Rotorcraft Parameters.

percent for the simple cycle, and 41.6 percent for the recuperated cycle relative to the reference engine. The fuel burn reduction for the simple cycle is approximately the same as the percent reduction in design point SFC (21.2 percent). For the recuperated cycle, however, the fuel burn reduction is greater than the percent SFC reduction at the design point (31.8 percent). This is due to the superior part-power performance of the recuperator engine. Takeoff gross weight has also been reduced by 6.9 and 4.5 percent for the simple and recuperated cycles, respectively compared to the reference engine.

Figure 32 shows the recuperated cycle to be superior in DOC to the simple cycle at both fuel prices. Despite the negative impact of weight, size, and cost incurred with the recuperated engine, the SFC benefit is large enough to offset these aspects.

Relative to the reference engine, as shown in Figure 33, the advanced engines reduce DOC by 7.0 and 7.4 percent, for simple and recuperated cycles respectively, at the low fuel price. At the high fuel price the year-2000 simple cycle can reduce DOC by 8.7 percent. However, the recuperated engine, which has a 41.6 percent reduction in fuel burned, has a DOC reduction of 11.4 percent.

2.4 Task IV - Small Engine Component Technology Plan

Task IV identifies and quantifies high payoff technologies for the rotorcraft engines and presents technology plans that are based on the benefits as projected for the high payoff technologies.

2.4.1 Technology Identification/Benefits

Tasks II and III performance and DOC results are based on a number of technology projections. These technologies have shown

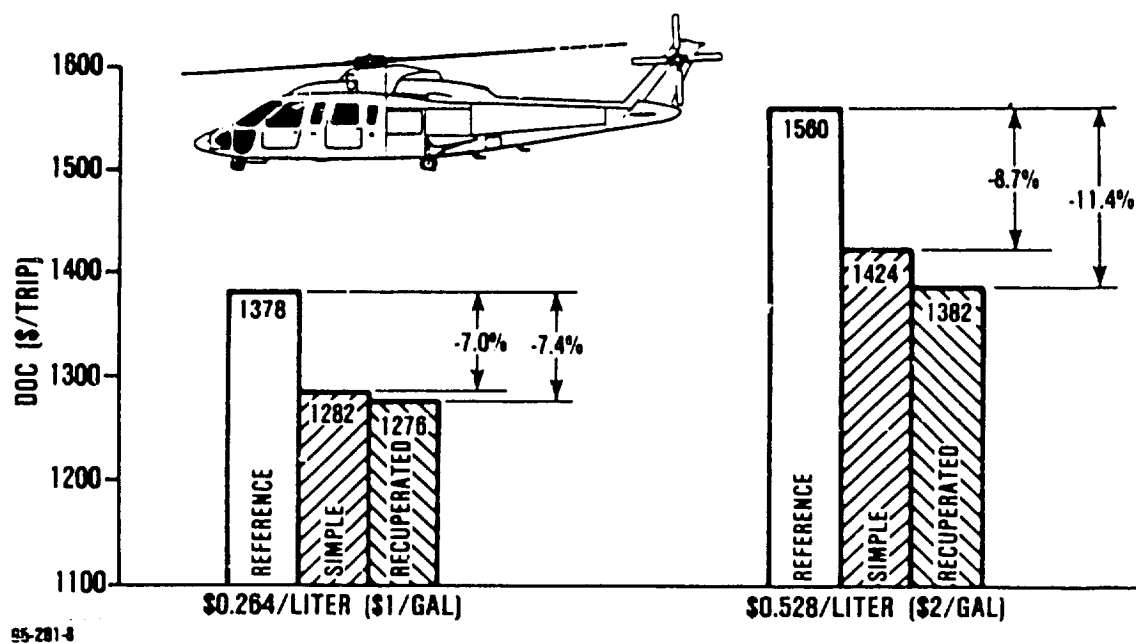
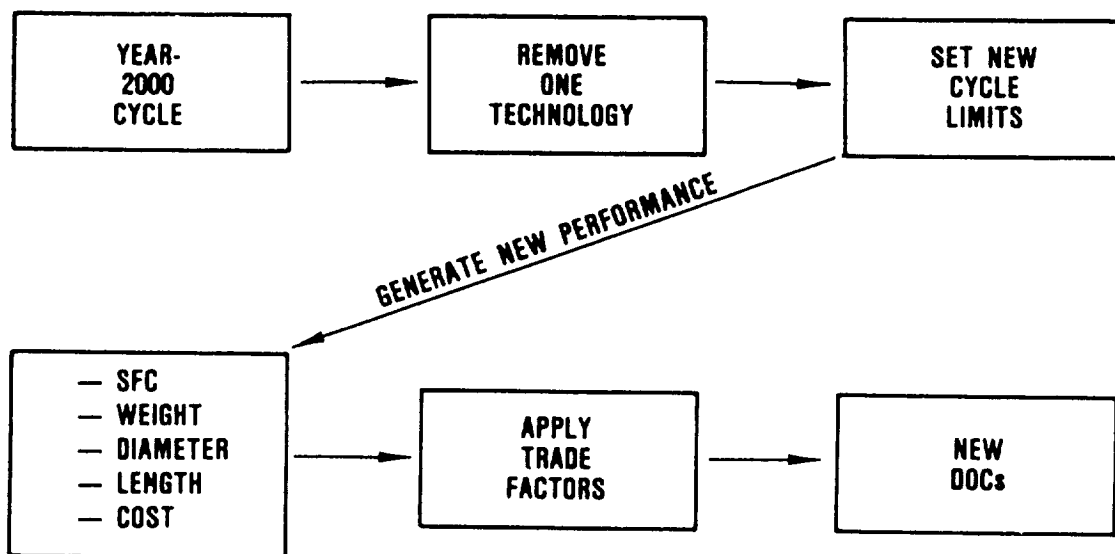


Figure 33. Helicopter DOC Results for Simple Cycle and Recuperated Engines.

benefit in terms of SFC, weight, size, or cost. Several of these technologies, such as metal matrix shafts, are difficult to quantify in terms of DOC, but their use is considered beneficial or necessary to meet engine design goals. The identified technologies are:

- o Component performance (aero)
 - Compressor η
 - Turbine η
 - Combustor $\Delta P/P$
- o Materials
 - Ceramics (for turbines, combustors, recuperators)
 - Ni_3Al disk (turbines)
 - Aluminum powder metal alloy (compressors)
 - Cast titanium (compressors)
- o Combustor
 - Low pattern factor
 - High heat release rate
- o System technologies
 - Metal matrix shafts
 - Noncontact face seals/brush seals
 - High-temperature lubricants

In order to estimate the benefits derived from the technologies listed above, GTEC isolated each technology using the technical approach summarized in Figure 34. This approach involved removing one technology from the year-2000 engines, setting new



06-201-22

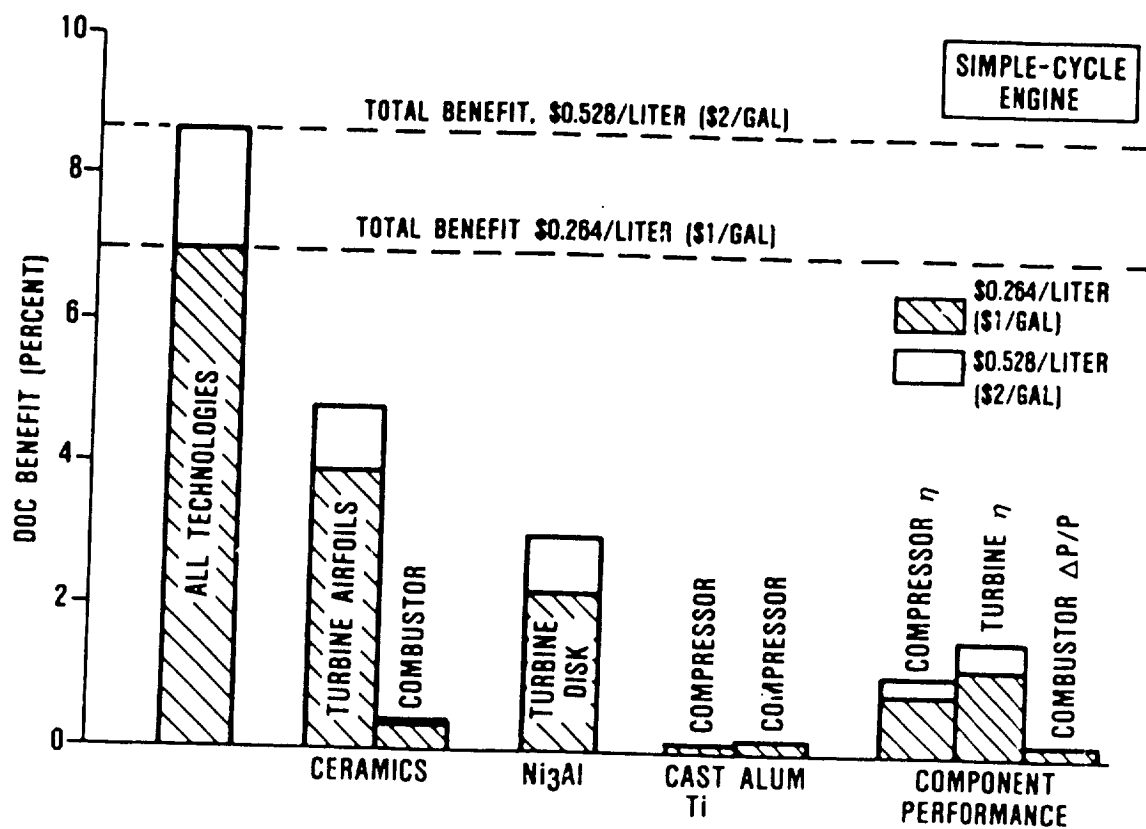
Figure 34. Technical Approach for Estimating Technology Benefits.

cycle limits as necessary, and generating new engine SFC, weight, diameter, length, and cost data. Finally, trade factors were applied to the new engine parameters, which resulted in new DOCs. Comparing the resultant DOC value to the DOC for the baseline year-2000 engine with all technologies shows the improvement derived from that technology. The selected technologies are not independent from one another and are therefore not additive.

Of the technologies quantitatively investigated, hot-end materials were found to have the greatest DOC impact, as shown in Figure 35. For example, ceramics for application in turbine airfoils contribute approximately half of the overall DOC improvement projected for the simple cycle engine. Ni₃Al for turbine disks was found to have the second greatest DOC benefit, following ceramics. Removal of Ni₃Al turbine disks and reducing hub speeds to values consistent with today's disk materials resulted in reduced efficiencies and increased turbine stage count for the simple cycle.

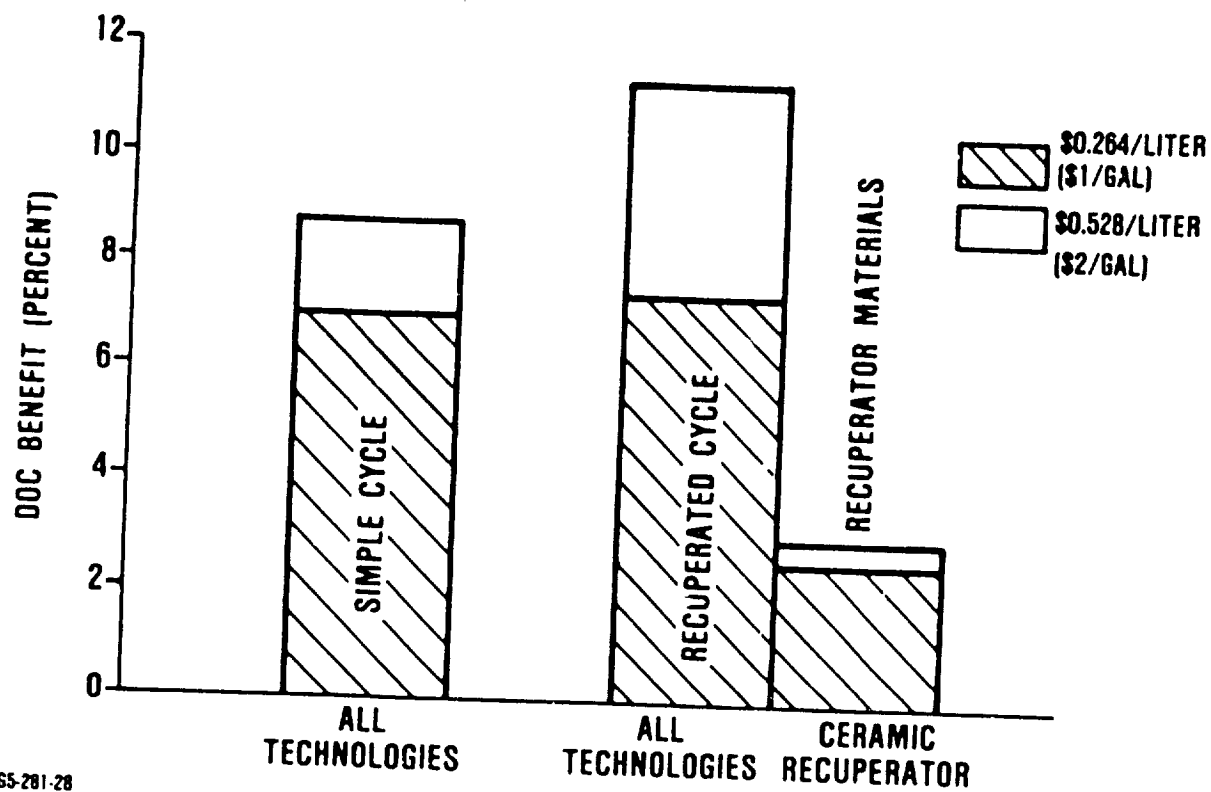
Compressor and turbine efficiency improvements also show significant DOC benefits. Combustor pressure drop reduction technology and improved compressor materials, however, resulted in only small improvements in DOC.

In addition to the technologies examined for the simple cycle, the impact of ceramic recuperator technology was quantified for the recuperated engine. As shown in Figure 36, the recuperated cycle has a DOC advantage over the simple cycle. Ceramics, both in the engine hot section and in the recuperator itself, are vital for the recuperated cycle. The use of a ceramic recuperator results in nearly a 3 percent decrease in DOC.



65-281-21

Figure 35. Projected DOC Benefits (Percent) for Isolated Technologies.



65-281-28

Figure 36. Comparison of Projected DOC Benefits (Percent) for Recuperated Versus Simple-Cycle Engines.

2.4.2 Technology Plan

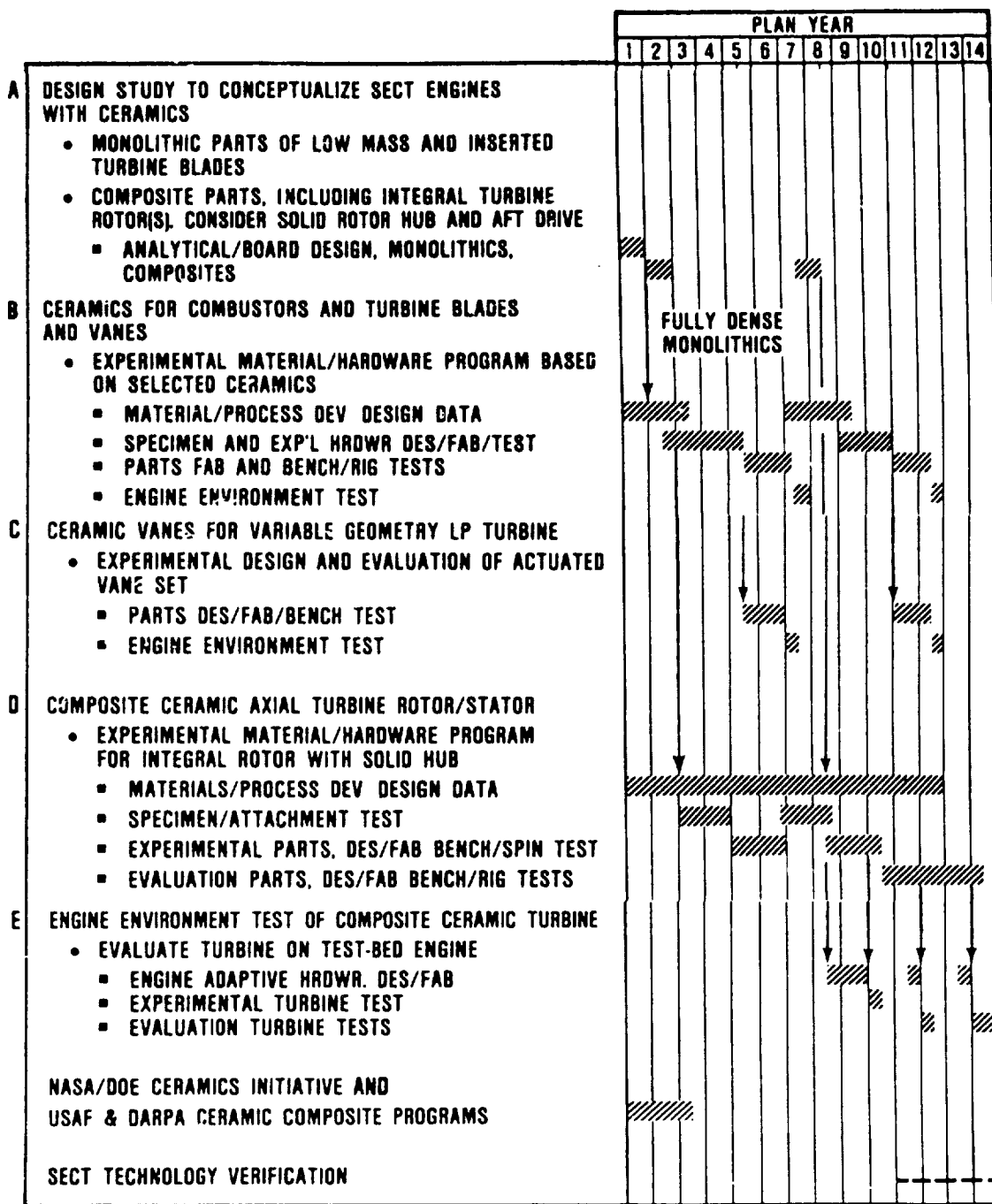
GTEC's recommended plan for Small Engine Component Technologies for year-2000 rotorcraft engines is presented in this section. This plan addresses a broad spectrum of technologies in keeping with the technology benefits as presented in paragraph 2.4.1. The plan is presented in sections for the following technologies:

- 2.4.2.1 Ceramics
- 2.4.2.2 Recuperators
- 2.4.2.3 Metallics for turbines
- 2.4.2.4 Turbine performance
- 2.4.2.5 Combustor performance
- 2.4.2.6 Compressor (centrifugal) performance
- 2.4.2.7 Materials for "cold" parts
- 2.4.2.8 System technologies

These plans address the high payoff technologies needed to obtain "technology readiness" by the year 2000. Some technologies may require verification and engine demonstration testing prior to commitment to an engine full-scale development. This activity is not included in the technology plans; it may be conducted during the latter program years (11 through 14).

2.4.2.1 Ceramics

Ceramics merit an all-out effort that should include engine conceptual design studies to assess the full potential of ceramics and materials technology/evaluation programs for monolithics and composites. Figure 37 presents the schedule for this plan, which is comprised of five discrete technology programs (identified as A through E). Program interdependencies are shown on the



06-281-51

schedule. The technology programs and interdependencies are discussed in the following paragraphs.

A. Design Study to Conceptualize SECT Engines with Ceramics

The current application of ceramics to hot engine parts is limited primarily to experimental parts of low mass such as vane segments, rotor blades, and thin-wall structures. A notable extension of this experimental technology can be found in the AGT101 automotive power plant as pioneered by the GTEC/Ford team for DOE/NASA. The AGT101 design, which is fully committed to ceramics (Figure 38), incorporates a small radial turbine wheel that is integrally cast of silicon nitride ceramic material.

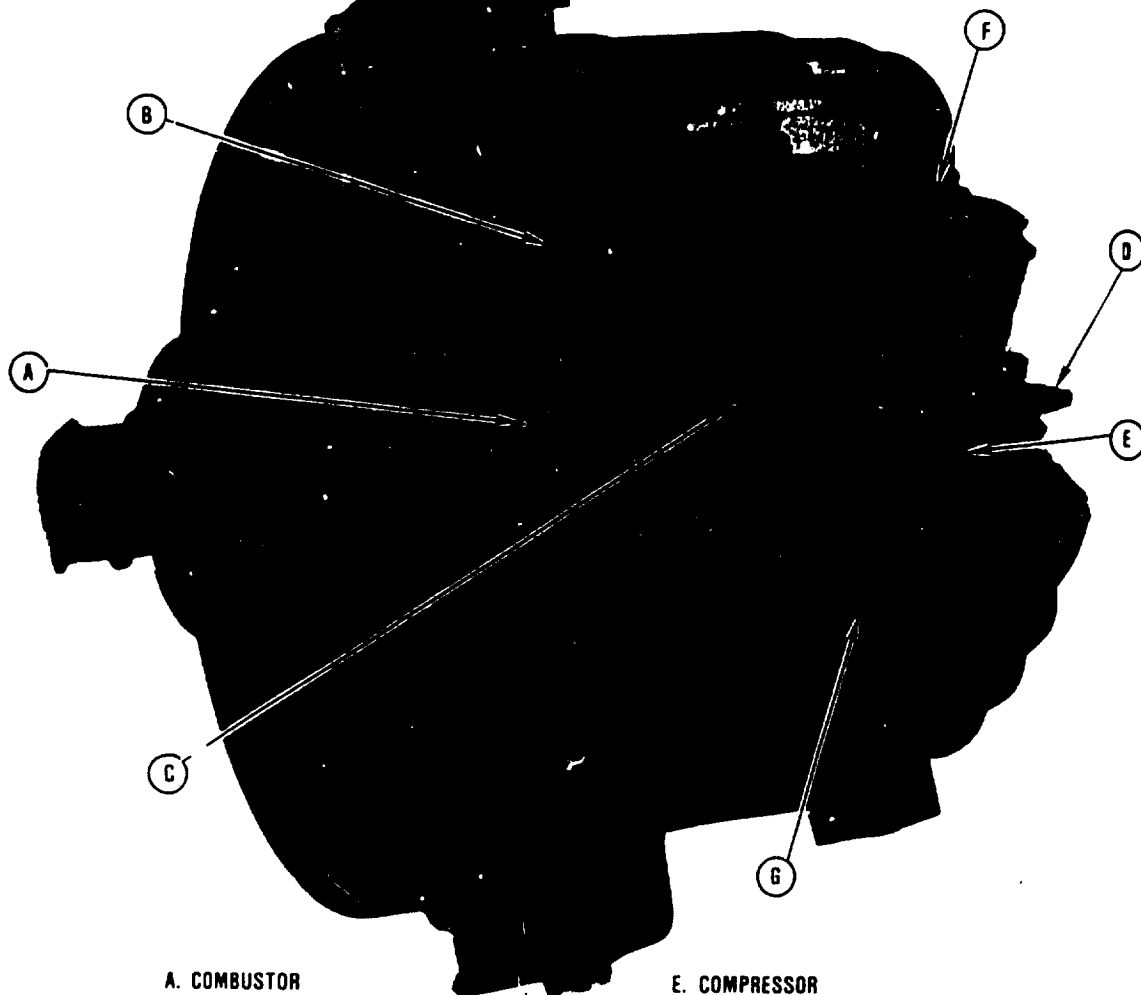
This program will explore the design opportunities of ceramics as conceptualized for year-2000 rotorcraft engines. The initial design effort will be based on the application of ceramics as limited to parts of low mass, and will be based on projected properties of fully dense monolithic ceramics.

A second design study will conceptualize a year-2000 rotorcraft engine fully committed to ceramics (monolithics and composites), including integrally cast axial turbine rotor(s). The study will include consideration of solid-hub rotor(s) based on projected properties of composite ceramics. It will use an aft-power drive arrangement to accommodate the solid turbine rotor(s). An update of this design is also proposed to establish rotor design and sizing for second-generation composite ceramic test parts (Reference Program D).

Program Description

This program consists of three conceptual design studies, as shown in Figure 37, Technical Program A, and described below.

ORIGINAL PAGE IS
OF POOR QUALITY



A. COMBUSTOR

- PREMIX/PREVAPORIZING
- CERAMIC MATERIAL

B. REGENERATOR

- CERAMIC MATERIAL
- ROTARY — EXTRUDED MATRIX
- DEVELOPED SEALS AND BEARINGS

C. TURBINE

- SINGLE STAGE, HIGH WORK RADIAL
- CERAMIC MATERIAL
- 1371C (2500F) MAXIMUM TURBINE INLET TEMPERATURE

D. BALL BEARING

- RADIAL AND THRUST LOADS

E. COMPRESSOR

- SINGLE STAGE CENTRIFUGAL
- 5:1 PRESSURE RATIO
- POWDER METAL ALUMINUM
- VARIABLE INLET GUIDE VANES

F. FOIL GAS BEARING

G. CERAMIC STRUCTURE

- TRANSITION LINERS, TURBINE SHROUD, TURBINE STATOR
- MATERIALS INCLUDE RBSN, SINTERED SIC, RSSIC

GS-281-35

Figure 38. AGT101 Power Plant.

Monolithics - Analytical design will include an assessment of fully-dense monolithic ceramic materials, manufacturing processes, and joining methods. Properties and geometry/mass limitations for design will be projected for a year-2000 rotorcraft engine. Preliminary sizing of components will be made and the SECT engine cycle (simple) will be reviewed and revised as necessary to track with the conceptual engine design.

Conceptual board design will be conducted to configure the engine based on technologies as projected for year 2000. Trade studies will be conducted as relevant to design options. A conceptual engine design will be depicted in cross section. Ceramic-to-metallic interface features will be conceptualized and depicted in supporting section views.

Composites - Analytical and conceptual engine designs will be conducted in the same manner as for monolithics except that ceramic properties and geometry/mass limitations will be based on projections for ceramic composites. Integral ceramic turbine rotors will be assumed for the HP turbine and for the first stage of the LP turbine. Components will be sized in accordance with projected properties. Solid-hub rotor(s) will be considered along with an aft-drive engine arrangement.

Analytical and conceptual engine design will be reviewed and updated in program years seven and eight, and will be based on updated ceramic material properties. Integral rotors will be reconfigured and resized (to define test parts for Program D).

Technical Approach

The simple-cycle rotorcraft engine, evaluated in Task III, will form the basis for this study program. The salient features of this engine are:

- o 746 kW (1000 shp), front drive
- o Two-stage centrifugal compressor
- o Reverse-flow annular combustor incorporating ceramic combustor and ceramic transition liners
- o One-stage HP turbine (TRIT = 1427C [2600F]) incorporating uncooled ceramic stator vanes and rotor blades (inserted)
- o Two-stage LP turbine incorporating uncooled ceramic stator vanes and rotor blades (inserted) for Stage 1, and advanced metallic uncooled stator vanes and rotor (integral, shrouded) for Stage 2

This engine will be conceptualized to more fully exploit ceramics in the hot section.

The feasibility of integral ceramic turbine rotors will be studied and will include engine arrangements that facilitate a solid rotor disk(s) with no hub bore(s). The arrangements will include cases for aft drive to accommodate the following:

- o Single-stage HP turbine featuring a solid ceramic rotor (no hub bore) with forward power transmission for compressor drive
- o Stage 1 LP turbine featuring a solid ceramic rotor (no hub bore) with aft power transmission for output power
- o Stage 2 LP turbine featuring a solid ceramic rotor or small-bore metallic rotor, as feasible

The feasibility of integral ceramic turbine rotors will be greatly enhanced by achieving a simple hub configuration with no hub bore. This will facilitate the lower hub stresses and stress concentrations necessary for the brittle ceramic materials.

Integral ceramic turbine rotors show the potential for greatly reduced material and machining costs and possible engine weight savings.

B. Ceramics for Combustors and Turbine Blades/Vanes

The development of ceramics for combustors and axial-flow turbine vanes, and blades, will result in uncooled components suitable for use at turbine rotor inlet temperatures up to 1427C (2600F). Ceramics are lighter in weight than comparable metal components, and they offer the potential for significantly lower cost when compared with cooled metal components. The feasibility of an axial rotor with ceramic blades inserted in a metal disk has been demonstrated for short-life engine applications under DARPA and Air Force funding. Ceramic combustor and turbine components are also being evaluated under the DOE/NASA AGT programs. These programs are investigating silicon nitride and silicon carbide monolithic ceramics.

Material selection for this program will depend on the state of demonstrated technology at program start. Fully dense silicon nitride and silicon carbide materials with improved high-temperature properties and high reliability are being developed under the DOE/NASA improved Si_3N_4 and SiC programs. It is anticipated that these improved fully dense materials will be available from vendors for experimental combustors and turbine blades and vanes for the early years of this program. Fabrication approaches will include net-shape techniques such as injection molding and slip casting. Moreover, ceramic composites are emerging materials

that offer the potential for higher toughness and consequent non-catastrophic failure modes. Progress of these composites resulting from separately funded activities or from Programs D and E should be assessed and incorporated if/as feasible for the later years of this program.

Ceramic technologies from this program will benefit both rotorcraft and commuter aircraft applications and APUs.

Program Description

This program is scheduled as four major activities, from material/process efforts through engine environment tests. Fully-dense monolithics are planned for the initial effort, which is scheduled for seven years. A second iteration is shown, for planning purposes, to establish technology readiness for the most suitable ceramic material (monolithics or composites) available in the 1992 time frame. Execution of the second iteration would depend on program results through the first iteration, on the outlook for higher-payoff integrally cast ceramic rotors (i.e., Technology Programs D and E).

A pilot combustor and turbine stage will be designed to be representative of the SECT rotorcraft engine and to be compatible with an existing GTEC test-bed engine. The pilot turbine stage would be designed to replace the first stage of the HP turbine.

Material vendors will be surveyed and the best available high-strength, high-temperature ceramic materials will be procured and tested to obtain the required design data. Ceramic vendors and fabrication processes (net or near net-shape) will be chosen for each ceramic component. Fabrication evaluations will be conducted to verify the fabricator's capability to produce high-quality components by the selected fabrication methods. Specimens and experimental hardware will be tested.

A separate study will be conducted to establish a compliant layer for the blade dovetail attachment to achieve long life and a high-temperature capability.

Ceramic component test parts will be procured. They will be evaluated dimensionally, and by appropriate NDE test methods, prior to rig testing. An iterative process, alternating between rig testing and design modifications, will be used to determine the final engine component design to be fabricated and verified during engine environment testing.

C. Ceramic Vanes for Variable-Geometry LP Turbine

The objective of this program is to test a set of ceramic variable-geometry LP turbine vanes as may be appropriate for a year-2000 recuperated rotorcraft engine. The vanes will be incorporated into the LP turbine section of an existing GTEC engine and operated at engine conditions.

This is an evaluation test program that will build on successful results of the Ceramic Materials Program as discussed for Program B.

Program Description

This program is scheduled to follow the materials and experimental testing of Program B. A second iteration is scheduled, for planning purposes, to achieve technology readiness for the latest materials as discussed for Program B.

Design - An existing GTEC engine will be selected as a test vehicle for variable-geometry LP turbine vanes. Analytical and board design will be conducted to configure a set of replacement

ceramic vanes. The vane design will be based on the test engine requirements, and on prevailing design and fabrication processes for monolithic or composite ceramics. Based on the detailed design, performance predictions will be made for comparison with test results.

Fabrication - A set of ceramic variable-geometry turbine vanes (and spare parts) will be fabricated/procured.

Test - A set of the ceramic vanes will be assembled, along with engine parts, into a test unit. This unit will be bench tested to verify proper function and to assess gas path leakages.

The unit will then be assembled into a test-bed engine and operated through its full range of operating temperatures, and with full gas path loads. Engine and turbine performance data will be obtained and compared with predicted values.

Technical Approach

The selection of an existing GTEC test-bed engine will be made to facilitate LP turbine operating conditions and test data that are representative of recuperated rotorcraft engines as configured by the SECT study program for year 2000. Analytical design, including engine cycle evaluation, will be conducted to configure a set of ceramic variable-geometry stator vanes for the LP turbine section. This design activity will be based on materials and manufacturing inputs for low-cost fabrication methods as envisioned for ceramics in the year 2000.

Testing of the vane set will include evaluation of leakage, performance, wear, and dynamic characteristics.

D. Composite Ceramic Axial Turbine Rotor/Stator

Ceramic materials have the potential for uncooled component use at high turbine inlet temperatures. Ceramics are lighter than comparable metal components and offer the potential for lower cost. The feasibility of a metal axial rotor with inserted ceramic blades has been demonstrated for short-life applications. However, the full benefit of ceramics is better realized in an integral axial rotor. This eliminates the costly ceramic and metal machining required for the blade dovetail attachment, and eliminates blade stagger angle constraints on the aerodynamic design of the airfoil.

Since the stresses around a bore hole at the center of the rotor are expected to exceed the material capability, the proposed rotor would use a solid disk with a stub shaft or other attachment concept not requiring a bore hole. In the long term, ceramic composites are the prime material candidates for improved toughness of the rotor and reduced potential of catastrophic failure.

The feasibility of ceramic radial rotors having a large hub mass is discussed for APUs in paragraph 5.4.2.1 as a parallel or follow-on technology program.

Program Description

This program is scheduled as four major activities, from materials/process development through bench tests. One generation of test parts is planned through bench/spin tests during the first six program years. Configuration of these parts will be established based on the engine conceptual design studies conducted in Program A. Second-, third-, and fourth-generation parts are envisioned for engine environment testing (Program E) in program years 10, 12, and 14, respectively.

Composite material systems will be surveyed and evaluated for properties and suitability of processes. Design data will be obtained for selected material systems. Specimen tests will be conducted along with attachment tests.

The design of a pilot turbine rotor with a solid hub (no bore hole) and a matching stator will be conducted, based on results from Program A. They will be configured to be representative, in size and shape, of the SECT rotorcraft engine (as conceptualized for the year 2000), and will be designed for compatibility with an existing GTEC test-bed engine. The aerodynamic and mechanical design of the pilot turbine parts will be based on attachment concepts, material systems, and fabrication approaches as selected during this task.

Fabrication and attachment development will be conducted for the pilot design/hardware. Rotor/shaft attachment schemes will be evaluated, and pilot parts will be bench- and spin-tested to demonstrate attachment concepts and other critical design features. The stators will undergo thermal shock tests.

Based on the results of the pilot design/test evaluation, a design update will be accomplished incorporating the latest aerodynamic technologies. The design will be completed and ceramic parts will be fabricated for bench/spin tests and for follow-on engine environment tests (Program E). Parts (metallic) will also be fabricated for cold aerodynamic rig tests, which will be conducted to fully map the turbine stage.

Based on the experimental results of this hardware, follow-on design/fabrication test cycles are projected for planning purposes to achieve technology readiness.

E. Engine Environment Test of Composite Ceramic Turbine

The objective of this program is to conduct engine test evaluations of an integral-ceramic, axial-turbine rotor and stator. This evaluation program assumes the successful progress of the composite ceramic materials/fabrication program for these parts, as described for Program D. Three generations of test parts are planned in order to achieve technology readiness.

Program Description

Major activities of this program include the design and fabrication of test-bed engine parts, and engine environment testing of one set of experimental parts and two sets of evaluation parts, as shown in Figure 37 and as discussed herein.

Analytical and board design will be conducted to modify the selected test-bed engine (such as the Garrett F109) to accommodate the ceramic test hardware, as provided by Program D. The gas generator section of the selected two-spool engine will be used for this testing. This will accommodate a solid-hub rotor (no bore) with a forward drive for the compressor section. Engine refurbishment and special adaptive hardware will be fabricated.

Engine gas-generator testing of the experimental ceramic turbine will be conducted (program year 10) to the design temperature for the ceramic parts. Performance and mechanical data will be obtained and compared with design predictions. A technical report will be published.

Two follow-on tests are planned for years 12 and 14, based on successful progress for the composite ceramics Program D.

Technical Approach

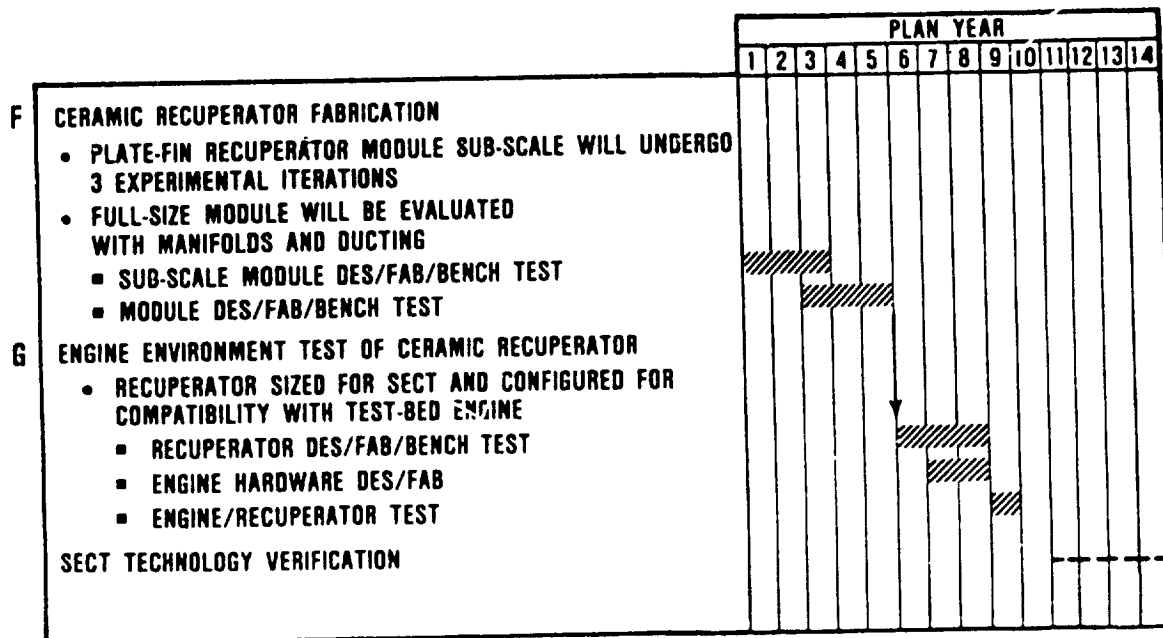
Specifications for a turbine stage will be established that are representative of the SECT rotorcraft and commuter engine requirements as envisioned for the year 2000. The specification will also be compatible with the selection of a suitable engine test bed for verification tests.

Analytical design of the integral-ceramic, axial-turbine rotor will draw from the latest technologies available for aerodynamic and mechanical design, materials properties, and fabrication/manufacturing processes. The aerodynamic design will take full advantage of high-blade stagger analyses as achievable with integral blade-disk rotors. The mechanical design will accept risks commensurate with engine benefits and will be based on the available material properties as established for the pilot and subsequent rotors.

2.4.2.2 Recuperator

This plan includes a comprehensive program to establish the fabrication technologies necessary for a ceramic platefin recuperator. The technologies would be applicable to a recuperated engine as envisioned for the year-2000 SECT rotorcraft. This plan provides for an experimental recuperator program and an engine environment test program. Figure 39 presents the schedule for this plan, which is comprised of two discrete technology programs (identified as F and G).

This plan does not include a technology initiative for regenerators. It is envisioned that this technology will be addressed separately by continuation of existing programs such as the NASA/DOE-sponsored AGT101 vehicular engine program.



65-281-63

Figure 39. Recuperator Technology Schedule.

F. Ceramic Recuperator Fabrication Development

Present metallic, fixed-boundary recuperator technology has limited application for future airborne propulsion systems due to excessive weight and insufficient temperature capability. The introduction of ceramic technology to recuperators reduces weight and increases the temperature operating range.

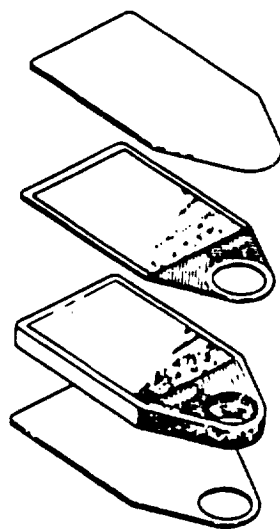
The SECT ceramic recuperator program objective is to evolve the appropriate fabrication technology to produce a finned-plate recuperator suitable for application to a specific small engine design. The specific goals of the study are:

- (a) Verify the fabrication technology necessary to produce full-size plate-fin recuperator modules and associated ceramic manifolds, ducting, and ceramic/metallic interfaces
- (b) Fabricate a full-size recuperator module
- (c) Test the full-size module under simulated engine conditions

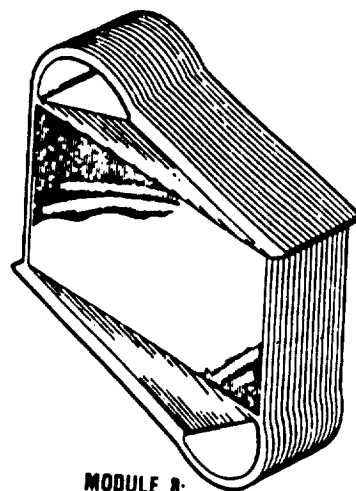
Program Description

This program, which is scheduled for 60 months, includes experimentation with both a subscale and a full-scale recuperator module. The program is based on feasibility work already completed on a core module. Figure 40 depicts these three modules of increasing complexity, while Figure 41 presents a detailed schedule for this technology program.

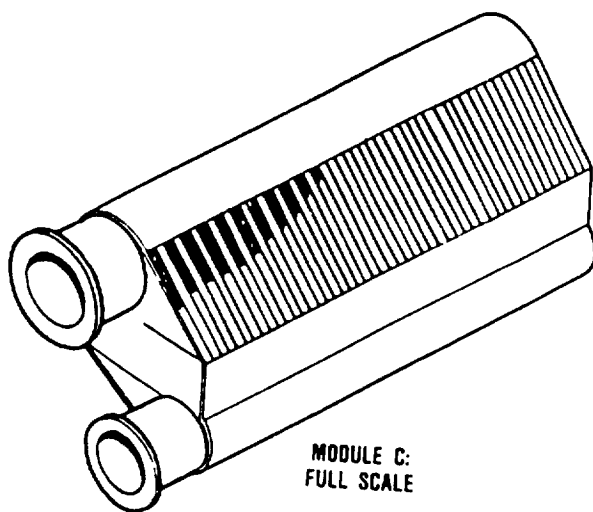
Task 1, Module B Design and Fabrication - The fabrication technology will be demonstrated by constructing a partial-stack-



MODULE A
(CORE MODULE)



MODULE B:
RECUPERATOR MODULE
(SUBSCALE)

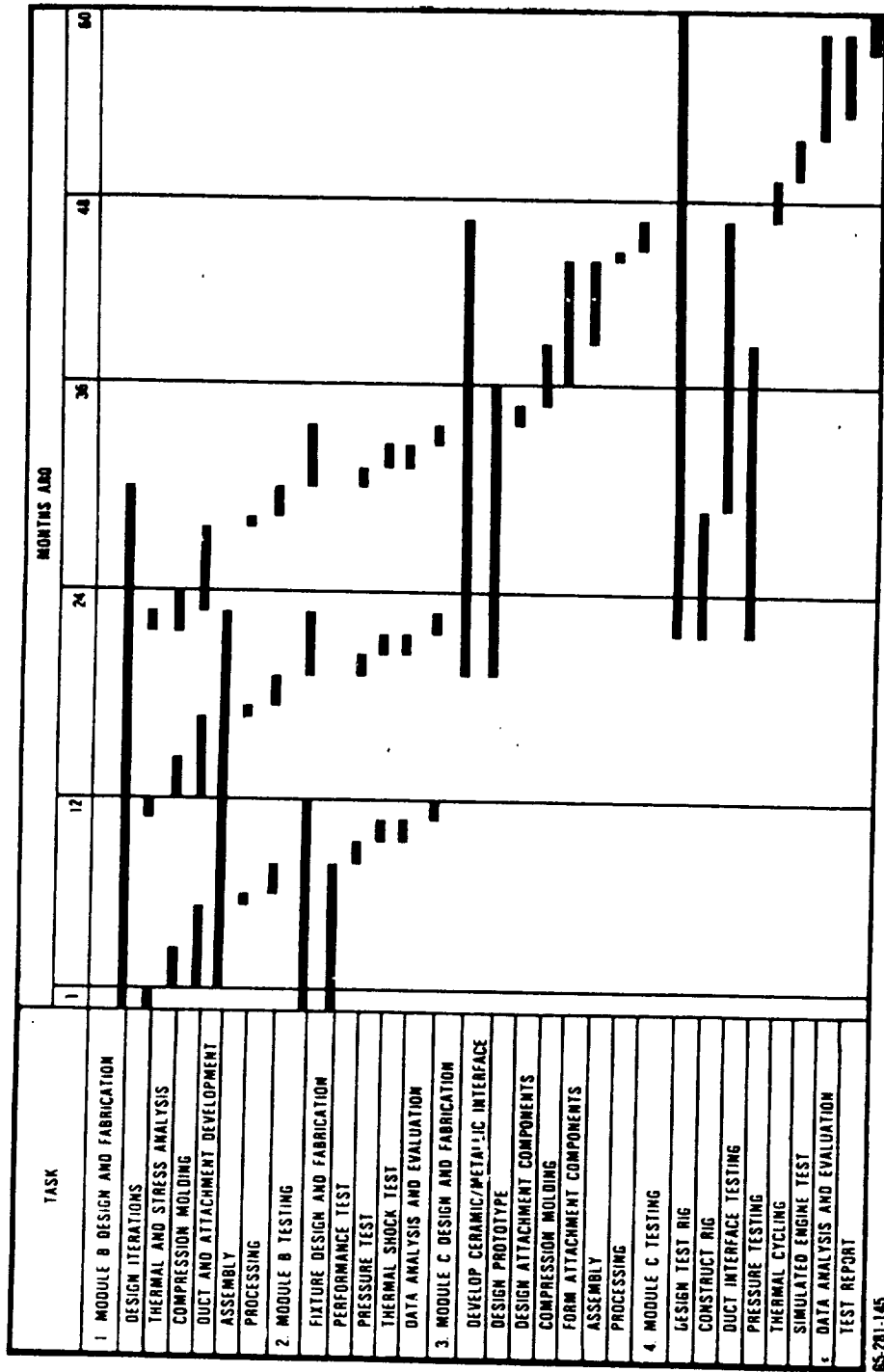


MODULE C:
FULL SCALE

65-281-10

Figure 40. Test Modules of Increasing Complexity.

ORIGINAL PAGE IS
OF POOR QUALITY



CS-281-145

Figure 41. Ceramic Recuperator Program Schedule.

height recuperator (Module B). The major effort of this task is to fabricate a working subscale recuperator module.

- o Design Iterations - The initial reference design established at the outset of the program will be based upon the results of the initial fabricate and test cycle for Module A. Three design iterations are expected to achieve program goals.
- o Thermal and Stress Analysis - This task will concentrate on structural analysis to keep the stresses in the ceramic components within the engineering material strength for the various environmental loadings to which the recuperator will be subjected. Because the engine may undergo significant transient operation, investigation of transient thermal stresses in the recuperator may be vital to ensure the structural integrity of the ceramic recuperator.

The recuperator operating conditions require that close attention be given to design for pressure containment. Manifolds, port connections, and manifold end closures will be analyzed. The analysis will include consideration of the loads and stresses in the core. Particular attention will be given to the bonding and sealing of ceramic ducts to the core. An objective of the design is to minimize stress concentrations in critical areas. A major portion of this task will be to determine the containment requirements/problems.

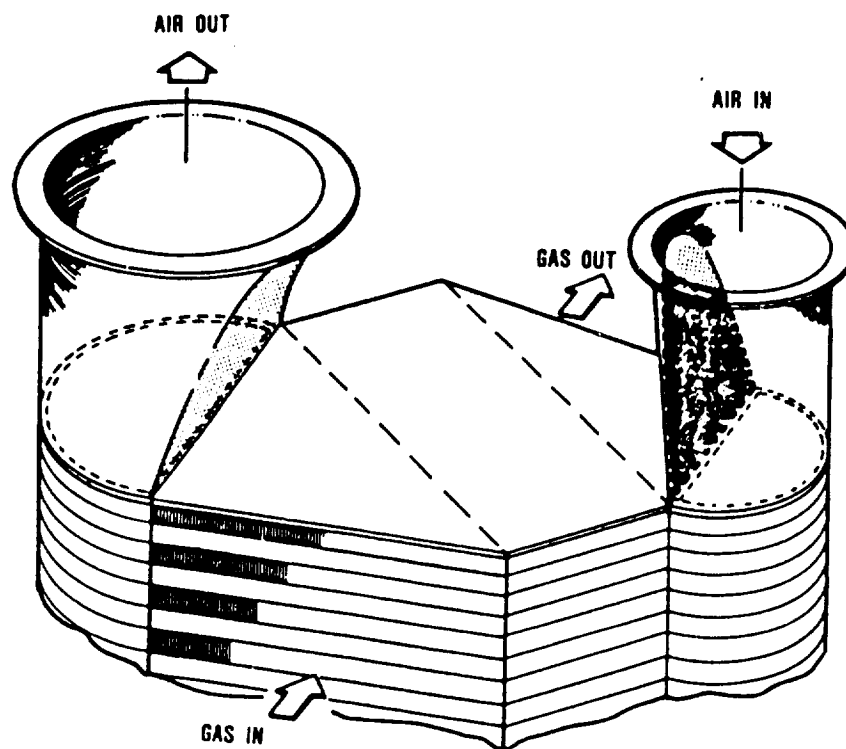
- o Compression Molding - The purpose of the compression molding task is to fabricate the finned plates required for the construction of the Module B cores. Forming ceramic finned-plate heat exchangers is an iterative process involving increasingly complex shapes. The

expertise gained in molding the Module A and sample recuperator plates during previous programs will be used to form the Module B recuperator.

Tooling for Module B will be procured as early as possible in the program in order to initiate compression molding studies. The fabrication effort has been structured to allow three iterations, with approximately four modules produced in each iteration. Forming parameters will be varied as necessary to produce acceptable individual finned plates. These plates will be used to assemble modules for use in performance, pressure, and thermal shock tests.

- o Duct and Attachment Development - Ceramic ducts provide the transition between the ceramic core and the metal engine ducts. Preliminary duct concepts are shown in Figure 42. These shapes are rather complicated and will probably require a strong development effort. Several sets of ducts will be fabricated and used for Module B testing. It is anticipated that the ducts will be fabricated from the same material as the recuperator core.

Because a significant effort will be required to develop a suitable method for forming the ducts, particularly if an unusual geometry is required, this task has been scheduled over a 22-month period. The forming method used to make the ducts (e.g., either slip casting or injection modeling) will dictate the type of bond used in attaching the duct to the recuperator core. This high-temperature, high-pressure seal is a key development area for ceramic recuperators.



GS-281-14

Figure 42. Conceptual Ceramic Duct Design for Recuperator Core.

- o Assembly - After all recuperator components are fabricated, they must be assembled to form modules for use in testing. Fixtures are needed to align and hold the various components during bonding. Good alignment is important so that dimensional tolerances are maintained. Techniques from the previous subtask that effect duct-to-core bonding will be used in assembling the modules.
- o Processing - The assembled modules must be run through binder extraction and nitriding cycles to convert the green module to a ceramic recuperator. Further processing cycle effort may be necessary to provide an acceptable strength recuperator for high-temperature, high-pressure service. For example, if the binder is extracted too rapidly, bloating may occur, seriously degrading the material strength.

Task 2, Module B Testing - The Module B testing program is designed to perform independent pressure, thermal shock, and performance tests on the partial-stack-height recuperators.

The modules fabricated in Task 1 will be subjected to the described tests to verify the recuperator's capability to function at the design pressure and temperature, as well as verify the heat transfer and pressure drop predictions. Thermal shock resistance also will be tested.

- o Fixture Design and Fabrication - A test fixture will be designed to pressurize Module B at ambient temperatures. Pressure differentials will be evaluated across the air- and gas-side layers, up to 1.25 times the design pressure differential. The test fixture will be

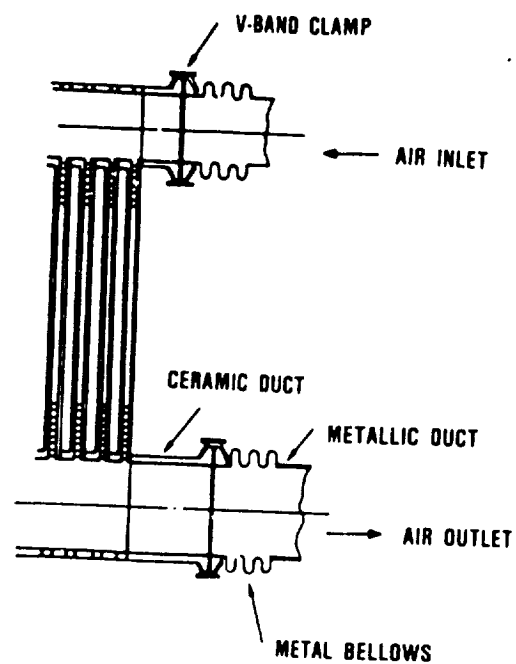
specifically designed and fabricated so that it can be used to subject Module B to low-temperature (less than 427C [800F]) performance tests.

- o Performance Test - The specifically designed pressure/flow test rig will be used to measure the module's heat transfer rates and pressure drops. These performance tests, conducted below 427C (800F), will be used to make accurate predictions for heat exchanger performance at high temperatures. This is a standard procedure for evaluating high-temperature heat exchangers.
- o Pressure Test - The pressure test is a nonflow test to check the pressure containment capability of the recuperator module. Pressurization to 1.25 times the design pressure differential is expected. If a module fails the test, fracture analysis will be conducted to identify the cause of failure (e.g., inadequate bonding, inadequate dimensional tolerances, or fabrication flaws). Efforts will then concentrate on the identified problem area to develop a solution.
- o Thermal Shock - When in service, the recuperator will be exposed to both a wide range of temperatures (ambient to 1260C [2300F]) and rapid temperature changes. To determine suitability for use under design conditions, modules will be placed in a furnace at 1260C (2300F). In addition, the thermal shock resistance will be tested by exposing the module to increasingly severe heating and cooling rates. To evaluate any possible thermal damage, modules will be pressure-tested after each thermal cycle.

- o Data Analysis and Evaluation - The data collected from the performance, pressure, and thermal shock tests will be evaluated and used to modify the Module C design, if necessary (i.e., if Module B fails many of the tests or the experimentally determined performance falls short of the predicted values).

Task 3, Module C Design and Fabrication - A full-size working recuperator module will be fabricated.

- o Ceramic/Metallic Interface - One of the key areas in the recuperator program is a method of attaching the unit to the engine. An 18-month time frame has been allotted for this effort. An adequate ceramic-to-metal joint is required for the high-temperature, high-pressure conditions. In addition to a mechanical seal, such as that shown in Figure 43, a permanent joint may be feasible. One such joint has been demonstrated by sputter-coating silicon nitride with titanium and brazing it to a compatible metal component. Several alternative solutions will be sought while researching this problem.
- o Design - Module C will replicate the plan form of Module B unless test results indicate the need for a design modification. The high-stress regions are expected to be localized at the air outlet manifold/gas inlet face region, based on previous analyses. To reduce the maximum stress level, changes in the recuperator plate configuration may be considered. The changes will be aimed at more uniformly heating the gas inlet face/air outlet manifold area. One possibility is to form channels or fins in the manifold to allow either the incoming gas or the exiting air to flow



65-281-16

Figure 43. Ceramic/Metallic Duct Attachment.

through the manifold wall and aid in heating. Alternatively, changes in edge and/or manifold thickness can alter the thermal mass or conduction path in a beneficial manner.

- o Design Attachment Components - A method of connecting the recuperator to an engine must be determined. The ceramic ducts from in Task 1 will be interfaced with metallic ducts connecting to the compressor and combustor. One such concept is shown in Figure 43. Cylindrical metallic ducts mate with cylindrical ceramic ducts via a V-band clamp. The ceramic air outlet duct may need to be flared to accommodate insulation for reducing the temperature to a point where a metallic V-band clamp can be used effectively. An alternative is the use of a ceramic duct all the way to the combustor.
- o Compression Molding - Tooling for Module C will be procured as the Module B fabrication effort nears completion. Module C is similar in shape to Module B, but is larger in stack height. Therefore, only fine tuning of the forming and processing parameters is anticipated. Three modules will be constructed for use in simulated engine tests.
- o Form Attachment Components - To complete the modules, ceramic ducts and other attachment components must be fabricated. The components required to effect a joint between ceramic and metallic ducts will be fabricated.
- o Assembly - The full-size core will be bonded and the ducts and other attachment components adjoined. The size of Module C dictates the use of large fixturing

tools to achieve the proper alignment. This assembly essentially replicates that of Module B, but on a larger scale.

- o Processing - The green modules must be converted to a ceramic material through binder extraction and nitriding cycles. Processing is expected to closely follow that of Module B except that larger furnaces and more complicated kiln furniture are needed to provide support for the module during binder extraction.

Task 4, Module C Testing - Full-size modules will be tested under simulated engine conditions. A test rig capable of simulating engine conditions will be designed and constructed. The simulated engine test will verify the viability and design of the ceramic finned-plate recuperator.

- o Design Test Rig - A relatively sophisticated rig is required to conduct high-temperature, high-pressure tests on Module C recuperators. This test facility must provide hot pressurized air at a high flow rate for the air-side stream and gas at approximately 1260C (2300F) for the gas-side stream. Control devices will be developed to maintain the desired temperatures, pressures, and flow rates for both air and gas streams.

The rig will be highly instrumented to record temperatures, pressures, and flow rates on both the inlet and outlet sides of the recuperator. This test rig will be used to qualify recuperator modules for installation in vehicles.

- o Construct Rig - After the test rig is designed, the unit will be constructed. The design task is scheduled

near the beginning of the program so that sufficient time is available to order and receive components for the test rig. Upon completion of the rig, a check run will be made to ensure that the unit can provide a sufficient quantity of air and gas at the temperatures and pressures of interest. Also, the rig will be calibrated before testing of any modules.

- o Duct Interface Testing - Potential ceramic/metallic duct joint designs resulting from Task 3 will be temperature- and pressure-tested. Laboratory tests are necessary to ensure that the components can survive the pressure and thermal stresses at elevated temperatures. In addition, joints will be tested for sealing integrity under these conditions.
- o Pressure Test - Module C will be pressure-tested at ambient temperature to verify the pressure containment capability of the prototype.
- o Thermal Cycling - Modules will be exposed to cyclic variations in temperatures of 21 to 1260C (70 to 2300F) to ensure that the recuperator module can withstand the thermal stresses resulting from these temperature extremes.
- o Simulated Engine Test - The simulated engine conditions test is the most significant test to be conducted during the program because it will verify the capability of the ceramic finned-plate recuperator to perform in a typical engine environment. Steady-state and transient test conditions are envisioned. The steady-state test

condition, which will be achieved by bringing the recuperator up to temperature slowly, will verify the predicted recuperator performance (heat transfer and pressure drop).

Transient tests simulate engine startup conditions. The transient test will generate operational-level stresses because of the temperature gradients imposed. Thermal stresses are known to be substantially higher than pressure stresses in the recuperator. Successful completion of these tests will provide confidence in the recuperator's ability to perform satisfactorily when attached to an engine. Modules passing these tests will be ready for use in an engine test.

- o Data Analysis and Evaluation - The data generated during all of the pressure, thermal, and simulated engine tests will be analyzed and evaluated. The results of this analysis will include pressure containment capability, pressure drop through the recuperator, thermal shock resistance, heat transfer effectiveness, and suitability for use in the intended application.
- o Test Report - At the conclusion of the Module C tests, a test report that will include data, discussions, conclusions, and a proposed engine testing program will be issued.

Technical Approach

Fabrication and testing of a full-size ceramic recuperator module is the major emphasis of this program. Garrett has defined three modules of increasing size and complexity to facilitate development in a logical manner while minimizing experimental costs (Figure 40).

Module A was constructed during a previous program to develop the fabrication technology required to make detailed finned-plate ceramic recuperators, as well as to test the pressure containment and high-temperature capability of these intricate matrices. Module A was able to support a 206 N/cm^2 (300-psi) pressure differential across the air and gas passages during a cold pressure test, demonstrating that the fabricated finned-plate matrices can withstand high operating pressures.

Module B will be a working recuperator, a reduced-stack-height heat exchanger (approximately 20 percent of a full-size recuperator module) that comprises alternating layers of air and gas passages. The shorter stack height will reduce the fabrication and testing costs, with little sacrifice in verifying the program objectives. This module, which will have the same plan form as the full-size version complete with integral air manifolds, will be used to determine the ceramic ducting and other support structures required for interfacing with engine components.

Module B will be performance-tested at temperatures up to 427C (800F) in order to generate heat transfer and pressure drop data. Since performance values measured at low temperatures can be accurately scaled to the higher operating temperatures, actual thermal performance of the module will be contrasted with predicted values to substantiate a full-size reference design recuperator.

Upon completion of performance testing, modules will be pressurized using large pressure differentials to determine the pressure containment capability of the design. Modules that survive the pressure tests will be exposed to increasingly severe thermal shocks to obtain thermal shock resistance of the unit.

After each thermal cycle, modules will be pressurized to determine whether any damage was incurred as a result of the thermal cycling.

The data collected from these tests will be used to generate the Module C design. Three design/fabricate/test cycles are anticipated to evolve a satisfactory design for this recuperator.

The full-size recuperator (Module C) will be constructed and tested under simulated operating conditions.

The reference recuperator design will be modified, if necessary, based upon the results of Module B tests. Also, the associated parts required to seal the ceramic recuperator to metallic engine components will be designed. After the tooling needed to form these parts is obtained, full-scale prototype modules will be fabricated.

These modules will be subjected to independent pressure and thermal cycling tests and will then be exposed to simulated engine conditions. These tests require the design and construction of a rig that produces the desired conditions. This design/construction effort is expected to last a significant period of time because of the sophistication required. The intent is to construct the test rig in such a way that it can be used for prooftesting of each production module before installation in a vehicle. Because of the high reliability desired, it is anticipated that each production recuperator module will be prooftested at stress levels in excess of design conditions to qualify it for installation in a vehicle.

Along with the two recuperator modules, the other components required to produce a functioning heat exchanger will be devel-

oped. These include the ceramic ducts that connect the recuperator core with the engine metal duct work, and the attendant seals and mechanical joints required at this interface.

A ceramic plate-fin recuperator shows the potential of solving the weight and temperature limitations associated with present metallic designs. The ceramic design could be the key to making the benefits of heat recovery (imposed fuel economy) available to airborne applications.

G. Engine Environment Test of Ceramic Recuperator

The objective of this program is to conduct engine environment tests of a ceramic plate-fin recuperator. This experimental program would be based on successful completion of the ceramic plate-fin recuperator Program F.

Program Description

This program consists of three tasks and provides for recuperator design, fabrication, and engine environment testing as scheduled in Figure 39.

The recuperator will be designed and sized for the power class of the year-2000 rotorcraft and commuter engines. Compatible engine parts will be selected from existing GTEC engines and incorporated into a recuperated engine system.

The ceramic recuperator and engine parts will be fabricated and component tests will be conducted. The components will be assembled into a recuperated engine test unit and instrumented for performance and mechanical data. The unit will be submitted to mechanical shakedown, performance and controls, and accelerated mission tests. Teardown inspection will be conducted at intervals and results will be documented in detailed reports.

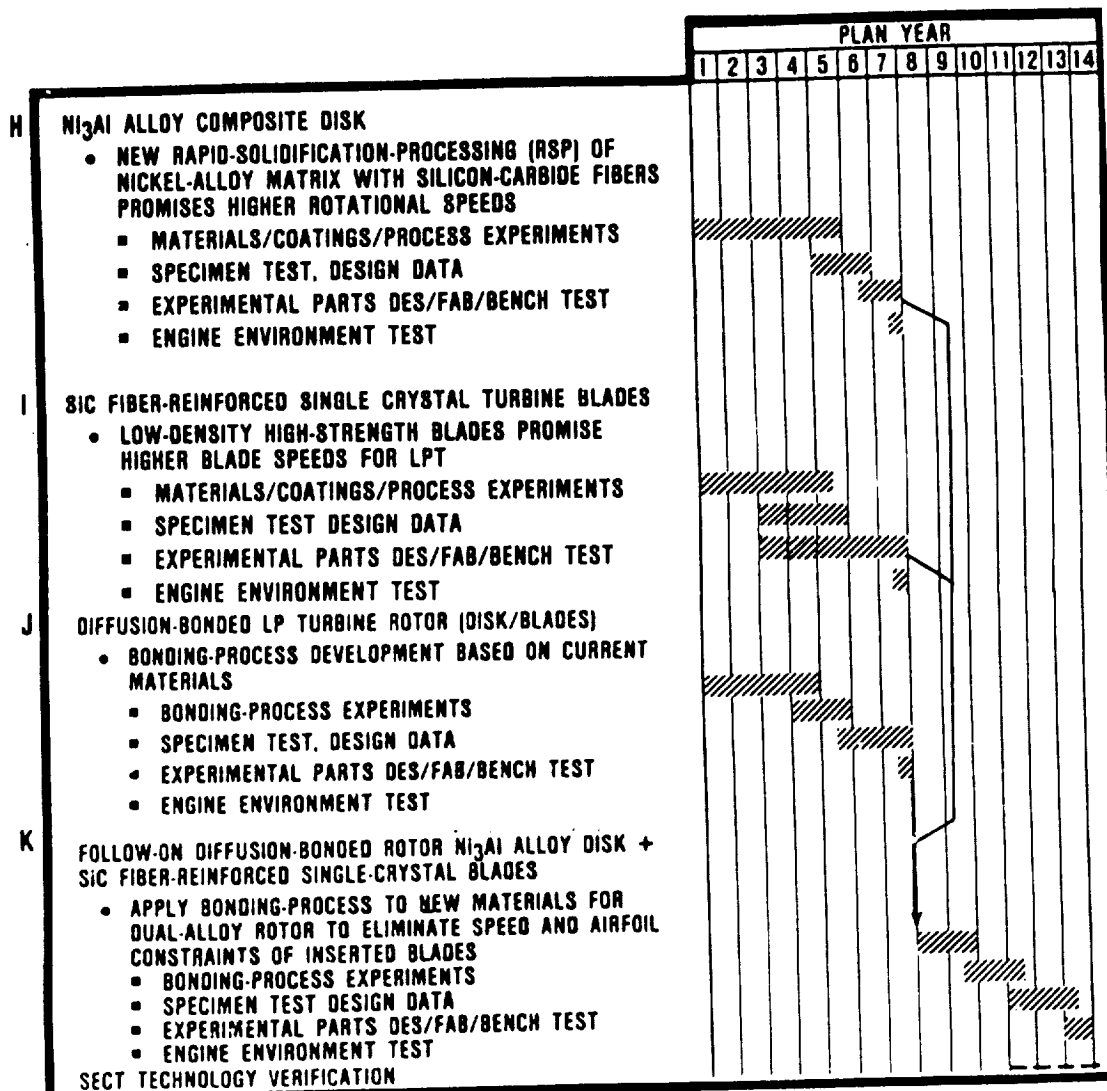
2.4.2.3 Metallics For Turbines

This plan comprises four interdependent technology programs identified as Programs H through K. As scheduled in Figure 44, the programs involve material and process efforts for turbine rotors with the objective of increasing operational speeds and temperature levels.

H. Ni₃Al Alloy Composite Disk

Current nickel-base alloy turbine disk materials such as René 95 and GatorizedTM IN100 are limited in specific strength by their relatively high densities and the inability of conventional gamma prime precipitation strengthening mechanisms to achieve very high strength without serious degradation of fracture properties. In order to overcome these strength deficiencies, the classical approach to turbine alloy development has been the addition of larger quantities of gamma prime forming elements, which also tends to reduce incipient melting temperatures. This approach results in a significant decrease in the temperature window between the grain recrystallization/growth temperature and the incipient melting temperature. This further restricts processing to controlled grain sizes for amelioration of unacceptably rapid crack growth and uncontrolled fracture. Reliance on gamma prime strengthening also inherently limits maximum service temperature of conventional alloys.

Lightweight, inherently stable turbine disk materials with acceptable strength and fracture properties can be developed through the revolutionary approach of metal matrix composites. Intermetallic (Ni₃Al) compounds display the low-density, oxidation resistance, and thermal stability necessary for turbine disk application; however, precipitate strengthening mechanisms are



95-281-80

Figure 44. Material Technology Schedule for Turbine Metallics.

not available to provide sufficiently high tensile capability in this class of materials. Addition of lightweight, high-strength fibers such as silicon carbide are therefore necessary to meet this requirement.

Previous difficulties in achieving SiC composite consolidation with a conventional high-strength nickel-alloy matrix have been largely related to the reactivity of silicon carbide in contact with the matrix at temperatures exceeding 1093C (2000F) (necessary to achieve satisfactory composite bonding). New fabrication approaches that employ rapid solidification processing (RSP) and/or stable carbide-coated fibers can eliminate this problem, allowing practical component processing. At the minimum, Ni₃Al/SiC-reinforced disks will equal the strength of today's strongest alloys, with a 10 percent reduction in density.

Program Description

This materials program consists of four major tasks, ranging from materials experiments through engine environment testing, as shown in Figure 44. It will be completed within seven program years and will establish high-strength Ni₃Al/SiC disk technology.

The program will establish the feasibility of RSP fabrication initially using uncoated SiC fiber. After determination of process/stability effects, a series of stable metallic carbide-type coatings such as tantalum carbide (TaC) will be considered to protect the core fiber from reaction. Composite panels and subscale components will initially be used to confirm mechanical properties for candidate materials and processing concepts. Preliminary subscale components will also be produced for spin cycling and burst evaluation prior to fabrication of full-scale parts for components in program years six and seven. Engine environment testing will be conducted in program year seven.

I. SiC Fiber-Reinforced Single-Crystal Turbine Blades

A lower density, higher creep-strength turbine blade material offers substantial LP turbine payoffs in the following areas:

- o Improved engine performance due to increased turbine temperatures and blade speeds
- o Increased disk rim speeds due to reduced blade loads
- o Reduced weight due to lighter blades and disks

Lower density turbine airfoils can be achieved by incorporating a significant volume fraction (e.g., 30 percent) of high-strength, low-density ceramic fibers (e.g., SiC) into a high-strength, single-crystal alloy matrix. Increases of 50 percent in density-corrected creep strength, or 56C (100F) in temperature capability above GTEC's SC alloy 180 are considered possible with this technology.

Program Description

This materials program consists of four major tasks, ranging from materials experiments through engine environment testing, as shown in Figure 44.

The technology program will focus on incorporating 30 percent of the high-strength SiC fibers into a directionally solidified (DS) single-crystal matrix. Since an unprotected SiC fiber will dissolve in a molten superalloy, the fibers must be coated with a compatible metal carbide such as TaC, which has demonstrated long-term stability in molten superalloys (e.g., TaC is an integral constituent of a DS eutectic superalloy). Thus,

coated SiC fibers will be evaluated for stability in candidate superalloys.

Following identification of an effective coating system for the SiC fibers, tasks will be undertaken to determine the solidification technology and optimize the fiber coating and the matrix alloy for mechanical properties and castability. This activity is vital to the manufacture of fiber-reinforced turbine blades. It will be supported by specimen tests for acquiring design mechanical properties and evaluating candidate coatings.

Experimental parts will then be designed and fabricated for bench tests (program years five through seven) and for engine tests. Engine environment testing is scheduled for program year seven.

J. Diffusion-Bonded LP Turbine Rotor (Disk/Blades)

The diffusion-bonding technology required for manufacturing uncooled turbine rotors for the LP turbine section will employ the most advanced blade and disk alloys available in designs of maximum mechanical efficiency. Current small engine production turbine rotors use either inserted blades with dissimilar materials for blades and disks, or integrally cast rotors of a single alloy.

In the inserted blade designs, turbine rotor speed and efficiency are limited by the stress concentrations in the disk rim as imposed by the mechanical attachments of the inserted blades. The need for mechanical attachments also imposes limitations on turbine blade hub solidity due to the limited space available for the attachments on the rim of a small-diameter turbine disk.

In integral cast designs, the mechanical attachment problems are eliminated, but maximum rotor speed is limited by the lower strength of a cast alloy hub versus a high-strength powder metallurgy alloy hub that is better for hub strength. The cast alloy hubs are also inferior to powder or forged alloys in low-cycle-fatigue life.

Advanced technology diffusion-bonded turbine rotors can combine the best single-crystal cast alloy with the highest strength/weight turbine disk alloy available in the time period of 1995 to 2000. The single-crystal alloys may have a 56C (100F) improvement in stress-rupture strength over the best of today's alloys, GTEC's SC-180. The turbine disk alloy will be a derivative of the Ni_3Al intermetallic compound. It is anticipated that this alloy will have strength characteristics equal to today's strongest alloys, with a 10 percent reduction in density.

When the technology is available the cooled diffusion-bonded bladed disk will be a candidate for use in the LP turbine sections of rotorcraft and commuter engines.

Program Description

This metal-joining program consists of four major activities, ranging from materials experiments through engine environment testing, as shown in Figure 44. It is a seven-year technology program to establish diffusion-bonded integral turbine wheel technology for the best blade and disk materials available today. This process should also be largely transferable to new metallics as envisioned for the year-2000 time frame.

Various diffusion-bonding concepts will be considered for final selection. The screening process will include specimen

testing of the different candidate alloys, bonding processes, and bonding geometries. A two-year effort is expected to select and verify the bonding method. Following selection of the bonding geometry and process, an effort of approximately two years will be necessary to develop the bonding process for the production environment. Efforts will be geared toward reducing production costs through minimizing scrap and process time. Nondestructive testing procedures will also be established at this time. Specimen tests will be conducted and design data will be obtained in parallel with these activities.

Following initiation of the process development, an initial design will be started. Selected for experimentation will be a turbine wheel from an existing GTEC gas turbine engine, such as the F109 turbofan. The detail design will examine the modifications necessary to incorporate an integral diffusion-bonded wheel in this existing configuration. This design will be fabricated and bench-tested.

A second design and fabrication phase will incorporate both design changes driven by iteration 1 and the benefits of an improved bonding process as the process efforts conclude.

The fabricated hardware from design iteration 1 will be evaluated by component and rig testing. Component testing will consist of a cold whirlpit overspeed test of several turbine wheels, either to the point of failure or to the point of verifying adequate burst margin. Hot testing will be conducted in an existing or a modified rig. Both steady-state and transient conditions will be simulated to determine actual stress and temperature levels.

Hardware from the second design iteration will undergo full engine testing in the selected engine. The engine will be cycled to expose the turbine to typical transient operation conditions.

Technical Discussion

The program will use a GTEC test-bed engine for the engine environment testing. The selected engine will be similar in size to that of the SECT rotorcraft engine. The technology program will use GTEC's SC-190 single-crystal alloy and a Udimet 720 powder alloy hub. These materials are the best turbine blade and disk alloys available today. The bonding process, design, and nondestructive evaluation process to be used will be developed for this alloy combination.

GTEC has developed a production diffusion-bonded dual-alloy turbine wheel for one of the turbine stages of the GTCP331 APU used in the Boeing 757 and 767 aircraft. The process to bond this wheel uses a cast blade ring. The initial concept selection and verification stages of this program will modify this proven process to adapt it to individually cast single-crystal blades.

K. Follow-On Diffusion-Bonded Rotor Ni₃Al Alloy Disk and SiC Fiber-Reinforced Single-Crystal Blades

This is a diffusion-bonding technology program for the manufacture of turbine rotors that is planned to build on the successful completion of related programs. This program will transfer the diffusion-bonding technology learned for current materials (Technology Program J) to similar rotors using new materials. The new materials envisioned for the year-2000 time frame are discussed in Technology Programs H and I of this section. These new blade and disk materials and an efficient diffusion-bonded joint could potentially maximize the benefits of higher

speed/temperature turbine rotors for year-2000 rotorcraft engines.

Program Description

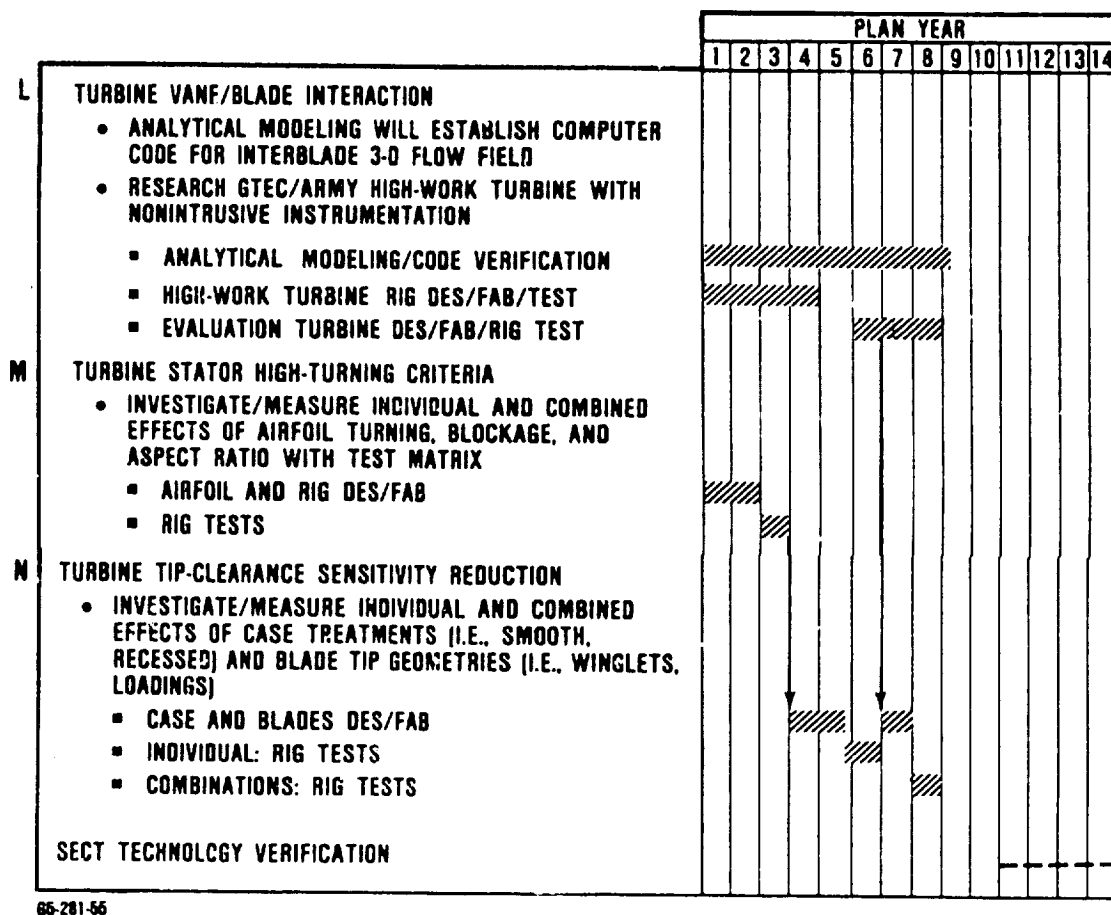
This technology program consists of four major activities, as shown in Figure 44. Its interdependency with Programs H, I, and J necessitates delaying the start of this program until plan year eight.

The program would include the same ingredients as discussed for Program J. However, the emphasis would shift from the initial highly experimental tasks to the later hardware evaluation tasks. This program and companion technology verification testing could achieve technology readiness for this concept for year-2000 engine designs.

2.4.2.4 Turbine Performance

This plan is made up of three discrete technology programs, identified as L through N in Figure 45. The first program, which is highly experimental, addresses the fundamental turbine aerodynamic prediction/design techniques that are necessary to achieve the turbine performance levels as predicted in this SECT study for the year 2000. The two other programs address specific turbine design features where large loss reductions are projected and necessary for year-2000 efficiencies.

The plan schedule shows interrelationships for optimum results. While the turbine tip clearance program (N) could be run to the SECT cycle independently, improved data validity can be expected with the interrelationships shown. Tip-clearance data, as planned here, will be obtained from blading that is compatible with a high-turning stator and blading that incorporates advanced vane/blade interaction concepts (L).



65-281-55

Figure 45. Turbine Technology Schedule.

L. Turbine Vane/Blade Interaction

Allowing for the SECT projected material and mechanical advances in technology, aerodynamic advances in optimizing rotor blade design to the stator exit flow field (vane/blade interaction) are required to achieve the year-2000 performance levels predicted for the rotorcraft, commuter, and turbojet engines. Year-2000 efficiencies reflect a 1 percent increase in efficiency due to optimizing vane/blade interaction.

The scope of the program will involve analytical and experimental work. Analytical work will consist of developing a design system tool for predicting interblade 3-D flow field to optimize the stator/rotor matching. The experimental work will include turbine component testing to understand rotor influence on the stator exit flow field. The test vehicle will be the GTEC/Army single-stage high-work turbine, which would be directly applicable to the rotorcraft HP turbine. The results of this technology program will extend to the axial turbine configurations of the rotorcraft, commuter, and turbojet engines.

Program Description

This program consists of three major tasks, from analytical modeling through rig testing of a turbine, as shown in Figure 45. The program is scheduled for eight years.

The program contains both the basic research and the analytical approaches, with a combination of the two in the sixth year. For the first two years, the research approach consists of rig design, fabrication, and instrumentation. The GTEC/Army high-work, single-stage turbine will be researched. Instrumentation used will be a nonintrusive type of measurement device such as a laser two-focus (L2F) system. The third and fourth years will include the rig testing program and analysis.

The analytical approach will begin during the first year and will extend to the third year. The main thrust of this approach will be to develop a 3-D code that will accurately predict the stator exit 3-D flow field. This activity could be either a Navier-Stokes solution or a Boyle-code-type analysis. In the fifth year, the results of the rig testing will be incorporated into the code. Results of the rig tests will include the rotor influence on the stator exit flow field.

The remaining three years (sixth through eighth) will involve use of the code to design a new turbine to the same velocity diagrams as the GTEC/Army high-work single-stage turbine, and testing the design. In the final year, a final report will be written on the results of the program.

Technical Discussion

Included in the year-2000 performance values is a one-point improvement in efficiency due to optimum matching of the stator exit and rotor inlet flow fields. This goal will require an extensive study of the effect of the rotor on the stator exit flow field. To date, a limited amount of work has been accomplished using a large-scale, low-speed test rig. The traditional probes that measure angle, pressure, and temperature cannot be used with the rotor in place. Nonintrusive instrumentation, such as an L2F system, will be required to map the interblade row flow field for the engine scale rigs.

After the interblade row flow field is understood, the results will be incorporated analytically. An accurate prediction of the 3-D stator exit flow field incorporating the stator viscous effects, interblade row endwall viscous effects, and the rotor influence of the flow field is needed to design the rotor. This analytical tool could be either a Navier-Stokes solver or a

quasi-3-D flow and boundary layer analysis such as the Boyle code. Particular attention will be given to the rotor leading edge design.

In summary, the program will include both experimental and analytical work. The experimental effort will involve component testing to understand rotor influence on stator exit flow field and optimization of vane/blade spacing for performance. The analytical work will consist of developing a design system tool to optimize the stator/rotor match.

M. Turbine Stator High-Turning Criteria

To allow close-coupling the HP and LP turbines on rotorcraft and commuter engines, high rotor shroud divergence, and high stator turning will be required.

The turbine design, as conceptualized, assumes ceramic inserted blades or a composite ceramic integral rotor. Either should eliminate or minimize the broach-angle constraints required for metallic inserted blades. This will permit increased blade stagger angles and higher reaction, which allows the higher stage performance required for the high-work, single-stage HP turbine of the simple cycle rotorcraft engine and the first-stage blades of the LP turbines of both the rotorcraft and commuter engines.

The high-work, single-stage HP turbine required by the rotorcraft engine incorporates a vane with high turning to achieve the performance needed for the year-2000 engine performance. To meet this performance goal, the limitations on the amount of turning that can efficiently be accomplished must be understood. The influence of the aspect ratio and the trailing edge blockage on the ability of the stator to meet the high turning requirements must also be known.

The program will consist of exploring stator performance and turning for stators designed for a range of exit flow angles from 77 to 81 degrees. A matrix of seven configurations will be rig tested, with variances in turning, trailing edge blockage, and aspect ratio from a baseline design. The results of this study will be incorporated into the design system (Program L) to aid configuration trade-off studies for the rotorcraft turbines.

Program Description

This program consists of two tasks, from airfoil design through rig tests, as shown in Figure 45. The program is scheduled for three years.

The program consists of testing seven configurations of a high turning vane. The first year will consist of designing the seven configurations, which will include a baseline vane and two variations each of turning, trailing edge blockage, and aspect ratio. The exit angles will range from 77 to 81 degrees. Thus, the matrix to be tested will include three variations each of exit angles, trailing edge blockage, and aspect ratio.

Testing of the seven configurations will be conducted in the third year. A report on the results of the rig testing will be issued at the end of the third year.

Technical Discussion

High-work, single-stage HP turbines required by rotorcraft engines use stators with high turning angles to achieve the work output. Industry has shown that turning of 79 to 80 degrees can be satisfied with nominal trailing edge blockage levels and high corrected flow stators. For the rotorcraft HP turbine to be successful, the turning technology must be verified in a lower

flow regime. With the lower corrected flows (smaller machines), the aspect ratio decreases and the trailing edge blockage increases due to size limitations. The increased blockage and decreased aspect ratio influence on stator performance at high turning must be evaluated and understood.

The program consists of designing seven stator configurations. This includes three stators at different exit angles at some nominal trailing-edge blockage. The stators will be typical of the size, aspect ratio, and solidity required for the rotorcraft engine. Using one of these stators as a baseline, two additional configurations each will be designed around the baseline stator with different trailing edge blockage levels and aspect ratios. The stators will be designed using the latest technology in 3-D design, which will include tangential lean and endwall contouring.

Following hardware procurement, each annular stator cascade will be tested. Testing will include a stator exit survey at various pressure ratios. Stator performance and turning will be evaluated for all seven stators. Particular attention will be given to the radial distributions as well as to the global results. Meeting turning and performance requirements globally would not necessarily achieve the optimum stage performance if the radial distributions are skewed.

N. Turbine Tip Clearance Sensitivity Reduction

To allow close-coupling the HP and LP turbines on the rotorcraft and commuter engines, high shroud divergence will be required for the LP turbine rotors. To achieve successful designs of this type, mechanical technology advances are required to reduce axial excursions during operating point changes. Reductions in axial excursions will allow closer running clear-

ances and will thus reduce performance penalties due to tip clearances. Furthermore, aerodynamic advances in the reduction of performance sensitivity to tip clearance are required to achieve the year-2000 performance levels predicted for the rotorcraft, commuter, and cruise missile engines. Year-2000 efficiencies reflect a 25 percent decrease in tip clearance sensitivity. The main thrust of this program is the continuation of GTEC studies already completed on casing treatment and rotor tip treatment.

The GTEC/USAF Case Treatment Study has shown that the smooth shroud has performance advantages over recessed shrouds. A goal of the proposed program is to extend this study using a high-work turbine as a testing vehicle. The high-work turbine will be used as a model for extending this technology into the rotorcraft and commuter engines, which will require high-work HP turbines.

The technical approach will extend the study on nonconventional tip geometry, such as winglets, into the high-work turbine technology. The GTEC/USAF LART program has shown significant performance advantages using winglets. A further aspect of the program will be to study the effects of aerodynamic loading on tip leakage. One approach will tailor the vector diagram so that the tip section is unloaded; another approach will vary the chordwise position of maximum loading.

Although the test rig will be a high-work, single-stage turbine, the results of the technology program would extend over all the axial turbine configurations of the rotorcraft, commuter, and turbojet engines.

Program Description

This program, which consists of three tasks, provides for screening tests and a second design iteration, as shown in Figure 45. It is scheduled to maximize the advantages of companion Programs L and M.

The program considers two areas for reducing tip clearance sensitivity, casing treatment, and rotor tip geometry. The rotor tip geometry will include nonconventional geometries such as winglets and experiments in blade loading.

The first year of the program will consist of defining the shroud and tip geometry to be tested, and designing the test configurations. The latter portion of the first year and the early portion of the second year will involve fabrication of the configurations followed by rig testing and analysis.

The final two years will follow the same procedure, superimposing the results of the two study areas into a conceptual design. A final report on the success of this effort will be submitted early in the sixth year.

Technical Discussion

Preliminary studies have demonstrated several approaches to reducing the stage performance sensitivity to tip clearance. Two approaches relate to geometry changes on either the shroud casing or the rotor blade tip. Past studies at GTEC have shown performance advantages for smooth shrouds and winglets on the tip sections. Continuation of the GTEC/USAF Case Treatment Study and the GTEC nonconventional tip geometry studies will be the main thrust of this program.

Another approach will include a tip section aerodynamic loading study. In this approach, the vector diagram will be tailored such that the tip section would be unloaded aerodynamically, thus reducing the pressure gradient across the airfoil. The position of the maximum aerodynamic loading influence on tip performance will also be studied.

In summary, reducing the performance sensitivity to tip clearance by 25 percent will require studies on shroud and tip geometry configurations, as well as on aerodynamic design philosophies.

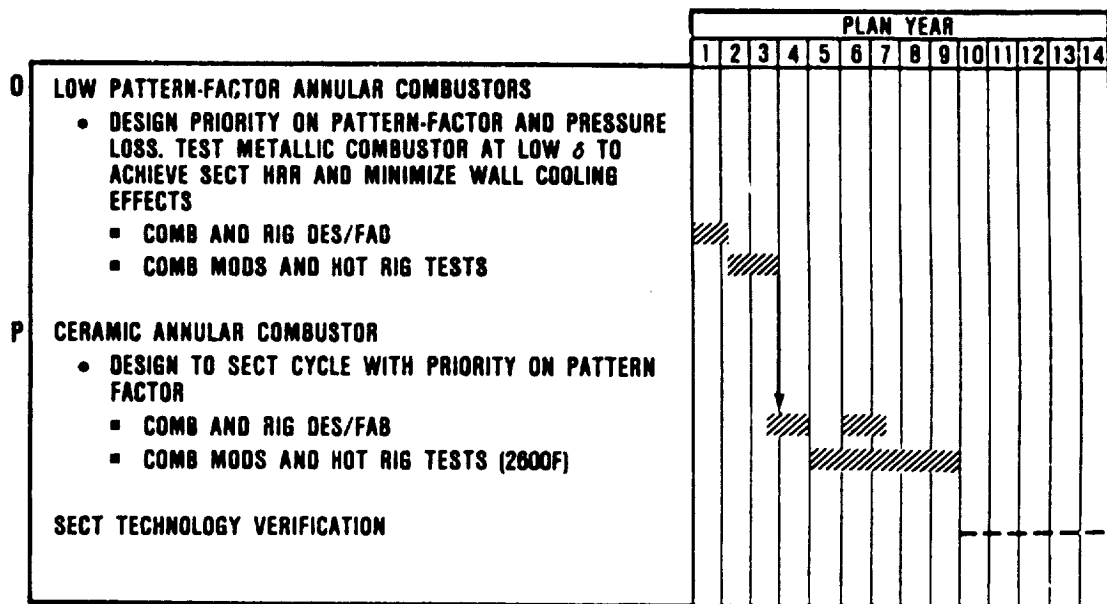
2.4.2.5 Combustor Performance

This section presents the technology plan for improving annular combustor performance for year-2000 rotorcraft engines. The plan consists of two discrete technology programs, identified as O and P in Figure 46.

The first program, which addresses pattern-factor for high heat release rate (HRR) combustors, will advance technologies applicable to ceramic combustors. It uses metallic combustors for rig testing. The second program will build on this advanced technology base to obtain experimental data on a ceramic combustor, which includes the combustor liner and hot transition liners.

O. Low Pattern Factor Annular Combustors

Significant performance requirement differences exist between the various SECT applications for annular combustors. The rotorcraft and commuter applications require a low pattern factor and a durable, efficient, stable combustion system with altitude relight capability. The cruise missile engine application requires a low pattern factor, volume-limited, short-life



86-281-132

Figure 46. Combustor Technology Schedule.

combustor to satisfy requirements for a low-cost, low-volume, low-weight engine. All SECT applications require nonmetallic materials to optimize combustion system performance for the high cycle temperatures of this study. Until non-metallic combustor materials are available, metallic combustors can be rig tested at increased cycle temperature levels to evaluate concepts.

As combustor temperatures rise, increased design priority on low pattern factor combustion systems will prevail to limit turbine inlet temperature hot spots. The additional goals of minimum combustor pressure drop and minimum combustor size make pattern factor reduction a difficult task. The use of nonmetallic materials will allow budgeting additional dilution air for pattern factor control by eliminating wall cooling requirements. Design concepts to minimize pattern factor can be evaluated with metallic combustors by rig testing at low pressures and using advanced wall cooling to minimize cooling air requirements. Testing will be directly applicable to rotorcraft, commuter, and APU reverse-flow combustion systems, and the analytical models will allow the extension of the results to through-flow combustors (cruise missile engines).

Program Description

This program consists of two primary tasks, from combustor design through hot rig tests, as scheduled in Figure 46.

The schedule is based on the use of an existing high-temperature combustion rig with combustors adapted to existing plenums. Existing analytical design tools will be used to define the initial combustor/liner geometries. Following initial testing, an iterative test-design modification procedure will be used on analytically predicted improvements, and each test sequence will

determine the degree of improvement obtained and will provide data on where further improvement is required.

The main program activities are summarized in the following:

- o Define a fuel injection system to provide uniform, well-atomized fuel distribution with coking resistance suitable for the cycle temperatures of this study (including 1427C [2600F] TRIT)
- o Define the combustion system to provide a well mixed, uniform, primary zone as well as an optimum mixing pattern dilution zone to provide minimum pattern factor
- o Rig test evaluate each configuration at selected test conditions to determine pattern factor, liner thermal gradients, and atomizer fuel passage wall temperature levels
- o Modify the configuration based on 3-D analysis and repeat tests, iterating until all design goals are achieved. A final redesign and test cycle will be used for the non-metallic design.

Technical Approach

Selection of design goals will include pattern-factor reductions of 35 percent (to 0.12 levels) for the rotorcraft simple cycle. Completely uniform wall temperatures are not achievable. However, hot-spot thermal gradients will be minimized via proper fuel injection and combustor aerodynamic design. The design goal level for wall thermal gradients will be as required for projected ceramic material properties.

Atomizer coking resistance is important for future rotorcraft and commuter applications with high combustor inlet temperature (particularly with recuperated cycles). The design goal will be to maintain fuel-passage wall temperatures at acceptable levels, currently estimated to be below 204C (400F). Effective thermal insulation will be required to minimize stem heat transfer and adequate tip cooling, with airblast atomization.

These programs will provide much needed information on design goal feasibility for pattern-factor control, fuel atomizer coking resistance, and liner thermal gradient control. Analytical design methods to optimize the aerodynamic design of nonmetallic combustors will also be initiated. Pattern factor will be a design priority for the ceramic combustor, with a goal of 0.12. This will allow the cycle temperature (TRIT) of 1427C (2600F) (as established in this study) with a hot-spot temperature of 1538 (2800F).

P. Ceramic Annular Combustor

This technology program will build on the advanced data base as established on metallic combustors (Program O) and on the ceramic materials program discussed in paragraph 2.4.2.1 (Program B). The aerothermal and mechanical design of a ceramic combustor (liner and transitions) will be accomplished based on existing analytical modeling, advanced data base (Program O), and ceramic material properties.

The system will be configured and sized for results applicable to the SECT rotorcraft engine (simple cycle) and to be compatible with existing rig and test equipment.

Program Description

This program consists of two primary tasks, as scheduled in Figure 46. Design and fabrication of the combustion system will be conducted along with combustion rig modifications. Two combustor/transitions will be completely fabricated and approximately eight ceramic combustors will be partially fabricated to facilitate experimental modifications. A second design-test iteration is scheduled to achieve technology readiness.

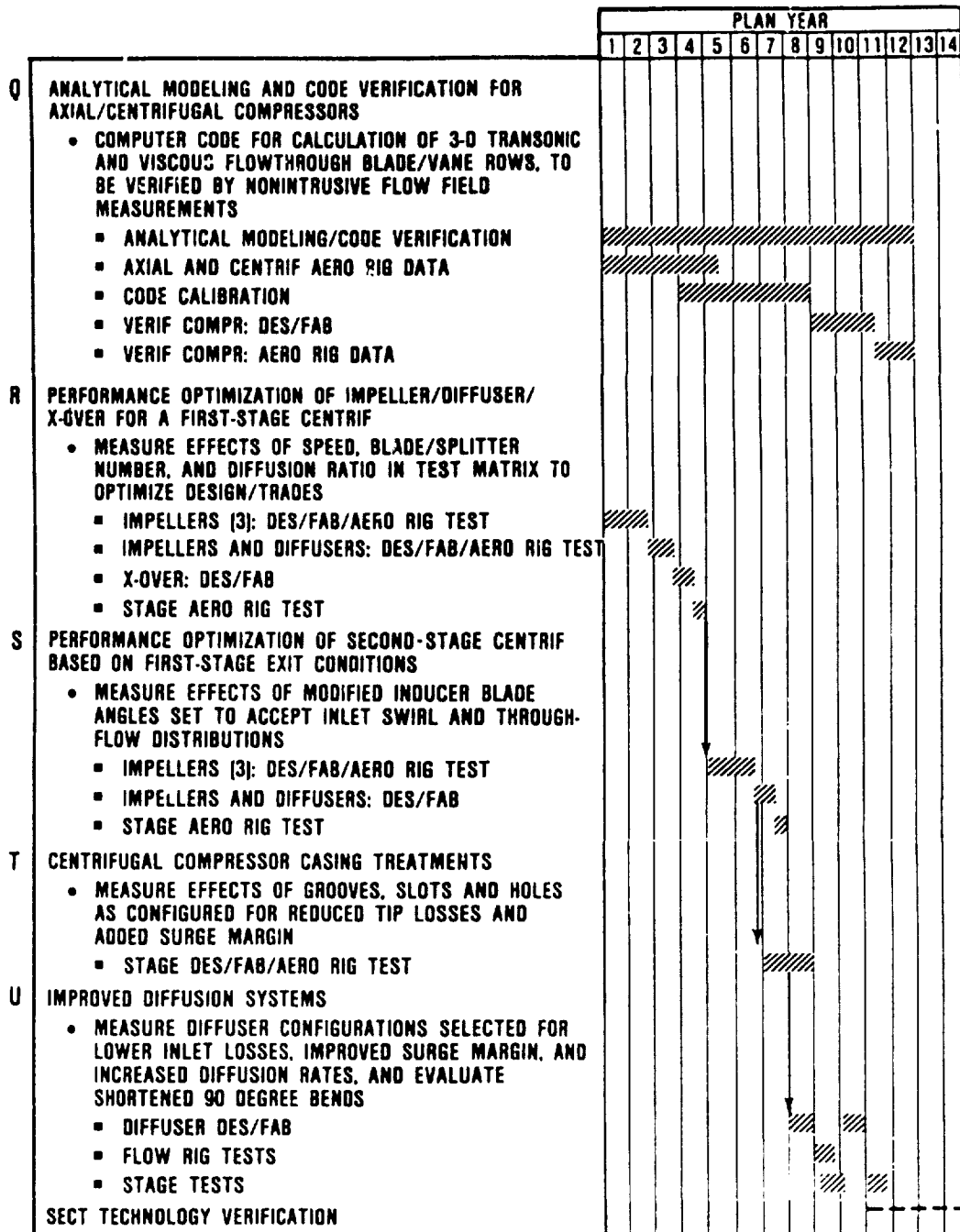
2.4.2.6 Compressor (Centrifugal) Performance

This plan consists of five discrete technology programs, identified as Q through U on Figure 47. The first program, which is highly experimental, addresses the fundamental aerodynamic prediction/design techniques for axial and centrifugal compressors that are necessary to achieve the centrifugal compressor levels as predicted in this SECT study for year-2000 rotorcraft engines. The other four programs address specific design features where large loss reductions are projected and necessary for year-2000 efficiencies.

The efficiency improvements projected to be attainable through these programs are as follows:

- | | | |
|---|--|---------------|
| o | Analytical Modeling | * |
| o | First-Stage Impeller/Diffuser Crossover Optimization | ≤ 0.5 percent |
| o | Optimization of Second-Stage Impeller | ≤ 0.5 percent |
| o | Case Treatments | ≤ 1.0 percent |
| o | Diffuser System | ≤ 1.0 percent |

*The analytical modeling tools are required to achieve the noted efficiency improvements. They will have an additional influence on performance dependent on configuration and application.



85-281-50

Figure 47. Compressor Technology Schedule.

Technology Programs R through U could be run independently to the SECT cycle. However, improved data validity can be expected with the interrelationships shown on the plan scheule.

Q. Analytical Modeling and Code Verification for
Axial/Centrifugal Compressors

To achieve the centrifugal compressor performance levels projected for the year-2000 time frame, compressor aerodynamic design technology must be improved in several areas. This is required in advance of full-stage compressor development in order to thoroughly explore compressor design options and ensure that proper design-parameter selections can be made.

The objective of this program is to develop 3-D viscous analytical codes as a design tool to significantly improve turbomachinery compressor performance. The obvious benefit of designing blade rows with improved predictions and reduced losses is the immediate application in all types of engine applications. The program is structured toward prediction and verification of internal flow calculations that have been substantiated by internal flow measurements so that the code can be used with confidence.

This ongoing program is the key to reducing compressor blade row losses, with reduction of as much as 60 percent anticipated for year-2000 applications.

Program Description

This program consists of five major tasks, from analytical modeling through aerodynamic rig testing of a verification compressor, as shown in Figure 47. The analytical activity for this program will be the development of a computer code to calculate

three-dimensional transonic and viscous flow through a turbomachinery blade/vane row. Concurrently, a test technique for non-intrusive flow-field measurements will be refined to aid in the modeling development and checkout of the analytical prediction code.

Technical Approach

3-D Viscous Modeling - The development of a 3-D viscous, transonic flow analysis code as an integral part of a design system requires an improved physical understanding of all relevant flow phenomena. The viscous flow calculation will model losses, work (rotating blade rows), and flow turning as well as quantitatively predict wake formation. The analysis will also include the effect of tip leakage flow through the clearance gap of a rotating blade row and a method for treating separated flow regions.

Three-dimensional viscous flow calculations are currently under development by several researchers. The extensive amount of literature available will be reviewed to evaluate the best approach to creating this code.

Development of the code will require calibration with test data, which is currently limited in open literature. Special emphasis will be placed on the development of a turbulent viscosity model for calculating shear stresses near walls and a tip leakage model for inclusion of this effect on flow development and losses in unshrouded rotors.

The code will be calibrated using the data acquired from the nonintrusive flow-field measurements. When a suitable number of comparisons are made, the test compressors will be redesigned using the 3-D code. The revised (verification) compressors will

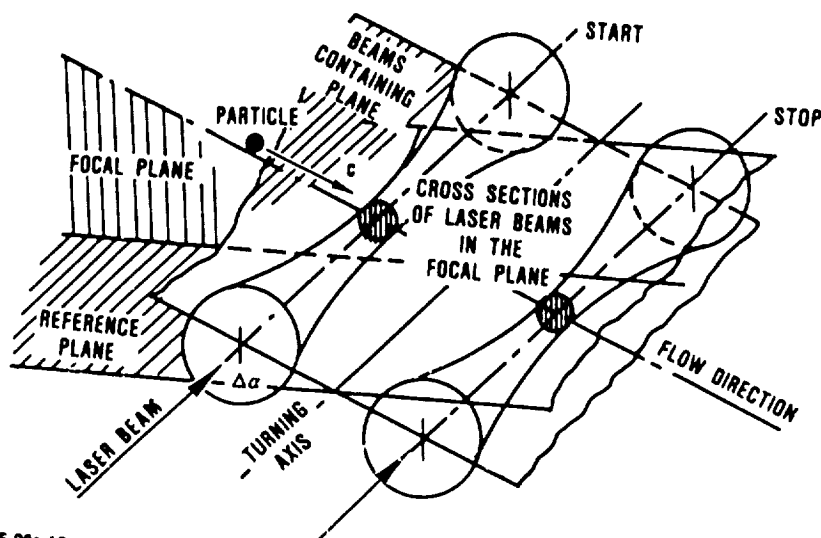
then be tested and compared to predictions, with the code models altered as required based on these comparisons.

Nonintrusive Flow-Field Measurements - Laser velocimeters provide a unique solution for measurements within the flow field of a rotating blade row. The most commonly used laser system is the laser Doppler velocimeter (LDV), but this system does not lend itself well to blade channels with small blade heights. A second system, the laser two-focus (L2F), is less commonly used but has several advantages over the LDV for the measurements required within small turbomachinery blade channels.

The L2F system (Figure 48) measures the time of flight between the two parallel light beams. Particles are seeded into the flow and follow very closely the mean flow direction. Due to the highly concentrated parallel light beams (approximately 100 times greater than in the LDV), the backscattered light from each particle gives a significantly higher signal-to-noise ratio. This feature allows the L2F to make measurements close to channel walls.

The basic accuracy of the L2F mean velocity measurement and low angle resolution is approximately ± 1 percent. This accuracy applies to lower turbulence levels that occur away from the walls. In the near-wall or high-turbulence region, and in zones of separated flows, the accuracy can decrease to ± 5 percent.

Initial measurements will be performed on a single-stage, axial-flow compressor. Velocity profiles will be measured within unbladed, stationary vane, and rotating blade portions of the flow path. To verify the accuracy of the initial L2F measurements, a traversing probe (hot wire and cobra types) will be used in the same portions of the unbladed flow path. These measurements will then be used to verify and calibrate the 3-D code.



65-281-18

Figure 48. L2F Measuring System.

Multistage axial compressor measurements will then be made, followed by measurements within a high-pressure-ratio centrifugal compressor stage. The data from these tests will be used to calibrate and model the 3-D code.

R. Performance Optimization of Impeller/Diffuser/Crossover for a First-Stage Centrifugal Compressor

The objective of this program is to determine the first-stage design parameters that maximize stage performance. Prior studies have shown that, for the largest impeller-exit blade angle allowed from stress considerations, impeller specific speed (rpm), and blade number (with splitters) are the two design parameters having the greatest impact on attainable stage efficiency. Impeller diffusion ratio appears to be of secondary importance as long as reasonable levels are employed. It is also known that detailed impeller-blading design has an important influence on efficiency. The effect of speed and blade number will be tested to establish the trade-off between viscous (friction) losses and blade-loading losses.

Program Description

This program consists of four major tasks, from impeller design through a stage aero rig test, as shown in Figure 47. The program, which is planned for three years, has the potential to improve overall compressor performance efficiency by as much as 0.5 percent.

Three first-stage impellers will be designed that independently vary blade number (with splitters) and treat specific speed relative to a baseline configuration. These impellers will be fabricated and tested in a rig to provide detailed performance and impeller-exit flow conditions. Blading design will employ

the most advanced quasi-3-D and full-3-D methods available to ensure high performance potential.

A diffusion system and crossover (deswirl) ducting will be designed based on the latest available technology. These areas will be tested using the best of the three impellers to establish first-stage performance capability.

Technical Approach

A preliminary design study will establish the exact range of the parameters to stay within reasonable limits on stress levels and practical fabrication methods as projected to the year 2000.

The compressor will be sized and configured to allow use of one of several existing basic compressor rigs. The compressor configuration will be based on GTEC-proven design techniques based on a recent state-of-the-art compressor.

To ensure high performance potential, the detail blading design will employ the most advanced, full 3-D methods available. Test instrumentation and the technique used will be the most advanced and definitive available.

S. Performance Optimization of Second-Stage Centrifugal Compressor Based on First-Stage Exit Conditions

The objective of this program is to establish optimum second-stage design parameters in view of the flow conditions exiting the crossover duct of the first stage of a two-stage centrifugal compressor. This technology is required in advance of full-stage compressor development in order to thoroughly explore compressor design options and ensure that proper design-parameter selections can be made.

By optimizing the second stage for the flow conditions exiting the first stage, inlet and secondary flow losses can be reduced, with a resulting improvement in stage efficiency. The potential benefit is estimated to be a 0.5 percent improvement in overall two-stage efficiency.

Program Description

This program consists of three major tasks, from impeller design through aerodynamic rig testing of a verification compressor, as shown in Figure 47. This program, as defined, will parametrically examine the effect of design parameters on stage performance. Typical flow conditions exiting the upstream stage will be established (from Program R), and inlet ducting designs (with variable vanes) will be developed to simulate those conditions. Three impellers will be designed for the second-stage centrifugal compressor design conditions of the rotorcraft (simple cycle) two-stage centrifugal compressor. These impellers will have modified inducer-blade angles to accept the different swirl and through-flow distributions, along with a baseline design for zero swirl. These impellers will be tested with the simulated upstream conditions over a range of swirl angles. Following evaluation of these test results, two diffusion systems will be designed for the best configuration and stage-performance potential established. A final report documenting these results will be written.

Technical Discussion

The typical flow conditions at the inlet to the second stage of two-stage centrifugal compressors have skewed profiles in both pressure ratio and angle. The present program is directed toward parametric investigation of design techniques to improve second-stage performance based on these skewed profiles. The impeller

designs will be modified to incorporate typical measured inlet gradients in pressure and swirl. Test results will be used to modify downstream diffusion systems to match any new impeller exit profiles as a result of the changes in impeller design. Subsequent tests will be made to verify the improvement in stage performance for this technology item.

T. Centrifugal Compressor Casing Treatments

The objective of this program is to reduce the tip-clearance sensitivity and improve the surge margin of centrifugal compressors. A reasonable amount of casing treatment study has been done for large axial compressors. A much smaller technology base is available for small centrifugal compressor stages. The benefit of this program will be to ascertain the impact of passive shroud treatments on surge margin and tip clearance of small compressor stages. These efforts are needed in advance of full-stage compressor development in order to thoroughly explore compressor design options and ensure that proper design-parameter selections can be made. It is projected that a one-point improvement in stage efficiency can be achieved at constant surge margin.

Program Description

This program is scheduled as one task, from stage design through aerodynamic rig, as shown in Figure 47. The program will evaluate a series of centrifugal-compressor casing-treatment concepts including grooves, slots, and holes in the impeller shroud. The position of these configurations will be varied along the shroud to determine their effect on tip clearance losses and surge margin. The proposed program will include design, fabrication, and test of these concepts.

Technical Approach

The proposed program will examine the effect of the various shroud configurations on surge margin and tip clearance losses. An existing rig that has a clearance control spindle capability will be used to evaluate the clearance effect. The shroud configurations will include some that are positioned in the knee and trailing-edge region for this clearance study.

Due to the strong interaction of the stages at part speed, the surge margin investigation will be done on a two-stage rig. In the two-stage configuration, the first stage operates to the left of its normal surge characteristic at part speed. Therefore, the casing treatment configurations have their most influence in this situation.

U. Improved Diffusion Systems

An extensive program is proposed for reducing diffusion system losses as well as maintaining existing performance in smaller envelope constraints. The benefits derived from this program are a higher-efficiency centrifugal stage and/or lower weight and reduced cost stages.

Program Description

This program, set up to establish technology for improved diffusion systems, consists of three major tasks, from diffuser design through stage tests, as shown in Figure 47. The program is directed at initial flow-rig testing to examine diffuser concepts followed by stage testing of the most promising configurations. Diffuser configurations will include those believed to lower inlet losses as well as improve surge margin, plus diffusers that increase the diffusion rate downstream of the throat

of the diffusers. Aggressive 90-degree bends will also be evaluated to lower the compressor envelope.

These configurations will be tested on a static-flow rig to be developed as part of the program. This flow rig will have the capability to simulate Mach and Reynold's numbers and to vary inlet total-pressure profiles and swirl distribution. Each of the 3-D diffuser designs will be fabricated and tested on both the static-flow rig and an existing in-house single-stage compressor rig. This dual evaluation will establish the validity of the static rig testing for subsequent diffuser effort. During the test sequence the analysis methods will be reviewed for possible improvement, and the test configuration will be reanalyzed as necessary.

At the completion of this analysis, the most promising concepts will be combined into a single-stage test configuration to demonstrate the benefit of this technology.

Technical Approach

Separate static-flow rig and full-stage tests will be conducted to sort potential diffuser configurations into two areas. The first application is to reduce losses in the inlet region of the diffuser. The second application is to maintain existing performance levels, but to reduce stage weight and cost by reducing compressor envelope diameter.

The first method involves determining the effects of swept leading-edge and nonsymmetric endwall configurations on compressor performance. In addition, the effects of endwall circumferential communication slots and diffuser bleed will be examined in terms of surge margin and rematch capability.

The second application is directed more toward reduced cost and lower weight by means of a reduced compressor envelope. Diffusion rates exceeding current technology will be evaluated, as will be the use of 90-degree bends (that are tighter than current design practice permits). The diffusers of increased diffusion rate will result in smaller envelopes because they will be designed for the same exit Mach number. Surge margin and efficiency will be evaluated in this test phase.

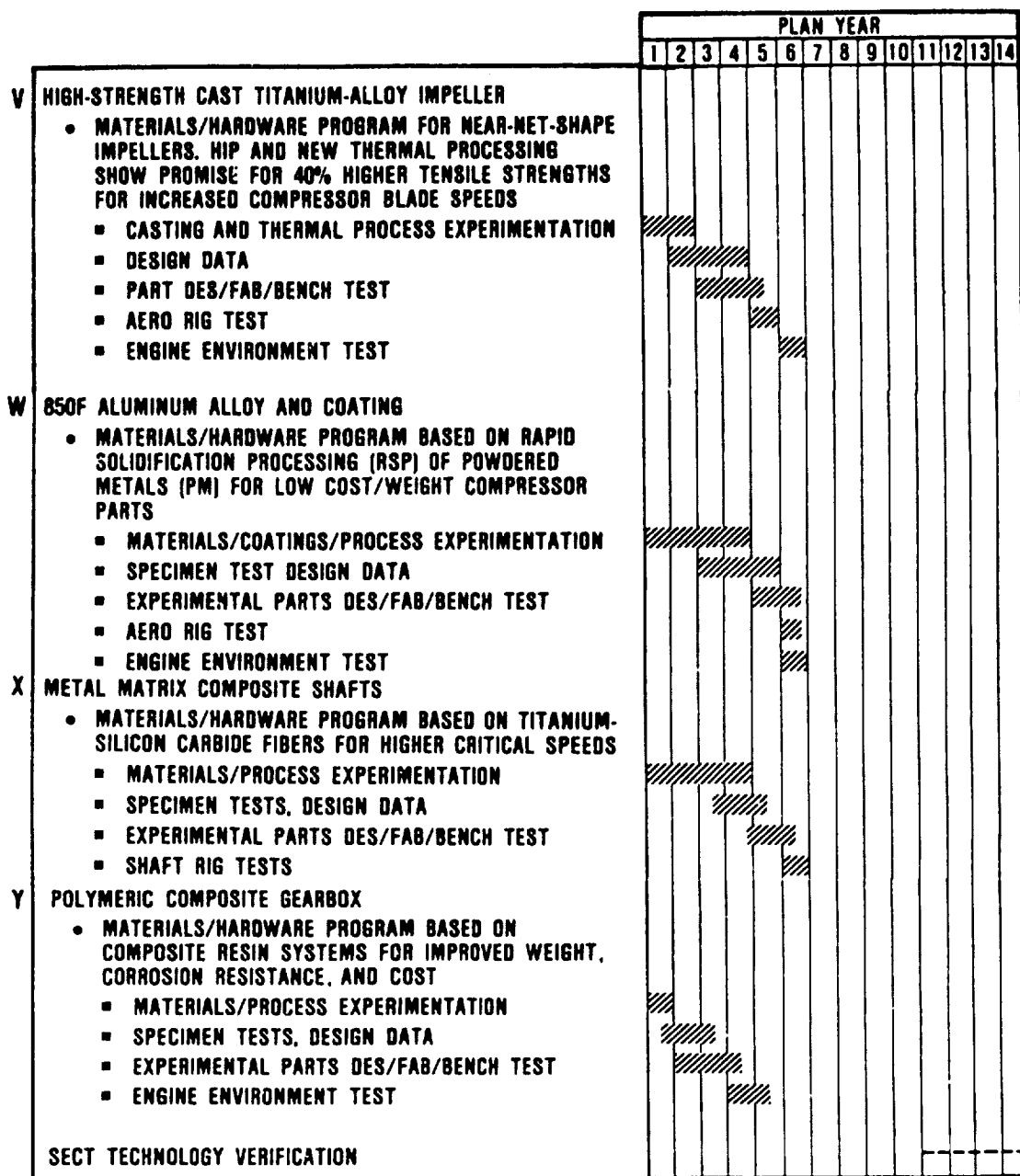
The benefits of this program will be applicable primarily to the rotorcraft and commuter applications.

2.4.2.7 Materials for "Cold Parts"

This plan consists of four discrete technology programs, identified as V through Y in Figure 49. Experimental materials programs that include evaluation testing, they are scheduled to be run independently.

V. High-Strength Cast Titanium-Alloy Impellers

Titanium alloys are often used in applications where a high ratio of mechanical-properties-to-weight is important. Specifically, such alloys are typically used in dynamic applications such as fan and compressor blades in gas turbine engines where a high level of tensile and fatigue strength is critical. However, these strength characteristics of the selected alloy must be accompanied by good toughness and high resistance to impact damage and crack propagation. The alpha/beta titanium alloys in which the alpha and beta phases are present at low temperatures are commonly used for these applications. To use these alloys effectively in such dynamic applications, the wrought material is conventionally used because of its superior fatigue strength compared with that of castings produced from the same alloys.



85-281-58

Figure 49. Material Technology Schedule for "Cold-Section Parts."

Recent advances in thermal processing of titanium alloys have demonstrated greatly improved mechanical properties of titanium castings, to a level equivalent to those of forged components. The constitutional solution treatment (CST) process developed by Howmet is a unique, nonconventional thermal processing concept that modifies the microstructures of titanium alloys, allowing them to achieve mechanical property levels superior to those attained by conventional heat treatments. The benefits of this new process include:

- o Highly uniform microstructure and properties not producible by any other technique
- o Insensitivity to section size
- o A wide range of uniform structures that can be produced to allow tailoring of properties
- o A highly controllable and reproducible process

In combination with advanced thermal processing concepts, the selection of high-strength titanium alloys such as Ti-6Al-2Sn-4Zr-6Mo (Ti-6246) optimizes material capability to meet advanced engine design requirements. Projected improvements in tensile and high-cycle fatigue strengths of up to 40 percent over forged Ti-6Al-4V are expected. These higher strengths will make possible the operation of compressor impellers at significantly higher speeds, permitting higher pressure rises per stage.

Program Description

This program consists of five major tasks, from casting experimentation through engine environment tests, as scheduled in Figure 49. The second-stage compressor impeller of an existing

turbofan engine has been selected as the component to verify this technology. The impeller will be mechanically redesigned to reduce its weight, using the higher strengths attainable in CST-processed Ti-6246. Ti-6246, having the highest strength capability among the alpha/beta family of titanium alloys, is the material selected for casting the compressor impeller.

Conventional investment casting techniques, as currently practiced by the industry, will be used in producing the net-shape-compressor impeller. This involves fabricating hard tooling to generate the impeller wax pattern, casting the impeller, and hot isostatic pressing (HIP) to fully densify the titanium casting. Casting iterations and tool rework will be required to establish dimensional reproducibility of the component as well as to optimize yield.

Concurrent with the casting process optimization, heat treat process development will be conducted. Its objective will be to achieve the best balance of mechanical properties in a cast Ti-6246 titanium impeller. Results of these programs will lead to the generation of a design data base. Component evaluation, followed ultimately by engine testing, will provide validation of the technology.

W. 454C (850F) Aluminum Alloy and Coating

The advanced gas turbine engines at GTEC for propulsion systems and auxiliary power units (APU) for both military and commercial aircraft, demand advanced alloy systems. Lightweight alloy systems possessing high-strength, high-temperature capabilities form the material basis for these modern gas turbine engines. At GTEC, aluminum alloys are used for applications below approximately 182C (360F), with titanium alloys used for applications from 182 to 482C (360 to 900F).

The emergence of rapid solidification processing (RSP) technologies has made possible the development of advanced metal alloy systems with significantly improved basic material properties. RSP powder metal (PM) aluminum alloys specifically made for elevated temperature service offer significant payoffs for gas turbine engines. These advanced aluminum alloys offer an enhancement of high-temperature strength via a large volume fraction of thermally stable, dispersed, intermetallic phases. These aluminum alloys demonstrate the potential for replacing titanium alloys in 182 to 343C (360 to 650F) applications, with a 35 percent weight savings. This weight change results in a decrease in inertial momentum and a more responsive engine. In addition, aluminum alloys are less costly than titanium alloys.

Advanced aluminum alloys that show great potential for high-temperature service are those based on the binary Al-Fe system, with ternary additions (Cr, Nb, Hf, Mo, Ti, Si, W, Zr, V, and rare earth elements) used to increase the thermal stability of the dispersed iron aluminide precipitates. Two PM aluminum alloy systems that have demonstrated superior mechanical properties up to 343C (650F) are the PM atomized Al-Fe-Mo (Pratt & Whitney) and Al-Fe-Ce (Alcoa) alloy systems. Two other alloy systems that have demonstrated high-temperature capabilities are the Al-Fe-V and the Al-Fe-Zr alloys produced by the planar flow casting (PFC) proprietary technique of Allied Chemical (based upon the melt-spinning principle). These metallic ribbon alloys have been shown to contain higher volume fractions of dispersed intermetallic phases than PM atomized alloys, a difference attributed to orders of magnitude difference in the maximum cooling rate available with the PFC technique (10^6 to 10^7 C/sec) as opposed to atomization techniques (10^4 to 10^5 C/sec).

A major drawback of these aluminum alloys is that they are more susceptible to particulate erosion damage than titanium

alloys. Small gas turbine engines in helicopters, ground power units, and other low-altitude applications (particularly over dusty, unimproved land areas) routinely ingest considerable amounts of sand and dust. Engine components operating directly in this erosive airflow consequently suffer progressive degradation in both physical and performance characteristics. Therefore, erosion protection for critical airfoil surfaces is needed to utilize the benefits of advanced aluminum alloys in these engine applications.

Program Description

This program consists of five major tasks, from materials experimentation through engine environment testing, as scheduled on Figure 49. Aluminum alloys produced by the Allied PFC technique represent a great potential for the development of 454C (850F) engineering material. Metallic ribbon alloys (which are later crushed to a powder form and consolidated into a billet) made by PFC have a larger volume fraction of dispersed phase than does PM-atomized aluminum alloy. This results in enhanced material strength properties. Research by Allied indicates that a 35 to 40 percent volume fraction of the dispersed intermetallic phases are required to meet the Air Force's 277 MPa (40 ksi) ultimate strength goal for a 454C (850F) aluminum alloy. Improved metallic ribbon alloy systems are the selected approach to achieve this goal.

If the ribbon alloys do not meet the 454C (850F) minimum property goals, alternative technologies will be pursued to improve the temperature capabilities of the optimized ribbon alloys. Previous research has indicated that minor elemental additions to the optimized PFC alloys can result in an improvement of the thermal stability or a modification to the dispersed

intermetallic precipitates, resulting in a subsequent increase in high-temperature properties. Another technique that has the potential to improve high-temperature material properties is to incorporate a reinforcing material into the aluminum matrix, which provides metal matrix composite (MMC) materials. Arco Metals Company's Silag Operation is a source of SiC whisker and particulate reinforcing materials, which have previously been very effective in improving the high-temperature strength of the matrix alloy when combined with an MMC. The incorporation of SiC has also been shown to improve the wear resistance of the MMC, which, in turn, should improve erosion resistance.

Even with enhanced erosion resistance due to SiC, a protective coating for the 454C (850F) material is required to further increase its erosion resistance. This coating will be similar to those being developed by GTEC for the Alcoa Al-Fe-Ce PM alloy.

The PFC metallic ribbon alloys effort will be performed concurrently with an effort on SiC reinforcement of PFC alloys. These phases of the program will subsequently interact with the fabrication of a compressor rotor. The coating aspect of this program will be concurrent with the later stages of alloy development and the early stages of compressor fabrication and testing. Preliminary results of the coating and prototype phases will be used to initiate the fabrication of an advanced 454C (850F) aluminum alloy compressor rotor with a particulate erosion-resistant coating, to be followed by testing for the evaluation of the coated component. Subsequent rig testing will be used to verify the feasibility of the component/coating system for engine applications described in this program.

The results of this program will lead to a class of aluminum alloy compressor rotors that can be substituted for titanium

alloys in engine applications up to 454C (850F). The alloys will be generically applicable to a wide variety of small gas turbine engines.

X. Metal Matrix Composite Shafts

High-speed gas turbine rotor dynamics experience has generally been restricted to relatively short, stiff rotors operating below the first bending mode critical speed. This restriction is due to the large rotor excursions and bearing loads encountered with operation near or through this critical speed. The resulting operating speed limitations place restrictions on the design configuration and performance of multispool turbine engines. Operation below the first bending mode is achieved by restricting rotor speeds, minimizing shaft lengths, and using large shaft diameters (especially for the low-pressure rotor). However, reduced LP rotor speeds reduce the maximum attainable turbine performance, while a large LP shaft diameter imposes larger bearing diameters and disk bores on the high-pressure (HP) rotor than are usually desirable. These size constraints impact the HP spool design by imposing higher bearing loads and greater rotor system size and weight for the required disk burst margins and low-cycle-fatigue lives.

Use of an advanced shaft material with a high ratio of elastic-modulus-to-density (E/ρ) will increase the shaft critical speeds and minimize the constraints as previously discussed. This critical speed advantage can be employed in one or more of the following ways:

- o The rotational speed of the shaft can be increased
- o The shaft diameters can be decreased
- o The unsupported length of the shafts can be increased

Increased shaft speeds can facilitate improved performance via lower airfoil loadings or reduced stage counts (for a given critical speed margin). Reduced shaft diameters or longer unsupported shaft lengths can provide reduced mechanical complexity of the shaft/bearing package and reduced engine weight. Reduced diameter shafts will be required to accommodate small disk bores (for bore stresses) for the high rotational speeds projected for year-2000 engines.

Silicon carbide fiber reinforced titanium is an advanced metal matrix composite material offering high E/p values for shafting applications in conjunction with high torsional strength capability and demonstrated fabricability. This material system exhibits E/p values two to three times higher than those of conventional shafting materials such as steel- and nickel-base alloys. In addition, titanium/silicon carbide turbine engine components have been fabricated at GTEC and elsewhere in the industry using established diffusion-bonding techniques.

Prior metal matrix composite shaft efforts have stressed retrofitting advanced shaft designs into existing engines, which necessarily sacrifices overall system benefits. The proposed program emphasizes the design of the rotor/shaft system with the power turbine rotors of SECT rotorcraft and commuter engines as prime candidates.

Program Description

This program consists of four major tasks, from materials experimentation through shaft rig tests, as scheduled on Figure 49. The program will be conducted on shafting and rotating groups sized to be representative of the SECT rotorcraft engine. The program will use Avco SCS-6 silicon carbide fiber in a Ti-6Al-4V matrix, with the fiber volume fraction and orientation

dependent upon the outcome of a preliminary rotor design study. After selection of the basic shaft manufacturing approach, a concept validation study will be conducted during which subscale shafts will be manufactured using the fiber loading and diffusion-bonding parameters required for full-scale shafts. These shafts will be subjected to torsion, bending, critical frequency, and nondestructive evaluations to validate the basic design and fabrication approaches selected for the full-scale shafts. Mechanical property design data will then be applied to panels fabricated using the fiber loading and processing parameters selected for the full-scale shafts, with a final shaft design iteration conducted based on the design data. A pilot manufacture demonstration involving 30 full-scale shafts, five of which will be fully machined for shaft rig dynamic testing, will follow. The remaining 25 shafts will be subjected to extensive bench and component tests to assess the consistency of the manufacturing process and methods for process scale-up.

Y. Polymeric Composite Gearbox

The development of polymeric composite gearboxes will result in a weight reduction of about 25 percent, as compared to cast aluminum gearboxes, and 10 percent compared to cast magnesium gearboxes. It will also eliminate the corrosion problems frequently encountered in magnesium gearboxes. In addition to the weight reduction, an initial cost reduction of about 25 percent is foreseen when the composite gearbox is compared with a cast aluminum or magnesium part. The composite gearboxes will be generically applicable to accessory gearboxes for rotorcraft and commuter engines, for APUs, and for the reduction gearboxes required in commuter turboshaft engines.

The composite gearbox will be made by compression-molding two pieces, which will be joined by a bolted flange at the split

line. The composite resin system will be chosen to meet the criteria of 204C (400F) stability, compatability with all anticipated lubricants, and ease of processing. The fiber reinforcements will be selected for stiffness, compatability with the selected resin system, and cost considerations.

The "building blocks" required for this advanced technology gearbox exist today, but the total problem of designing and constructing a composite gearbox for small turbine engines has not yet been addressed. Sikorsky has made considerable progress in developing a large composite gearbox for a helicopter transmission. Many of the lessons learned by Sikorsky on this effort will be directly applicable to the smaller turbine engine gearboxes.

Program Description

This program consists of four major tasks, from materials experimentation through engine environment testing, as scheduled on Figure 49. Slightly more than four years will be required to develop and engine-test a prototype polymeric composite gearbox. The program consists of five major activities.

Concept - The initial program activity will be to select the fabrication concept and material system to be employed. This task will emphasize materials and processing approaches that will produce net-shape components with minimum manufacturing costs in production.

Gearbox Design - Design efforts will be based on an existing engine as a verification vehicle.

The design of a composite accessory gearbox will be an iterative approach that will involve the selected composites fabricator. Thus, the gearbox will be designed for manufacture with composite materials, rather than by specifying composite material for a component designed to be a metal casting. In addition, material design data for the selected material system will be generated to adequately support the design effort.

Tooling and Fabrication - Polymeric gearboxes will require new tooling, which will be designed and manufactured after the gearbox design concept is established. Four prototype gearboxes will be fabricated for testing purposes during this phase.

Bench and Rig Tests - Of the four fabricated gearboxes, one will be instrumented and used for static load tests to destruction to verify that satisfactory design margins are met. A second gearbox will be extensively rig tested. The rig tests will subject the gearbox to the transient loadings expected in an actual engine environment.

Engine Testing - The remaining two gearboxes will be installed on test bed engines and will be tested on a piggy-back basis.

Technical Approach

The technology program will fully demonstrate a lightweight, durable, corrosion-resistant gearbox on an existing GTEC engine. The program will develop the rules and tools to permit successful design and fabrication of composite gearboxes for other small engines, including rotorcraft, commuter, and APUs.

The program will use an existing engine and gearbox as a test bed vehicle.

2.4.2.8 System Technologies

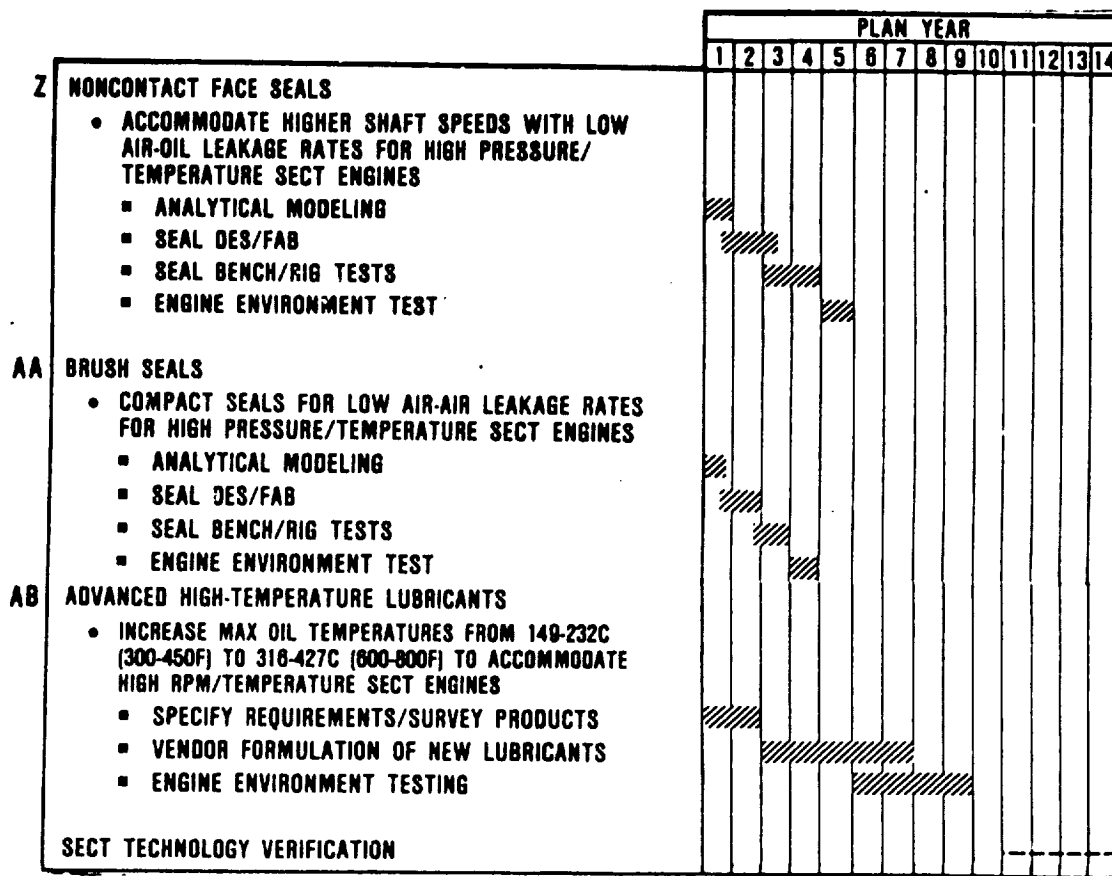
This plan consists of three discrete technology programs, identified as Z through AB in Figure 50. These programs address the mechanical requirements as projected for year-2000 rotorcraft engines.

Z. Noncontact Face Seals

The performance and durability of high-speed gas turbine engines significantly depend on the mainshaft bearing compartment seals. Labyrinth, face, and ring seals are commonly employed as mainshaft seals to seal the oil system from the engine air/gas path working fluids. Even with technological advances in seal materials, coatings, lubrications, and heat transfer, current labyrinth, rubbing contact face, and ring seals demonstrate limited growth potential to withstand the increasingly severe environment projected for future advanced gas turbine engines.

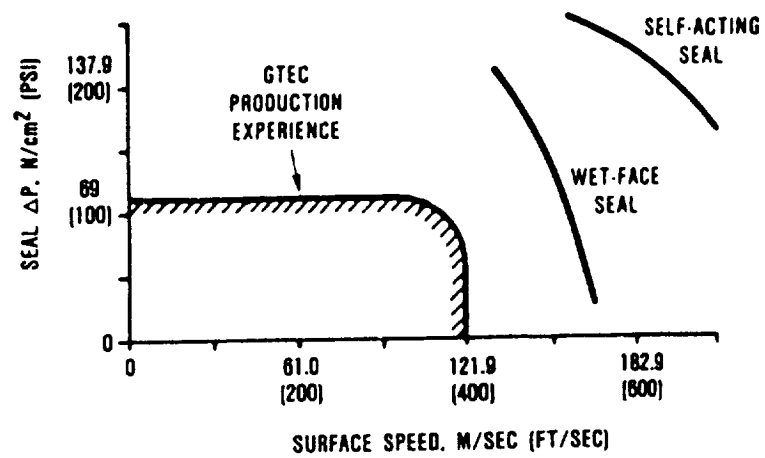
Future generation gas turbine engines will require sealing to be performed at higher speeds, pressures, and temperatures. They will also require lower leakage rates than are achievable for labyrinth and current carbon face and ring seal designs. These same engines will approach mainshaft seal operating conditions of 304 m/sec (1000 ft/sec) surface speed, 206.9 N/cm² (300 psi) pressure differential, and 649C (1200F) sealed gas temperature. In addition, these engines will be compact and lightweight.

Figure 51 shows GTEC's current production engine mainshaft carbon face seal operating conditions and future requirements. Current operating conditions for rubbing-contact carbon face seals at GTEC are approximately 121.9 m/sec (400 ft/sec), 79.3 N/cm² (115 psi), and 316C (600F).



85-281-82

Figure 50. Engine Systems Technology Schedule.



65-281-1

Figure 51. GTEC Experience and Projections for Seal Capabilities.

Labyrinth seals, although not imposing the surface speed limitations of conventional face seals, do have other design limitations. These seals result in greater leakage and, consequently, higher heat input and increased debris contamination of the bearing cavities.

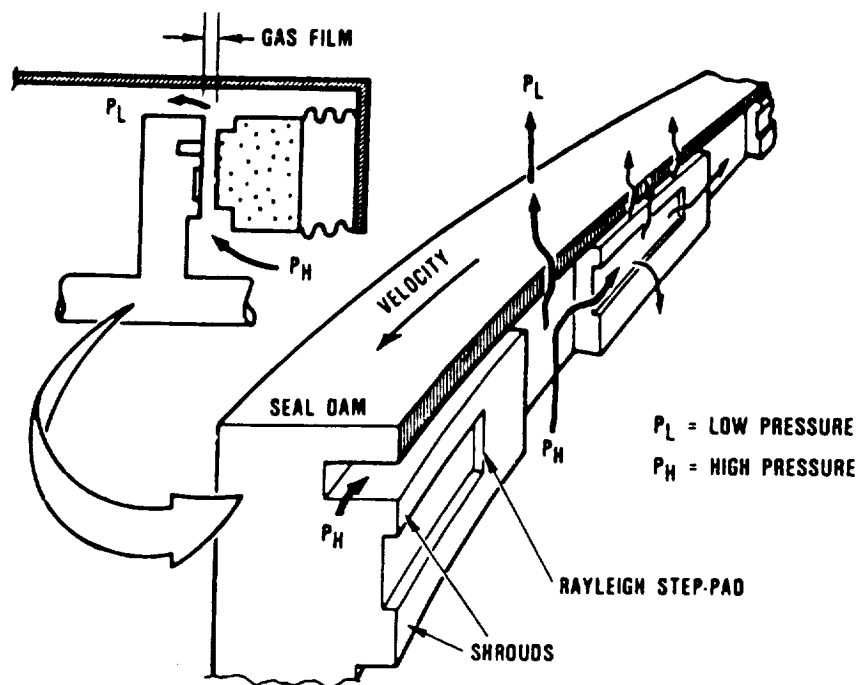
Floating ring seals have operating limits similar to those of face seals. However, a major drawback is that leakage from this type of seal, as it wears, approaches that of a labyrinth seal. This is especially true at higher speed, pressure, temperature, and excursion conditions.

The noncontact, self-acting gas film seal concept offers the best potential to meet the sealing requirements of advanced gas turbines. Figure 52 shows the details of a Rayleigh step-pad noncontact seal geometry. This is one example of many lift-pad geometries that can be used for noncontact seal operation.

The effect of self-acting lift pads is depicted in Figure 53, which shows parallel sealing faces operating without rubbing contact because of a balance between the opening and closing forces. If the seal tends to close, the lift pad hydrodynamic force increases to prevent a rubbing contact. Thus, a condition of no rubbing contact will prevail except at start-up and shut-down.

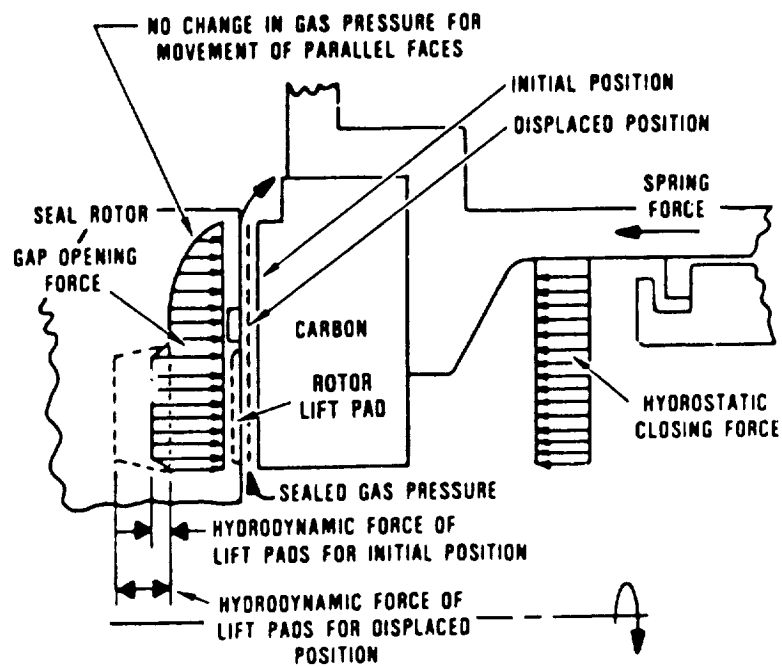
Program Description

This program consists of four major tasks, from analytical modeling through engine environment testing, as scheduled on Figure 50. The noncontact face seals program will entail extensive analytical and experimental efforts. Various aspects of the seal operational modes have been analytically modeled, and it is a topic of considerable current interest. As in the case of most



65-281-3

Figure 52. Rayleigh Pad Seal Operation.



65-281-4

Figure 53. Mechanical, Pneumatic, and Self-Acting Forces on a Rayleigh Pad Seal.

analyses, however, only special cases have been considered, and many modes of operation observed in practice remain untreated by analysis. The noncontact face seals will remain principally an experimental effort, with the analysis as an aid to understanding the physical principles involved.

The method of fabrication of the intricate lift-pad geometries and the identification of suitable materials for these geometries are also significant problems to be resolved.

Extensive analysis will be performed on the lift-pad geometry and seal steady-state operating characteristics during the initial seal design phase. These analyses will include:

- o Seal leak rates using compressible-flow analysis
- o Lifting pad hydrodynamic analysis
- o Pressure balance computations
- o Seal stability analysis
- o Thermal and mechanical distortion analysis.

Technical Approach

This program will be initiated with the design and fabrication of a seal test rig specifically designed to evaluate noncontact face seal operating parameters. To investigate the full operating range of noncontact face seals, the test rig must be capable of operation beyond 10,470 rad/s (100,000-rpm) speed, 206.9 N/cm² (300-psi) differential pressure, and 1200F sealed gas temperatures.

Current GTEC-sponsored R&D efforts will provide a technical basis for the initial lift pad geometry selection. These designs will then be tested to the full extent of the seal operating

parameters. Performance deficiencies will be determined and the design will be iterated and retested.

Seal operational qualities to be determined in this advanced seal test rig include:

- o Rubbing contact operation power loss
- o Rubbing contact seal distortion
- o Carbon lift-off speed
- o Carbon touchdown speed
- o Noncontact power loss
- o Noncontact seal distortion
- o Seal dynamic modes
- o Seal leak rates
- o Seal wear rates

Appropriate fabrication techniques and proper material must be defined. The rotor surface must withstand contact seal operation at low speeds and during many start/stop cycles. The requirement for a hard protective coating to satisfy these requirements compounds the problem of machining intricate lift-pad geometries into this surface. Some processes have already been attempted, with limited degrees of success.

An important consideration is the influence of tolerance on lift-pad operation. Due to the small dimensions involved, large-percentage tolerances may be required to allow for the use of conventional machining processes. The final selection of lift-pad geometry may be determined by the particular design's operational sensitivity to tolerance.

An important requirement for a stable, low-leakage face seal is that the mating surfaces remain plane during operation. Extensive mechanical and thermal distortion analysis will be performed to ensure that this operating condition is satisfied.

Seal performance testing to intermediate speed, differential pressure, and gas temperature of 4188 rad/s (40,000 rpm), 103.4 N/cm² (150 psi), and 316C (600F), respectively, can be initiated on an existing GTEC seal test rig. A new high-speed test rig specifically designed to run noncontact seals to operating limits of 10,470 rad/s (100,000 rpm), 206.9 N/cm² (300 psi), and 649C (1200F) is currently under construction and will be available for this program.

The ongoing GTEC R&D efforts on noncontact seal effort for gas turbine mainshaft sealing applications ensure a solid technical base from which the designs for the extended operating conditions can be achieved. The availability of a suitable test rig that requires only minor modifications to accommodate a wide range of noncontact seal designs and operating experience on an R&D Rayleigh pad noncontact seal enhances the probability of a successful design with program cost effectiveness.

AA. Brush Seals

The performance and reliability of high-speed gas turbine engines depend on the seals. Labyrinth-type seals have been used as the primary air-to-air seal in gas turbine engines. However, these seals cannot meet the increased demands of performance and the required low leakage rates of the small gas turbine engines as conceptualized for the SECT Program.

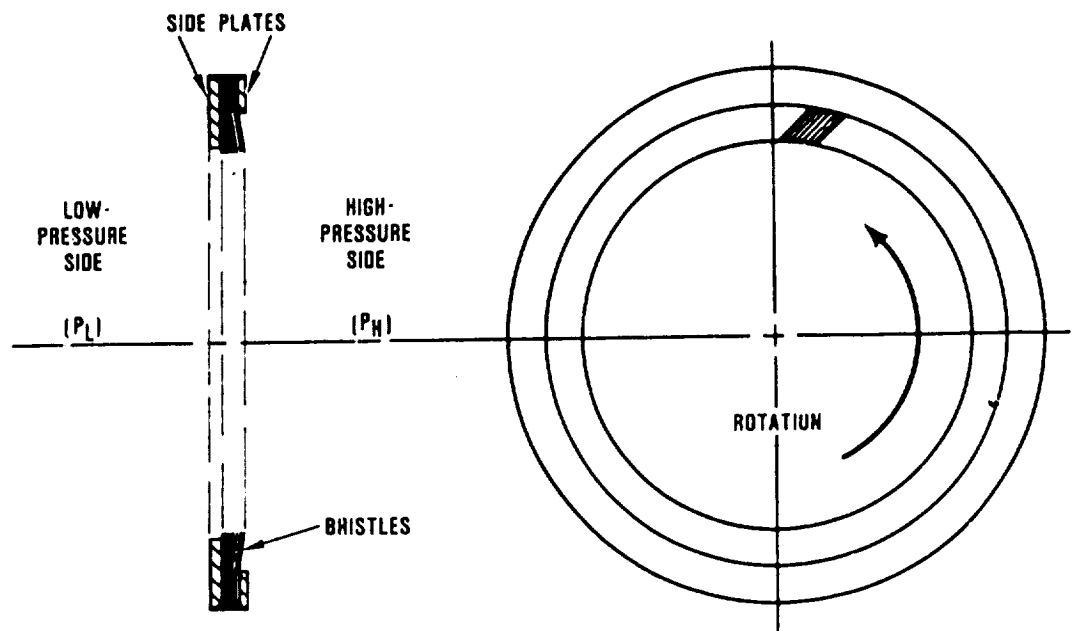
Future gas turbine engines will require seals to perform at higher temperatures, pressures, and peripheral speeds. To meet the increased performance demands, lower leakage rates are also required. Even with the technology advancements in labyrinth seal land materials and coatings, the advanced operating requirements limit growth potential. Labyrinth seals, unaffected by increased temperature and peripheral speed, do have other design

limitations. These seals, which operate with a running clearance, result in high leakage rates and potentially decrease the engine performance. Radial excursions of the shaft typically lead to labyrinth seal run-in and higher leakage rates than is acceptable for future gas turbine engines. In addition, advanced gas turbines are required to be lightweight and compact. Increasing the number of seal knives on a labyrinth seal increases seal performance, but it also increases seal axial length. To meet the requirements of advanced gas turbines, high density air-to-air restrictors for rotating shafts are required.

The brush seal concept offers the potential to meet the increased sealing requirements of gas turbine engines. Figure 54 shows a typical brush seal tested at GTEC. The lay of the bristles and the bristle stiffnesses permit a low starting torque requirement and reduced power consumption. The brush seal offers the reduced leakage rates that are required for advanced gas turbine engines. Besides offering excellent leakage characteristics for air-to-air type applications, brush seals might also be considered for air-to-oil bearing sump sealing if the initial debris generated from the bristles can be diverted around the bearings.

Program Description

This program consists of four major tasks, from analytical modeling through engine environment testing, as scheduled on Figure 50. Development of brush seals will entail extensive analytical modeling and testing. Some aspects of the seal operating characteristics have already been tested. From this testing, certain geometries have shown to be superior. Continued development of this seal geometry will be conducted, primarily with rig testing. Analytical tools will be used as an aid to understanding the sealing physics. The analytical tools will be used to evaluate seal leakage rates, power consumption, initial starting torque, and life predictions.



65-281-15

Figure 54. Typical Brush Seal.

A sizable effort will be devoted to the fabrication of the brush seal. Fabrication techniques are a large portion of the seal cost. Methods will be investigated to reduce fabrication cost without impeding seal performance.

Technical Approach

Current GTEC efforts have defined a base brush seal geometry. This design will be tested to define seal operating parameters. Areas of improvement will be identified, modifications made, and the new design tested. Seal operating parameters to be determined by rig testing include:

- o Air leakage rates relative to:
 - Rotor speed
 - Shaft eccentricity
 - Bristle density
 - Bristle-to-rotor interference
 - Operating time
- o Power consumption
- o Bristle wear rates
- o Rotor coating wear rates
- o Extended life characteristics

The seal will be tested over the entire operating conditions of temperature, pressure differential, and peripheral speed. After extensive rig testing has verified the seal design, the seal will be evaluated in an appropriate engine test bed.

Attention will be given to the material selections for the brush seal bristles and the rotating journal. The journal surface must be capable of withstanding the bristle contact for the

associated speeds and temperatures. Wear of the the journal surface will decrease sealing performance. The bristles must withstand high temperatures and be compatible with the journal coating. Some materials have been identified, and initial GTEC test results are promising.

AB. High-Temperature Lubricants

Advanced technology engines will operate with higher internal pressures, temperatures, and shaft speeds (approximately 65 percent higher) than current designs. At the same time, the size of these engines will become smaller as the components are made more efficient. These factors will place a higher demand on the oil used to lubricate and cool the mechanical components in the engine. This increased requirement on the oil comes from two factors: increased heat generation and sizing of lubrication system components.

The higher temperatures, pressures, and speeds will increase the lubrication system heat load due to increased bearing, gear, and seal losses. The conduction losses into the bearing cavities (in the turbine end) will be increased because of hotter secondary cooling air, and because there will be less room for insulation on the cavity walls (due to reduced engine size). Moreover, churning losses will be increased because of smaller bearing cavity size.

Because the heat load will increase, the lubrication system components (especially the oil cooler) must grow in size and weight in order to keep current oils at an acceptable temperature level. Currently, this temperature requirement is 135 to 149C (275 to 300F). At some point, the size and weight of the lubrication system components become large enough to be considered unacceptable.

There are some oils with temperature capabilities of 204 to 232C (400 to 450F), but they either degrade quickly or are very expensive and therefore not suited for general gas turbine use.

The solution to this problem will be advanced gas turbine lubricants that can operate at much higher temperatures of 316 to 427C (600 to 800F). This will permit the lubrication components, and other engine components, to be smaller.

Program Description

This program consists of three major tasks, from specification requirements through engine environment testing, as scheduled in Figure 50. Creating a high-temperature lubricant for use in gas turbines is a project that will require coordination with oil companies like Exxon, Mobil, and others that are heavily involved in the research and development of lubricants.

The program will be conducted in five primary activities:

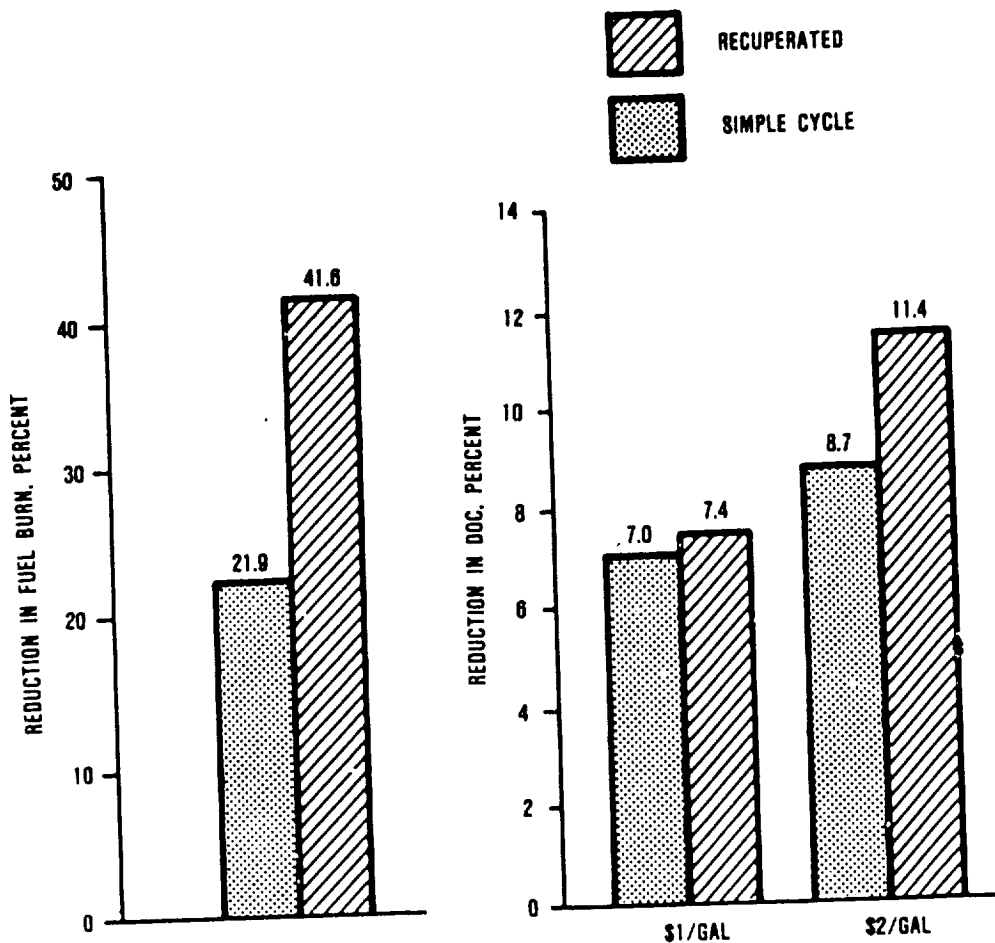
- o Establish the detailed requirements for an advanced high-temperature lubricant. This will include foaming, viscosity, storage, compatibility with elastomers, temperature capability, and cost.
- o Survey the commercially available lubricants to determine the capabilities of current technology. Determine which type of lubricant, if any, would be the most likely candidate for development into a high-temperature lubricant. This will require discussion with a number of lubricant manufacturers.

- o Based on the survey, establish a program with the most qualified vendor. This program should provide some funding to the vendor to encourage work on the program. It would also provide a means of controlling the program's activities.
- o Test the candidate lubricants per GTEC's standard oil certification process, which includes laboratory and engine testing. Engine testing should include cold starting, altitude, storage, and environmental conditions typically required in military programs.
- o When a lubricant has met all of the testing requirements, it would be released for general use in industry.

2.5 Summary

The rotorcraft mission analysis revealed significant reductions in fuel burn, of 21.9 and 41.6 percent, for the simple and recuperated cycles, respectively (Figure 55). The selection of either a recuperated or a simple cycle is strongly dependent on fuel price. The recuperated and simple cycles have similar DOCs at \$1/gallon: approximately 7 percent lower than the reference engine. At the higher fuel price, the advantage clearly shifts toward recuperation (11.4 percent reduction versus 8.7 percent for the simple cycle).

These fuel burn and DOC reductions are strongly dependent on several key technologies, shown in Figure 55. These include advanced materials, component performance, and system technologies.



KEY TECHNOLOGIES

- ADVANCED MATERIALS
(CERAMICS, Ni_3Al ,
CERAMIC RECUPERATOR)
- IMPROVED COMPONENT
PERFORMANCE
(TURBINE, COMBUSTOR,
COMPRESSOR AERO)
- SYSTEM TECHNOLOGIES
(METAL MATRIX SHAFTS,
SEALS)

Figure 55. Rotorcraft Mission Analysis Results.

Fairchild Metro III, for which considerable data exists, as the current technology baseline.

The baseline Metro cross section was modified to provide a standup cabin, as shown in Figure 56. In addition to the cross section modification, the following technologies were applied to the baseline Metro III:

- o Aft-mounted tractor engines
- o Composite construction for the wings, empennage, nacelles, and interior furnishings
- o Bonded lithium aluminum fuselage
- o Higher aspect ratio wings
- o Increased wing loading
- o High lift, low drag flap system
- o Standup cabin with 183-cm (72-inch) aisle height and noncircular cross section
- o Low-drag cockpit
- o T-tail

With the introduction of SFAR 41, the FAR 23 takeoff weight limit of 5670 kg (12,500 lb) has been discontinued for small aircraft used for commuters. Since this rule has been favorably received, it was assumed for this study that it will prevail for year-2000 commuters. Therefore, aircraft takeoff weight for this study was allowed to increase or decrease with engine weight as long as the aircraft can take off at the given maximum power available, 746 kW (1000 shp) per engine. In addition, a change in engine weight was accompanied by a change in nacelle and structural weight.

Aerodynamic improvements were added to the baseline aircraft via wing area/aircraft drag reductions as follows:

3.0 COMMUTER TURBOPROP ENGINES

This section presents Garrett's SECT study approach, methodology, and results as established for the commuter turboprop engines envisioned for the year 2000. The presentation is organized into four major tasks as conducted and described in paragraph 1.2 of this report.

3.1 Task I - Selection of Evaluation Procedures and Assumptions

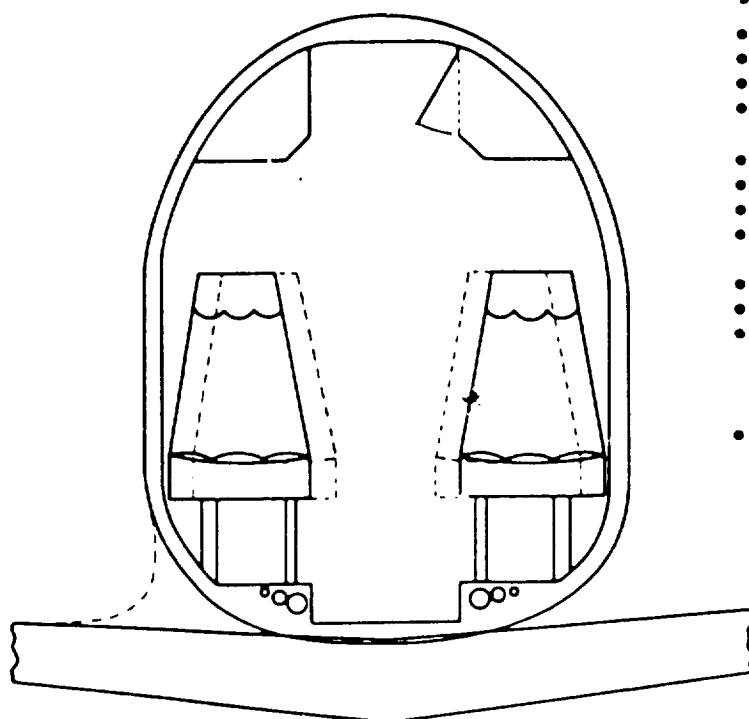
The following paragraphs present the study results for the reference aircraft, mission, engine, projected environmental constraints, economic model, and the trade factors.

3.1.1 Reference Aircraft for Commuter

A reference aircraft was configured and sized for this study based on the following primary assumptions:

- o FAA Regulations, FAR Part 23, Part 135(A), and Part 41
- o Two-engine installation (based on reference engines as defined in paragraph 2.1.3).

These assumptions led to the selection of a 19-passenger size class aircraft. Study efforts included a survey of existing 19-passenger commuters as well as potential year-2000 airframe technologies. NASA-funded studies (reference 4) conducted by Boeing, Cessna, Lockheed, General Dynamics, and Beech, were reviewed for possible airframes and technologies. Based on this review, an aircraft employing technologies from several of these studies was characterized. The derived aircraft is based on the



DIMENSIONS

- 48-CM (18-INCH) AISLE WIDTH
- 183-CM (72-INCH) AISLE HEIGHT
- 48-CM (18-INCH) SEAT WIDTH
- 38-CM (15-INCH) FLOOR-TO-SEAT CUSHION BOTTOM
- 2.5 M³/M OVERHEAD STORAGE
- 30-CM (12-INCH) WINDOW HEIGHT
- 8.35-CM (2.5-INCH) CABIN WALL THICKNESS
- 8.98-CM (2.75-INCH) FLOOR THICKNESS UNDER AISLE
- 152-CM (60-INCH) EXTERNAL WIDTH
- 198-CM (78-INCH) EXTERNAL HEIGHT
- SEATS MOVE 5-8 CM (2-3 INCHES) INTO AISLE DURING FLIGHT FOR GREATER COMFORT. SEAT RETURNED TO POSITION AGAINST WALL FOR EASIER BOARDING
- 2.58 M² (27.60 FT²) FRONTAL AREA

65-281-68

Figure 56. Standup Cabin for Reference Commuter.

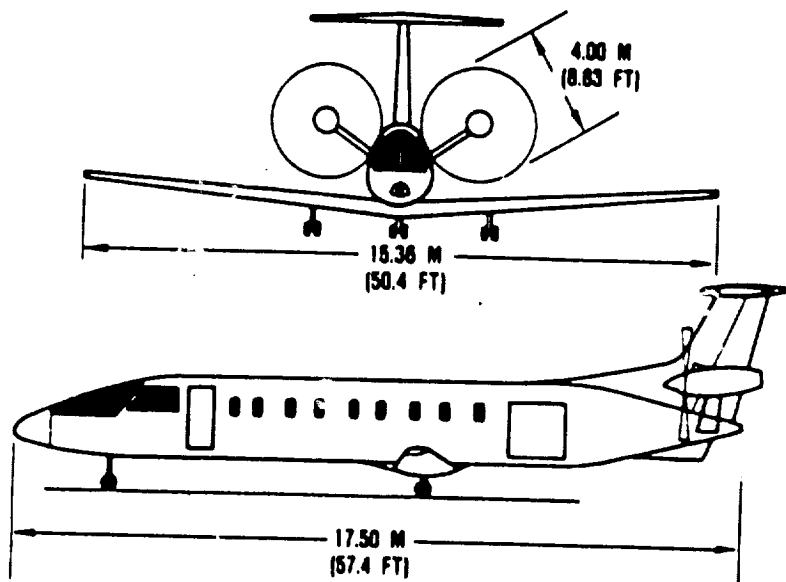
- o Reduction of aircraft weights through the use of composite materials
- o Strut-mounting the engines/nacelles to eliminate the interference drag at the wing-fuselage-nacelle channel and to avoid the ineffective area of the wing covered by the nacelle
- o Allowing for improved surface finish due to use of composites

With the baseline configuration established, the aerodynamics for the reference engine were then estimated. The methodology used for estimating aircraft drag was calibrated by generating the known Metro III polar. The same methodology was then used to calculate the drag polar for the year-2000 technology commuter aircraft.

Figure 57 shows side and front views of the SECT reference aircraft and presents a data summary.

3.1.2 Reference Mission For Commuter

A turboprop commuter mission typically consists of several stages with varying lengths. The operator/owner of a 19-passenger commuter would typically have a different route than does the operator/owner of a larger or a smaller airliner. Therefore, a statistical examination was made of route analysis requests made to a 19-passenger commuter airframe manufacturer. Results are shown in Figures 58 and 59. Current mission stage lengths range primarily between 139 km (75 nm) and 278 km (150 nm). The mean route segment is 272 km (147 nm); the most often recurring route segment is 139 km (75 nm). Figure 58 shows that more than 50 percent of the takeoffs and landings occur below 305m (1,000 ft) altitude, and approximately 70 percent of them occur below 610m (2,000 ft).



- 19 PASSENGERS
- TWIN ENGINE 746 KW (1000 SHP) EACH
- CRUISE L/D = 7 TO 8
- EMPTY WEIGHT = 3088 KG (6808 LBS)
- OPERATING WEIGHT EMPTY (OWE) = 3343 KG (7370 LBS)
- PAYLOAD = 1637 KG (3610 LBS)
- FUEL = 953 KG (2100 LBS)
- TOGW = 5933 KG (13,080 LBS)

FEATURES

- BONDED ALUMINUM LITHIUM ALLOYS — FUSELAGE
- COMPOSITES — EMPENNAGE, NACELLES, MAIN WING

65-281-52

Figure 57. SECT Reference Commuter Aircraft.

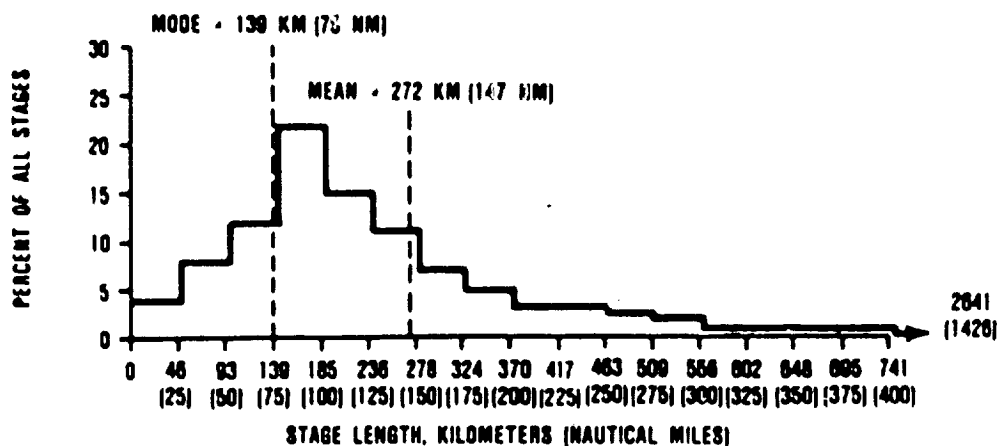


Figure 58. Present Commuter Aircraft Stage Lengths.

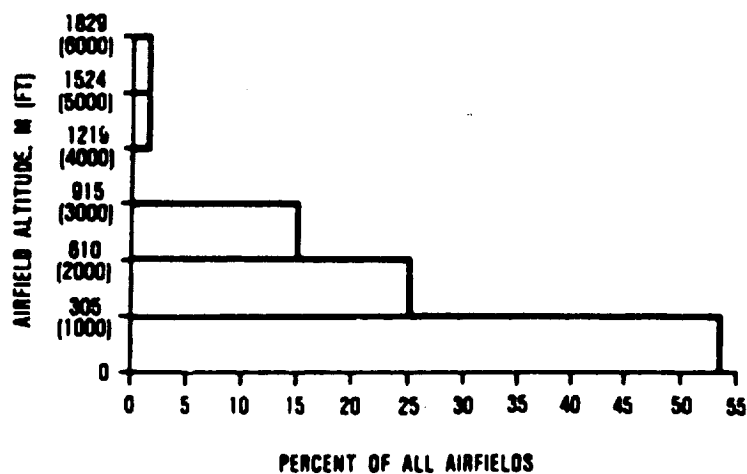


Figure 59. Survey Results of Present Airfield Altitudes.

Based on the statistical survey, a year-2000 reference commuter mission was established as follows:

- o Route Segments A four-segment mission was selected with the following stage lengths:

Stage	1	2	3	4
Length, km	139	278	185	139
(nm)	(75)	(150)	(100)	(75)

- o Takeoff Altitude Since most takeoffs occur at low altitude, sea level was used for takeoff and landing.
- o Ambient Conditions ISA conditions were selected for the flight envelope.
- o Cruise Altitude This was computed for the reference case and will be engine-dependent for the year-2000 engine commuter systems.

An analysis of optimum altitudes based on reference aircraft (paragraph 3.1.1) and the reference engine (paragraph 3.1.3) shows a dependence on block-time parameters. Since block time is controlled mainly by the time to climb to a cruise altitude and maximum cruise speed, the optimum altitude is selected based on the trade between maximum cruise speed versus altitude and time to climb. The maximum cruise speed varies only slightly with altitude for this case. Thus, the gain in maximum cruise speed possible at higher altitudes does not offset the time to climb to higher altitudes. The optimum altitudes for minimum operating cost for the stage lengths studied, therefore, was found to be at the altitude where V_{MO} (maximum operating

speed) intersects maximum cruise speed (approximately 2438m (8000 ft)).

- o Cruise and Climb Speeds Because time is normally the most expensive parameter in a route analysis, the cruise and climb speeds are set by engine max cruise and max climb power settings.
- o Ground Handling A constant five minutes at idle for taxi on the ground was used between each route segment.
- o Fuel Tankage The fuel tankage on the commuter aircraft design was sized at a maximum to allow the largest number of route segments before refueling is required.
- o Fuel Reserves The flight fuel reserves were selected to be 45 minutes at maximum cruise speed at the cruise altitude for the last 139 km (75 nm) route segment. Since the shortest route segment is flown at the lowest altitude, this segment will result in the maximum reserve fuel.
- o Payload The missions were flown with a full 19-passenger load. A passenger weight of 86.2 kg (190 lb) (passenger plus baggage) was used.
- o Approach One minute at flight idle was used for the approach leg.
- o Refueling Time Penalty If the weight and/or SFC of an engine did not allow the aircraft to fly all route segments without refueling, a 15-minute refueling time penalty was scored against the engine/aircraft block time.

Figure 60 depicts the reference mission for the commuter and summarizes primary data.

3.1.3 Reference Engine For Commuter

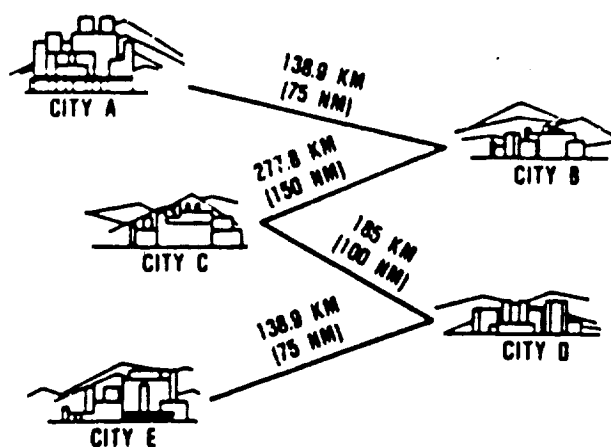
The reference engine for the turboprop commuter application uses the same engine core technology as derived for the rotorcraft reference engine (paragraph 2.1.3); as such, it is based on component performance that represents 1985 engine demonstrated levels.

Configuration - The reference engine has the same general configuration as the rotorcraft reference engine and is shown in Figure 61. Differences, as shown, consist of deletion of the IPS and the addition of an offset propeller gearbox and an annular segment inlet.

Materials - The materials used in the SECT reference commuter engine are identical to those listed for the reference rotorcraft engine as presented in Table 4. Additionally, the commuter engine requires a propeller gearbox with an aluminum housing.

Performance - The commuter reference engine performance is based on the same component performance levels as the rotorcraft reference engine. The engine is sized for 746 kW (1000 shp) at takeoff and is matched for optimum performance at a cruise flight condition as summarized below:

- o Engine Sizing Point - ISA, SL, static condition at takeoff (T/O) power setting (TRIT = 1149 C (2100F), kW = 746 (shp = 1000)



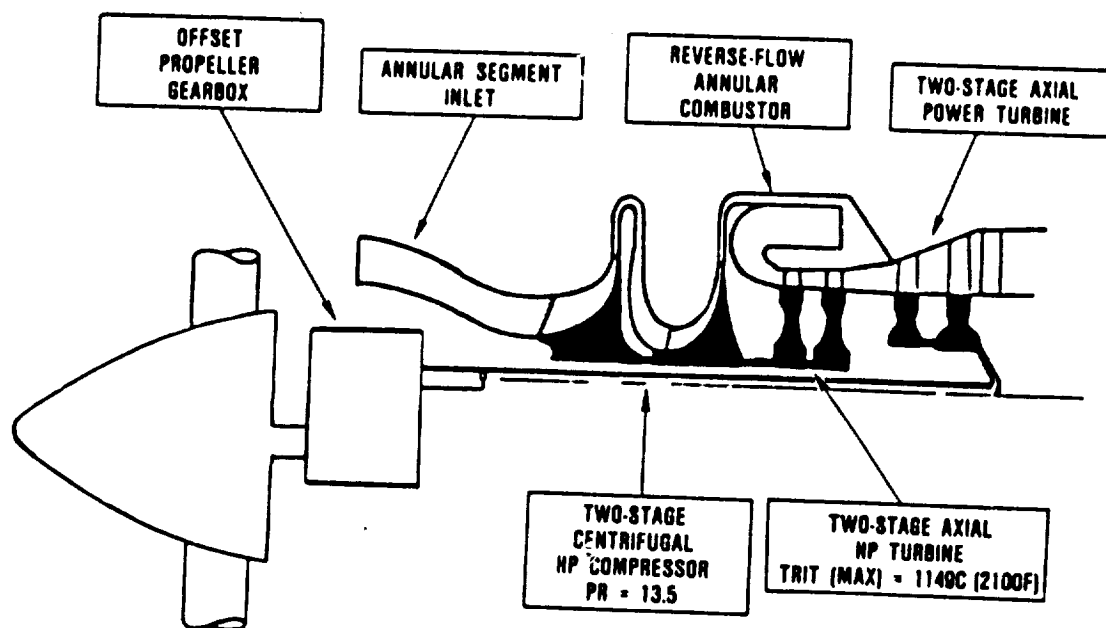
ORIGIN DESTINATION	STAGE DISTANCES, KILOMETERS (NAUTICAL MILES)	PASSENGERS CARRIED	CRUISE SPEED
A-B	139 (75)	19	470 (254)
B-C	278 (150)	19	472 (255)
C-D	185 (100)	19	472 (255)
D-E	139 (75)	19	472 (255)

85-281-104

- MAX CRUISE POWER
- CRUISE ALTITUDE = 2438 M (8000 FT)
- TOTAL DISTANCE = 741 KM (400 NM)
- FUEL CAPACITY = 953 KG (2100 LBS)
- BLOCK FUEL = 817 KG (1801 LBS)*
- BLOCK TIME = 2 HOURS, 37 MINUTES

*INCLUDES 45 MINUTE/RESERVE

Figure 60. Commuter Reference Mission.



85-281-34

Figure 61. Commuter Reference Engine Configuration.

- o Engine Design Point - ISA, 5486m (18,000 ft), 569 km/hr (307 knots) TAS condition at maximum cruise power setting (TRIT = 1093C (2000F))

In sizing the engine, an iteration between the off-design sizing point and the selected design point was necessary. As a result of the off-design operation at the sizing point, the compressor inlet flow of the commuter reference engine is slightly greater than that of the rotorcraft reference engine 3.2 kg/s (7.1 lb/sec) versus 3.0 kg/s (6.7 lb/sec). The resulting turboprop engine and component performance data for these cases are summarized in Tables 14 and 15.

The commuter reference engine achieves 521 kW (699 shp) (2 percent propeller gearbox loss assumed) at the design point. For this case the TRIT has been defined as 56C (100F) below the 1149C (2100F) takeoff power setting. Design point SFC for the reference engine is 0.261 (kg/hr)/kW, (0.430 [(lb/hr)/hp]).

Weight - The commuter reference engine weight has been estimated at 191 kg (422 lb), including accessories and propeller gearbox, as shown in Table 16. This weight was generated by the WATE-S program, which included F109/TSE109 measured and calculated weights for accessories and controls and typical measured propeller gearbox weights from current turboprop engines. Length and diameter were estimated at 42.1 and 15.4 inches, respectively.

Cost - As with the rotorcraft reference engine, cost was estimated based on a mean sell price as depicted on Figure 62A. The sell price range is based on a GTEC market survey of presently available turboprop engines in the 447 to 895 kW (600 to 1200 shp) range. The resulting commuter reference engine cost is \$195,000 (1985 dollars).

TABLE 14. COMPUTER REFERENCE ENGINE DESIGN POINT DATA

Overall Engine Performance		Component Performance	
Design Point Performance - 3,486m (11,437 ft), 569 km/hr (307 knots) TAS, ISA, Uninstalled With No Production Margins			
		<u>HP Compressor</u>	
		<u>1st Stage</u>	
Engine Rating, kW (shp)	521 (699)	o PR	4.73
SFC, (kg/hr)/kW, (lb/hr)/hp	0.261 (0.430)	o η_{AD}	81.8
Turbine Inlet Temperature		o η_{Poly}	85.3
o HP Turbine, C (F)	1093 (2000)	<u>2nd Stage</u>	
o LP Turbine, C (F)	737 (1359)	o PR	2.85
Overall Cycle PR	13.36	o η_{AD}	81.6
Inlet \dot{W}/δ , kg/s (lb/sec)	3.230 (7.120)	o η_{Poly}	85.3
\dot{W}_{LP} , rad/s (rpm)	2408 (23,000)	<u>Overall</u>	
\dot{W}_{HP} , rad/s (rpm)	4542 (43,380)	o PR	13.5
Fuel LHV, kJ/kg (Btu/lb)	42,798 (18,400)	o η_{AD} , %	78.7
		o η_{Poly} , %	84.7
		o Exit \dot{W}/δ , kg/s (lb/sec)	0.34 (0.74)
		<u>Compressor</u>	
		o η , %	99.94
		o $\Delta P/P$, %	4
		<u>HP Turbine</u>	
		o \dot{W}/δ , kg/s (lb/sec)	0.53 (1.16)
		o η_{AD} , %	87.0
		o Cooling Flow, %	6.8
		o Interturbine, % ($\Delta P/P$)	1.4
		<u>LP Turbine</u>	
		o \dot{W}/δ , kg/s (lb/sec)	1.96 (4.31)
		o η_{AD} , %	88.5
		o LPT-MO2 $\Delta P/P$, %	2.5
		<u>Propeller Gearbox</u>	
		o η , %	98.0

*Stator and blade cooling flows are shown. The second-stage stator and blades are uncooled. The balance of the cooling flows (4.9%) are used for disk and firtree cooling.

*Stator and blade cooling flows are shown. The second-stage stator and blades are uncooled. The balance of the cooling flows (4.9%) are used for disk and firtree cooling.

TABLE 15. COMMUTER REFERENCE ENGINE SEA LEVEL DATA

Sea Level Performance - Sea Level, Static, ISA, T/O, Uninstalled With No Production Margins	
Overall Engine Performance	Component Performance
Engine Rating, kW (shp)	746 (1000)
SFC, (kg/hr)/kW, (lb/hr)/hp	0.295 (0.491)
Turbine Inlet Temperature	
o HP Turbine, C (F)	1149 (2100)
o LP Turbine, C (F)	783 (1441)
Overall Cycle PR	12.68
Inlet $\dot{W}\sqrt{\theta}/\delta$, kg/s (lb/sec)	3.109 (6.854)
\dot{W}_{LP} , rad/s (rpm)	2408 (23,000)
\dot{W}_{HP} , rad/s (rpm)	4542 (43,333)
Fuel LHV, kJ/kg (Btu/lb)	42,798 (18,400)
	<u>HP Compressor</u>
	<u>1st Stage</u>
	o PR 4.58
	o η_{AD} 82.6
	o η_{Poly} 85.9
	<u>2nd Stage</u>
	o PR 2.78
	o η_{AD} 82.0
	o η_{Poly} 84.3
	<u>Overall</u>
	o PR 12.7
	o η_{AD} 79.7
	o η_{Poly} 85.4
	o Exit $\dot{W}\sqrt{\theta}/\delta$, kg/s (lb/sec) 0.34 (0.74)
	<u>Combustor</u>
	o η , % 99.97
	o $\Delta P/P$, % 4.03
	<u>HP Turbine</u>
	o $\dot{W}\sqrt{\theta}/\delta$, kg/s (lb/sec) 0.53 (1.16)
	o η_{AD} , % 87.0
	o Cooling Flow, % 6.8
	o Interturbine, % (AP/P) 1.38
	<u>LP Turbine</u>
	o $\dot{W}\sqrt{\theta}/\delta$, kg/s (lb/sec) 1.94 (4.28)
	o η_{AD} , % 88.0
	o LPT-NOX $\Delta P/P$, % 1.79
	<u>Propeller Gearbox</u>
	o η , % 98.0

*Stator and blade cooling flows are shown. The second-stage stator and blades are uncooled. The balance of the cooling flows (4.9%) are used for disk and firtree cooling.

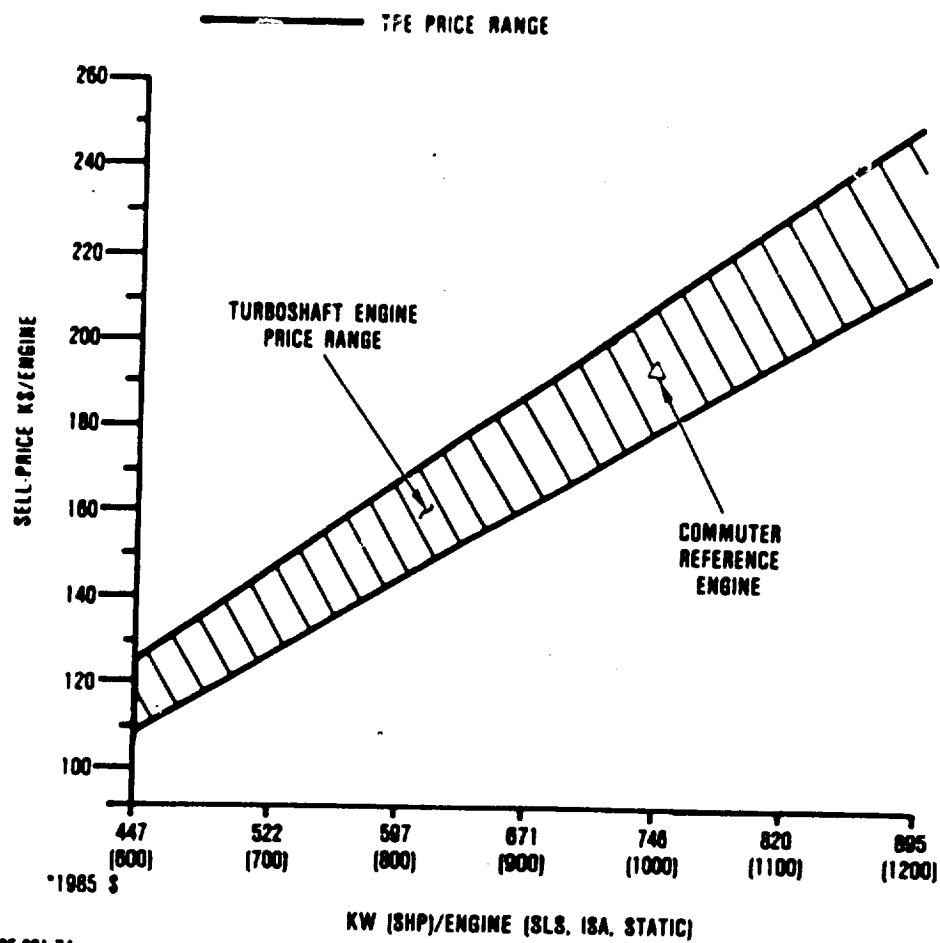
Table 16. Modular Weight Breakdown.

<u>Module</u>	<u>Weight (lb.)</u>
Propeller Gearbox	151.7
Compressor	36.5
Combustor	51.6
HP Turbine	36.0
LP Turbine	81.3
Accessories	64.6
<u>Total</u>	<u>421.7</u>

3.1.4 Environmental Constraints

Environmental constraints for the year-2000 were projected for commuter turboprop engines based on the sources as given for the rotorcraft engine study in paragraph 2.1.4.

In-depth studies performed in the early 1980s by the organizations listed in paragraph 2.1.4 concluded that any increased stringency in the existing rules and standards would result in negligible benefits to the environment, especially in the commuter and small business jet aircraft classes. In addition, further significant reductions in aircraft noise are not likely without substantial increases in the funding of the applicable acoustic technologies. Therefore, it is reasonable to assume that noise limits imposed in the year 2000 will be equal or similar to the most stringent rules existing today.



GS-281-74

Figure 62A. Reference Engine Costs Based on Mean Market Sell Price.

For the purpose of the Garrett SECT study, the Stage 3 takeoff, sideline, and approach noise limits of the FAA FAR, Part 36 regulations for large commuter aircraft (those carrying more than 19 passengers) were used. ICAO Annex 16, Chapter 3 noise standards are essentially identical to the FAA Stage 3 limits. Small commuter aircraft studies should use the FAA FAR, Part 36, Appendix F regulations that set noise limits for a 305m (1000 ft) level flyover. The ICAO Annex 16 standards are identical. A new takeoff noise measurement procedure currently is being developed by the FAA and ICAO to replace the existing level flyover procedure for small aircraft. However, this procedure should not increase the stringency of the level flyover, and its use in this study was not considered to be of any additional benefit on a comparison basis.

The EPA regulations do not limit gaseous emissions from turboprop engines. Moreover, no smoke constraints exist for small turboprop engines less than 999 kW (1340 hp).

The U.S. Air Force emission goals for engines are described in AFR 19-1 and are applicable to fixed wing, manned aircraft only. Smoke emission levels are to be below the visibility threshold, based on exhaust diameter, with a maximum limit of $SN = 65$. Carbon monoxide and hydrocarbon goals are aggressive and require levels that result in an idle combustion efficiency of 99.5 percent for engines with an idle pressure ratio above 3:1, and a combustion efficiency of 99.0 percent for engines with an idle pressure ratio below or equal to 3:1. NO_x goal levels are to be less than 50 percent of the Air Force defined "uncontrolled" level at takeoff and climbout modes. These stringent emission goals, however, will not impact flight safety or combat effectiveness for Air Force engines.

Small aircraft engines have been found to cause only a minor impact on overall pollution levels and hence have no required gaseous emission standards (ICAO, EPA) for commercial usage. Moreover, the stringent emission goals for military engines may be exceeded for small engines to prevent any impact on combat effectiveness. The engine specification for emissions levels is typically selected by the engine manufacturer consistent with small engine, state-of-the-art combustion efficiency predictions.

Emission levels likely to be required by the year 2000 for a 746 kW (1000 shp) size class turboprop are as follows:

- o Smoke levels - below the level of visibility, smoke number (SN) = 50
- o Gaseous emissions - unregulated for civil engines

3.1.5 Economic Model for Commuters

This paragraph presents the economic modeling as used for the commuter engines of this study.

A GTEC DOC economic model was used that is similar to the one in a 1980 NASA Report (reference 5). The cost estimating models are based on the vehicle partitions as shown in Table 17. The basic aircraft parameters for the economic models are listed in Table 18.

In synthesizing the total weight of an aircraft, it is convenient to partition the weight into a number of major components. GTEC LCC and DOC models used for this study made use of a

TABLE 17. COMMUTER VEHICLE PARTITIONS

Component	Cost
Airframe minus nacelle	Fixed
Nacelle	Variable
Propeller	Fixed
Payload	Fixed
Missions	Fixed
Fuel tankage	Variable
TOGW limit	Variable
Fuel load	Variable
Engine	Variable
Engine cost	Variable

TABLE 18. AIRCRAFT PARAMETERS FOR THE ECONOMIC MODEL

No. of Engines, excluding spares	1000
Spares	10%
Potential aircraft	500
Annual use	2000
Service life	15
TOGW (structural limit) kg (lb)	5,670 (12,700)
Payload [Passengers at 86.2 (190 lb) each]	1637 (3610)
Range km (nm) (Reference Engine)	741 (400)

TOGW model consisting of four major elements: airframe fixed weight, airframe variable weight, installed engine weight, fuel and tankage weight. These can be expressed as fractions of TOGW.

3.1.5.1 Airframe Weight Partitions

The fixed weight for all the commuter airframes consists of the crew, support systems, instruments, avionics, fuselage (minus the engine nacelles/pods), wings, empennage, landing gear, and systems (controls, actuation, pumps, wiring, and piping). These parts are fixed weights due to the structure of the study. The crew, support systems, instruments, and avionics are fixed because they are not affected by the engine. Since the upper limit of power has been fixed at 746 kW (1000 shp) per engine for the study, the aircraft size is also fixed. As weight decreases, block time is reduced, which improves DOC. This, in turn, fixes the fuselage (minus the engine nacelles/pods which are affected by engine volume and weight), the wing, the empennage, the landing gear, and the systems weight.

Some other weights were fixed or variable due to the influence of regulation, or of design/market approaches of typical manufactures. These are described, following, for each airframe.

The fuel tankage except the fuel bladder (including pumps, pipes, collector plenums) is fixed. This is assumed because many commuter airframe manufacturers design the airframe with the maximum tankage that the wings can hold. This is done so that the resulting airframe can then be used for both the executive and the commuter market. For the executive market, a large fuel supply is desirable to ensure that the aircraft appeals to the largest market. The maximum fuel tankage also allows a commuter to make several stops before refueling, thus minimizing block time. The maximum tankage is normally limited by the wing size.

On-board tankage is normally sold as a special kit and will not be considered for this study. Where fuel could be reduced, the fuel load was reduced to fly the missions.

The payload for this study was limited to 19 passengers. This was due to the assumption that SFAR 41 type regulations will be in effect in the year 2000 for this class of commuter aircraft; SFAR 41 defines a small aircraft at 19 passengers, maximum. A typical industry weight of 86.2 kg, (190 lb) for passenger and baggage was assumed.

The change in aircraft drag due to increase in engine volume is approximated by the following:

$$\text{DRAG} = C_D q S_w = K_2 \frac{AL}{A_{f_r} L_r} q S_w$$

Where:

- C_D = Coefficient of drag
- q = Dynamic pressure
- S_w = Wing area
- K_2 = Constant, from other aircraft nacelle studies
- A, A_{f_r} = Frontal area of new engine and reference engine
- L, L_r = Length of new engine and reference engine

The turboprop commuter airframe used in this study is similar to the Fairchild Metro III, but it has modifications from the NASA Small Transport Aircraft Technology study to upgrade it to a year-2000 airframe, as discussed in paragraph 3.1.1. The basic cost parameters are generally based upon the data from the turboprop aircraft operating and maintenance parameters from NASA Report CR-165176 (reference 5). The fuel burn and block time to fly the mission was obtained by computing these parameters on the GTEC mission computer programs, SUPERM.

The calculations performed herein assume that the commuter can take off at the maximum all-up weight of the reference aircraft plus or minus some additional weight for year-2600 technology engines (which may have additional components such as regenerators). This assumption was examined by reviewing the maximum weight at takeoff of the present Metro III. The Metro III has a Garrett TPE331-10 engine that has 746 kW (1000 shp) thermodynamic power and is gearbox flat-rated at 701 kW (940 shp). That places the Metro III in the same size class as the SECT commuter. The maximum all-up weight of the Metro III is 6577 kg (14,500 lb). With 701 kW (940 shp), it can take off at ISA at 6577 kg (14,500 lb) up to 2438m (8000 ft) altitude. This allows for 816 kg (1800 lb) of additional installed engine weight (IEW). Thus, the assumption of adequate takeoff weight capability of the reference aircraft appears reasonable.

The engine and nacelle weights can vary with the engine. The IEW consists of the bare engine weight, the weight of the cowlings, engine mounts, inlet, starter/generator, batteries, connections, pipes/hoses, lubricants, oil cooling system, and exhaust system. The ratio of the nacelle plus engine weight is related to the engine weight by a constant, K_1 . K_1 was obtained from a study of GTEC designs of turboprop engines and nacelles in this shp category.

$$IEW = K_1 \times \text{engine weight}$$

The fuel (plus reserves) weight was varied with the engine performance. Only enough fuel was put on board to fly the four mission segments plus reserves. Thus, reducing engine weight improved specific range and reduced fuel burn (holding the engine SFC constant). A good dispatcher would normally load only enough fuel to fly the mission.

The commuter TOGW was calculated in the following form:

$$\text{TOGW} = \text{AFFW} + K_1 \times \text{engine weight} + \text{fuel (burned + reserves)}$$

where

AFFW = Airframe fixed weight

TOGW can be approximated by manipulating the Brequet range equation for fuel burn fraction.

3.1.5.2 Operating Cost Model

The annual cost of owning and operating the referenced commuter aircraft was structured into fixed and variable costs, as shown in Table 19.

TABLE 19. COMMUTER OWNER/OPERATOR COSTS

Fixed Cost	Variable Costs
Loan interest rate	Fuel
Imputed interest rate on equity	Airframe maintenance
Depreciation	Engine maintenance
Crew wages plus benefits	Crew expenses
Insurance	Landing fees
Taxes	
Hanger rent	
Miscellaneous	

While these costs are fixed and variable with respect to aircraft usage, they are recategorized for evaluation of changes in the engine. For nonrevenue operation as computed here, the

imputed interest on equity investment should be included. The fuel cost in the modeling uses the fuel burn from the computer mission analysis results.

$$FC = (W_f)(F_p)(TOH)$$

where:

FC = Fuel cost
W_f = Fuel weight
F_p = Fuel price/lb
TOH = Total operating hours (lifetime)

The other costs are modeled as:

$$CINT + CIINT = QA[(LYRS)(RINT)AC + (LYRS)(RIINT)EQ]$$

Where:

CINT = Interest cost
CIINT = Imputed interest cost on equity
QA = Quantity of aircraft
LYRS = Loan years
RINT = Interest rate
AC = Airframe cost
RIINT = Inputed interest rate
EQ = Equity

3.1.5.3 Development Cost Model

Development engine costs were estimated based on engine configuration and technologies employed.

Based on empty weight, the model prepared by J.R. Humphreys (Reference 6) was used to determine business aircraft development cost. Its mathematical form is:

$$ADC = 741,000 \left(\frac{ACEW}{1000} \right)^{1.49}$$

Where:

ADC = Airframe development cost

ACEW = Aircraft empty weight

The basic airframe cost, except for nacelles, is fixed. The changed development cost for nacelles was not considered to have a significant impact on total development cost, so a constant was used.

3.1.5.4 Manufacturing Cost Model

Like development cost, manufacturing cost can also be estimated as a function of aircraft weight and engine thrust. The airframe and engine manufacturing cost inputs to the equations described below are based on acquisition cost (sell price). The airframe manufacturing cost model selected, which is based on data from several business aircraft manufacturers, considers only fixed and variable airframe weight. Its mathematical form is:

$$AMC = [BMW \times BMC + CW \times CC + EC] QA$$

Where:

AMC = Airframe manufacturing cost

BMW = Bonded metal components weight

BMC = Bonded metal cost per pound

CW = Composite components weight
CC = Composite components cost per pound electronics packages
EC = Cost of electronics packages
QA = Number of aircraft

Engine costs were estimated for each engine separately. Costs for the reference engine were based on estimated market sell prices for 1985 as described in paragraph 3.1.3. Costs for advanced technology, year-2000 engines were based on cost factors/adders as applied to the reference engine costs for parts/components replaced by new technologies. These cost adjustments included a projected 15 percent cost reduction by year 2000 for current technology parts.

3.1.5.5 Maintenance Cost Model

Aircraft maintenance costs can be distributed to three major categories: airframe, engine, and burden, as shown:

$$(1) \text{ Total Maintenance Cost} = \text{AM} + \text{EM} + \text{MB}$$

Where:

AM = Total airframe maintenance cost

EM = Total engine maintenance cost

MB = Total maintenance burden

The model selected to represent airframe maintenance cost was prepared by the Aerospace Corporation and reported in "A Direct Operating Cost Model for Commuter and Local Services Airlines."

$$(2) \text{ AM (per flight hour) } = 0.02308 (\text{EW})^{0.813} \\ - 0.1562 \text{ ASL} + 23.7730$$

Where:

EW = Aircraft empty weight (lb)

ASL = Average stage length (statute miles)

Engine-related maintenance costs are based on GTEC experience (GTEC maintenance contracts) and on the 1985 reference engine. Engine maintenance consists of three major components:

$$(3) \text{ EM } = \text{Routine maintenance} + \text{Unscheduled power section} \\ \text{maintenance} + \text{Unscheduled line replaceable unit} \\ \text{maintenance}$$

Maintenance burden, which was also estimated by the Aerospace Corporation model, is dependent on the magnitude of airframe and engine maintenance costs:

$$(4) \text{ MB } = 0.152 (\text{AM} + \text{EM}) + 6.4445$$

For the year-2000 recuperated engine, a number of changes were required to properly reflect the additional complexity of the year-2000 recuperated engine. Airframe maintenance was considered to be the same as Equation 2.

Engine maintenance and maintenance burden, however, required further definition. Engine maintenance costs can be categorized as labor and materials costs, and as scheduled or unscheduled. Based on this definition, the maintenance cost for the year-2000 recuperated engine can be modeled as shown in Equation 5.

$$(5) \quad EM = 1.15 \text{ (Unscheduled labor maintenance*)} \\ + 0.75 \text{ (Scheduled labor maintenance*)} \\ + \text{ (Scheduled and unscheduled material maintenance*)}$$

The maintenance burden definition was also revised to reflect the additional support equipment and parts stock required for the recuperators and associated hardware.

$$(6) \quad MB = 0.152 (AM + EM) + NE (1.14 \text{ SEC} + 1.15 \text{ BSPSC}) + 5.135$$

Where:

NE = Number of engines
 SEC = Support equipment cost
 BSPSC = Base supply parts storage cost

3.1.6 Trade Factors for Commuters

This section presents trade factors for the commuter turbo-prop engine application as computed for Task II evaluation of beneficial engine changes that may be possible due to projected technology advancements.

The trade factors relate commuter owner-operator costs to engine parameter changes. The trade factors, as generated, are based on the SECT reference aircraft (year 2000) and mission (year 2000), and on the SECT reference engine (year 1985).

*Value for 1985 reference

The trade factors constitute partial differentials for the listed parameters and are presented in Table 20 for the fuel prices* selected for this study. The DOC breakdown (Figure 62B) indicates that a number of factors contribute to aircraft DOC. Of these factors, the majority are only indirectly influenced by the propulsion system. One exception is fuel cost, which is directly influenced by engine SFC. As shown, this engine-sensitive portion of DOC constitutes only 20 to 40 percent of the total, depending on the fuel price.

TABLE 20. COMMUTER TRADE FACTORS

	\$0.264/liter (\$1/gal)	\$0.528/liter (\$2/gal)
$\Delta \text{DOC}/1\% \Delta \text{ engine SFC}$	\$2.88	\$5.69
$\Delta \text{DOC}/1\% \Delta \text{ engine weight}$	\$0.26	\$0.29
$\Delta \text{DOC}/1\% \Delta \text{ engine diameter}$	\$0.12	\$0.14
$\Delta \text{DOC}/1\% \Delta \text{ engine length}$	\$0.03	\$0.04
$\Delta \text{DOC}/1\% \Delta \text{ engine cost}$	\$1.93	\$1.93

The values shown are DOC changes in trip cost for each 1 percent change in the given parameter. The DOC/trip values are \$1221 and \$1500, respectively, for the low and high fuel prices selected for this study.*

*Low fuel price: \$0.264/liter (\$1/gal)
High fuel price: \$0.528/liter (\$2/gal)

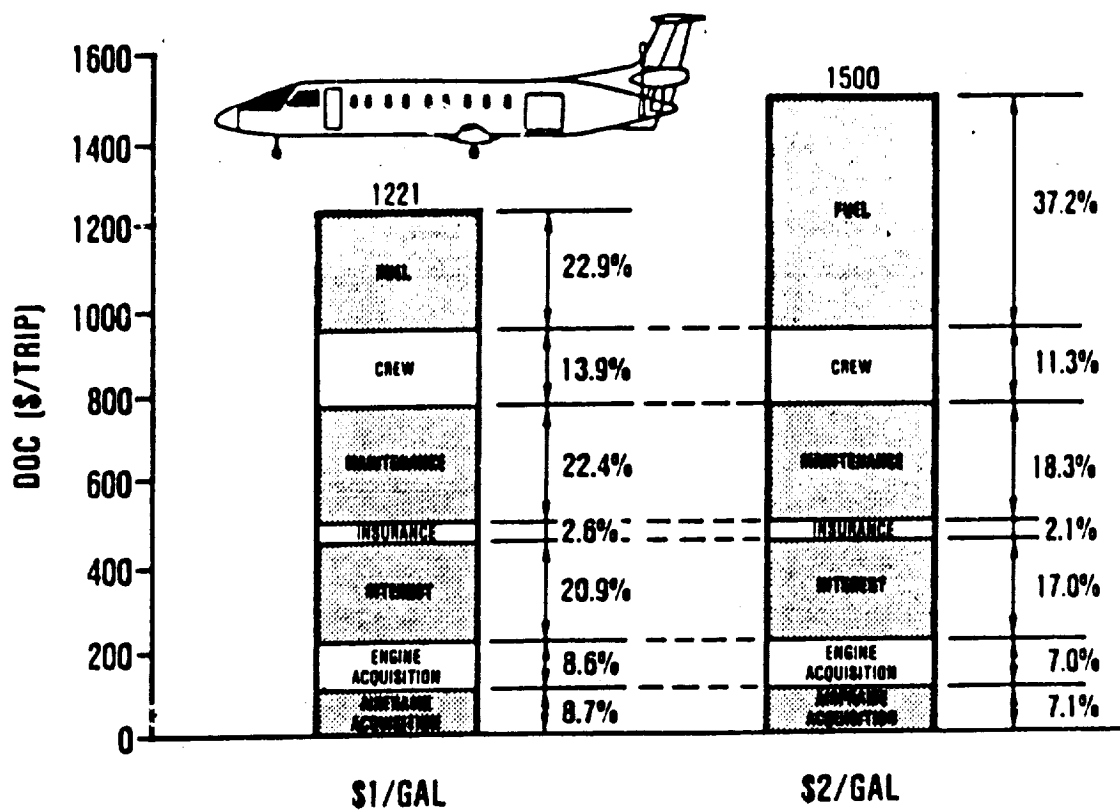


Figure 62B. Commuter DOC Breakdown - Reference Engine.

3.2 Task II - Engine Configuration and Cycle Evaluation

The cycle/configuration studies for the commuter application parametrically considered a range of potential combinations in terms of turbine rotor inlet temperature (TRIT), cycle pressure ratio (CPR), component types, materials and associated efficiencies, cooling flows, pressure drops, and leakages as projected for year-2000 capabilities. From the range of engines considered, a final engine selection for Task III evaluation was made on the basis of payoff in aircraft direct operating cost (DOC). The DOC improvements were estimated through the trade factors established in Task I, which relate changes in DOC in terms of changes in engine performance (SFC), weight, diameter, length, and cost (changes are relative to the 1985 reference engine). Size, weight, and cost were quantified for each engine of interest.

3.2.1 Technology Projections

The initial task in configuring potential commuter engines for the year 2000 was to establish the expected level of technology in that time frame. Inherent in these technology projections is the assumption that they will be available by the year 2000. Technologies have been identified in three major areas: materials, aerodynamics, and mechanical improvements. These technologies impact the cycle study in terms of efficiency levels, TRIT limits, and cooling flow requirements, as well as turbine stage count and hub speed limits.

The technology projections for the commuter application are essentially identical to those discussed for the rotorcraft application and therefore will not be repeated here. Material projections are outlined in paragraph 2.2.1.1, followed by aerodynamic technologies in paragraph 2.2.1.2. Recuperator and

mechanical technologies, as well as cost, weight, and size estimates are discussed in paragraphs 2.2.1.3 through 2.2.1.5.

Technology improvements for regenerators were investigated for both the commuter and the rotorcraft applications. The projections for regenerators are based on GTEC experience with the NASA/DOE-sponsored AGT101 automotive engine, shown in Figure 63. As shown, a 7 percent leakage rate is projected for advanced seals with a 1000-hour life. Temperature capabilities up to 1093C (2000F) are projected for the regenerator core.

3.2.2 Cycle/Engine Studies

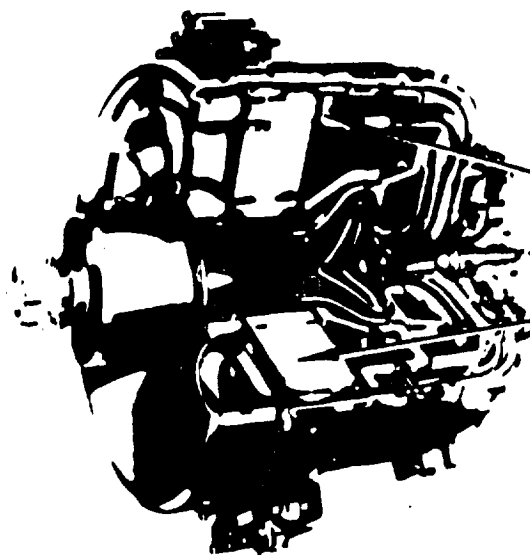
The parametric cycle study for the commuter application has been generated with essentially the same ground rules and methods as discussed for the rotorcraft application in paragraph 2.2.2. For the commuter application, three cycle types have been evaluated: two heat recovery cycles (recuperated and regenerated) and a conventional simple cycle.

3.2.2.1 Recuperated Cycle Study

The primary emphasis of the commuter study was placed on cycles with waste heat recovery, particularly recuperation. A wide range of configurations and cycle parameters were considered, as outlined in Figure 64.

The initial configuration consists of a single-stage centrifugal compressor, reverse-flow combustor, single-stage HP turbine, and two-stage LP turbine. Ceramics are used in the combustor and turbine vanes and stators. In addition to the initial configuration, a number of component and material options were considered for the compressor and turbines.

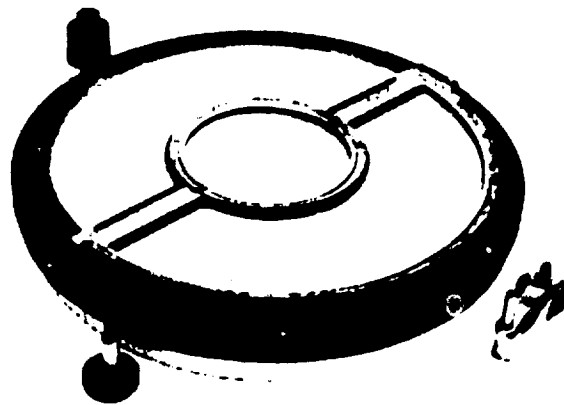
ORIGINAL PAGE IS
OF POOR QUALITY



TECHNOLOGY PROJECTIONS:

- LOW-LEAKAGE, LONG-LIFE SEALS
(7% AT 1000-HOUR LIFE)
- HIGHER-TEMPERATURE CAPABILITY CORE
(INLET TEMPERATURE = 1093C (2000F))

APPLICATION - AUTOMOTIVE
POWER - 74.6 KW (100 SHP)
SFC - 0.183 (0.30)



GS-281-128

Figure 63. Regenerator Technology Projections Based on AGT101 Experience.

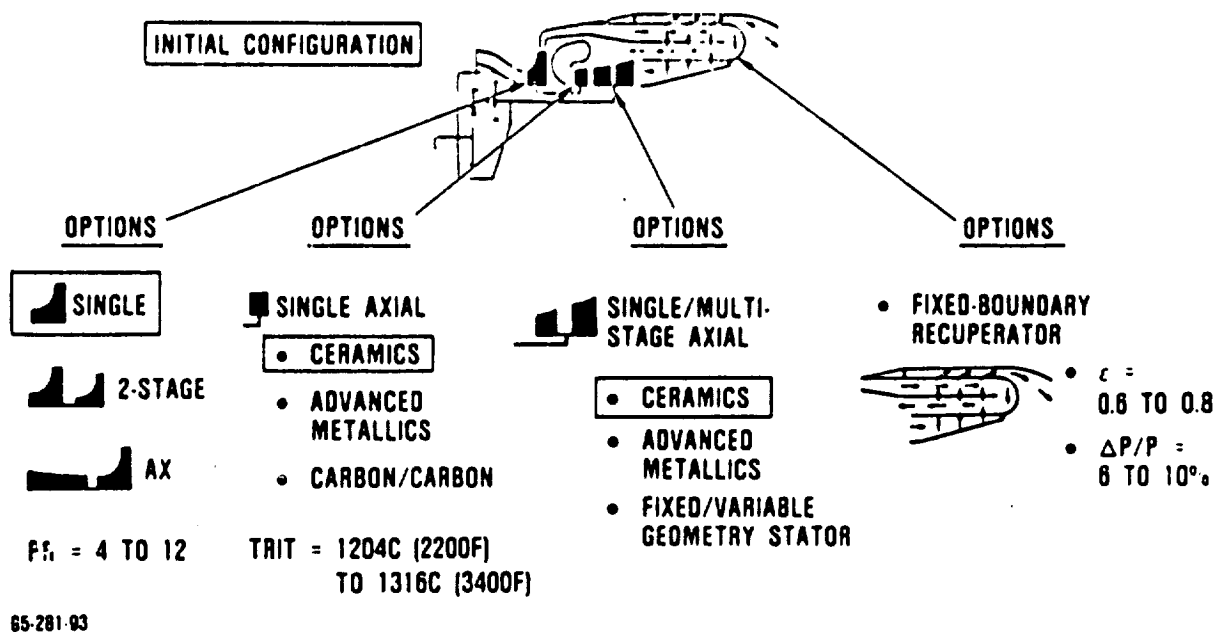


Figure 64. Commuter Recuperated-Cycle Study Configurations and Options.

For the compressor, both two-stage centrifugal and axial-centrifugal configurations were compared with the single centrifugal design. Pressure ratios were evaluated from 4:1 to 12:1.

For the HP turbine, only axial configurations were considered; however, both advanced metallics and carbon-carbon were examined and compared with ceramics. TRITs ranging from 1204 to 1872C (2200 to 3400F) were investigated.

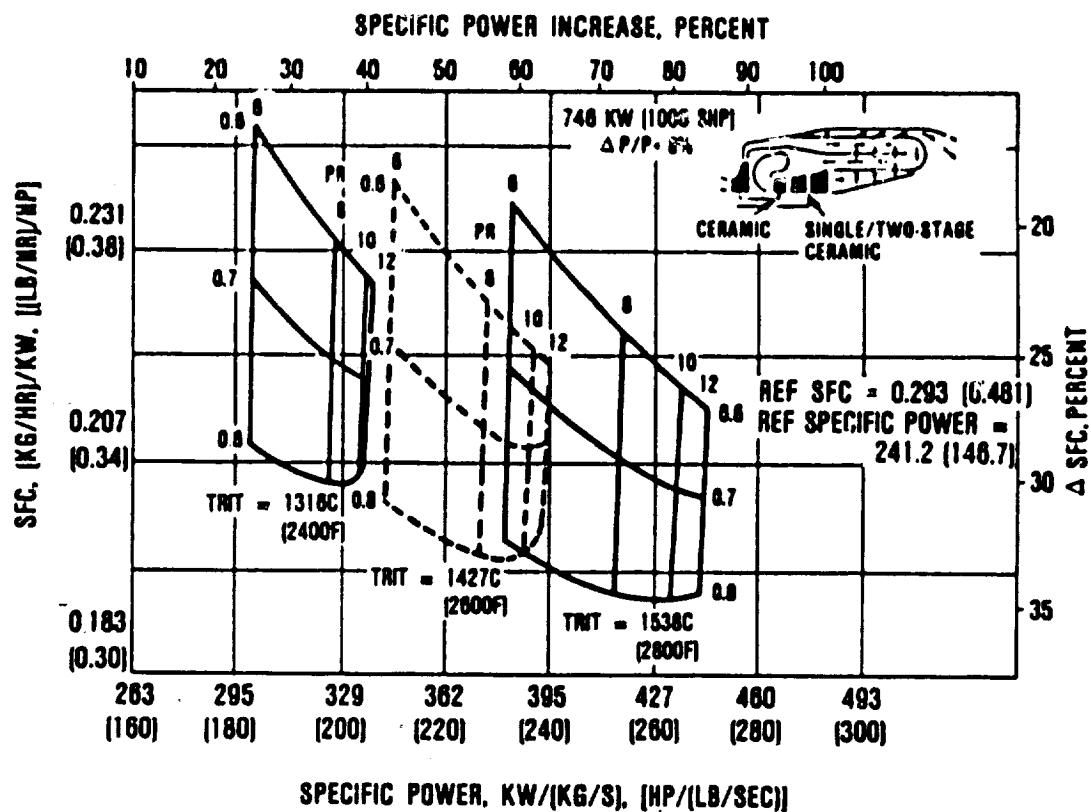
Axial stages only were considered for the LP turbine. Advanced metallics, in addition to the initial ceramic material, were evaluated. Both fixed-geometry and variable-geometry LP turbines have been examined.

A range of effectiveness from 0.6 to 0.8 was evaluated for the fixed-boundary recuperator. Pressure drops from 6 to 10 percent were evaluated. A ceramic counterflow plate-fin recuperator was considered as the initial configuration.

3.2.2.1.a Performance

The performance (SFC versus specific power) of the initial configuration over a range of CPRs (6 to 12), TRITs of 1316 to 1538C (2400 to 2800F), and effectiveness (0.6 to 0.8) reveals that an SFC improvement of 35 percent is possible relative to the 1985 reference engine. As shown in Figure 65, increases in specific power of up to 85 percent are also possible. The optimum CPR, which depends on both TRIT and effectiveness, falls between 8:1 and 10:1.

The cycles shown assume that uncooled ceramic turbines are used across the TRIT range evaluated. With a material temperature limit of 1538C (2800F), the practical TRIT limit of ceramics is considered to be 1427C (2600F) in light of expected year-2000



66-281-113

Figure 65. Recuperated-Cycle Performance Results for Commuter Application.

combustor pattern factors. The 1538C (2800F) cycles would therefore require some cooling, thus reducing their performance and desirability. In terms of performance, it is clear that the highest effectiveness and temperature (0.8 and 1427C [2600F]) result in the best SFC and specific power (at a CPR between 8:1 and 10.1).

One of the penalties incurred with a recuperated cycle is the pressure drop in the recuperator itself and associated manifolding and ducting. To determine the impact on engine performance, a range of pressure drops from 6 to 10 percent was investigated, as shown in Figure 66. The pressure drop variations studied pertain to the total incurred in both the hot and cold streams in the recuperator.

Varying recuperator pressure drop has little impact on the optimum cycle pressure ratio, but results in approximately a 0.5 percent increase in SFC per one percent increase in pressure drop. Therefore, the recuperated cycles inherently desire high effectiveness and low pressure drop in terms of performance, which unfortunately have an unfavorable impact on recuperator size and weight, as well as on cost.

3.2.2.1.b Size and Weight

The impact of effectiveness and pressure drop ($\Delta P/P$) on size and weight can be found in Figure 67. As shown, both weight and size increase with effectiveness and with decreasing pressure drop. A reduced pressure drop has a large impact on recuperator length, which in turn, increases overall weight.

Several other recuperator configurations were also examined, including plate-fin and tubular designs in metallic or ceramic, and with either counterflow and cross-counterflow flow paths, as

CERAMIC PLATE-FIN
COUNTERFLOW
PLENUM HEIGHT = 7.62 CM (3 IN.)
TURBINE DUCT RADIUS = 15.24 CM (6 IN.)
TRIT = 1427C (2600F), PR = 8

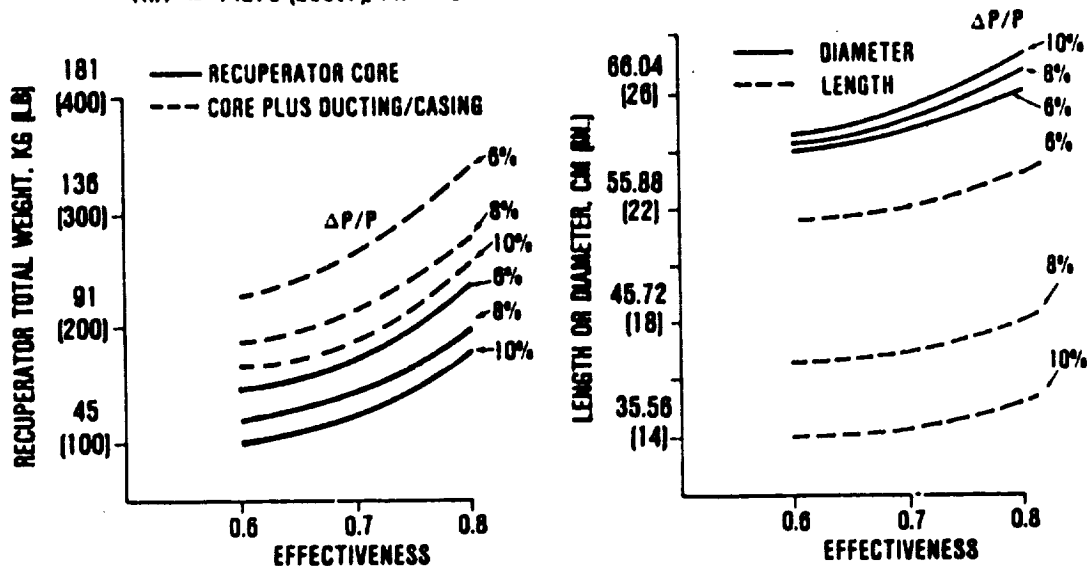


Figure 67. Impact of Recuperator Effectiveness and Pressure Drop on Weight and Size.

shown in Figure 68. The optimized design is dependent upon weight and cost, and possibly, size constraints. With respect to weight, it is clear that either the metallic tubular two-pass crossflow design or the ceramic plate-fin counterflow designs are the most desirable, depending upon selected effectiveness.

Specific power is considered an indicator of engine size and weight. As such, several engines have been selected to present the trend of weight as a function of specific power. A constant TRIT line at 1427C (2600F) (varying pressure ratio) as well as a constant pressure ratio line at 10:1 (varying TRIT) is shown in Figure 69. Overall engine weight, as well as recuperator and engine core weight, decreases with specific power, as indicated. Limiting the investigation to TRITs of 1427C (2600F) and lower shows that weight is starting to minimize in the 10 to 12 pressure ratio range.

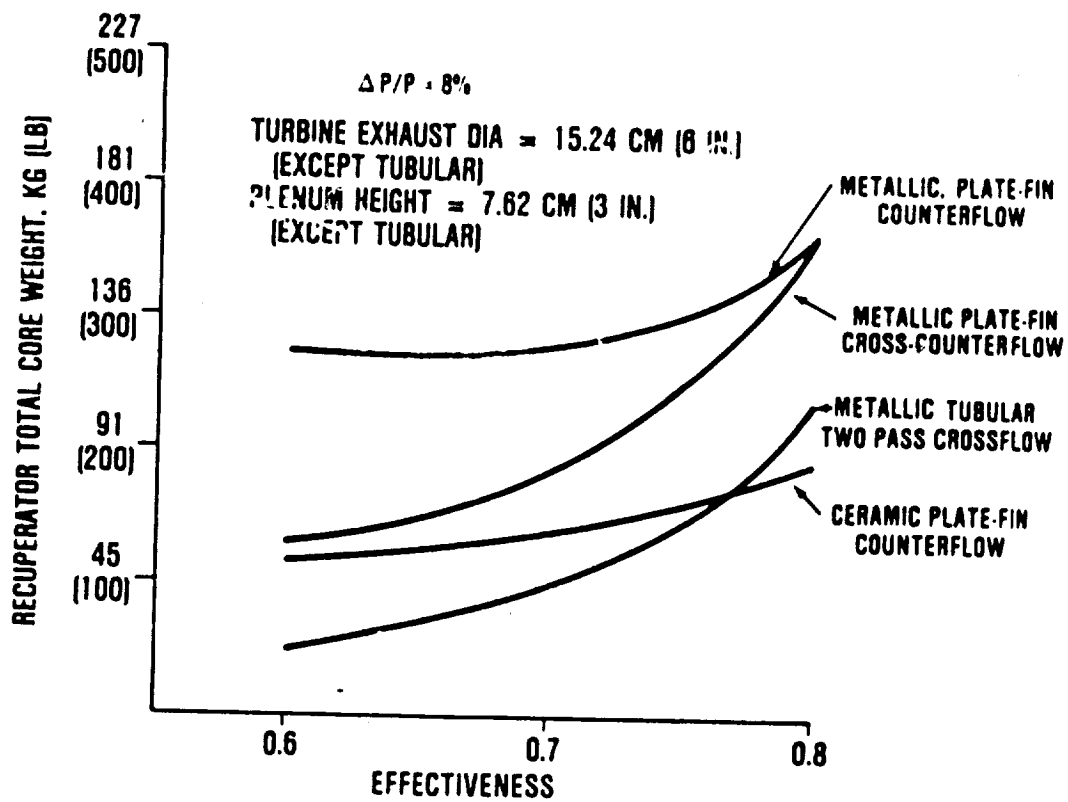
3.2.2.1.c Cost

It has been shown that weight decreases with specific power. Referring to Figure 70, it can be seen that cost exhibits similar characteristics. Once again, engine cost is minimized in the 10 to 12 pressure ratio range.

Recuperator cost also decreases with flow, but it increases dramatically with effectiveness and reduced pressure drop, as shown in Figure 71. The impact of effectiveness on cost is particularly evident in the estimates as reassessed for Task III. Decreasing pressure drop from 10 to 6 percent results in a 50 percent module cost increase.

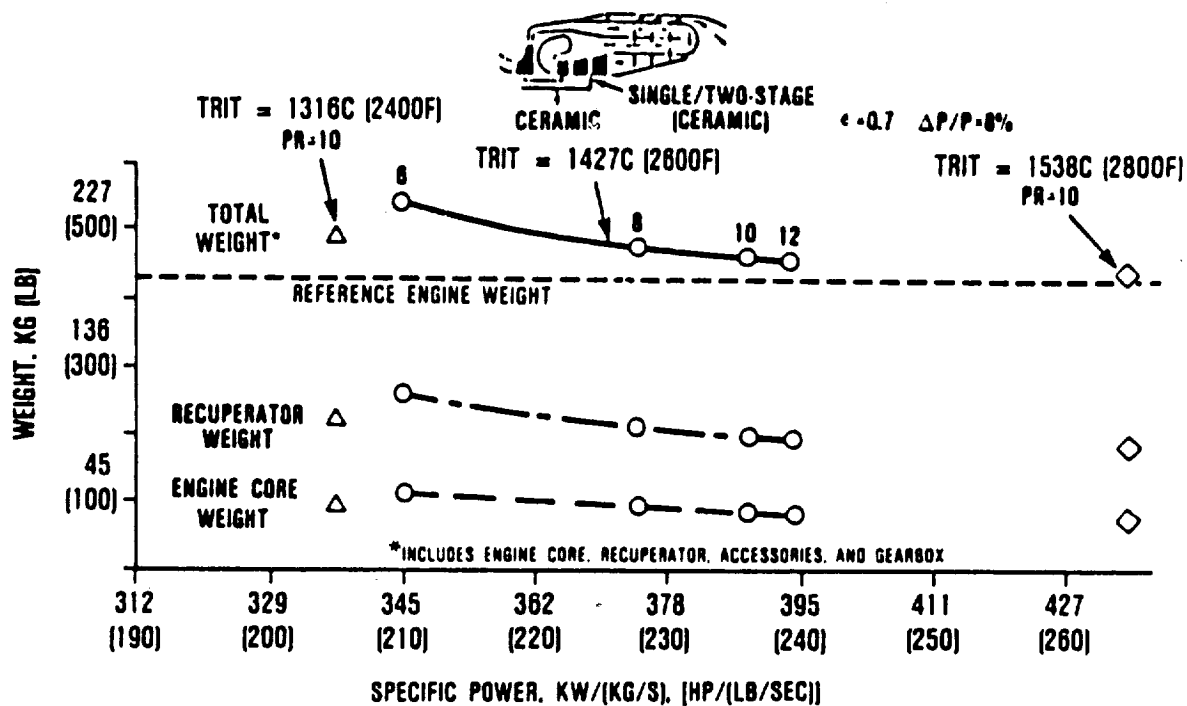
3.2.2.1.d Direct Operating Cost

Changes in SFC, size, weight, and cost were evaluated through the trade factors generated in Task I to determine their



85-281-117

Figure 68. Weight Comparison of Recuperator Types.



65-281-122

Figure 69. Recuperated Engine Weight Trend As a Function of Specific Power.

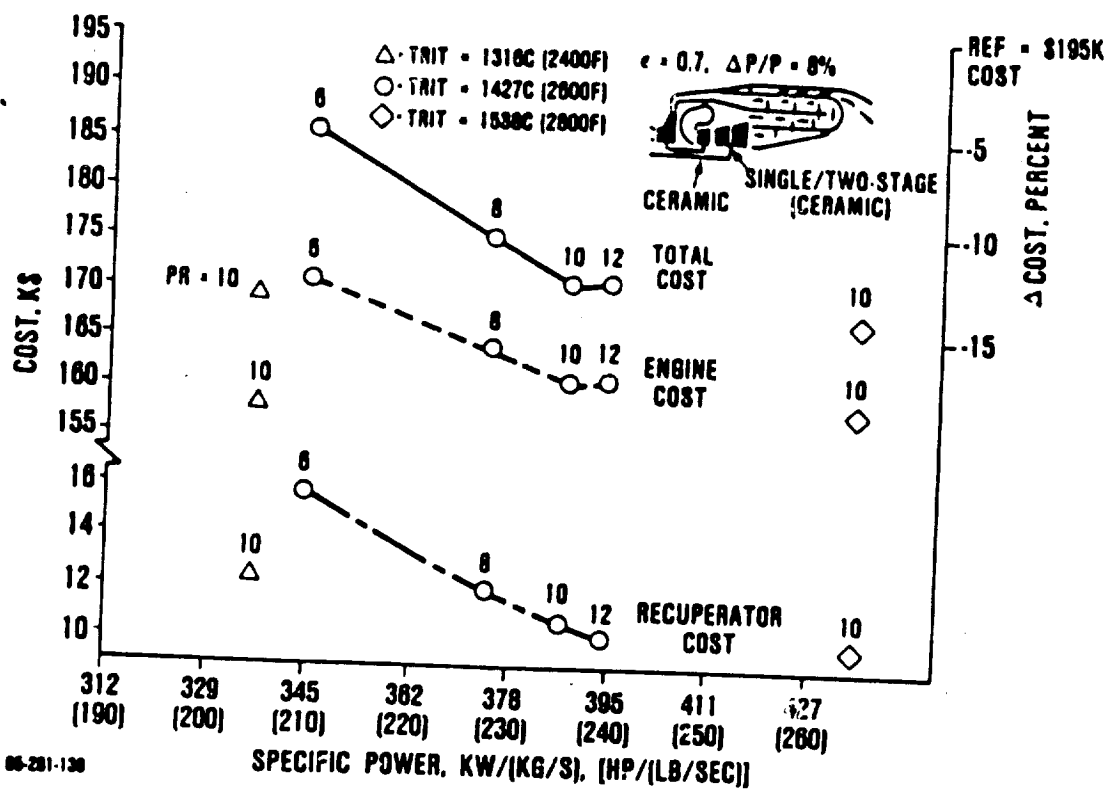
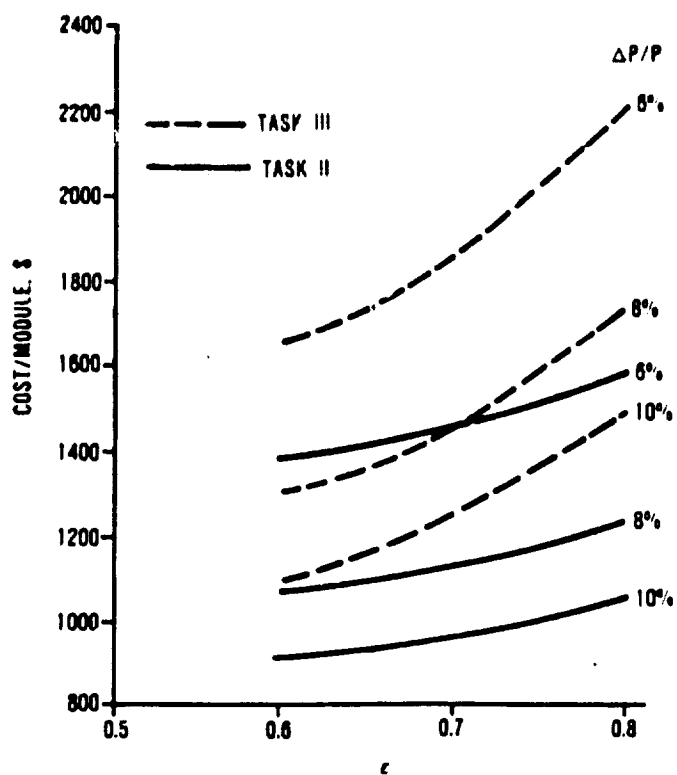


Figure 70. Recuperated Engine Cost Trend As a Function of Specific Power.

CERAMIC PLATE-FIN
COUNTERFLOW
PLENUM HEIGHT = 7.62 CM (3 IN)
TURBINE DUCT RADIUS = 15.24 CM (6 IN)
TRIT = 1427C (2600F), PR = 8



85-281-121

Figure 71. Impact of Effectiveness and Pressure Drop On Recuperator Cost.

impact on mission performance (DOC). The trade factors, generated with the year-2000 aircraft and the 1985 reference engine, place the greatest emphasis on SFC and cost.

Plotting DOC per trip as a function of SFC and specific power (Figure 72) shows that improving these two parameters does in fact result in DOC savings. As indicated, DOC optimizes at a pressure ratio of 10:1 at the 1427C (2600F) TRIT.

It has been demonstrated that although high recuperator effectiveness and low pressure drop are highly desirable in terms of engine performance, a penalty is paid in terms of size, weight, and cost. The DOC results ultimately determine where these tradeoffs optimize in terms of recuperator effectiveness and pressure drop. As shown in Figure 73, the recuperator optimizes near 0.8 at the low fuel price, but at the high price an effectiveness above 0.8 is indicated. Pressure drop, on the other hand, has little impact on DOC (for the range evaluated) at either fuel price. Clearly, the need for pressure drops below 8 percent is not indicated.

For the initial recuperated configuration, the DOC results point to the selection of a pressure ratio of 10:1 at a TRIT of 1427C (2600F), with a recuperator effectiveness and pressure drop of 0.8 and 8 percent, respectively. Further, trades involving compressor configuration and turbine materials were made as discussed in the following paragraphs prior to a final recuperated engine selection.

3.2.2.1.e Configuration Trade Studies

Both two-stage centrifugal and axial centrifugal compressors were considered in comparison to single centrifugals. As shown in Figure 74, there is some improvement in performance to be gained, particularly at higher pressure ratios.

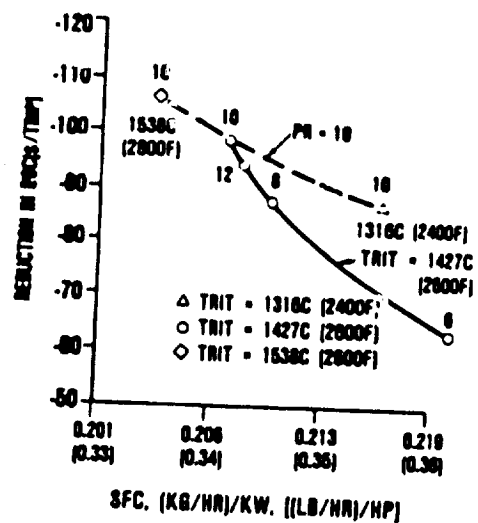
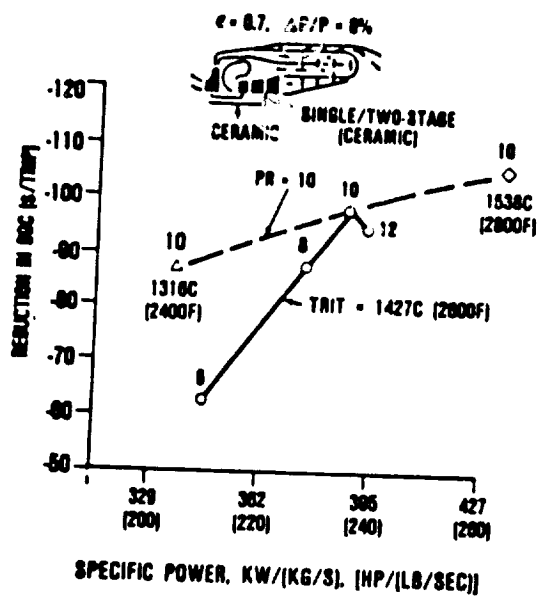


Figure 72. Reduction in Commuter DOC As a Function of SFC and Specific Power.

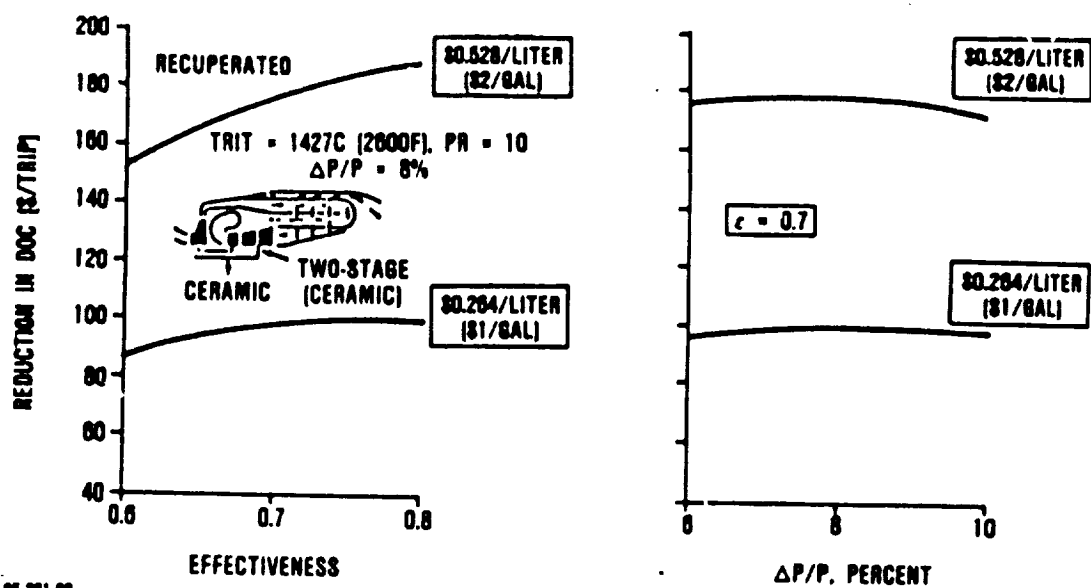


Figure 73. Reduction in Commuter DOC As a Function of Recuperator Effectiveness and Pressure Drop.

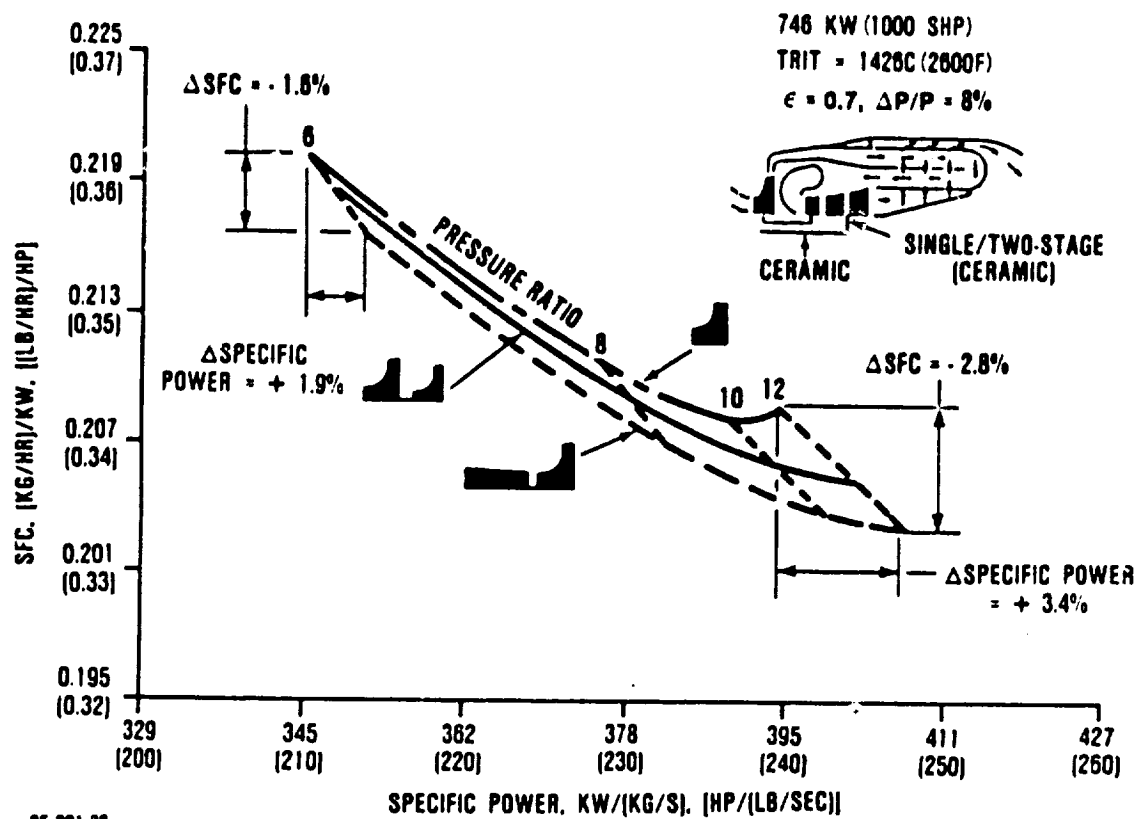


Figure 74. Compressor Configuration Effects on Commuter Engine Performance.

The penalty for these alternate compressor configurations is in added complexity, weight, size, and cost. The DOC results, as shown in Figure 75, indicate that little or no benefit is derived from the added compressor complexity, particularly in the 10:1 PR range.

Other configuration trades considered were in the turbine materials, where both advanced metallics and carbon-carbon were evaluated. Advanced metallic cycles/configurations are compared to the ceramic cycles/configurations in Figure 76.

Replacing the cooled metallic turbines with uncooled ceramic turbines has a substantial impact on the cycle. The use of ceramics can further improve SFC by 10 to 15 percent relative to the advanced metallic engines. Also, the metallic turbines show SFC increasing with TRIT due to the impact of increasing cooling flow.

Carbon-carbon versus ceramics is compared as shown in Figure 77. Carbon-carbon allows TRIT to be increased substantially without the penalty of cooling. The cycle, as shown, clearly benefits. Unfortunately, carbon-carbon is not expected to be available in man-rated engines (turbine section) by the year 2000.

In terms of DOC, the ceramic turbines are clearly more desirable than advanced metallic designs, as shown in Figure 78. The use of ceramics can reduce DOC by \$50 to \$100 per trip (4 to 7 percent additional DOC reduction) relative to advanced metallics. Carbon-carbon does have a DOC advantage over ceramics, but as previously discussed, it is not projected to be available for this application.

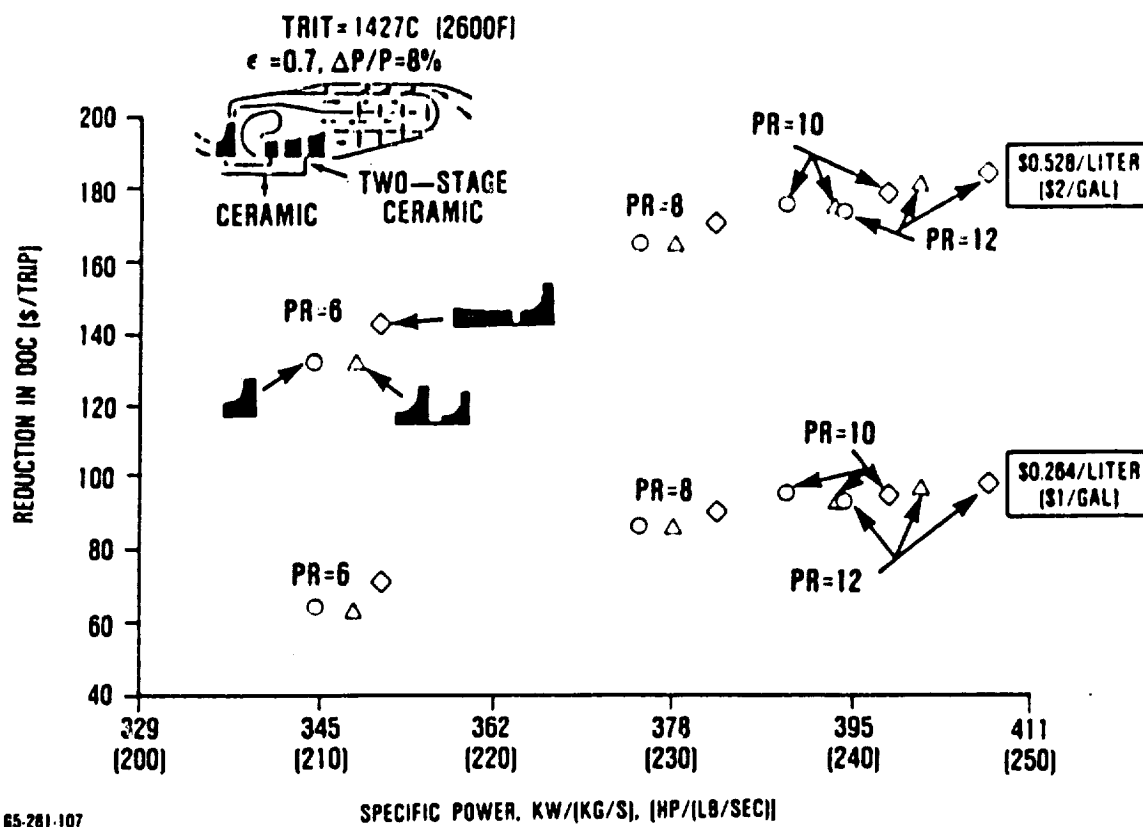
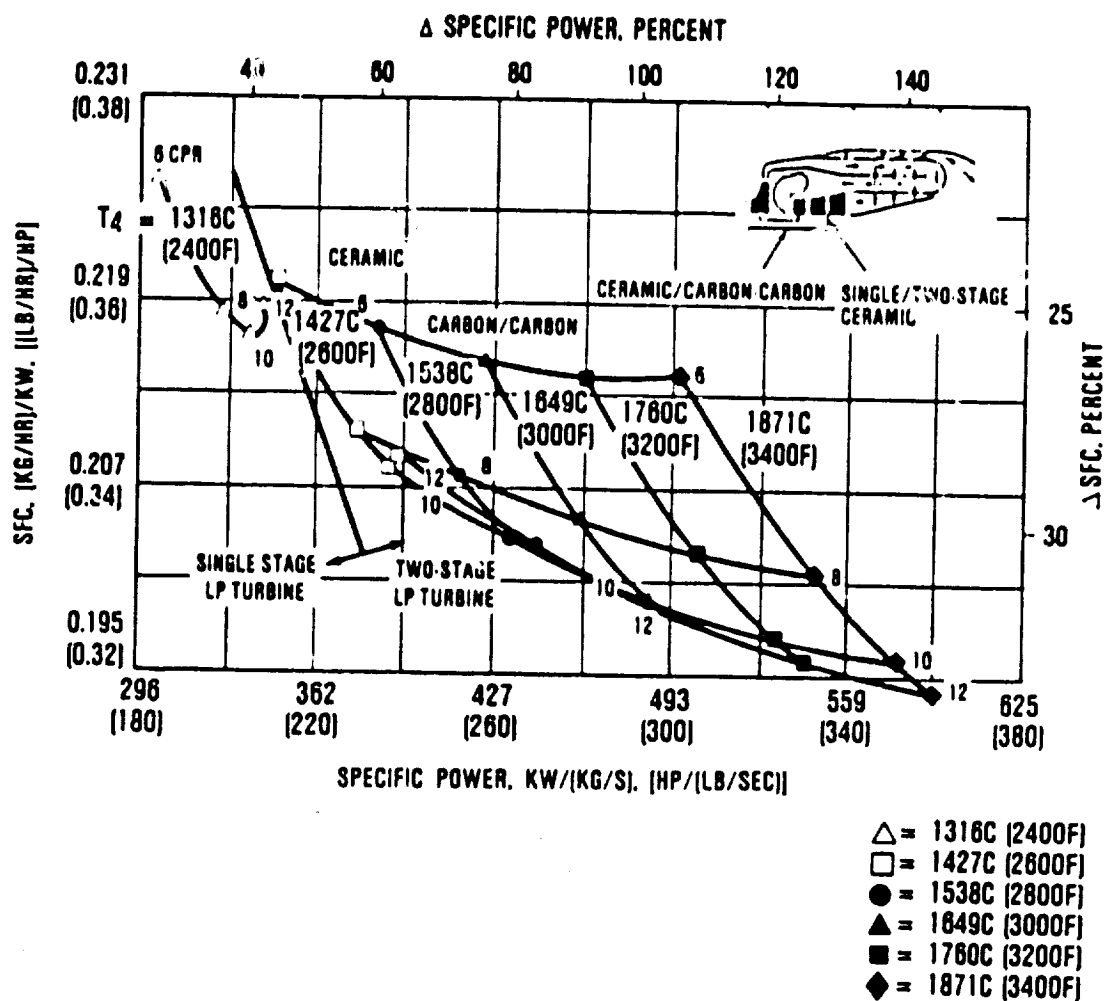


Figure 75. DOC Comparison for Different Compressor Configurations.



05-281-123

Figure 77. Performance Comparison of Ceramic Versus Carbon-Carbon Turbines.

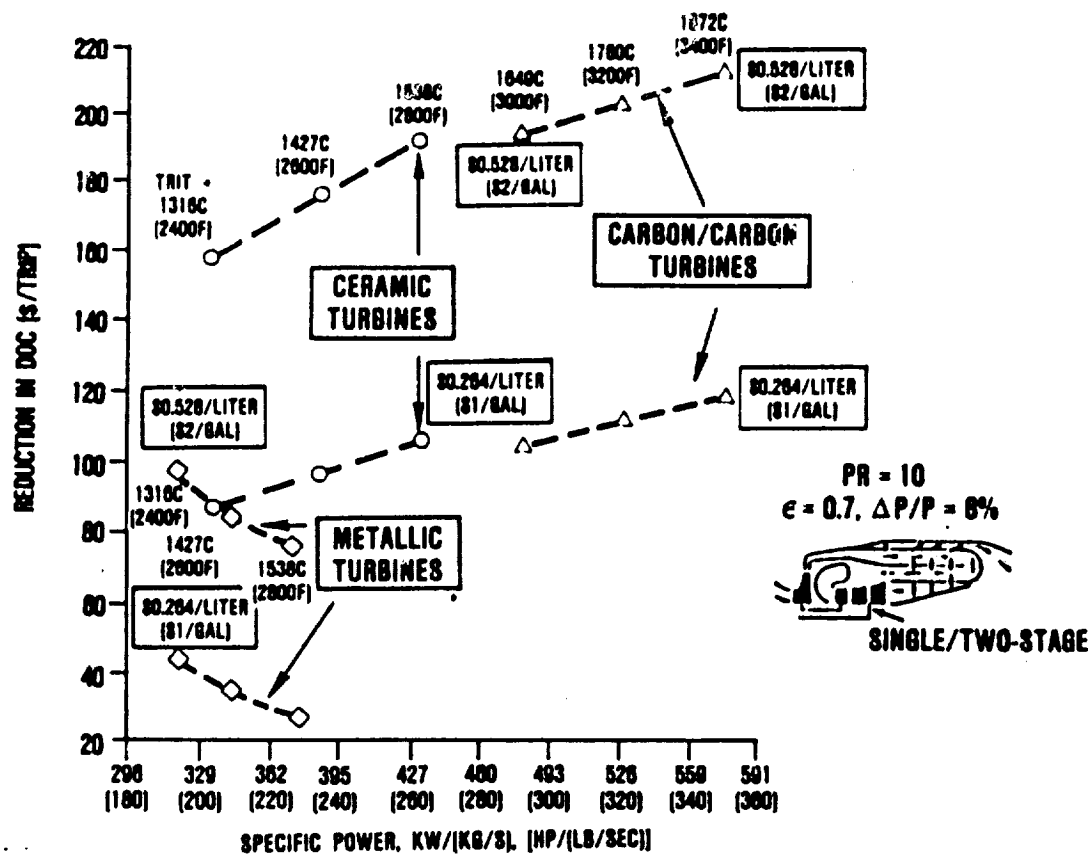


Figure 78. DOC Comparison of Ceramic Versus Advanced Metallic and Carbon-Carbon Turbines.

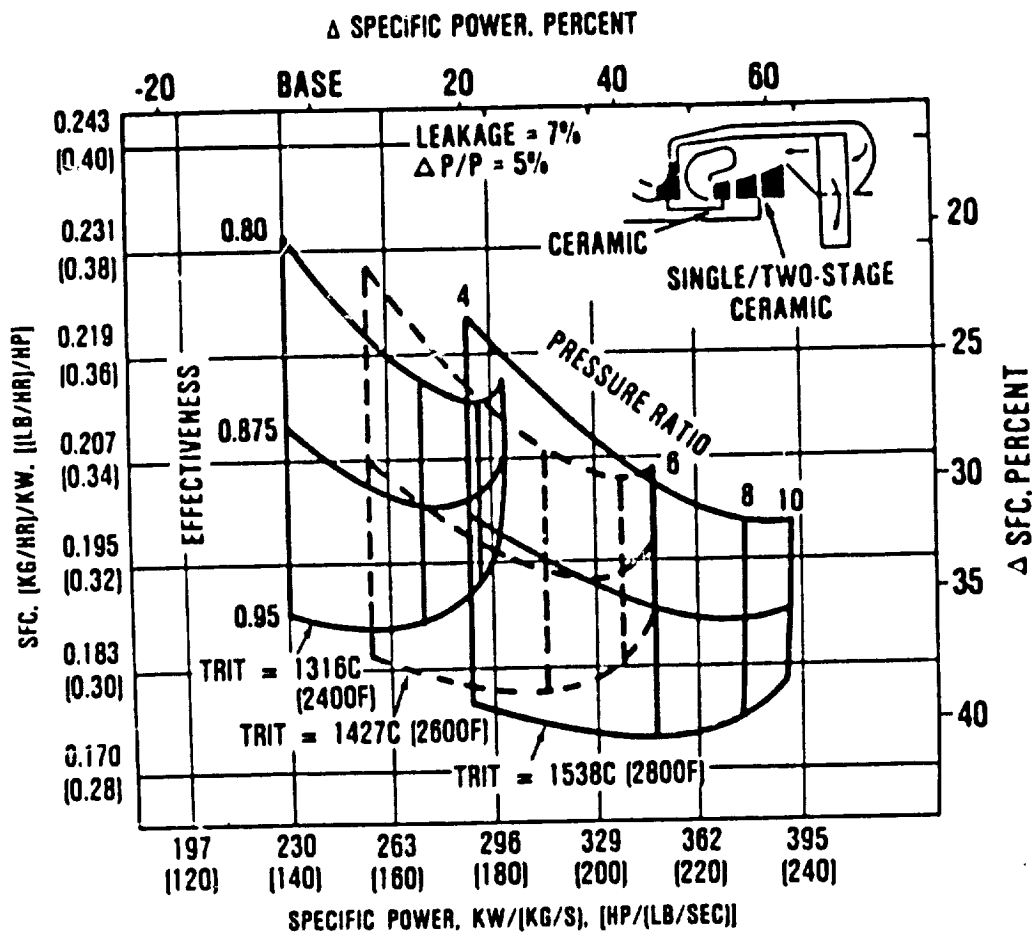
3.2.2.2 Regenerated Cycle Study

The regenerated cycle evaluation is similar to the recuperated study, with the added complexity of leakage. Only one engine configuration was considered that consisted of a single-stage centrifugal compressor, axial ceramic turbines, and a ceramic rotary regenerator.

Figure 79 shows a plot of SFC versus specific power with a range of pressure ratios from 4:1 to 10:1, TRT from 1316 to 1538C (2400 to 2800F), and regenerator effectiveness from 0.8 to 0.95. Regenerator pressure drop and leakage are held constant at 5 and 7 percent, respectively. As shown, SFCs below 0.3 (nearly a 40 percent improvement relative to the reference engine) are possible. Cycle pressure ratio optimizes at approximately 6:1, compared to 10:1 for recuperated cycles due to the higher level of effectiveness.

The key performance penalty incurred in a regenerated engine is leakage (including carry-by). To determine its impact, leakage was varied from 4 to 10 percent. As shown in Figure 80, if leakage increases from 4 to 10 percent, specific power can be reduced by 15 percent and SFC can increase by 5 percent. Clearly, high effectiveness and low leakage are important in a regenerated engine. As with recuperators however, high effectiveness and low leakage translate into increased size and weight, as shown in Figure 81.

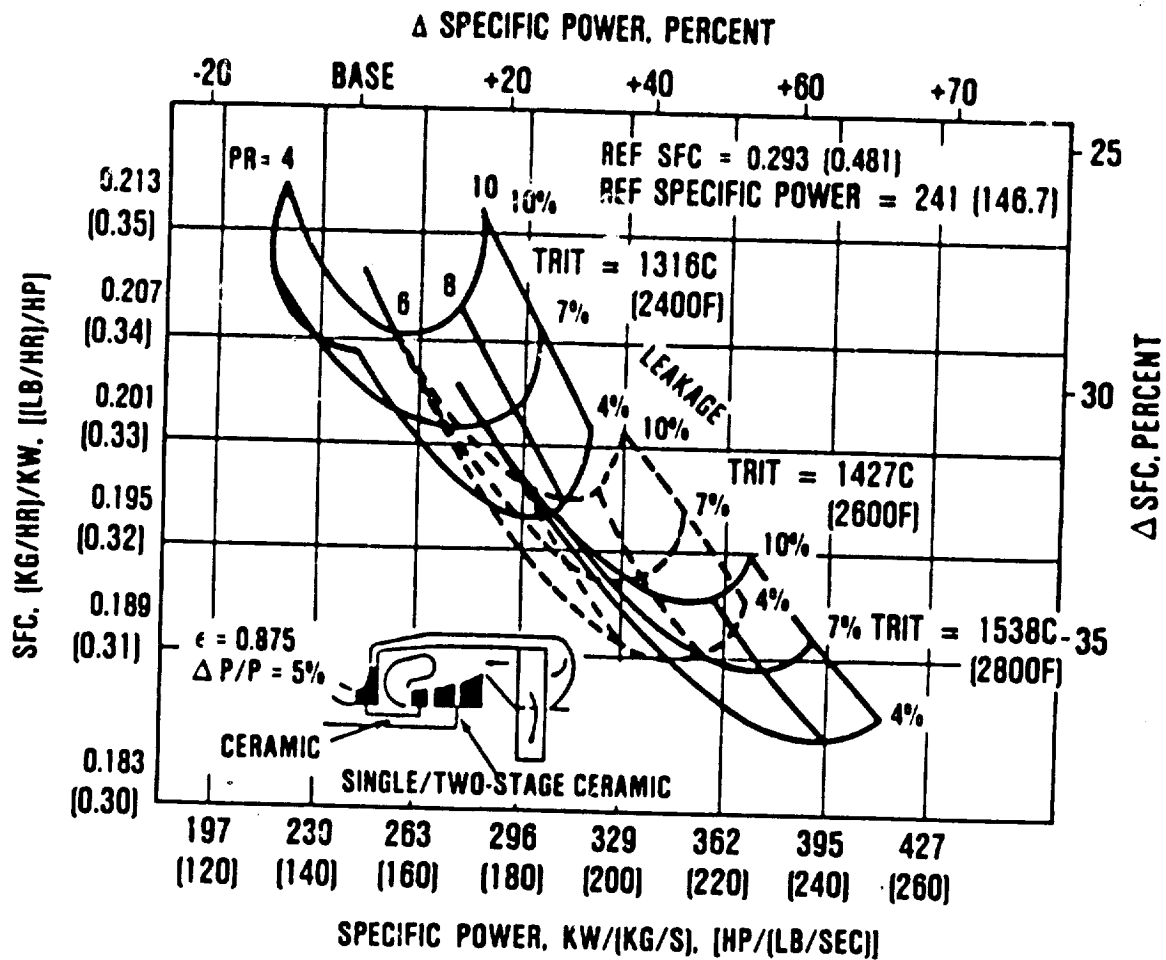
In terms of DOC, recuperated and regenerated cycles have similar trends, as indicated in Figure 82. Again, effectiveness optimizes at a lower value (near 0.88) for the low fuel price than for fuel at the high price (0.92 to 0.93). Leakage has less of an impact on DOC than might be expected. Leakages below 6 to 7 percent show little payoff for this application. Also,



REF SFC = 0.293 (0.481)
REF SPECIFIC POWER = 241 (146.7)

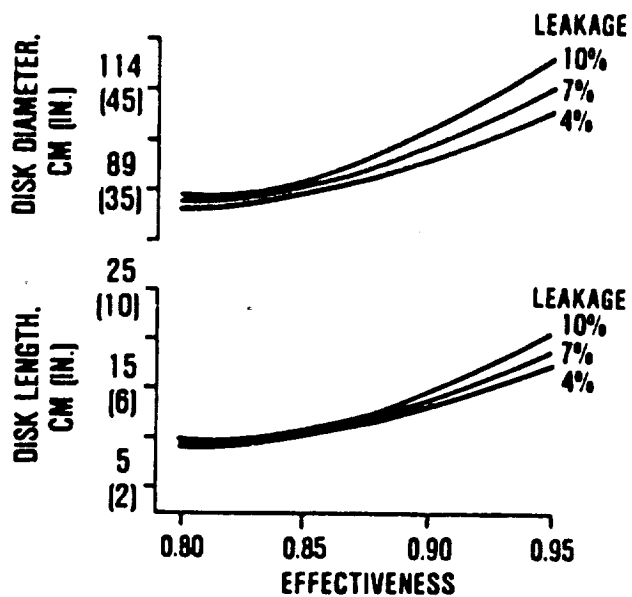
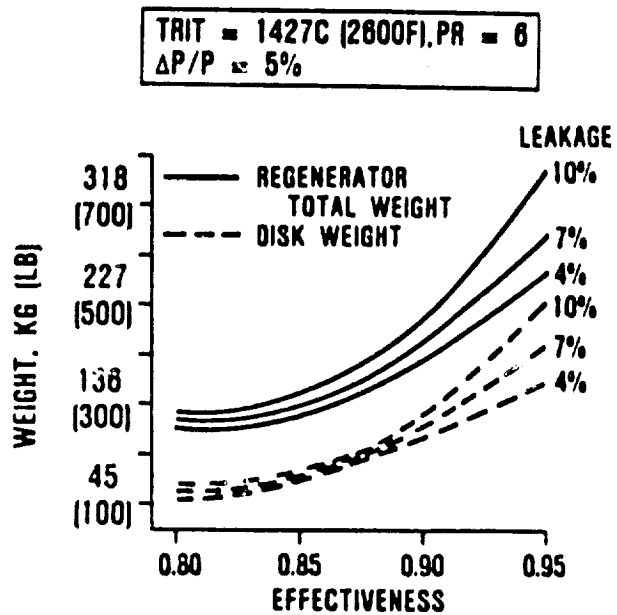
65-281-128

Figure 79. Regenerated Cycle Performance Results for Commuter Application.



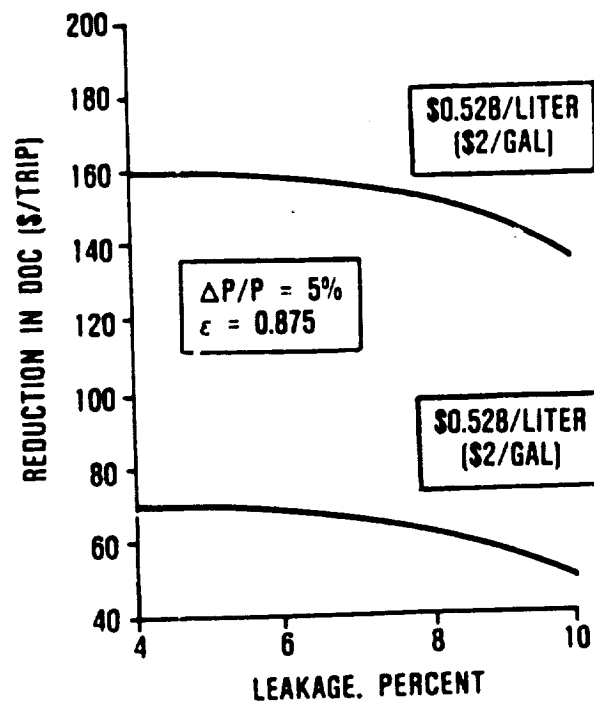
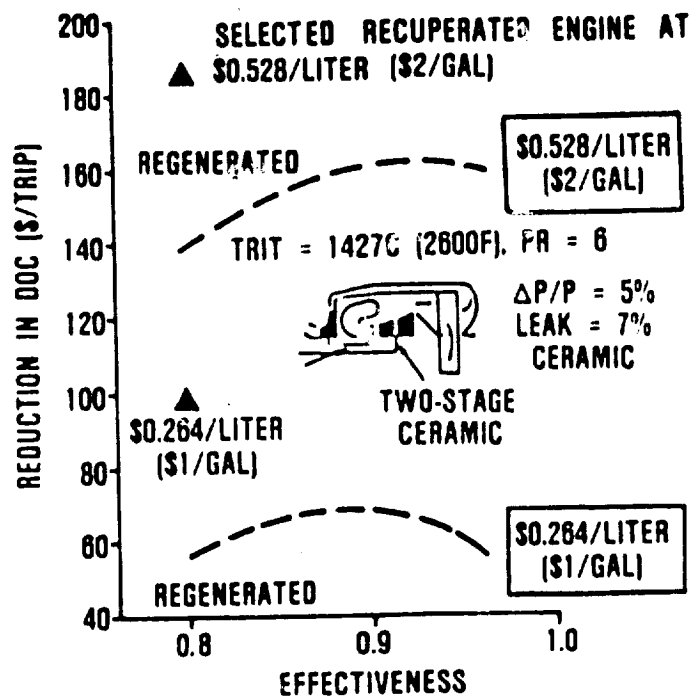
85-281-120

Figure 80. Impact of Regenerator Leakage on Performance.



85-281-118

Figure 81. Impact of Regenerator Effectiveness and Leakage on Size and Weight.



65-281-25

Figure 82. Impact of Regenerator Effectiveness and Leakage on DOC.

regenerated engines cannot match the improvement in DOC achieved by the ceramic recuperated engine at either of the fuel prices selected for this study.

3.2.2.3 Simple-Cycle Study

A conventional simple-cycle engine was also selected for the commuter application, based on the results from the rotorcraft simple-cycle study as discussed in paragraph 2.2. Due to the similarities between the commuter and rotorcraft trade factors, similar DOC trends were expected for the two applications, thereby not affecting cycle selection. As shown in Figure 83, an engine with ceramic turbines at a pressure ratio of 22:1 and a TRIT of 1427C (2600F) had been selected for the rotorcraft application. This cycle was rematched to include a proper accounting of the inlet, propeller gearbox, and associated losses, as shown.

3.2.3 Cycle/Engine Selection

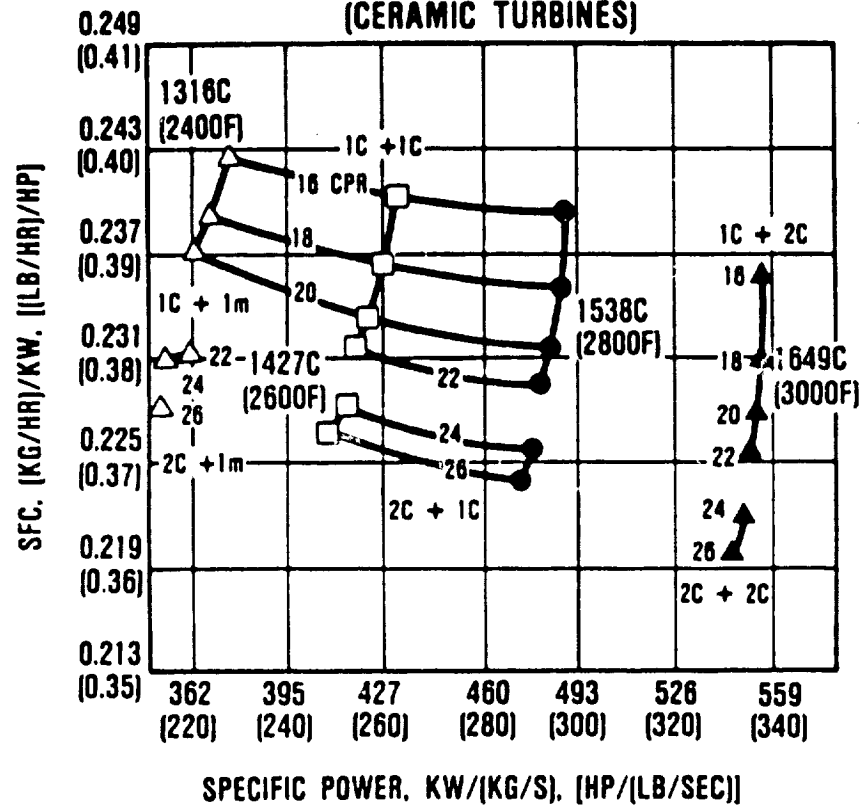
Three cycle types have been investigated for the commuter application: recuperated, regenerated, and simple. All three are compared in terms of DOC in Figure 84. As shown, the recuperated cycle is the clear winner in terms of total DOC at the high fuel price of this study. At the low fuel price, it is a toss up between recuperated and the conventional simple-cycle approach.

Despite its SFC advantage, the regenerated engine loses out at both fuel prices. As indicated, the unfavorable contributions of weight, size, and cost are enough to offset the SFC advantage.

Based on the DOC results at the high fuel price, only the recuperated engine, as described below, was considered for further evaluation in Task III:

- o Compressor - Single-stage centrifugal, PR = 10:1

ROTORCRAFT STUDY (CERAMIC TURBINES)



REMATCHED COMMUTER ENGINE DATA

- TRIT = 1427C (2600F)
- PR = 22
- SFC = 0.238 (0.392)
- SPECIFIC POWER = 406 (247)
- WEIGHT = 131 KG (288 LB)
- LENGTH = 58.4 CM (23.0 IN.)
- DIAMETER = 23.4 CM (9.2 IN.)
- COST = \$154,100

65-281-125

Figure 83. Simple Cycle for Commuter Selected from Rotorcraft Study.

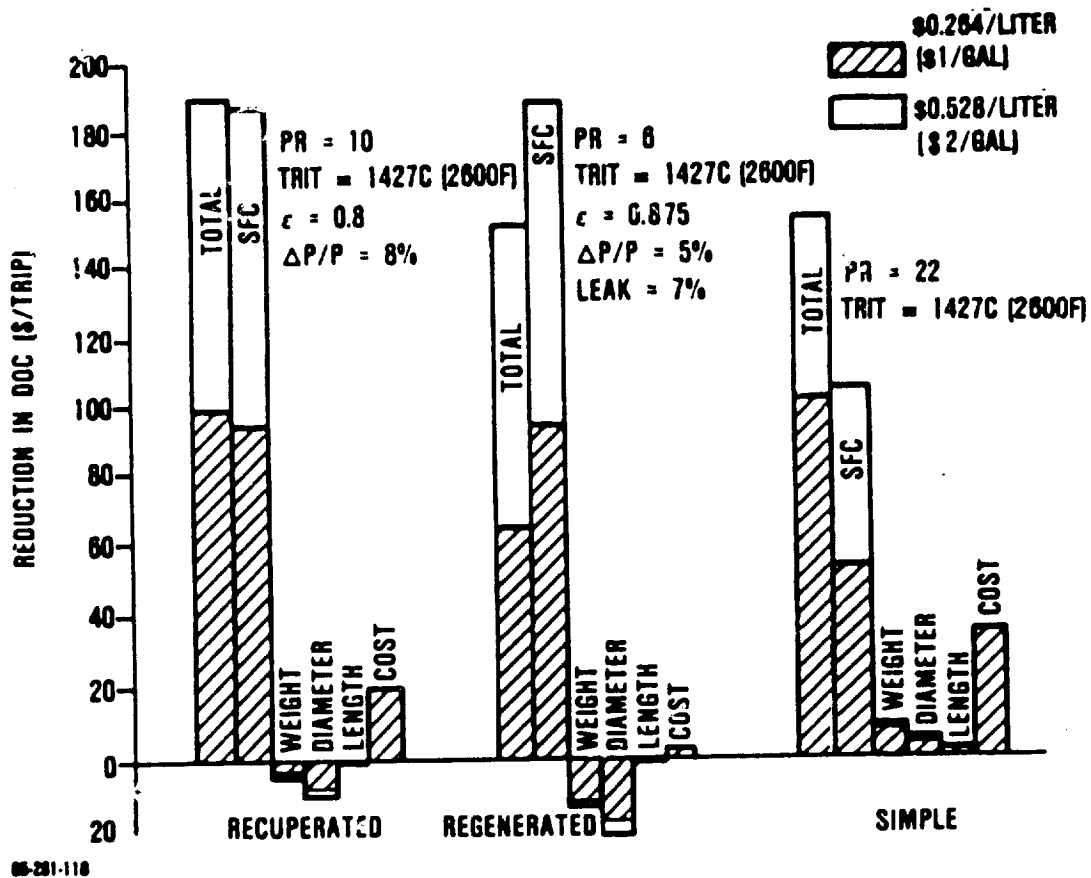


Figure 84. DOC Comparison of Recuperated, Regenerated, and Simple Cycles.

- o HP turbine - Single-stage axial, ceramic, uncooled, unshrouded, TRIT = 1427C (2600F)
- o LP turbine - Multistage axial, uncooled (ceramic as necessary)
- o Recuperator - Ceramic plate-fin, $\epsilon = 0.8$, $\Delta P/P = 8$ percent

3.3 Task III - System Performance Evaluation

The selected engine from Task II was evaluated in terms of its impact on overall aircraft system performance. A detailed mission analysis was conducted for the aircraft/engine system, requiring an extensive matrix of off-design performance. Finally, the selected engine was evaluated in detail with the GTEC economic model to determine direct operating costs (DOC).

Prior to the system performance evaluation, the recuperated engine cycle and configuration were further refined by the typical GTEC preliminary design process.

3.3.1 Engine/Cycle Refinements

Several minor engine refinements were made to the year-2000 engine selected in Task II. These refinements were made following a more detailed design analysis of each engine component. The identified refinements and the resulting performance effects are summarized in Table 21.

For the recuperated cycle, engine performance has changed only slightly; however, weight, size, and cost estimates were revised. These changes are due primarily to a reassessment of the recuperator design and cost estimates. This results in a

TABLE 21. PERFORMANCE REFINEMENTS FROM TASK II

Sea Level, Static, ISA, τ/θ

	Task II	Task III	Comments
SPC, kg/hr-kw (lb/hr-hp)	0.196 (0.323)	0.196 (0.323)*	o Design point change
Specific Power, kW/kg-s (hp/lb-sec)	387.3 (235.6)	371.7 (226.1)*	SLS to 18,000 feet, 569 km/hr (307 knots) TAS
Weight, kg (lb)	235.6 (519.5)	229.9 (506.8)**	o Cost and weight
Length, cm (in)	106.7 (42.0)	102.4 (40.3)	- Ni3Al disk
Diameter, cm (in)	68.8 (27.1)	64.8 (25.5)	- Recuperator cost/weight
Cost, K\$	175.1	194.1	- reassessed
			- Sell price reassessed
Compressor			
- $W/\theta/\delta_{INLET}$, kg/s (lb/sec)	1.95 (4.29)	2.02 (4.46)	o Task III efficiencies
- $W/\theta/\delta_{EXIT}$, kg/s (lb/sec)	0.27 (0.597)	0.306 (0.674)	per GTEC preliminary
- PR	10	10	design program
- η_{AD}	0.818	0.818	
- η_{poly}	0.866	0.866	
Combustor			
- TRIT, R(P)	1427 (2600)	1427 (2600)	
- $\Delta P/P$, percent	5	5	
HP Turbine			
- $W/\theta/\delta$, kg/s (lb/sec)	0.508 (1.12)	0.576 (1.27)	
- η	0.904	0.898	
- $\Delta H/U2$	1.23	1.09	
- NHP, rpm	63,480	60,149	
LP Turbine			
- $W/\theta/\delta$, kg/s (lb/sec)	1.09 (2.41)	1.21 (2.66)	
- η	0.872	0.884	
- $\Delta H/U2$	1.76	2.34	
- NLP, rpm	34,893	31,159	

*Off-design

**Includes recuperator weight, 107.1 kg (236.1 lb)

size and weight reduction of 2 to 6 percent, and a cost increase of 11 percent. These refinements were analyzed and found to have no effect on the optimum cycle selection.

3.3.2 Mission/Economic Analysis

The mission and economic analyses for the commuter application were conducted with the reference mission and aircraft using the GTEC mission/economic model as defined in Task I.

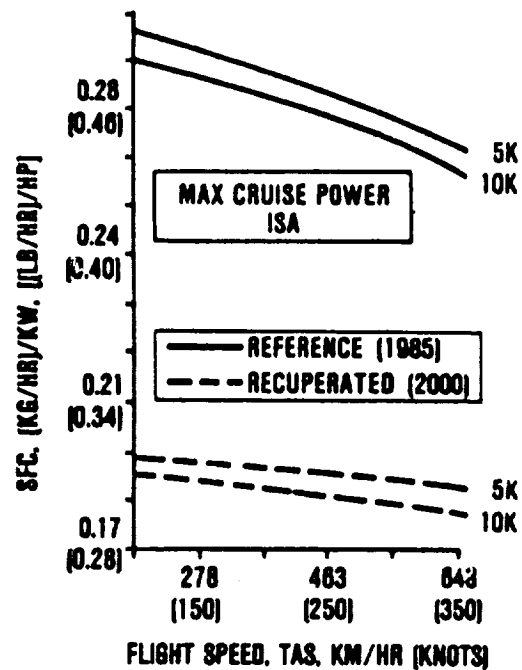
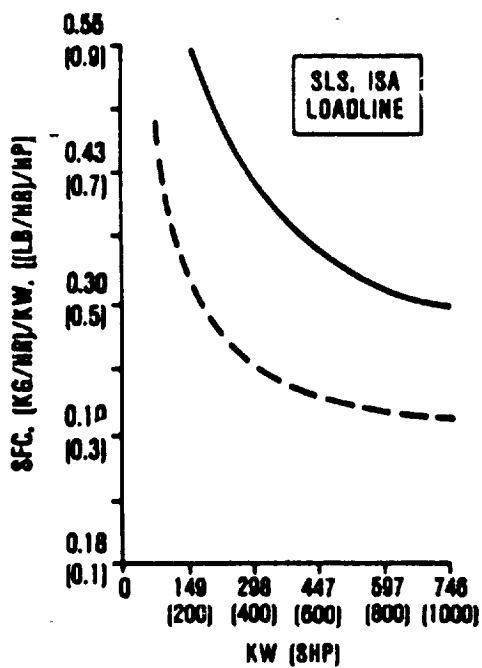
To support the mission analysis, a matrix of off-design performance conditions and power settings was generated. A comparison of sea level, static loadlines, shown in Figure 85, indicates that the recuperated engine has superior part-power SFC over the reference engine. A flight speed, SFC lapse rate comparison shows SFC improvements of 30 to 35 percent.

The resulting mission performance has been summarized in Figure 86. As shown, the key change is a 35 percent reduction in fuel burn relative to the reference engine. Takeoff gross weight has also been reduced by 2.9 percent. Drag, cruise speed, and block time compare unfavorably with the reference due to the increased size of the recuperated engine.

Figure 87 shows the study results in terms of DOC. The recuperated cycle is shown to significantly reduce DOC by 5.7 and 11.1 percent, relative to the reference engine at the low and high fuel prices, respectively.

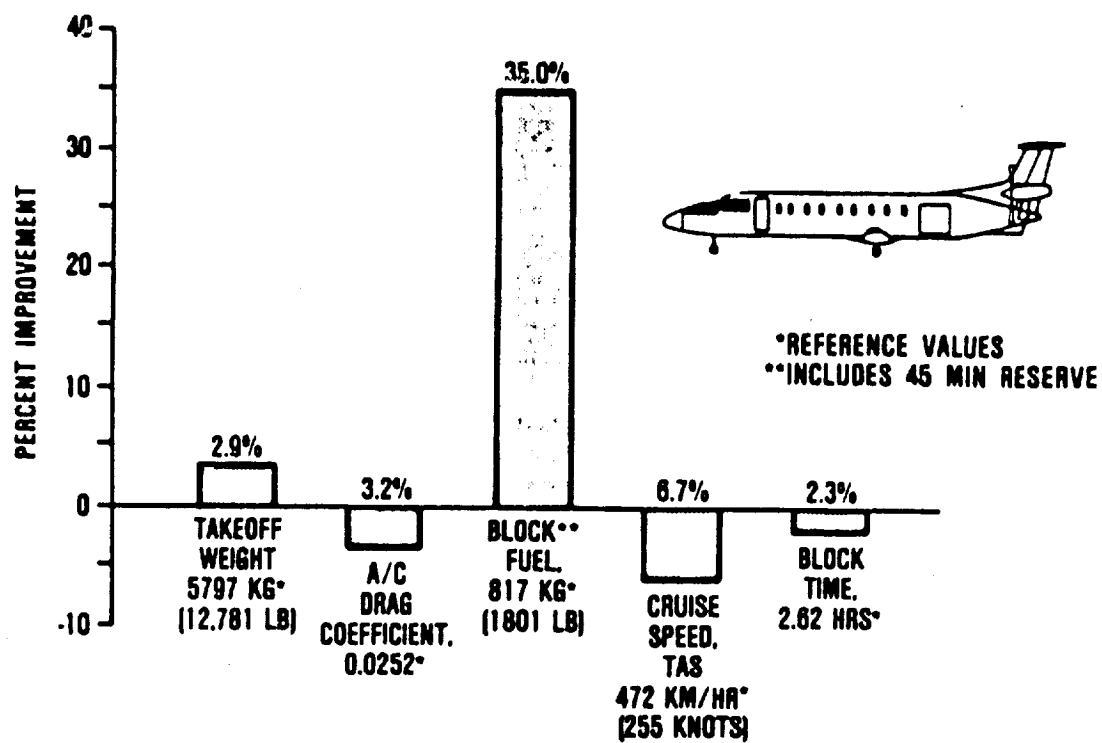
3.4 Task IV - Small Engine Component Technology Plan

Task IV identifies and quantifies high payoff technologies for the commuter engines. It also presents technology plans that are based on the projected benefits.



85-251-127

Figure 85. Part-Power Performance Comparison for the Commuter Application.



05-281-114

Figure 86. Projected Reductions in Commuter Parameters, Recuperated Engine Mission Results.

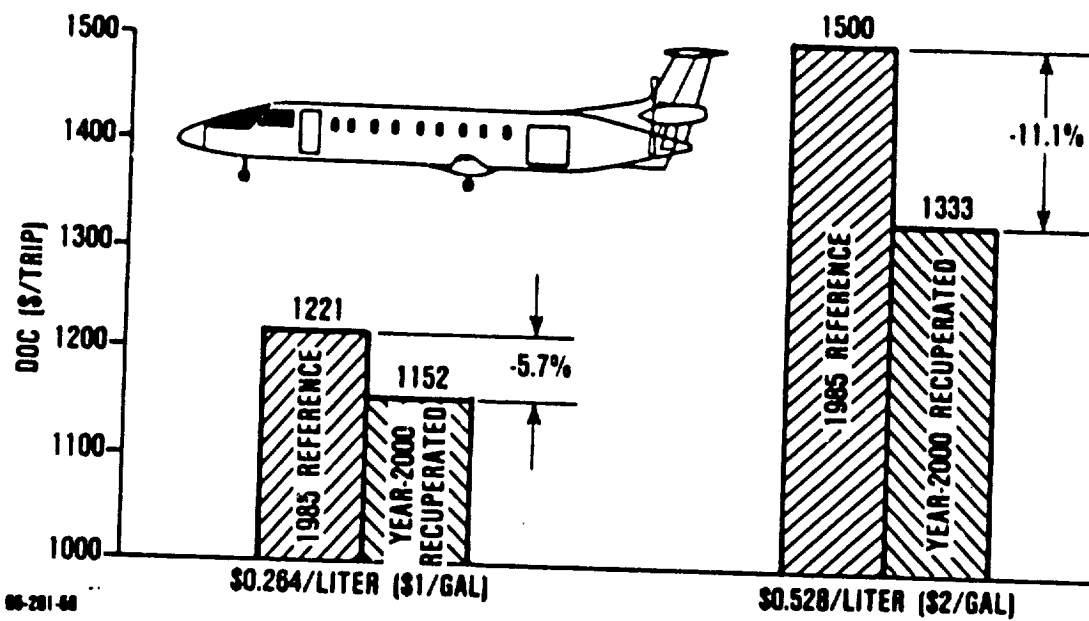


Figure 87. Commuter DOC Results for Recuperated Engines.

3.4.1 Technology Identification/Benefits

A number of technologies have been identified by the performance and DOC results from Task II and Task III. They are essentially identical to those discussed for the rotorcraft application in paragraph 2.4.1. These technologies have benefits in terms of SFC, weight, size, or cost. Several of these technologies, such as metal matrix shafts, are difficult to quantify in terms of DOC, but their use is considered beneficial or necessary to meet engine design goals. The identified technologies are:

- o Component performance (aero)
 - Compressor η
 - Turbine η
 - Combustor $\Delta P/P$
- o Materials
 - Ceramics (for turbines, combustors, recuperators)
 - Polymeric composites (propeller gearbox)
 - Ni₃Al disk (turbines)
 - Aluminum powder metal alloys (compressors)
 - Cast titanium (compressors)
- o Combustor
 - Low pattern factor
 - High heat release rate
- o System technologies
 - Metal matrix shafts
 - Noncontact face seals/brush seals

In order to estimate the benefits derived from these technologies, GTEC isolated each technology using the technical

approach as discussed for the rotorcraft engine in paragraph 2.4 and as summarized in Figure 88. This approach involves removing one technology from the year-2000 engine, setting new cycle limits as necessary, and generating new engine performance, specifically SFC, weight, diameter, length, and cost data. Finally, trade factors were applied to the new engine parameters, which result in new DOCs. Comparing the resultant DOC values to the DOC for the baseline year-2000 engine with all technologies shows the improvement derived from that technology. The selected technologies are not independent from one another and are therefore not additive.

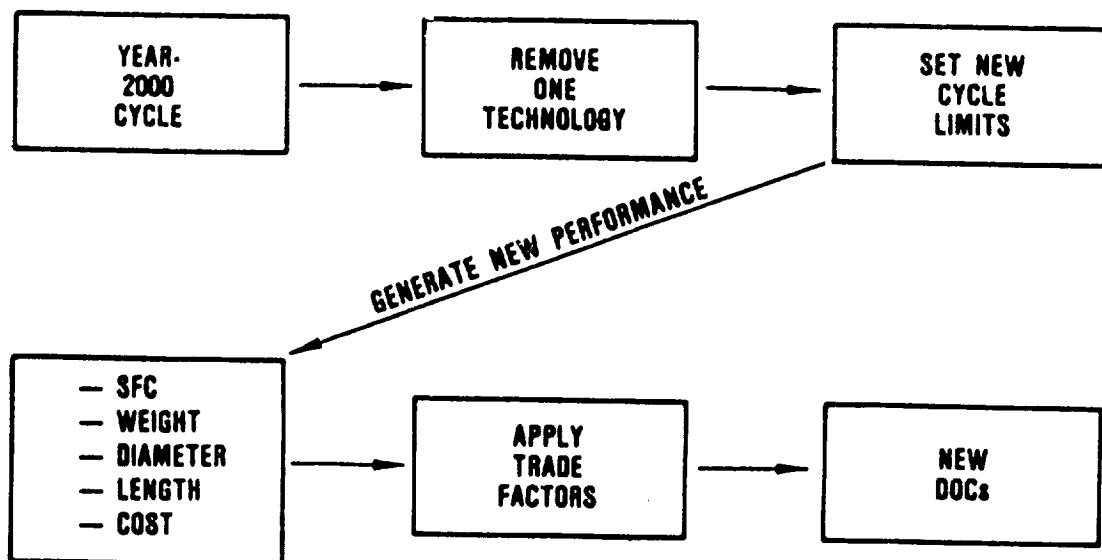
Of the technologies quantitatively investigated, hot-end materials were found to have the greatest DOC impact, as shown in Figure 89. For example, ceramics for application in turbine airfoils contribute approximately half of the overall DOC improvement projected. Ceramics in the recuperator contributes approximately one-fourth of the overall DOC improvement.

Compressor and turbine efficiency improvements also show significant DOC benefit. Combustor technologies for lower pressure drop and improved compressor materials resulted in only small improvements in DOC.

Unlike the simple-cycle engines for the rotorcraft application, Ni₃Al did not pay off in DOC benefits. This can be attributed to the much lower aerodynamic loading levels in the HP turbine (and therefore, lower acceptable blade and disk speeds) for the recuperated engine.

3.4.2 Technology Plan

GTEC's recommended plan for the technologies applicable to year-2000 commuter engines is discussed in this section. The



05-251-47

Figure 88. Technical Approach for Estimating Technology Benefits.

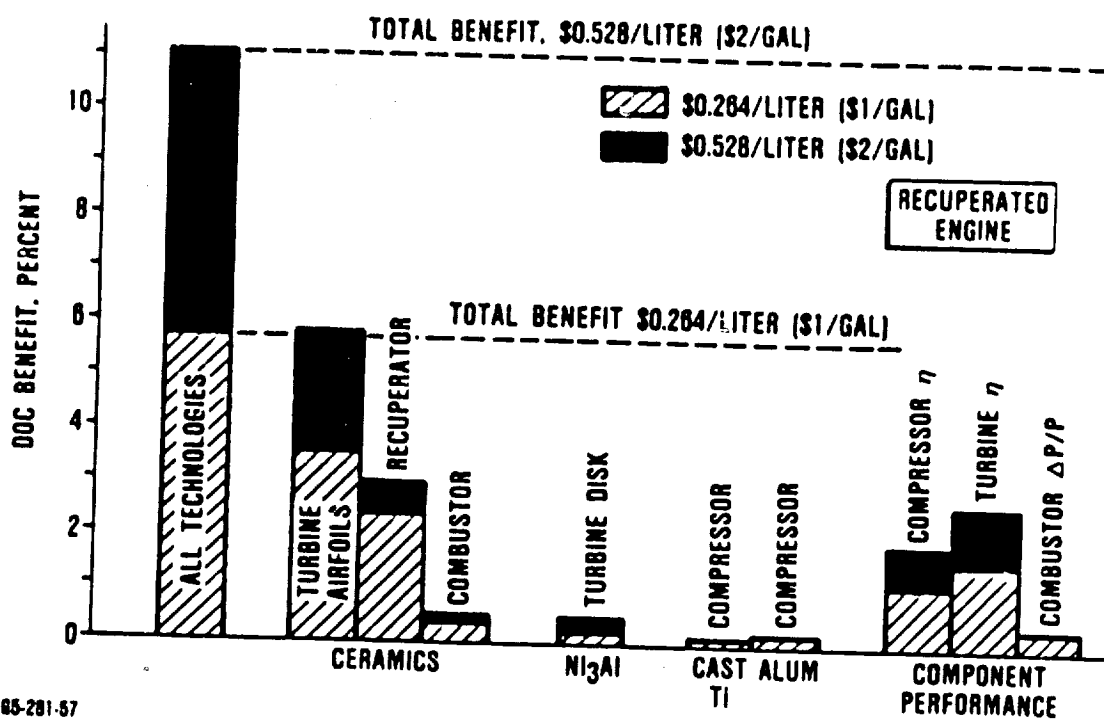


Figure 89. Projected DOC Benefits (Percent) for Isolated Technologies.

objective of this plan is to address high payoff technologies in keeping with the technology benefits presented in paragraph 3.4.1. These high-payoff technologies consist of those with quantified DOC benefits and other system technologies considered vital to future turboprop engines, as envisioned for year-2000 commuters.

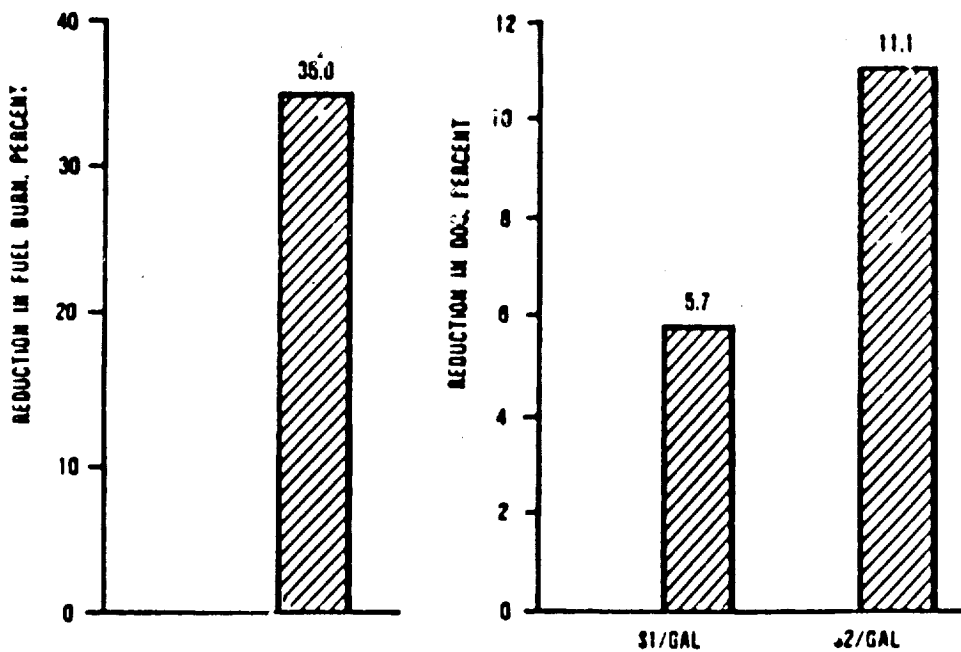
These high-payoff technologies, as discussed in paragraph 3.4.1, are essentially the same as those identified for year-2000 rotorcraft engines and presented in paragraph 2.4. Moreover, the technology benefits for these two engine applications are similar. For these reasons, a technology plan common to both of these engines is recommended here. The technology plan for commuter engines is the same as outlined for the rotorcraft, which is repeated here for reference purposes.

- 2.4.2.1 Ceramics
- 2.4.2.2 Recuperators
- 2.4.2.3 Metallics for turbines
- 2.4.2.4 Turbine performance
- 2.4.2.5 Combustor performance
- 2.4.2.6 Compressor (centrifugal) performance
- 2.4.2.7 Materials for "cold" parts
- 2.4.2.8 System technologies

3.5 Summary

The commuter mission performance achieved with the selected year-2000 recuperated engine is summarized in Figure 90. As shown, the key improvement is a 35 percent reduction in fuel burn relative to the reference engine. With this fuel burn advantage, the recuperated engine achieves a reduction in DOC of 5.7 and 11.1 percent, respectively, at the low and high fuel price.

These fuel burn and DOC reductions are dependent on several key technologies. These include advanced materials, component performance, and system technologies.



KEY TECHNOLOGIES

- CERAMICS (TURBINE, RECUPERATOR)
- IMPROVED COMPONENT PERFORMANCE (TURBINE, COMBUSTOR, COMPRESSOR AERO)
- SYSTEM TECHNOLOGIES (METAL MATRIX SHAFTS, SEALS)

Figure 90. Commuter Mission Analysis Results.

4.0 SUPERSONIC CRUISE MISSILE ENGINES

This section presents Garrett's SECT study approach, methodology, and results as established for the cruise missile engines envisioned for the year 2000. This section is organized into four major tasks as conducted and described in paragraph 1.2 of this report.

4.1 Task I - Selection of Evaluation Procedures and Assumptions

In Task I, reference missiles are defined to represent year-2000 vehicle technology, and reference propulsion systems are defined to represent current rocket and near-term gas turbine engine technology. A representative year-2000 mission is established and the reference airframe/engine is evaluated for missile range for a constrained missile volume.

The impact of environmental constraints on the year-2000 missile is also considered as appropriate, and an economic model is defined to facilitate evaluation of missile costs. Finally, trade factors are computed for primary engine interface parameters in order to quantify the improvements in missile range and missile cost/range for the advanced turbomachinery cycles/configurations considered in Task II.

4.1.1 Reference Missiles

Two reference missiles were configured for the supersonic, tactical mission that is discussed in paragraph 4.1.2. The selection of these configurations was based on discussions held with various missile manufacturers, in particular, Martin Marietta.

The first reference missile discussed is rocket-powered and is representative of a current (1985) technology weapon system. The estimated range and cost of this missile establish the performance benchmark for current supersonic, tactical missile systems.

Due to the requirement for increased range, it is projected that advanced missiles will require the more efficient turbine engine to replace the rocket engine. For this reason, a second missile was configured to represent a turbojet-powered missile system.

The dimensions of both of these missiles are defined by the packaging limitations of an existing rotary launch envelope: they are confined to a maximum length of 424 cm (168 in.), a maximum width of 46 cm (18 in.), and a maximum height of 86 cm (34 in.). The cross-section dimensions represent a triangular portion of the total payload area.

4.1.1.1 Reference Missile (Rocket Propulsion System)

The configuration for the rocket-powered missile, shown in Figure 91, is of conventional cylindrical shape. It is 36 cm (14 in.) in diameter and 427 cm (168 in.) in length. The payload, avionics, and controls are located in the forward section of the missile in a 165 cm (65 in.) long conical housing. The propulsion system, which is in the aft section, accounts for 262 cm (103 in.) of the missile's total length.

The estimated weight of the missile is 729 to 771 kg (1600 to 1700 lb). The missile's basic aerodynamic characteristics are similar to those of the turbojet-powered missile.

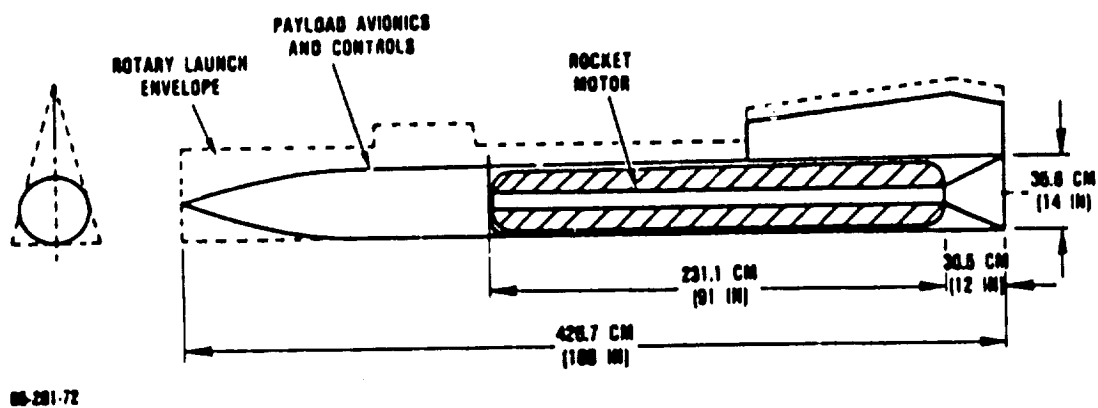


Figure 91. Reference Missile Configuration with Rocket Propulsion System.

4.1.1.2 Reference Missile (Turbojet Propulsion System)

The configuration of the turbojet-powered missile, shown in Figure 92, is generally trapezoid shaped. The forward section of the missile contains the payload, avionics, and controls in a 165 cm (65 in.) long conical housing. The aft section of the missile (the trapezoidal section) contains the fuel, the turbojet engine, and the engine inlet duct, and accounts for the aft 262 cm (103 in.) of the 428-cm (169-in.) total missile length. The frontal view of the missile shows a cross section with a maximum height and width of 53 and 36 cm (21 and 18 in.), respectively. The engine inlet is a fixed area Pitot design, which minimizes cost while maintaining adequate inlet pressure recovery. A flush-type inlet design is not being considered in this study due to high-inlet pressure losses associated with supersonic flight conditions.

The calculated missile weight is displayed in Table 22. The aerodynamics generated for the missile are summarized in Table 23.

TABLE 22. TURBOJET-POWERED MISSILE WEIGHTS

Component	Weight kg (lb)
Payload/Avionics/Controls	227 (500)
Structure	229 (505)
Fuel	129 (284)
Engine	<u>96 (211)</u>
Total	680 (1500)

4.1.2 Reference Engines

Two reference engines are defined for the supersonic, tactical mission that is outlined in paragraph 4.1.3. A two-stage

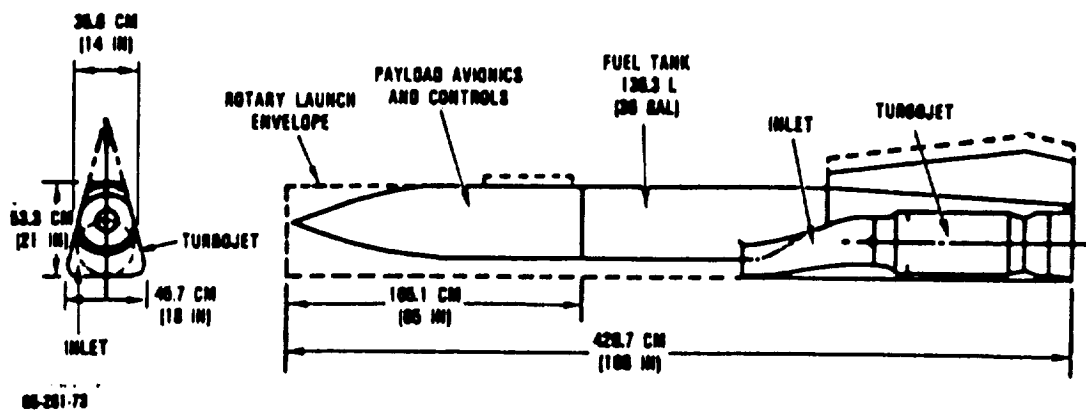


Figure 92. Reference Missile Configuration with Turbojet Propulsion System.

TABLE 23. TURBOJET-POWERED MISSILE AERODYNAMICS

<u>C_L</u>	<u>C_{D_I}</u>	<u>Mach No.</u>	<u>C_{D_0}</u>
0.005	0.0003	0.8	0.0011
0.015	0.0017	1.0	0.0227
0.025	0.0037	1.2	0.0297
0.035	0.0062	1.4	0.0306
0.045	0.0090	1.6	0.0277
0.055	0.0122	1.8	0.0233
0.065	0.0157	2.0	0.0195
0.075	0.0194	2.2	0.0174
		2.4	0.0158
		2.6	0.0146

Missile Reference Area = 1.95 m^2 (21 ft^2)

C_L = Lift Coefficient

C_D = Drag Coefficient = $C_{D_I} + C_{D_0}$

C_{D_I} = Induced Drag Coefficient

C_{D_0} = Parasitic Drag Coefficient

rocket engine that is representative of a current-technology (1985) engine system is first defined. The estimated missile range and missile cost/range for the rocket-powered missile are used in the final payoff assessment in Task III.

Also defined is a turbojet engine that is representative of near-term (✓1989) turbomachinery technology. No turbine engine currently exists that is suitable for completing the outlined supersonic mission. This turbojet engine is defined so that realistic trade factors can be generated for the evaluation of year-2000 engines in Task II.

4.1.2.1 Reference Engine (Rocket)

A two-stage, conventional solid-rocket propulsion system is used to meet the mission requirements. The performance, weight, and cost of the rocket motor were not calculated by GTEC for this study. However, based on discussions with airframers and rocket engine designers, it is considered feasible to design a rocket engine with adequate performance levels to meet the stated mission requirements. As the actual cost of a rocket engine of this type is not available, a cost of \$60,000 was assumed for the SECT study.

4.1.2.2 Reference Engine (Turbojet)

The reference (turbojet) engine is based on a conceptualized GTEC turbojet engine of near-term (✓1989) technology that is suitable for supersonic tactical missile applications. The performance, operating parameters, and configuration of this engine reflect component technology levels beyond 1985 demonstrated technology.

Configuration

The turbojet engine configuration is shown schematically in Figure 93 along with summary data as established in this study. The engine is a single-spool turbojet design that uses a mixed-flow and axial-compressor system and is driven by a single-stage axial turbine. The through-flow combustor allows for a minimal-diameter design, which is required for integration into the missile system. Additionally, the engine features a fixed-geometry expansion/deflection nozzle and a combined electric power generator/fuel pump and metering unit mounted on the mainshaft of the engine.

Materials

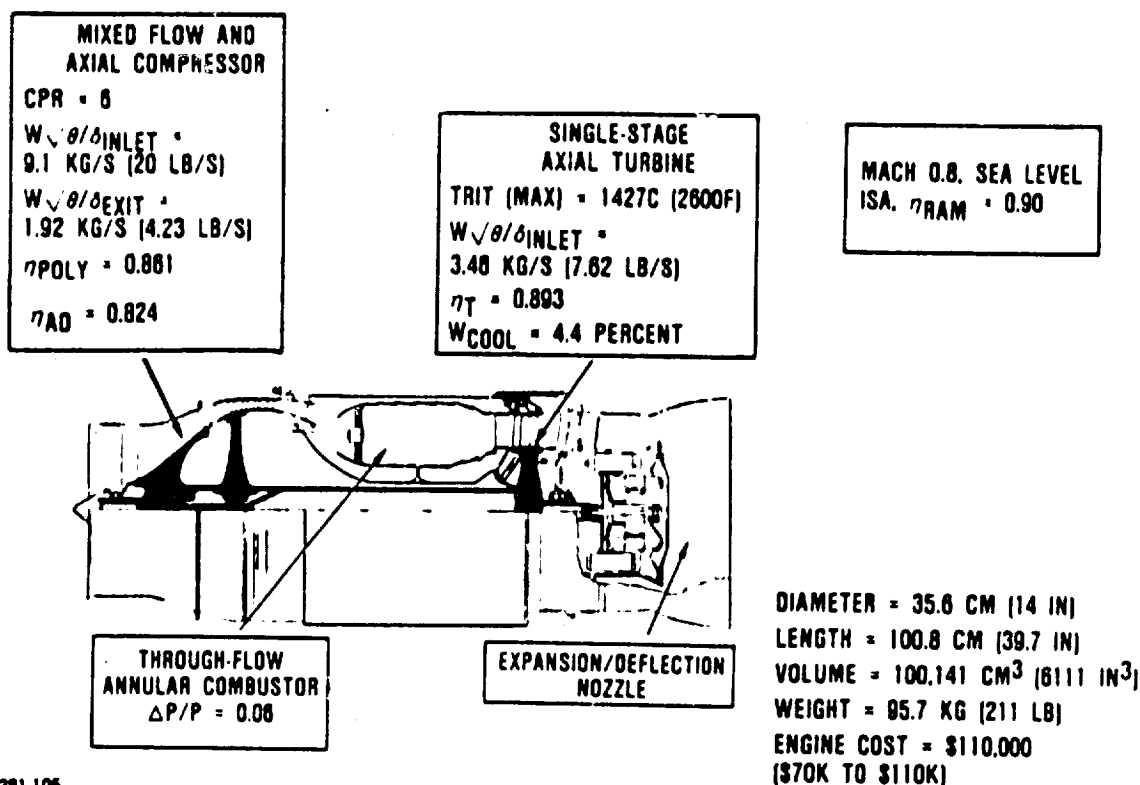
The materials selected for the reference (turbojet) engine are listed in Table 24. It is anticipated that all materials included will be available for use in a near-term (1989) demonstration engine.

TABLE 24. REFERENCE TURBOJET COMPONENT MATERIALS

Part	Material
Compressor	Disk: Titanium Airfoil: Titanium
Combustor	Hastalloy X
HP Turbine	Disk: Powder-Metal Astroloy Airfoil: CMSX-3 Stator: Columbium
Shaft	INCO 718

Engine Performance

Engine performance is predicted using component technology levels representative of near-term (1989) demonstration engines.



65-281-105

Figure 93. Reference Turbojet Engine Configuration and Data Summary.

Several engine performance conditions must be considered because of the range of operating conditions required by the mission. Figure 94 shows the thrust of the reference (turbojet) engine and missile drag as a function of flight Mach number. Highlighted in this figure are several critical performance levels that are discussed in the following paragraphs.

The engine thermodynamic design point is selected at the missile launch condition (Mach 0.8, sea level). Table 25 summarizes the performance at this condition. The selection of this design point assures that adequate thrust is available to sustain and accelerate the missile after launch. It also provides for balanced performance between the missile launch and cruise conditions.

Another critical engine condition is max power cruise. Table 26 summarizes the engine performance at this condition. The engine performance at Mach 2.5, sea level, is important since the engine operates at this condition for most of the mission duration. The max power condition indicates that excess thrust is available for maneuver requirements. It is also an indicator of engine efficiency. It is at this condition that the TSFCs of the advanced engines were evaluated in Task II.

Other engine performance included is the sea-level, static, uninstalled condition. The engine performance at this condition is summarized in Table 27.

Engine Weight

The reference (turbojet) engine weight, including accessories, has been estimated at 96 kg (211 lb). This weight was calculated in a manner similar to the rotorcraft and commuter engines, using the WATE-S Computer Program. The WATE-S program was also used to determine advanced engine weights in Task II.

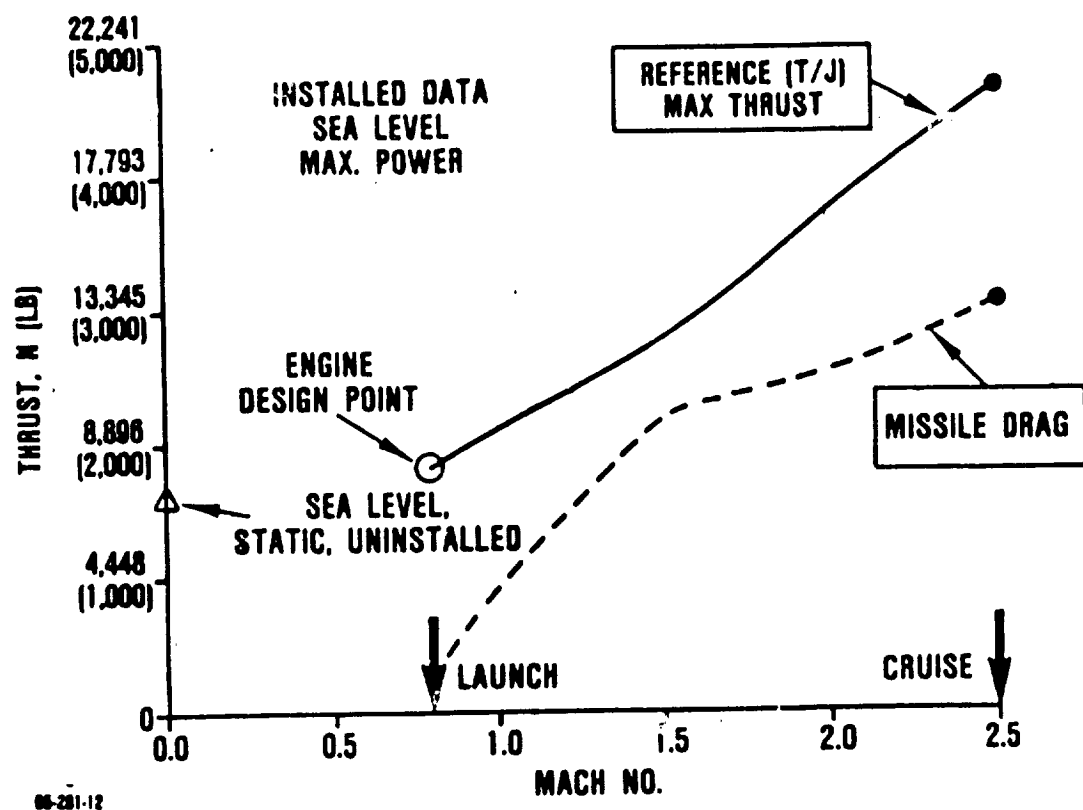


Figure 94. Missile Thrust and Drag.

TABLE 25. REFERENCE (TURBOJET) ENGINE - DESIGN POINT DATA

Design Point Performance - Sea Level, Mach 0.8, ISA,
Installed With No Production Margin

Overall Engine Performance		Component Performance	
		<u>HP Compressor</u>	
Engine Rating, N (lbg)	8194 (1842)	o PR	6.0
TSFC, (kg/hr)/N	0.167	o η_{AD} , %	82.4
Turbine Inlet Temp, C (F)	1427 (2600)	o η_{poly}	86.1
Overall Cycle PR	6.0	o Exit flow	1.92 (4.23)
Inlet Wt/δ, kg/s (lb/sec)	9.1 (20.0)	<u>Combustor</u>	
Physical Speed, rad/s (rpm)	3.657 (34,925)	o η , %	99.5
JP-10 Fuel, LHV, kJ/kg (Btu/lb)	42,100 (18,100)	o ΔP , %	5.8
		<u>HP Turbine</u>	
		o Wt/δ, kg/s (lb/sec)	3.46 (7.62)
		o η_{AD} , %	89.3
		o Cooling Flow, %	4.4
		<u>Inlet</u>	
		o Ram efficiency, %	90

TABLE 26. REFERENCE (TURBOJET) ENGINE -
MAX POWER CRUISE DATA

Max Power Cruise Performance - Sea Level, Mach 2.5, ISA,
Installed With No Production Margin

Overall Engine Performance		Component Performance	
		<u>HP Compressor</u>	
Engine Rating, N (lbf)	20,813 (4,679)	o PR	2.60
		o η_{AD} , %	83.2
TSFC, (kg/hr)/N (lb/hr)/lb	0.200 (1.958)	o η_{poly}	85.3
		o Exit flow	5.14
Turbine Inlet Temp, C (F)	1427 (2600)	<u>Combustor</u>	
Overall Cycle PR	2.80	o η , %	99.6
Inlet W/0/6, kg/s (lb/sec)	5.87 (12.95)	o ΔP , %	0.076
Physical Speed, rad/s (rpm)	3.683 (35,176)	<u>HP Turbine</u>	
JP-10 Fuel, LHV, k ^o /kg (Btu/lb)	42,100 (18,100)	o W/0/6, kg/s (lb/sec)	3.59 (7.91)
		o η_{AD} , %	89.3
		o Cooling Flow, %	4.4
		<u>Inlet</u>	
		o Ram efficiency, %	70

TABLE 27. REFERENCE (TURBOJET) ENGINE -
SLS, UNINSTALLED DATA

SLS, Uninstalled Performance - Sea Level, Mach 0.0, ISA,
Uninstalled With No Production Margin

Overall Engine Performance		Component Performance	
		<u>HP Compressor</u>	
Engine Rating, N (lbg)	7099 (1596)	o PR	5.98
		o η_{AD} , %	82.3
TSFC, (kg/hr)/N (lb/hr)/lb	0.128 (1.253)	o η_{poly}	86.1
		o Exit flow	4.25
Turbine Inlet Temp, C (F)	1237 (2259)	<u>Combustor</u>	
Overall Cycle PR	5.98	o η , %	99.6
Inlet W/0/δ, kg/s (lb/sec)	9.1 (20.0)	o ΔP, %	5.9
Physical Speed, rad/s (rpm)	3,443 (32,884)	<u>HP Turbine</u>	
JP-10 Fuel, LHV, kJ/kg (Btu/lb)	42,100 (18,100)	o W/0/δ, kg/s (lb/sec)	3.59 (7.92)
		o η_{AD} , %	89.1
		o Cooling Flow, %	4.4
		<u>Inlet</u>	
		o Ram efficiency, %	100

Engine Cost

The manufacturing cost of the reference (turbojet) engine was estimated based on current fabrication technologies. The acquisition cost for the reference (turbojet) engine is estimated to be in the \$70,000 to \$110,000 range. A conservative cost of \$110,000 is assumed for the SECT study. This same method of engine cost estimating was used to determine manufacturing costs of advanced engines in Task II.

4.1.3 Reference Mission

Cruise missile mission types have been considered by GTEC from among a number of possible future requirements. Figure 95 summarizes these requirements into five generic classes that embody different cruise Mach numbers and ranges.

After consultation with airframe manufacturers and the Government, it was established that the supersonic tactical missile propulsion system should be given the highest priority in this study. This is the result of a perceived need for supersonic speeds with payload/range requirements beyond that which can efficiently be provided by a rocket or a ramjet. Moreover, turbomachinery component technology is felt to be lacking for a low-cost, supersonic turbojet.

The mission objectives for the supersonic tactical missile are tactical defense suppression, and/or ship attack (collateral sea control). For these cases, both speed and low signature are required for successful defense penetration. Based on these mission objectives, it was decided that a low-altitude supersonic flight profile should be evaluated. This mission type, which is illustrated in Figure 96, was used to evaluate the potential payoff of engine technologies as projected in the year 2000.

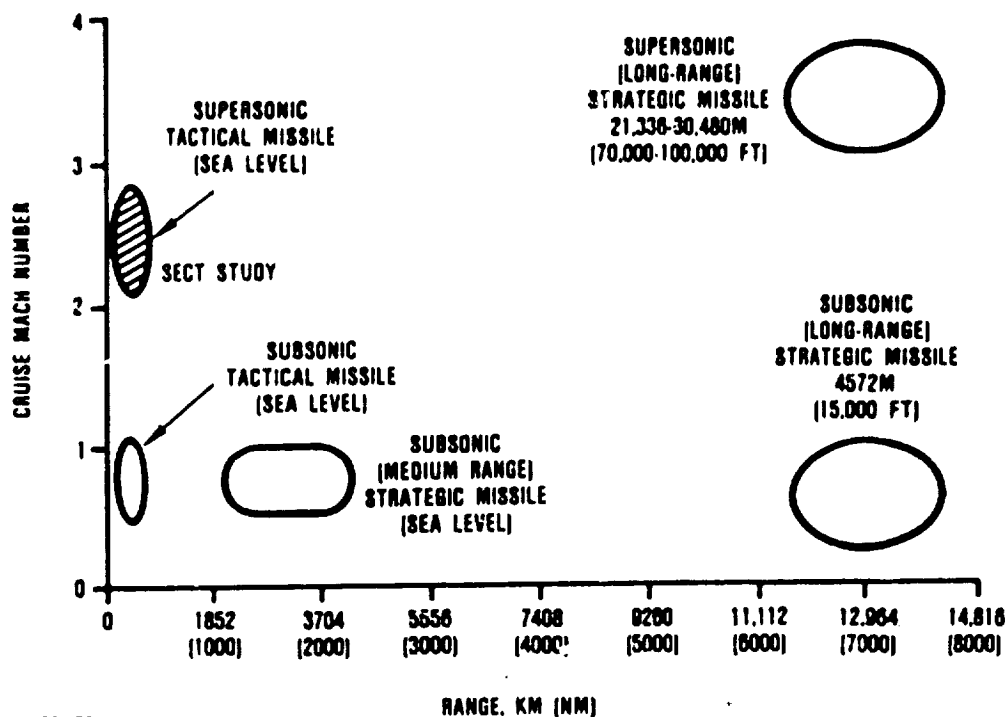
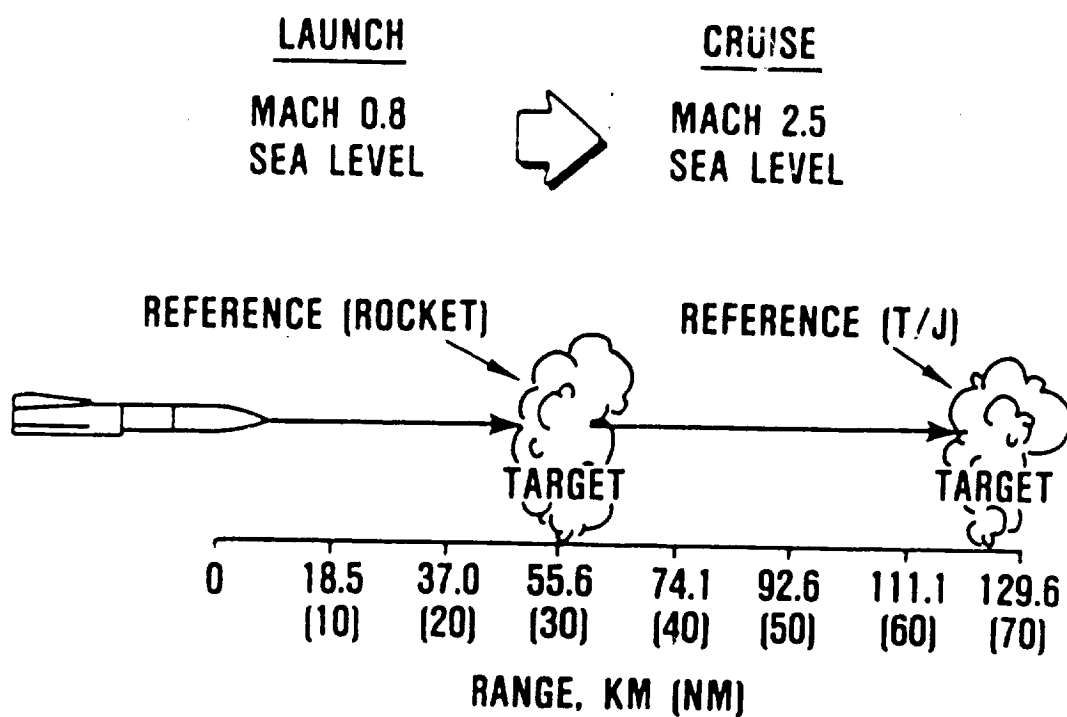


Figure 95. Several Missile Scenarios for the Future.



35-281-47

Figure 96. Representative Reference Mission.

4.1.3.1 Mission-Reference Missile (Rocket)

The mission for the rocket-powered missile was not calculated by GTEC for this study. However, a range of 57 km (30 nm) was suggested by airframers to be representative of today's rocket technology for a sea level trajectory. This value is useful for comparative purposes in the final payoff evaluation of Task II.

4.1.3.2 Mission-Reference Missile (Turbojet)

The mission for the turbojet-powered missile was calculated from an in-house mission analysis program. It was modeled in the following manner:

- o The missile is launched from sea-level carrier aircraft at Mach 0.8.
- o The missile accelerates at sea level at maximum thrust until it reaches Mach 2.5.
- o The missile cruises at Mach 2.5, sea level, until fuel exhaustion.
- o Range is the total distance traveled at fuel exhaustion.

The range calculated for the turbojet-powered missile is 126 km (68 nm). This mission type was used to determine trade factors for evaluation of year-2000 engines and for the Task III mission analysis.

4.1.4 Economic Model

The economic model used for the supersonic cruise missile is a modified model that was used in the rotorcraft and commuter applications.

The economic calculation addressed the missile fixed costs and variable costs while adhering to a set of assumptions that are summarized in Table 28. The missile fixed costs consider the airframe and the fuel costs of JP-10 selected for this study.* The missile variable costs consider the engine and total on-board fuel costs. The variable costs are dependent on the particular cycle/configuration that is evaluated in Task II.

These major contributing costs can be added in the following manner to determine total missile cost:

Total Missile Cost = Airframe Cost + Engine Cost + Fuel Cost

Airframe Cost = Cost of Airframe Structure, Payload, Avionics, and Controls. These costs are based on discussions with airframers.

Engine Cost = Cost of Engine System, including Accessories

Fuel Cost = Cost of Total On-board Fuel (JP-10)

Other costs associated with the acquisition costs of a missile system, such as engine spares costs, were not considered in this study for reasons of simplicity.

4.1.5 Environmental Constraints

The environmental constraints imposed on supersonic cruise missile systems are generally quite different from those on commercial or military aircraft. There are no universal guidelines or standards governing missile environmental constraints; they

*Fuel price assumed \$2.64/liter (\$10/gal)

TABLE 28. ECONOMIC MODEL FOR THE CRUISE MISSILE

Assumptions		Fixed Cost	Variable Cost
No. of Engines	2000	Airframe (\$390,000) Fuel Price (\$10/gal)	Engine
Spares	-		Fuel Volume
Missiles	2000		
Annual Use	-		
Storage Life, yrs	15		
Gross Weight, kg (lb)	680 (1500)		
Payload, kg, (lb)	227 (500)		

depend on analyses of specific threats. Missile designers are concerned with the overall missile observables. It is essential that the missile penetrate enemy defenses undetected. In order to limit a missile's signature, its visual, noise, infrared, and radar signatures must be design considerations.

An important area that must be minimized is the radar cross section (RCS) of the engine inlet. The most effective means of minimizing the missile's vulnerability to RCS is to reduce the inlet flow requirement. Technology advancements in the turbojet cycle will enable the engine to operate at higher turbine inlet temperatures. These advancements, in turn, lead to higher specific thrust systems (thrust/airflow), thereby requiring smaller engine airflows. Minimizing the airflow required by the engine decreases the missile inlet and reduces the RCS of the system. The advanced missiles, therefore, will be less vulnerable to RCS than present systems.

Infrared signatures typically are a concern for present missile systems. Supersonic tactical missiles, however, will not be as vulnerable to infrared signature due to the high mission flight speeds. At these speeds ($M = 2.5$), no other system would be able to deploy and pursue from the rear.

4.1.6 Trade Factors

Trade factors have been generated for the supersonic tactical missile system relating missile range and acquisition costs to small changes in primary engine-missile interface parameters (TSFC, weight, volume) for constant missile volume. The trade factors are based on the reference missile (year 2000) and mission (year 2000), and the reference (turbojet) engine representing near-term (1989) technology.

The trade factors constitute differentials for the listed parameters and are based on a one percent change. These values are summarized in Table 29 for a fuel price (JP-10) of \$2.64/liter (\$10/gal). The missile costs are calculated directly.

TABLE 29. MISSILE TRADE FACTORS (CONSTANT MISSILE VOLUME)

Missile Range/1% Engine TSFC (nm/%)	0.82
Missile Range/1% Engine Weight (nm/%)	0.04
Missile Range/1% Engine Volume (nm/%)	0.56

The missile range and missile cost/range (\$/nm) is used in the evaluation of the advanced engines. It is desired that improvements to these parameters be maximized in order to provide for the best year-2000 missile system.

4.2 Task II - Engine Configuration and Cycle Evaluation

The cycle/configuration studies for the cruise missile application parametrically considered a range of potential engine combinations in terms of turbine rotor inlet temperature (TRIT), cycle pressure ratio (CPR), component types, materials and associated efficiencies, and cooling flows, as projected for the year 2000. From the range of engines considered, a final engine selection was made for Task III evaluation on the basis of payoff in missile range and missile cost per mile. These improvements were estimated through the trade factors (established in Task I) that relate changes in range and missile cost per mile in terms of changes in engine performance (TSFC), weight, diameter, length, and cost (changes are relative to the reference turbojet engine). Engine volume, weight, and cost were quantified for each engine of interest.

4.2.1 Technology Projections

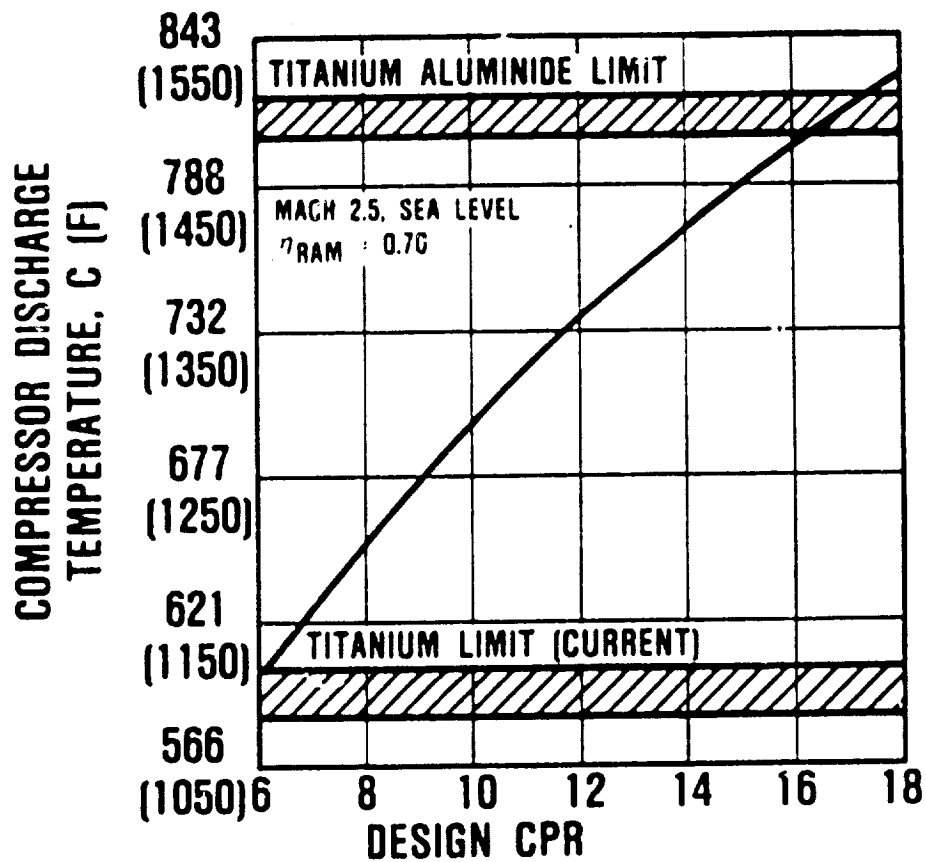
The initial task in configuring potential cruise missile engines for the year 2000 was to establish the expected level of technology in that time frame. Inherent in these projections is the assumption that the technologies will be available by the year 2000. Technologies have been identified in three major areas: materials, aerodynamics, and mechanical improvements. These technologies impact the cycle study in terms of efficiency levels, turbine inlet temperature limits, and cooling flow requirements, as well as turbine stage count and hub speed limits.

Materials

Several additional material technologies must be considered for the cruise missile engine beyond those considered for the rotorcraft and commuter engines. The materials, titanium aluminides and carbon-carbon, primarily allow for higher temperatures in the compressor and turbine components of the engine.

Titanium aluminide (Ti_3Al) is ideally suited for use in compressor vanes, blades, and rotors, due to its high strength/weight and capability of meeting the high temperature demands at supersonic flight speeds. Figure 97 shows that the expected maximum temperature capability for Ti_3Al is $816^{\circ}C$ ($1500^{\circ}F$). This limit allows for a compressor design pressure ratio up to 17:1 at the supersonic flight conditions of this study.

Carbon-carbon, which is projected for use in the engine hot-section, has properties that provide for high strength and high temperature exceeding that of conventional hot-section materials, as discussed in paragraph 2.2.1.1. The maximum temperature projected for carbon-carbon in the year 2000 is $2205^{\circ}C$ ($4000^{\circ}F$), based



05-281-31

Figure 97. Advanced Compressor High-Temperature Material Requirements.

on the existence of a suitable coating. Additional material properties for Ti_3Al and carbon-carbon are summarized in Table 30.

Aerodynamics

The component performance projections for the year-2000 cruise missile engine addresses low volume, low cost technologies. These projections affect the component efficiency levels predicted.

Compressor - The compressor performance projections are generally dependent on compressor type, flow size, and manufacturing cost. Figure 98 shows a plot of compressor polytropic efficiency for a multistage axial compressor as a function of compressor exit corrected flow. A decrement in efficiency taken for low cost cast compressor stages versus machined stages is also shown. The assumptions for the efficiency projection include aggressive stage loading ($P/P > 1.85$ for first stage), compressor exit Mach number of 0.5, and a 1 percent clearance/height ratio. An additional assumption limits the compressor last stage blade height to 1.1 cm (0.43 in.) or more. This limit is very aggressive for axial compressors and is considered to be a practical limit on size for low cost, efficient airfoils.

Technology advances required to achieve these efficiency projections include further development of 3-D analytical methods, desensitization of blade rows to rotor tip clearances, and the reduction of airfoil and secondary-flow losses. Additional technology advances, aimed at reducing compressor manufacturing costs, include increased stage loading capacity in a small size, and maintained performance (efficiency) with increased leading- and trailing-edge thickness.

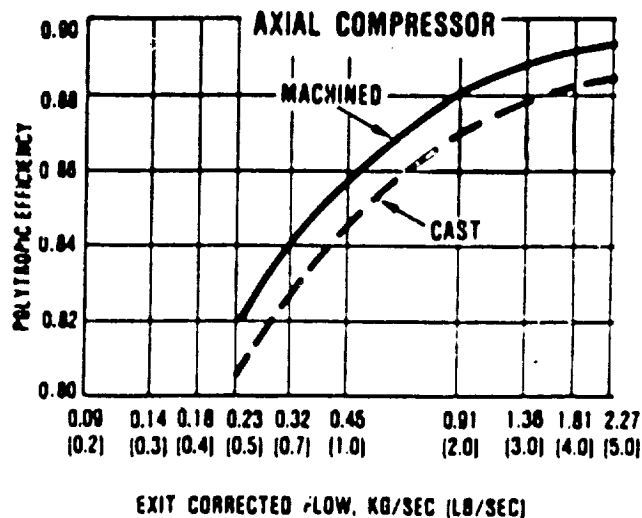
Combustor - The combustor technology projections for year-2000 cruise missile engines emphasize increased temperatures in a

TABLE 30. ADDITIONAL MATERIAL TECHNOLOGIES FOR
CRUISE MISSILE ENGINE

Application	Titanium Aluminides	Carbon- Carbon
	Compressor Vanes, Blades, Rotors	Turbine Vanes, Blades, Rotors, Combustor, Nozzle
Density, kg/cm ³ (lb/in ³)	0.005 (0.17)	0.002 (0.065)
Material Temperature Limit, C(°F) (Uncooled)	816 (1500)	2205 (4000)
Design Strength, kN/cm ² (ksi)*	20.7 (30)	34.5-68.9 (50-100)
Cost Factor**	1.5	2

*For 1-hour life at design temperature

**1.0 is 1985 metallic engine part



- STAGE LOADING FIRST STAGE
P/P > 1.85
- 0.5 EXIT MACH NUMBER
- 1 PERCENT CLEARANCE/HEIGHT
[0.0127 CM (0.005 IN) MIN.]
- EXIT BLADE HEIGHT LIMIT
≥ 1.09 CM (0.43 IN)
- EFFICIENCY DECREMENT FOR
CASTING 2 TO 4 POINTS

EFFICIENCY IMPROVEMENT PROJECTIONS

- FURTHER DEVELOPMENT OF 3-D ANALYTICAL METHODS (60%)
- DESENSITIZE BLADE ROWS TO TIP CLEARANCES (20%)
- REDUCE AIRFOIL AND SECONDARY-FLOW LOSSES (20%)

OTHER IMPROVEMENTS (COST)

- INCREASE STAGE LOADING CAPACITY IN SMALL SIZE
- MAINTAIN EFFICIENCY WITH THICKER EDGES

65-781-50

Figure 98. Axial Compressor Performance Projections.

small volume while maintaining good performance. Specifically, low pattern factors are critical at rotor inlet temperatures of 1927C (3500F). Also, in order to achieve a small volume, a very high reference velocity and a low combustor residence time is desired. A comparison of the critical operating parameters of the reference (turbojet) engine and the year-2000 engine is shown in Figure 99.

Technology advances required to achieve the tabulated performance and geometry projections include the further development of 3-D combustor performance modeling, the evolution of advanced diffuser design tools, and the improvement of fuel nozzle/dome airflow interaction for improved ignition and lean blow-out characteristics.

Slurry fuel is also an attractive technology for volume-limited applications due to its inherent high energy-to-volume characteristics.

Technology advances will address aluminum slurry, carbon slurry, and boron slurry. Only boron slurry, however, is evaluated in Task IV in order to show the additional improvements possible beyond conventional fuel (JP-10).

Turbine - The HP turbine performance projections are generally a function of stage mean work coefficient and turbine flow size. Figure 100 shows the turbine efficiency for these parameters. As shown, efficiency is reduced as turbine flow is decreased and turbine loading is increased.

The efficiency curves assume a two-stage axial configuration, no fabrication constraints on turbine blade design, an unshrouded blade with 2 percent tip clearance, and an uncooled

ENGINE PARAMETER*	REFERENCE ENGINE (TURBOJET)	YEAR 2000 CRUISE MISSILE
COMBUSTOR DISCHARGE TEMPERATURE, C (F)	1427 (2600)	1826 (3500)
PATTERN FACTOR	0.35	≤ 0.25
COMBUSTOR $\Delta P/P$	8.0%	7.5%
COMBUSTOR η	0.998	0.998
HEAT RELEASE RATE, W/(M ³ /kPa) [(BTU/HR)/(FT ³ /ATM)]	1048 (11 x 10 ⁶)	1764 (18.5 x 10 ⁶)
REFERENCE VELOCITY, M/S (FT/SEC)	46+ (150+)	46+ (150+)
RESIDENCE TIME, MS	3.6	3.4

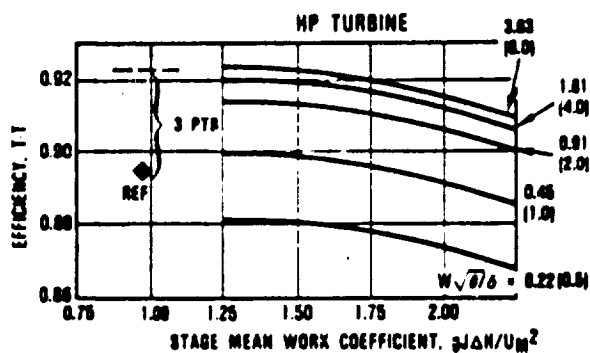
*MACH 2.5, S/L

- FURTHER DEVELOPMENT OF 3-D COMBUSTOR PERFORMANCE MODEL
- DEVELOPMENT OF ADVANCED DIFFUSER DESIGN TOOLS
- IMPROVE FUEL NOZZLE/DOME AIRFLOW INTERACTION

201-43



Figure 99. Cruise Missile Combustor Technology Projections.



EFFICIENCY IMPROVEMENT PROJECTIONS

- REDUCED ROTOR TIP LOSSES (55%)
- MINIMIZE VANE/BLADE INTERACTION LOSSES (45%)

OTHER IMPROVEMENTS (COST)

- IMPROVED PERFORMANCE/LIFE OPTIMIZATION IN PRELIMINARY DESIGN

- NO FAB CONSTRAINTS
- UNSHROUDED BLADE
- 2 PERCENT TIP CLEARANCE
- UNCOOLED
- TWO-STAGE AXIAL

88-281-48

Figure 100. Cruise Missile HP Turbine Projections.

blade. These efficiency curves are the same as shown for the rotorcraft application except that the stage work coefficient limit is increased.

Technology advances required to achieve these turbine efficiency projections include reduced rotor tip losses and minimized vane/blade interaction losses. Additional technology advances, primarily aimed at reducing costs, and improved performance/life optimization in the preliminary design phase can minimize the "overdesign" inherent in short life or expendable missile systems, resulting in reduced costs.

Mechanical

The mechanical projections for the year-2000 cruise missile engine are the same as for the rotorcraft and commuter applications discussed in paragraph 2.2.1.4. Refer to that section for the definition and limits of these projections.

System Technologies

Several additional technology projections were considered for the year-2000 cruise missile engines. These technologies include high-temperature, low-cost accessories, high-temperature minimum-lubricated bearings, and expansion deflection thrust nozzles. High-temperature, low-cost accessories and high-temperature, minimum-lubricated bearings are needed because of the high-temperature operating conditions experienced at supersonic flight conditions.

4.2.2 Engine Cycle/Configuration Study

The cycle/configuration study for the cruise-missile application consists of a range of cycle parameters and component

types representing a number of potential engine options for the year 2000. A turbojet cycle is considered in this study because of the high Mach number (Mach 2.5, sea level) and the importance of high specific thrust.

The thermodynamic cycle study considers a range of turbine rotor inlet temperatures from 1427 to 1927C (2600 to 3500F), and cycle-pressure ratios from 6:1 to 14:1. Also, several engine configurations are considered, as shown in Figure 101. The compressor configurations addressed include multistage axial compressors (stage count depending on pressure ratio) and axial/centrifugal compressors. The turbine configuration addresses an uncooled single-stage axial with carbon-carbon rotor and airfoils.

Three key operating conditions were found to be important for the cruise missile application, sea-level operation at the (1) Mach = 0.8 launch, (2) Mach = 1.5 minimum acceleration point, and (3) Mach = 2.5 cruise.

The engine design point was selected at the Mach = 0.8 launch condition. The cycle parametric study assumes a compressor inlet corrected flow of 9.1 kg/s (20 lb/sec) at this condition, and component efficiency levels based on the aerodynamic and mechanical projections as discussed in paragraph 4.2.1. Also, a fixed-geometry inlet (η_{ram} ranging from 0.7 to 0.9) and a fixed-geometry expansion/deflection nozzle were assumed.

Designing the engine at the Mach 0.8 operating point avoids overspeed at the higher flight speeds. Although designed at this condition, the engines were sized for the Mach 1.5 operating point. As shown in Figure 102, the Mach 1.5 operating point is

CYCLE

CPR = 6 TO 14. TRIT = 1427 TO 1926C (2600 TO 3500F)

CONFIGURATION

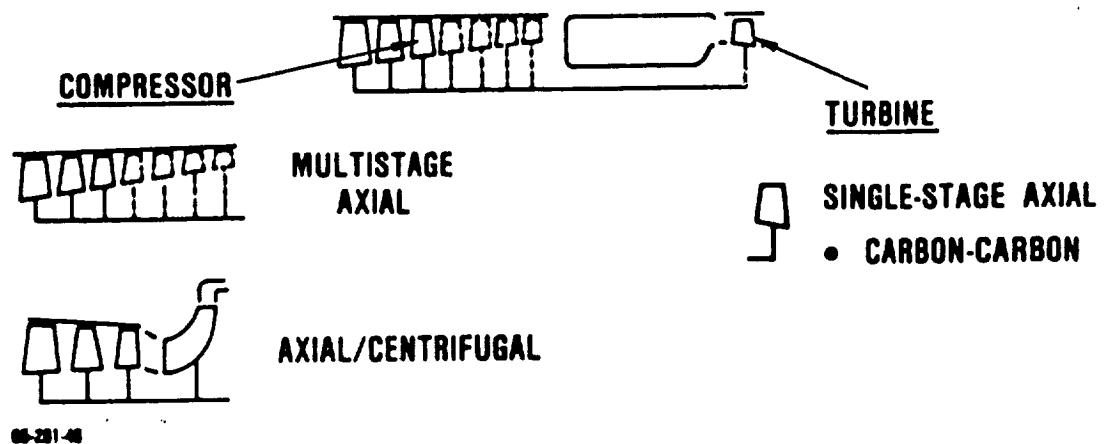


Figure 101. Missile Cycle/Configuration Study Engine Options.

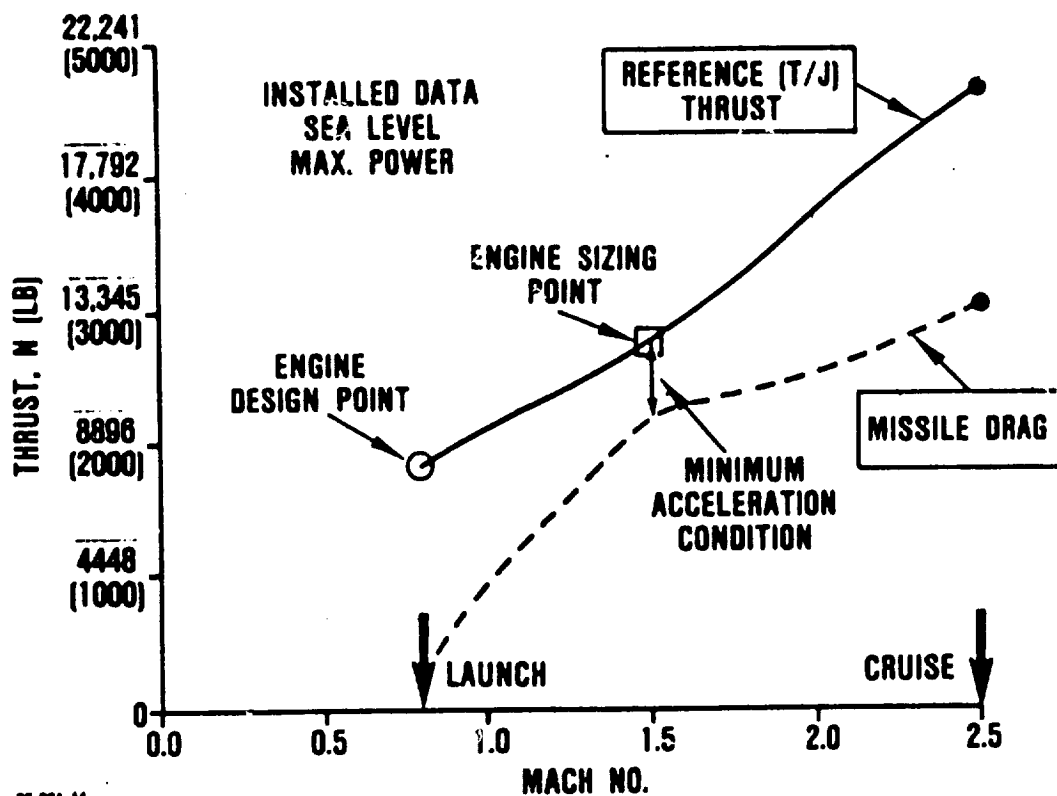


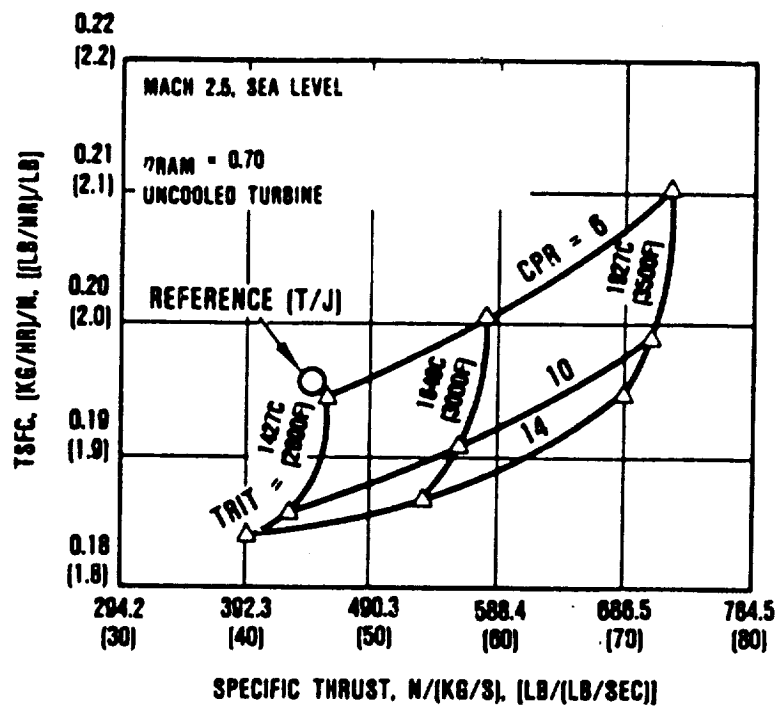
Figure 102. Engines Sized by Minimum Acceleration Condition.

the missile's minimum accel condition, or the point where the difference between engine thrust and missile drag is at a minimum during missile acceleration.

The scaled engines were then run at the Mach 2.5 cruise condition. The effect of scaling on performance was not addressed during this phase of the parametric study. The component efficiencies are therefore based on the initial design point flow size of 20 lb/sec.

The results of this parametric study, shown in Figure 103, show that TSFC improvements can be made as cycle pressure ratio is increased. This is accompanied, however, by decreased specific thrust. Also shown is that significant specific thrust improvements are possible with increased rotor inlet temperature at the expense of TSFC. It is expected then, that a combination of increased cycle pressure ratio and rotor inlet temperature will achieve the best year-2000 engine cycle. Another result from the cycle parametric study can be seen by referring to Figure 95 (where compressor discharge temperature is shown as a function of cycle pressure ratio). At the Mach 2.5, sea-level condition, it is clear that T_{13A1} is critical if a cycle pressure ratio above 6:1 is desired.

The resulting engine size requirements, on the basis of engine inlet corrected flow, are shown in Figure 104A. As shown, less flow is required to deliver the minimum accel thrust as the compressor pressure ratio and rotor inlet temperature are increased. Increasing the pressure ratio and temperature, however, results in the very small compressor-corrected exit flows of 0.9 to 1.4 kg/sec (2 to 3 lb/sec), as shown in Figure 104B. These small flow sizes would preclude the use of an axial compressor configuration for today's technologies because of the

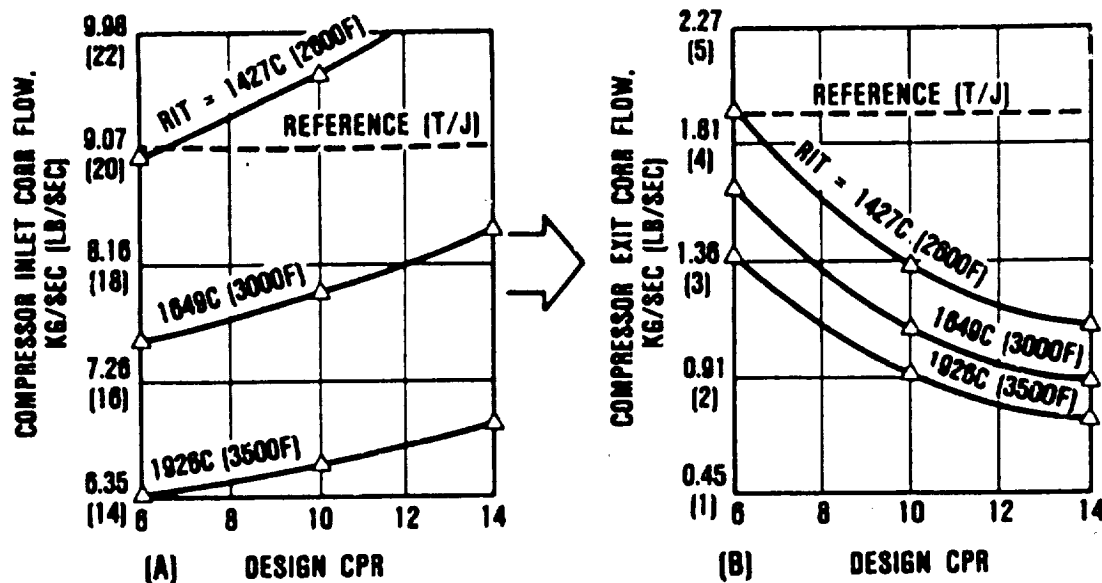


65-281-103

NOTE: COMPONENT EFFICIENCIES ARE BASED ON
20 LB/SEC COMPRESSOR INLET FLOW SIZE

Figure 103. Missile Cycle Study Results.

SIZED AT MACH 1.5, SEA LEVEL
 DESIGN POINT: MACH 0.8, SEA LEVEL
 $\eta_{RAM} = 0.90$



66-291-46

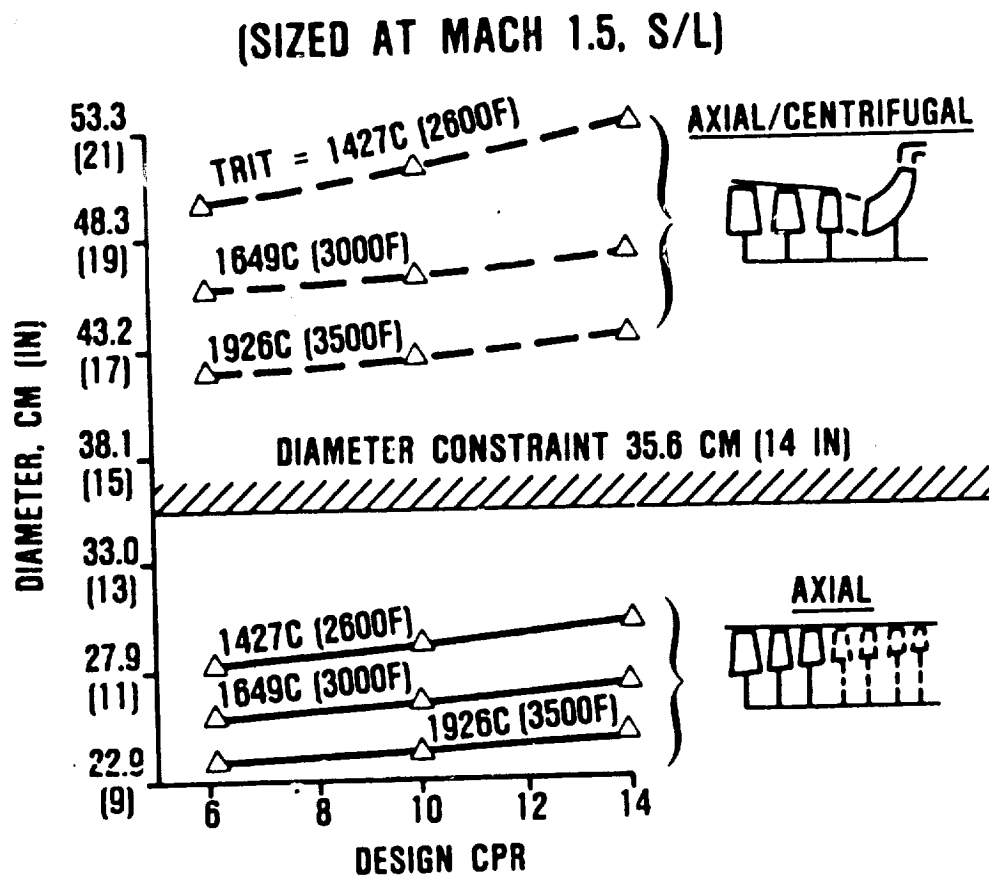
Figure 104. Compressor Inlet and Exit Corrected Flow Variation.

small last-stage blade heights. Today this would typically require the use of axial/centrifugal compressor configurations.

Typical diameter relationships were calculated for axial and axial-centrifugal compressors. The results are shown in Figure 105. For a diameter-constrained (limited volume) application, axial/centrifugal compressor configurations were eliminated because of the large diameter requirements of the centrifugal stage. Axial compressors, however, lie within the diameter constraint and were selected for further study.

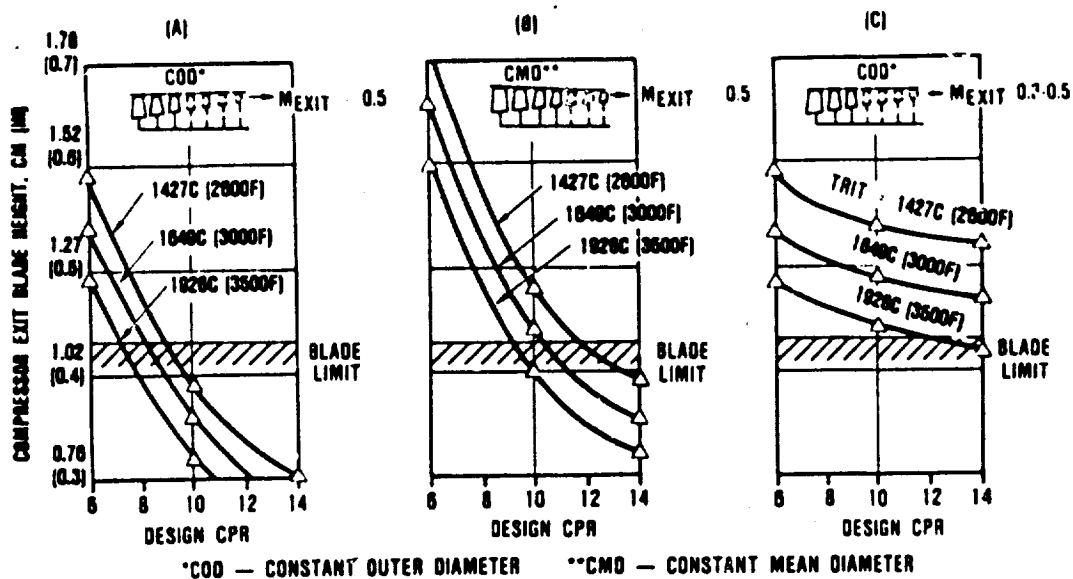
There are many axial compressor configuration types that can be addressed. The goal of this study was to determine a configuration type that would give the greatest potential in cycle selection. GTEC first considered a constant outer diameter (COD) compressor configuration with an exit Mach number of 0.5. A high Mach number was chosen in order to allow for higher loading/stage, thereby reducing stage count. This configuration type resulted in acceptable compressor exit stage blade heights for pressure ratios of 7 to 9:1 (Figure 106A). To extend the P/P range, a constant mean diameter (CMD) compressor configuration was considered next. This configuration results in acceptable compressor exit stage blade heights for pressure ratios of 9 to 11:1 (Figure 106B). Figure 106C shows the results of a COD compressor configuration with the exit Mach number decreasing from 0.5 to 0.3 as pressure ratio is increased (stage count increased). This configuration type allows for the greatest pressure ratio selection since more favorable blade heights are achieved. This compressor configuration type was selected and used for the remainder of this study.

Candidate engine volumes, weights, and costs were then calculated. As shown in Figures 107A and 107B, engine volume and weight are cycle-dependent. Engine, volume and weight can be



65-281-49

Figure 105. Axial and Axial-Centrifugal Compressor Diameter Comparison.



65-281-42

Figure 106. Compressor Axial Blade Height Limits.

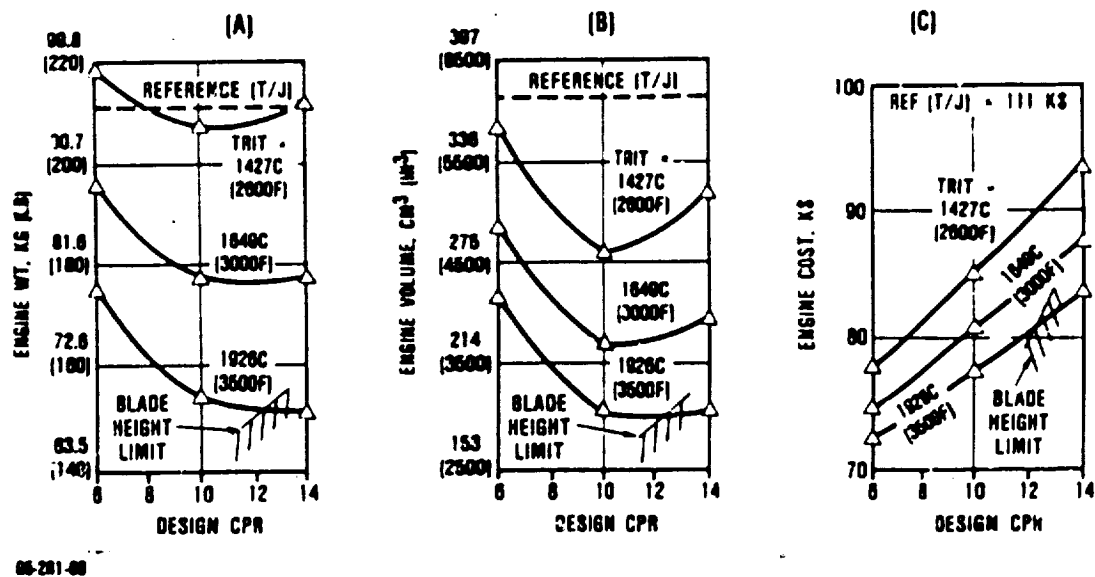


Figure 107. Missile Engine Weight, Size, and Cost Trends.

minimized, as expected, at higher turbine rotor inlet temperatures and, to a degree, at increased cycle pressure ratios. Engine costs tend to decrease with smaller engine sizes (see Figure 107C). However, engine costs tend to increase with increasing cycle pressure ratio because of increased compressor stage count.

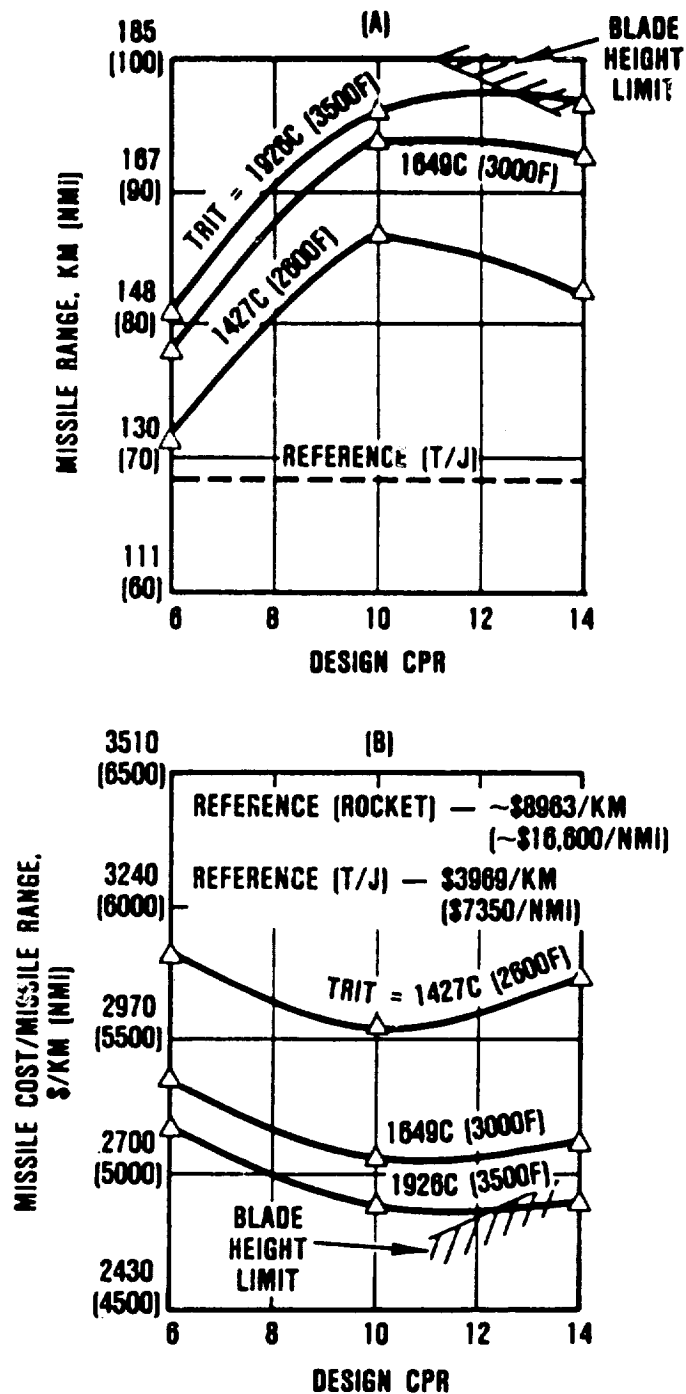
4.2.3 Cycle/Configuration Selection

The trade factors that were generated in Task I were used to calculate the missile range and missile cost/range of the year-2000 missile. This was done for the candidate engines by using their respective TSFC, volume, weight, and cost values. The results of this calculation are shown in Figure 108A for range, and Figure 108B for missile cost/range. These figures show that the cycle/configuration, with a rotor inlet temperature of (1926C) 3500F and a cycle pressure ratio of 12:1, results in the maximum improvement. This cycle and configuration, as illustrated in Figure 109, were selected for further evaluation in Task III.

4.3 Task III - System Performance Evaluation

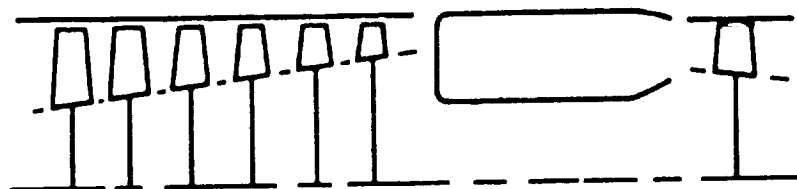
In Task III, the selected engine from Task II was evaluated in terms of its impact on overall missile system performance. A detailed mission analysis was conducted that required extensive off-design performance. Finally, the missile range and cost/range were determined and compared to the reference values calculated in Task I.

Prior to these system evaluations, the selected engine configuration was further refined based on the GTEC preliminary design process.



68-261-71

Figure 108. Missile Engine Range and Cost/Range Trends.



- COMPRESSOR — 6-STAGE AXIAL (C.O.D.)
— CPR = 12:1
- COMBUSTOR — ANNULAR THROUGH FLOW
— CARBON-CARBON
- HP TURBINE — SINGLE-STAGE AXIAL
— TRIT = 1926C (3500F), UNCOOLED
— CARBON-CARBON

05-281-32

Figure 109. Selected Missile Engine.

4.3.1 Engine/Cycle Refinements

Several minor engine refinements were made to the year-2000 engine selected in Task II. These refinements were made following a more detailed design analysis of each engine component. The identified refinements and the resulting performance effects are summarized in Table 31. The following paragraphs discuss each of these refinements and their effects on component and engine performance.

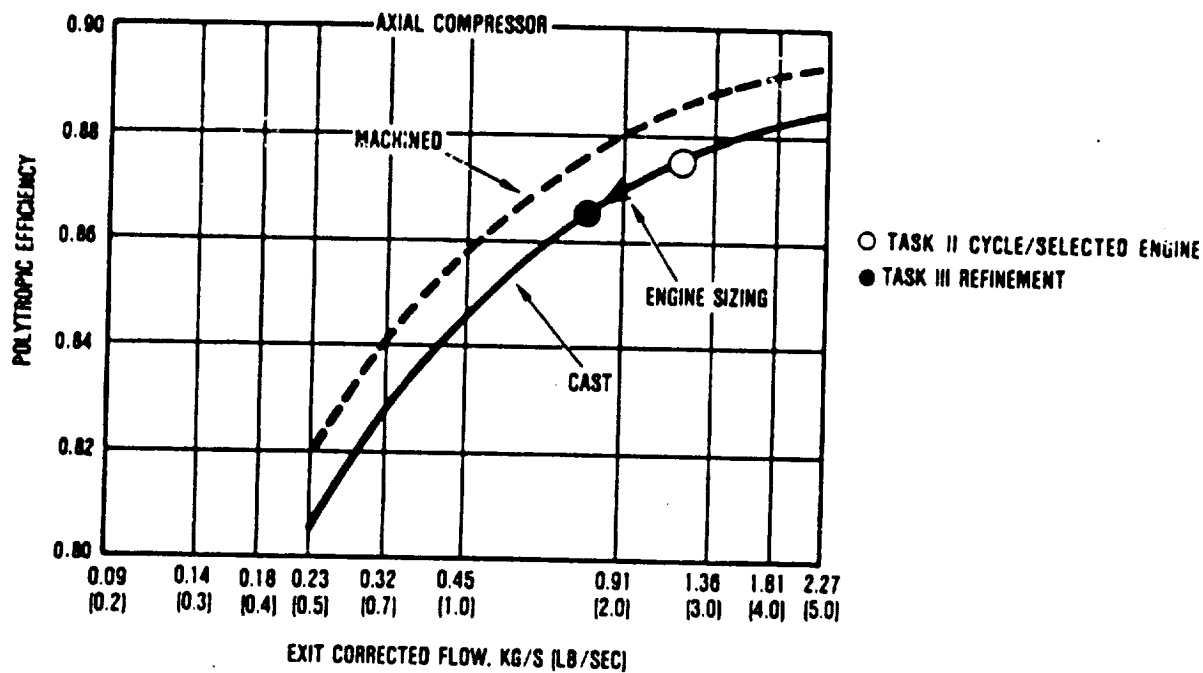
As previously discussed, the cycle parametric study of Task II was conducted with component efficiencies based on a compressor inlet corrected flow (at Mach 0.8, sea level) of 9.1 kg/s (20 lb/sec). A design point flow size of 6.8 kg/s (15.0 lb/sec) actually results for the engine when it is sized for minimum accel thrust at Mach 1.5. This smaller flow size results in a reduction in compressor projected efficiency, as shown in the curve in Figure 110. This engine sizing effect was not taken into account in the Task II study. Also, additional analyses have determined that variable geometry is required for the first two stages of the compressor, at the expense of increased engine diameter and engine cost.

The turbine efficiency was decreased by 4.1 points (0.920 to 0.879) as shown in Table 31. This decrease resulted from engine sizing and from turbine diameter and aerodynamic loading changes, as shown in Figure 111. The sizing changes are due to scaling the engine to meet the minimum acceleration condition. The turbine diameter (and mean blade radius) was reduced with no change in rotational speed; this increased the stage work coefficient (from 1.65 to 2.65), thereby degrading the efficiency by 2 points. A final correction was made to account for a single turbine stage (curves are for two-stage turbines with implicit reheat effects) with exit guide vanes.

TABLE 31. MISSILE ENGINE PERFORMANCE REFINEMENTS

Parameter*	Task II	Task III	Comments
TSFC, (kg/hr)/N (lb/hr)/lb	0.161 (1.575)	0.167 (1.642)	<ul style="list-style-type: none"> o Variable geometry o Refined design o Cost reassessed
Thrust, N (lbf)	9457 (2110)	9150 (2057)	
Diameter, cm (in)	24.4 (9.6)	27.2 (10.7)	
Length, cm (in)	106.7 (42.0)	101.6 (40.0)	
Weight, kg (lb)	66.9 (147.5)	68.0 (150)	
Cost, \$	80,600	87,600	
Compressor			<ul style="list-style-type: none"> o Efficiency projections reassessed
- $W/\theta/\delta_{INLET}$, kg/s (lb/sec)	6.8 (15.0)	6.8 (15.0)	
- $W/\theta/\delta_{EXIT}$, kg/s (lb/sec)	0.83 (1.83)	0.83 (1.83)	
- CPR	12	12	
- η_{POLY}	0.874	0.865	
- η_{AD}	0.825	0.813	
Turbine			<ul style="list-style-type: none"> o Efficiency projections reassessed o Increased aerodynamic loadings
- TRIT, C (F)	1927 (3500)	1927 (3500)	
- $W/\theta/\delta_{INLET}$, kg/s (lb/sec)	1.61 (3.55)	1.61 (3.55)	
- η_{AD}	0.920	0.879	

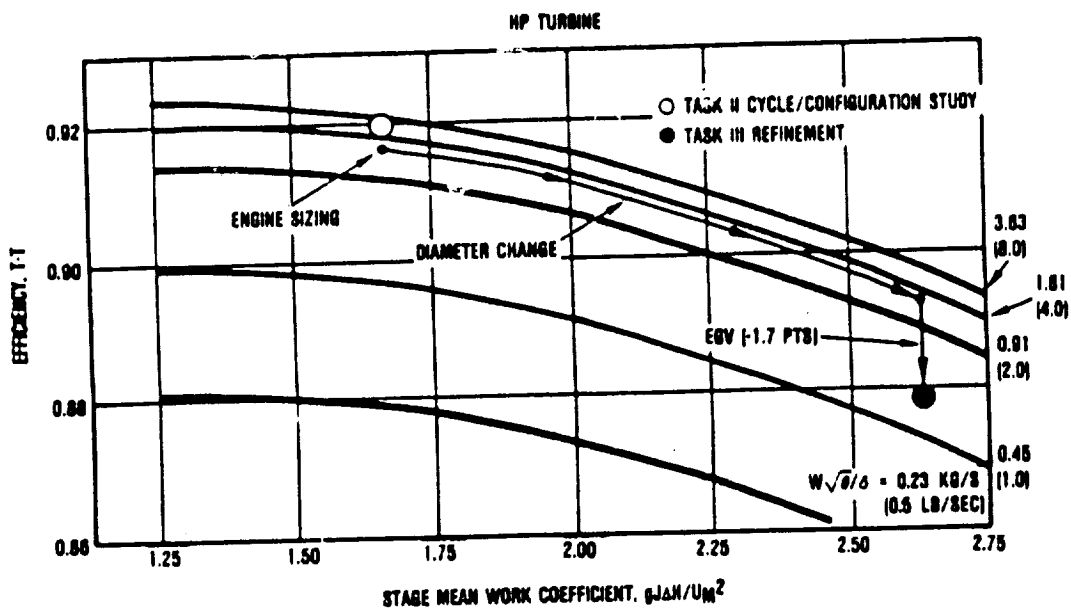
*Design point: Mach 0.8, sea level, $\eta_{RAM} = 0.90$



- STAGE LOADING FIRST STAGE P/P > 1.85
- 0.5 EXIT MACH NUMBER
- 1 PERCENT CLEARANCE/HEIGHT 0.013 CM(0.005 INCH) MINIMUM
- EXIT BLADE HEIGHT LIMIT 1.09 CM ≥ [0.43 IN]

85-281-143

Figure 110. Impact of Compressor Size Change.



- NO "FAB" CONSTRAINTS
- UNSHROUDED BLADE
- 2 PERCENT TIP CLEARANCE
- UNCOOLED
- TWO-STAGE AXIAL

86-281-142

Figure 111. Impact of Turbine Size and Loading Change.

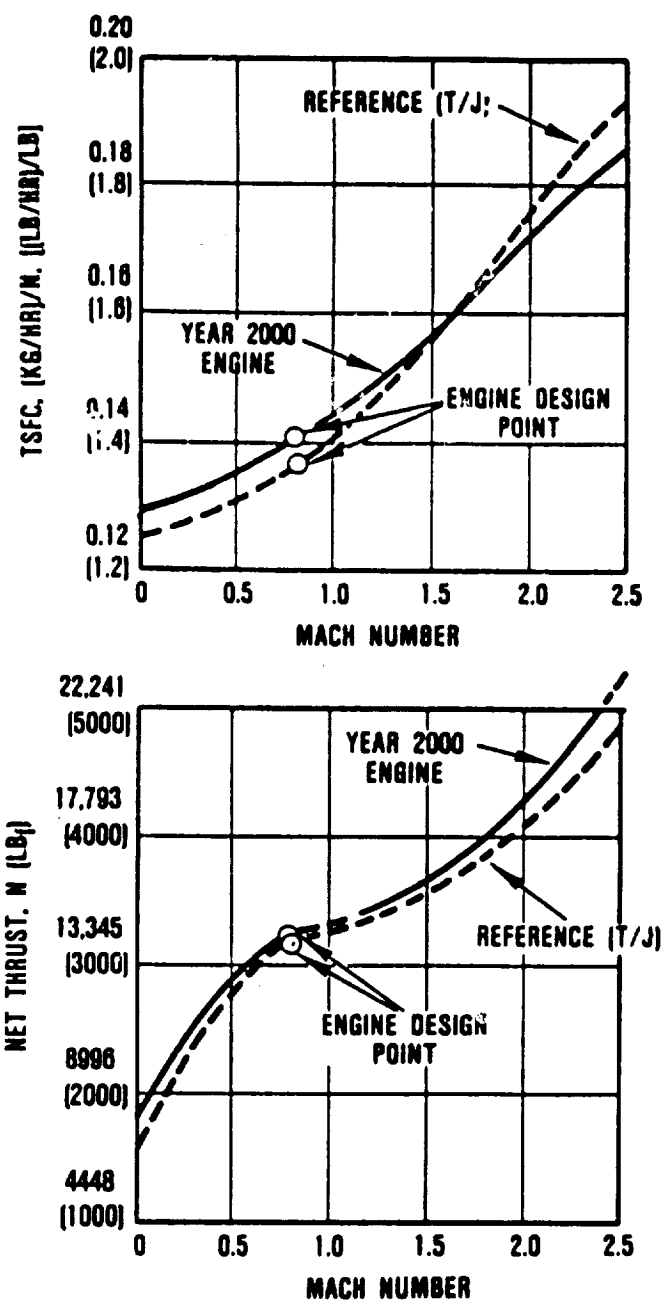
Other refinements that affect the engine include a better definition of the component geometry and a revised cost assessment. The refined component geometry results in a shorter engine from Task II. Also, an engine cost revision was made for a change in the estimated engine sell cost.

These engine refinements result in a year-2000 engine concept that displays engine performance characteristics that are similar to those determined in Task II. Also, these refinements apply to each of the engine concepts considered in Task II. For these reasons, it was concluded that these engine refinements have no effect on the engine/cycle selection, and the refinements actually provide for a better determination of the optimum engine available in the year 2000.

4.3.2 Mission Analysis

The mission analysis for the year-2000 missile system was conducted using the reference missile and mission defined in Task I and the year-2000 engine selected in Task II.

To support the mission analysis, off-design engine performance of the revised year-2000 engine was predicted. Figure 112 summarizes the engine thrust and TSFC as a function of Mach number and altitude. As shown in the figure, the year-2000 engine displays similar performance characteristics to the reference (turbojet) engine. The year-2000 engine, however, has a greatly reduced engine envelope. Both the year-2000 engine and the reference (turbojet) engine are sized to the same thrust level at the minimum acceleration condition (Mach 1.5, sea level). This off-design engine performance, in addition to part-power engine performance, is used in the mission analysis model for calculation of the year-2000 missile range and missile cost/range."



88-281-110

Figure 112. Performance Comparison of Reference and Year-2000 Turbojet Engines.

The results of the mission analysis are summarized in Figure 113 for both the missile range and missile cost/range payoff assessment. The missile range calculated for the year-2000 engine is 167 km (90 nm). This compares to 56 km (30 nm) for the reference (rocket) and 126 km (68 nm) for the reference (turbojet) engine. The year-2000 range exceeds the missile range of the rocket-powered missile by nearly 200 percent and the turbojet-powered missile by more than 30 percent. Similarly, the missile cost/range for the year-2000 engine is \$2867/km (\$5310/nm). This shows the year-2000 engine to have a missile cost/range improvement of 68 percent for the reference (rocket) engine and 27 percent for the reference (turbojet) engine.

4.4 Task IV - Small Engine Component Technology (SECT) Plan for Missile Application

Task IV identifies and quantifies high payoff technologies for the cruise missile engine and presents technology plans that are based on the benefits.

4.4.1 Advanced Technology Identification and Benefits

Based on the results of Tasks II and III, a number of key technologies have been identified. The technologies that follow include those that show performance benefits in terms of TSFC, envelope, weight, and cost, as well as other technologies that are considered beneficial or necessary to meet year-2000 design goals. These technologies are:

- o Materials
 - Cast titanium (compressor)
 - Titanium aluminide (compressor)
 - Carbon-carbon (turbine, combustor, nozzle)

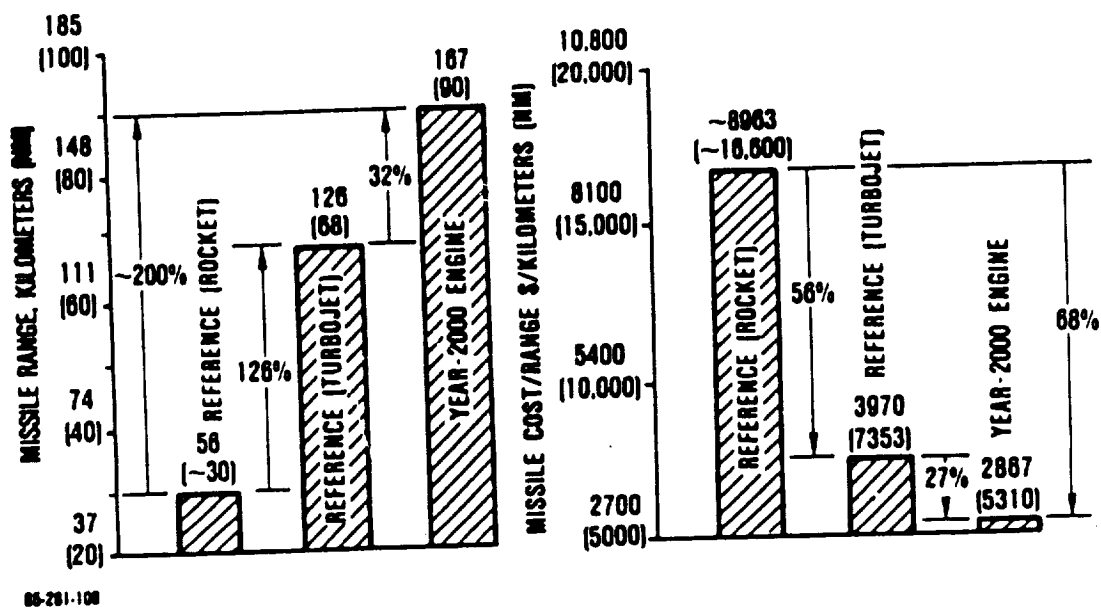


Figure 113. Missile Range and Cost Per Range Comparison of Reference and Year-2000 Turbojet Engines.

- o Component Performance
 - Compressor aero
 - Compressor casing treatments
 - Compressor casting/tooling techniques
 - Turbine aero
 - Shaped carbon-carbon airfoils
- o Combustor
 - Low pattern factor
 - High temperature rise
- o System technologies
 - Slurry fuels
 - Expansion/deflection (E/D) exhaust nozzle
 - Metal matrix shaft
 - High-temperature accessories
 - High-temperature bearings

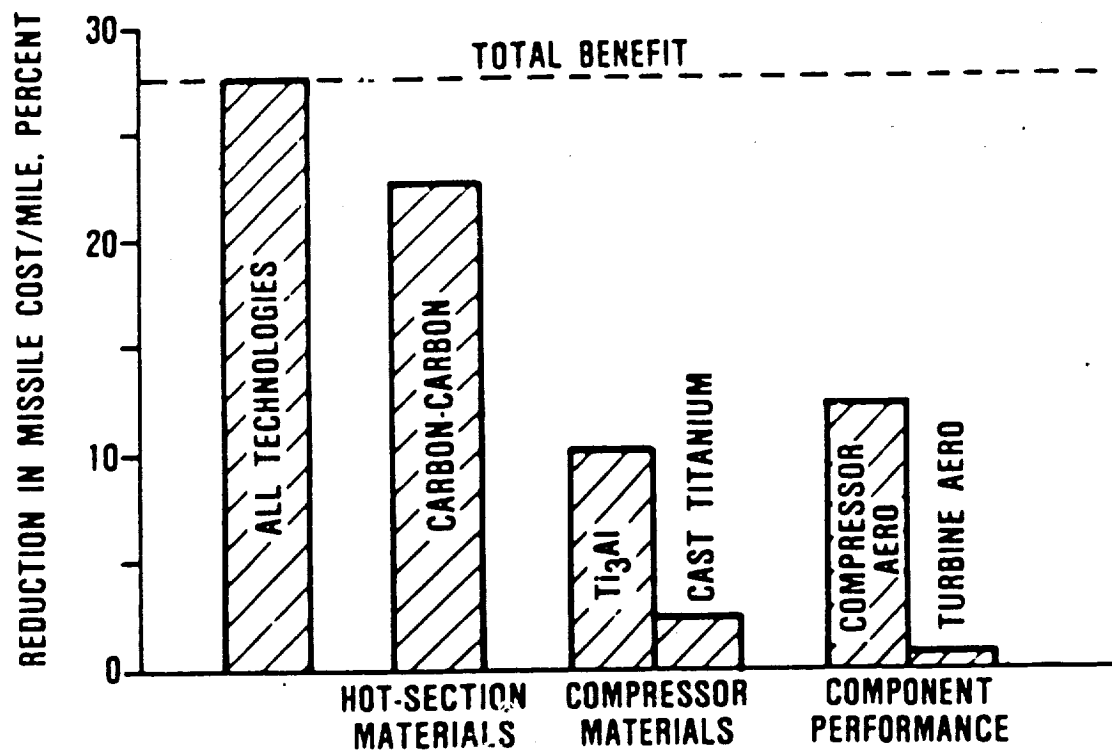
In order to estimate the benefits derived from the above technologies, each was isolated using the technical approach discussed for the rotorcraft engines in paragraph 2.4. This approach involves removing one technology from the year-2000 engine, setting new cycle limits as necessary, and generating new engine performance, specifically, engine TSFC, weight, volume, and cost. Finally, the trade factors were applied to the new engine parameters, which resulted in new missile range and cost per mile estimates. Comparing the resultant values to those for the baseline year-2000 missile shows the improvement derived from that technology. The selected technologies evaluated in this manner are not independent from one another and, therefore, are not additive.

Of the technologies quantitatively investigated, material technologies were found to have the greatest improvement in mis-

side cost per mile as shown in Figure 114. For example, most of the cost improvement is due to the use of carbon-carbon in the entire hot section of the engine. Ti_3Al for the compressors was also found to provide a significant unit cost improvement. Removal of Ti_3Al limits the achievable compressor discharge temperature, which results in greatly reduced cycle pressure ratio and mission benefits.

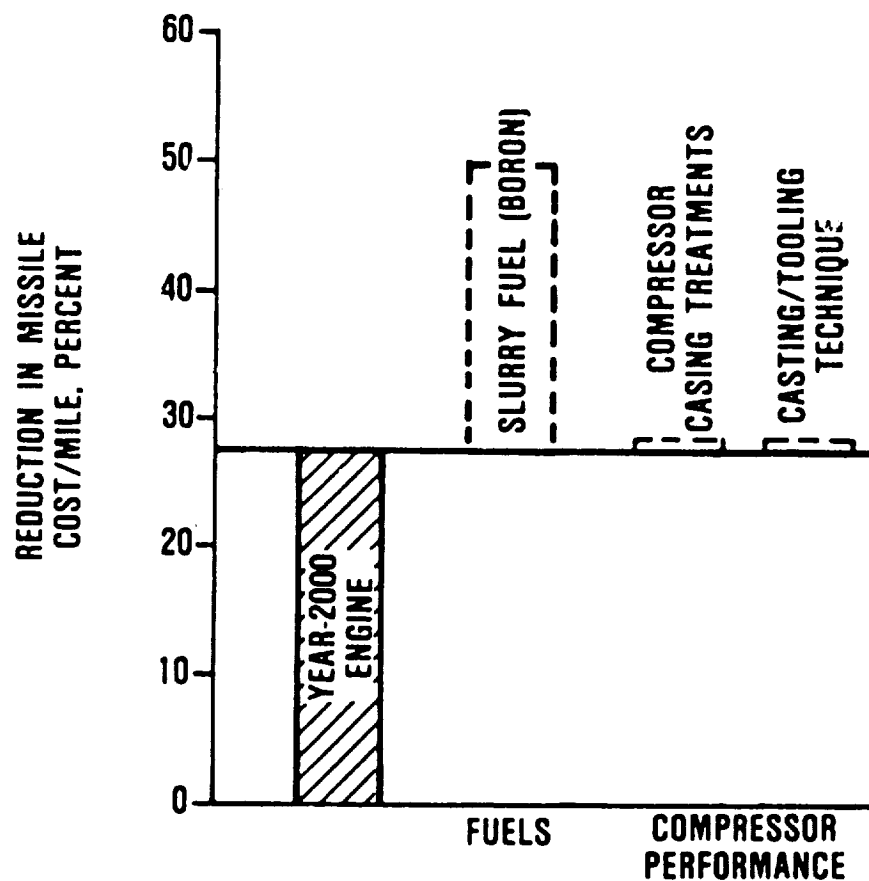
Component aerodynamics were also proven to be important in cost per mile improvements, specifically the compressor aerodynamics, where good efficiency with small axial blading is critical.

In addition to the technologies examined in the baseline year-2000 engine, several technologies were evaluated to determine further improvements in missile costs. The additional technologies evaluated are slurry fuels (boron), compressor casing treatments, and compressor casting/tooling techniques. As shown in Figures 115 and 116, the use of boron slurry fuels can significantly improve missile cost per mile and increase range to approximately 130 nmi, which is significantly greater than that of the baseline year-2000 value. Compressor casing treatments and compressor casting/tooling techniques, although important, show a much smaller improvement. The results of this technology evaluation leads to the conclusion that carbon-carbon, slurry fuels, and component performance are key technologies for the cruise missile engine.



GS-281-111

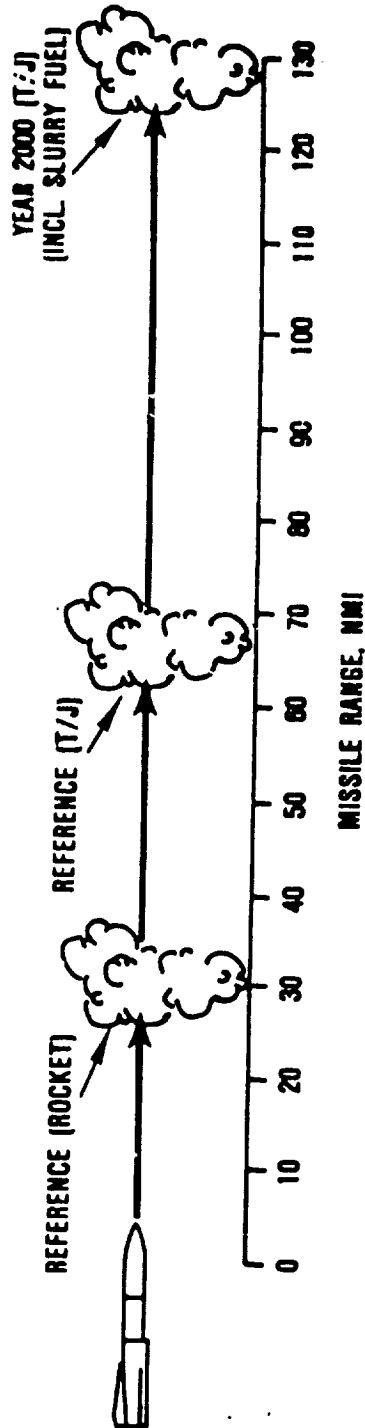
Figure 114. Comparison of Technology Benefits to Missile System.



GS-281-112

Figure 115. Benefits of Additional Technologies.

MACH 2.5, SEA LEVEL



KEY TECHNOLOGIES

- ADVANCED MATERIALS (CARBON-CARBON, Ti_3Al)
- ADVANCED FUELS (BORON SLURRY)
- IMPROVED COMPONENT PERFORMANCE

Figure 116. Missile Range Comparison.

4.4.2 Technology Plan

GTEC's recommended plan for Small Engine Component Technologies for year-2000 cruise missile engines is presented in this section. This plan addresses technologies in keeping with the technology benefits as presented in paragraph 4.4.1. The technologies addressed are as follows:

- 4.4.2.1 Materials
- 4.4.2.2 Combustor Technologies
- 4.4.2.3 Compressor (Axial) Performance
- 4.4.2.4 Turbine Performance
- 4.4.2.5 Systems Technologies

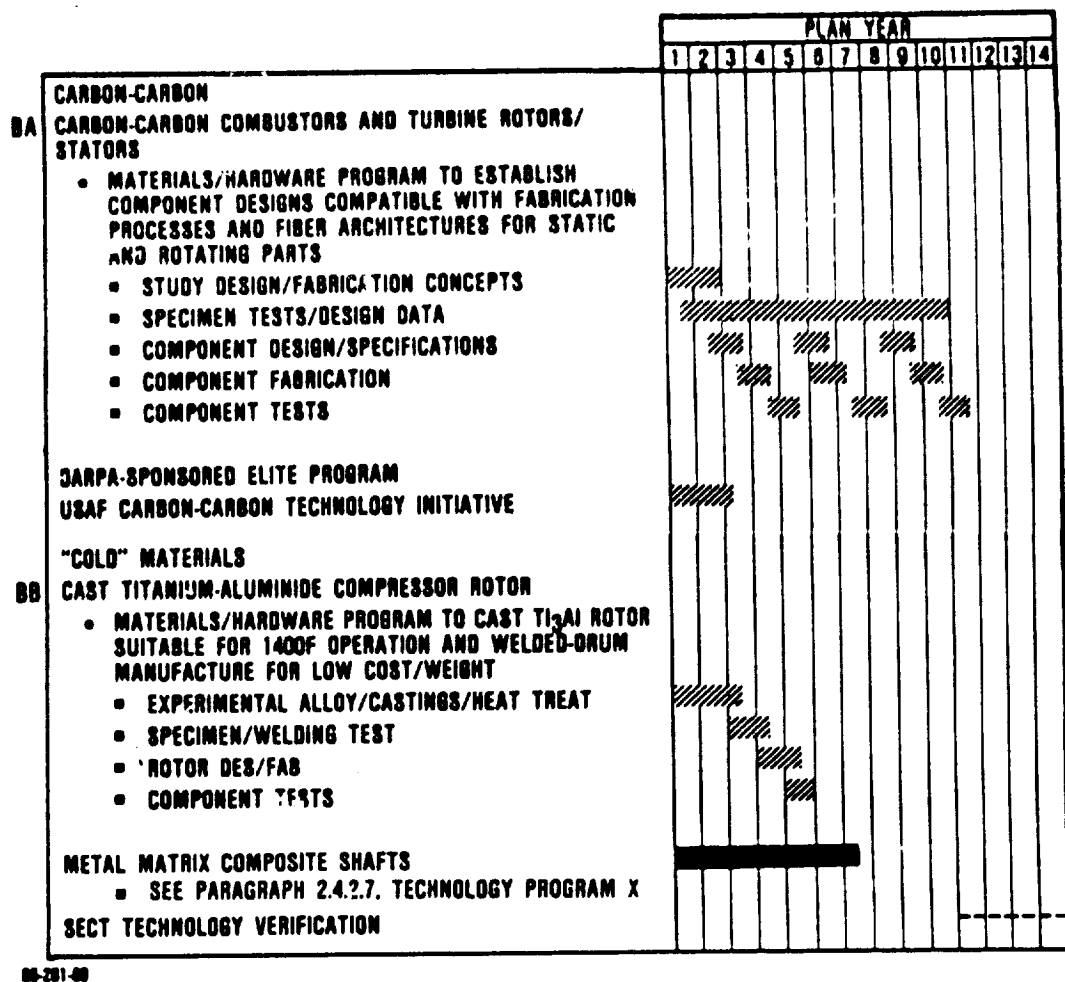
These plans address the high payoff technologies needed to obtain "technology readiness" by the year 2000. Some technologies may require verification and engine demonstration testing prior to commitment to an engine full-scale development. This activity is not included in the technology plans; it may be conducted during the latter program years (11 through 14).

4.4.2.1 Materials

This plan consists of two discrete technology programs that are identified as BA and BB in Figure 117. The metal matrix composite shafts program that was previously discussed for rotorcraft engines (paragraph 2.4.2.7, Program X) is shown here for reference and applies to the cruise missile engine as well.

BA. Carbon-Carbon Combustors and Turbine Rotors/Stators

Coated carbon-carbon (C-C) composite components will have the capability of higher turbine inlet temperatures and lighter-



00-201-00

Figure 117. Materials Technology Schedule.

weight engines. In addition, the ability to operate uncooled components will result in additional specific fuel consumption (SFC) improvements. The use of these materials also adds engine design flexibility in handling high ram inlet temperatures and the resulting high compressor discharge temperatures.

Carbon-carbon materials consist of high-strength carbon fibers imbedded in an amorphous carbon matrix. Since carbon oxidizes at significant rates above 427C (800F), a coating is mandatory to protect the composite. In an inert atmosphere, C-C maintains or increases its strength characteristics up to 2205C (4000F). This high temperature capability has led to its use in rocket nozzles and missile nose tips. It is also being widely used in aircraft brake disks and rotors. The successful use of coated C-C as the wing leading edge and the nose cap for the space shuttle has spurred interest in its use as an engine material.

The composite nature of C-C means that the fiber architecture can be tailored to meet the component stress requirements. In the case of axial rotors, this primarily means hoop reinforcement in the disk and radial reinforcement in the blades. A polar weave fabric layup, which is densified either by pyrolysis of a resin or pitch impregnate, or by chemical vapor deposition (CVD), is a natural starting point. The blades would be machined into a densified billet to form an integral rotor. The coating would be the final step, although oxidation inhibitors would also be incorporated into the carbon matrix and, ultimately, into the fibers themselves.

Combustor liners and exhaust nozzles will also be made as fabric layup with primary and secondary cooling holes drilled into the combustor liner prior to coating. The low stress requirements for the turbine stators result in additional fabrication options, including compression molding of a chopped fabric.

Based on current programs, the basic capability appears feasible for C-C substrates to be fabricated in the required component shapes and to meet the strength requirements. The major question is whether 2-D reinforcement of rotors is adequate or whether 3-D reinforcement is required to achieve improved interlaminar shear properties.

A number of programs are addressing the coatings technology. This includes adding oxidation inhibitors to the substrate as well as using overlay coatings. Based on current DARPA and USAF programs, 1371 to 1649C (2500 to 3000F) protection appears feasible in the near term, while 1927C (3500F) coatings are in development for longer term use. A major hurdle is a reliable oxidation protection system that can be cycled repeatedly over a wide temperature range.

Program Description

This program consists of five major tasks, from the design study through component tests, as scheduled in Figure 117. Three iterations are scheduled to achieve technology readiness.

The initial program task is to select preliminary designs for the coated C-C components. This includes the fiber architecture, attachment schemes, and fabrication approaches. Preliminary material requirements are thus established. Vendors will be surveyed to determine the state-of-the-art capabilities for component fabrication approaches. Vendor capabilities will then be evaluated to determine the best long-range approaches and capabilities.

Basic fabrication approaches will be evaluated in subcomponent trials. Typical questions addressed for the rotor include polar weave versus other fiber architectures, high interlaminar

strength constructions, aerodynamic shape capabilities, shaft attachment schemes, and low-cost densification approaches. Typical questions for the stator include integral versus segmented construction, chopped fabric versus laminate, aerodynamic shape capabilities, attachment schemes, and low-cost densification approaches. Subcomponents will be fabricated for testing, and NDE techniques will be established.

Under the specimen test activities, vendor material will be evaluated in terms of strength (before and after coating), oxidation resistance, and mechanical property changes after exposure. Candidate fabrication approaches will be evaluated by disk spin tests, attachment tests, and mechanical load tests. Substrate, coating, and fabrication approaches will be selected on the basis of these tests.

Test specimens will then be fabricated to obtain mechanical design property data. Those specimens will have relevant fiber architectures and coatings and will be tested over the appropriate range of temperature and environment. A significant number of specimens will be tested to compile an adequate data base.

A detail design for experimental parts is planned, along with two follow-on iterations that will have the benefit of the full design data base. The detail design will consider all material and fabrication constraints.

Three fabrication cycles are planned. They provide hardware for component and rig tests, hardware for the engine test, and they support the development of NDE technologies for in-process inspections.

Fabricated components will be bench tested individually to assess mechanical and aerodynamic performance. These component

tests will be used to qualify components for subsequent rig tests. Test results will influence the second detail design effort.

Rig tests will evaluate component performance and durability under simulated engine conditions. Results will guide subsequent design and fabrication tasks.

BB. Cast Titanium-Aluminide Compressor Rotor

The SECT advanced cruise missile engine, as conceptualized for the year 2000, has a six-stage axial compressor with a maximum compressor discharge temperature of 732 to 760C (1350 to 1400F). To minimize the cost for a missile engine, the most desirable method of manufacture of the compressor rotor is to cast all rotors and weld them together into a drum rotor.

To minimize compressor weight, the forward stages (one through three or four) should be cast of a conventional titanium alloy and given the high strength processing as discussed for the program: "High-Strength Cast Titanium-Alloy Impeller" (paragraph 2.4.2.7, Program V). No difficulty is anticipated in fusion welding these stages by electron beam or laser welding processes. The aft stages of the compressor would ideally be cast of a titanium aluminide alloy such as Ti₃Al due to favorable strength/density characteristics at high temperatures.

Research conducted in the Air Force Materials Laboratory and performed for the Air Force by Pratt and Whitney Aircraft has shown that viable Ti₃Al alloys retain useful strength to the 704 to 760C (1300 to 1400F) region and can be fusion welded with care. The Air Force-sponsored research will need to be expanded for the manufacture of integrally cast axial flow compressor rotors.

Program Description

This program consists of four major tasks, from alloy selection through component tests, as scheduled on Figure 117.

The alloy selection task would review the results of the latest alloy studies, including GTEC IR&D work, to select an alloy with adequate high-temperature strength for the SECT cruise missile engine. The selected alloy composition would be produced as a master heat, which would provide the required metal for subsequently producing castings.

Trial castings will be expeditiously procured by using existing GTEC wax patterns for integrally bladed turboprop engine turbine wheels. Appropriate casting parameters will be fine-tuned to produce sound castings for further evaluation. Heat treatments of the alloys will be studied to optimize microstructure, strength, and ductility. Mechanical properties of the cast alloy with the best heat treatment will be determined up to 816C (1500F). Emphasis will be placed on tensile, short-time creep, and high-cycle-fatigue properties.

An evaluation will be made of the weldability of the cast, heat-treated alloy. The purpose of this evaluation is to identify a welding process adequate to weld Ti₃Al compressor rotors to one another and to cast conventional titanium alloys. Processes to be evaluated include electron beam, laser, and friction welding. Preheating and postheating will be studied as means of eliminating weld cracking.

Based on the properties and the results of the welding study, a single-stage representative of the cruise missile compressor will be designed, manufactured, and component-tested. The component testing will include overspeed burst tests, cyclic

whirlpit tests, and sectioning and testing of finished castings to verify material properties.

4.4.2.2 Combustor Performance

This section presents the technology plan for combustors as applicable to year-2000 cruise missile engines. The plan consists of three discrete technology programs, identified as Programs BC to BE in Figure 118.

The first program (BC), which addresses diffusion systems suitable for the cruise missile engine cycle, is limited to cold flow tests. It is scheduled to start, after Plan Year 2, to incorporate the results of an Air Force/NASA combustor diffuser interaction (CDI) program currently in progress.

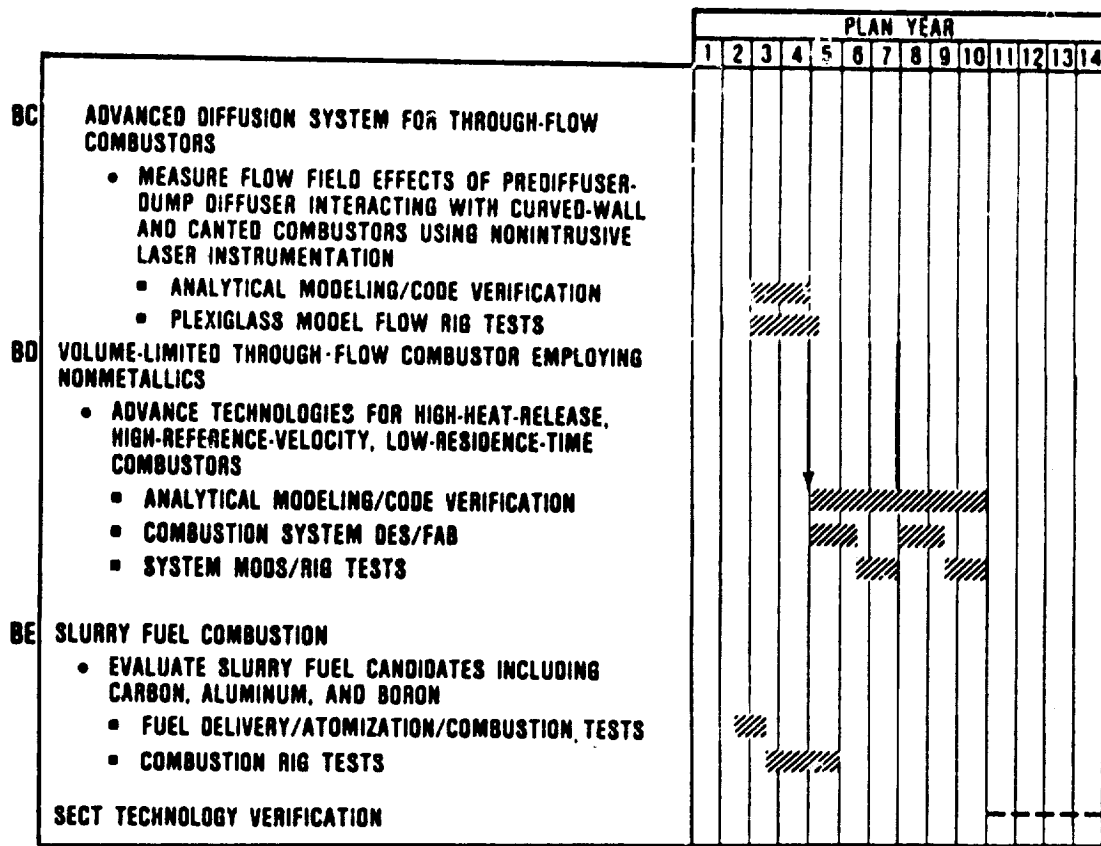
The second program (BD), which is for a nonmetallic combustor, is scheduled to build on the diffusion technology of Program BC and on the carbon-carbon materials program discussed in paragraph 4.4.2.1 (Technology Program BA).

The third program (BE), which addresses slurry fuels, is scheduled to start in Plan Year 2. It builds on the results of a DARPA ELITE program currently in progress.

BC. Advanced Diffusion System for Through-Flow Combustors

Advanced diffuser systems are needed for cruise missile engine (CME) applications to reduce engine length and weight and to improve cycle performance by reducing combustor pressure drop.

Low pattern factor, volume-limited combustor design goals provide significant risk for SECT cruise missile engine combustors. The CME combustor reference velocity (V_{ref}) and heat



06-201-131

Figure 118. Combustor Technology Schedule.

release rate (HRR) are approximately 45.7 m/s (150 ft/sec) and 1.89×10^6 w/(m³·kPa) (18.5×10^6 Btu/(hr·ft³·atm)), respectively. Current state-of-the-art propulsion engines have V_{ref} and heat release rates (HRR) of about 27.4 m/s (90 ft/sec) and 0.613×10^6 w/(m³·kPa) (6×10^6 Btu/(hr·ft³·atm)). The design goal pattern factor for the CME is 0.25, which is approximately 30 percent lower than the projected 0.35 pattern factor based on current technology.

Program Description

This program consists of two major tasks, from analytical modeling through Plexiglas flow tests, as scheduled in Figure 118.

The first activity will be a CDI program review and analytical design evaluation of advanced diffuser systems. After identifying the diffuser types of most interest, the selected diffusers will be fabricated and tested in a Plexiglas rig (CDI type). Nonintrusive laser flow-field measurements will be taken to determine the detailed flow field for comparison with predictions. Pressure recovery data will also be obtained. The second activity will involve rig testing to identify promising configurations with respect to diffuser type and combustor geometry that produce low-pressure-loss, stable airflow patterns for high-through-flow combustion systems.

The final activity of the diffuser program is an analytical model to more accurately match measured data. This will allow increased confidence in predicting advanced diffuser performance for future engines.

Technical Discussion

The diffusion system length must be minimized for future engines while retaining high effectiveness. This will require identifying the optimum advanced diffuser types to provide the least amount of pressure loss in the minimum length. The interaction between combustor and diffuser will require improved analytical models to adequately predict pressure recovery for advanced diffusers.

Analytical predictions will be compared with Plexiglas rig test data to identify an optimum advanced diffuser geometry while verifying analytical model accuracy. The start of this program will be delayed two years in order to incorporate the results of the ongoing Air Force/NASA CDI program for current state-of-the-art diffusers. The advanced diffuser program will employ the 3-D LDV measurement technology being developed in the CDI program and apply it to nonsymmetric advanced, curved-wall, vortex-controlled diffuser geometries.

The goal of this program is to verify the aerodynamic model accuracy for determining pressure loss and flow field in an advanced prediffuser, dump diffuser system. The current CDI program evaluates combustor-diffuser interaction with current state-of-the-art prediffusers. The proposed program will extend that study to more aggressive diffuser designs, including curved-wall and canted combustor (nonsymmetric) effects.

BD. Volume-Limited Through-flow Combustor Employing Nonmetallics

The use of uncooled nonmetallic combustors will significantly reduce combustion system problems associated with high-cycle

temperatures. The crucial requirement for initiating nonmetallic combustor technology programs is a suitable material. The material should allow "arbitrary" placement of air orifices and be capable of withstanding relatively high thermal gradients and mechanical shock/vibration levels. Cooling air will not be required so that it will be available for improved pattern-factor control.

Fuel atomizer-combustor dome swirler optimization will minimize the severity of thermal gradients in the combustor primary zone, which is crucial for nonmetallic material. Due to the strong interrelationship between atomizer and combustor performance, both areas will be evaluated simultaneously in full annular rigs. Pattern factor control and thermal gradient reduction will be addressed. Atomizer coking resistance will not be evaluated in this program due to the limited operational life required.

A high-pressure combustion rig will be used to evaluate high-reference-velocity, high-HRR combustors. Three-dimensional, reacting flow, combustion analytical models will be used to determine the initial geometry for advanced systems with between 1.02 and $2.04 \times 10^6 \text{ w}/(\text{m}^3 \cdot \text{kPa})$ (10 and $20 \times 10^6 \text{ Btu}/[\text{hr} \cdot \text{ft}^3 \cdot \text{atm}]$) HRRs. Pattern factor, combustion efficiency, stability, and ignition characteristics will be evaluated for each system to determine the practical size limits for combustors depending on engine application.

Program Description

This program consists of three primary tasks, from analytical modeling through rig tests, as scheduled in Figure 118.

Existing analytical models and the advanced diffuser data from the foregoing program (BC) will be used to design the combustor. Mechanical design will be based on C-C data from the materials programs discussed in paragraph 4.4.2.1, Technical Program BA. Two C-C combustion liners, complete with hole patterns will be fabricated. Approximately eight additional liners will be partially fabricated to facilitate experimental modifications. A second design-test iteration is scheduled to achieve technology readiness.

Test results will be compared with analysis predictions of combustor performance to verify accuracy or identify areas where additional modeling development is required.

Pattern factor and combustion efficiency levels are expected to be the limiting parameters in reducing combustor volume. Ignition and stability characteristics will be determined for each configuration.

Following initial test evaluation, each combustor will be modified to determine optimum performance for each configuration. Iterative analysis and testing will allow up to five modifications for each configuration during the test program to achieve optimum performance. Analysis prediction and test result comparisons will be available for all modifications to verify model accuracy for low-residence-time combustors.

At the conclusion of the test program, the impact of reduced combustor volume on pattern factor, combustion efficiency, ignition, and stability will be evident. This data will allow more precise combustor sizing for given applications. Analytical model prediction accuracy will also be established to allow increased use of the model as a design tool for future volume-limited combustion systems.

BE. Slurry Fuels Technology Plan

Introduction and Discussion

The performance of gas turbine powered cruise missiles can be improved by the development of suitable fuels with increased energy-per-unit volume; the range of the vehicles can be increased without altering their size. Therefore, existing launch aircraft can be used and the number of available targets increased. Figure 119 shows the potential range increase as a function of fuel energy.

Slurry fuels, composed of powdered solid materials suspended in a liquid carrier, offer the potential for dramatic increases in fuel energy on a volume basis as compared to the conventional distillate fuels such as JP-4 and JP-10. The most common slurries being considered as potential fuels are carbon, aluminum, and boron. Slurries composed of these materials have their own specific advantages and disadvantages and each requires its own evaluation. Considerable research has been performed on carbon slurries, both with respect to fuel formulation and combustion demonstration, and limited work is in progress on boron slurry. However, to date very little has been done with aluminum slurry.

GTEC has experience with all three types of slurry fuels. In 1979, GTEC performed fuel characterization and combustion tests on 15 different carbon slurry formulations from three fuel suppliers. These tests involved atomization tests, flame visualization, and ignition and stability tests.

High combustion efficiencies were obtained for carbon slurry fuels in a test rig, provided that sufficient combustor pressure (750 psia) and combustor length were available (compared to conventional liquid fuel combustors). The combustion efficiency was

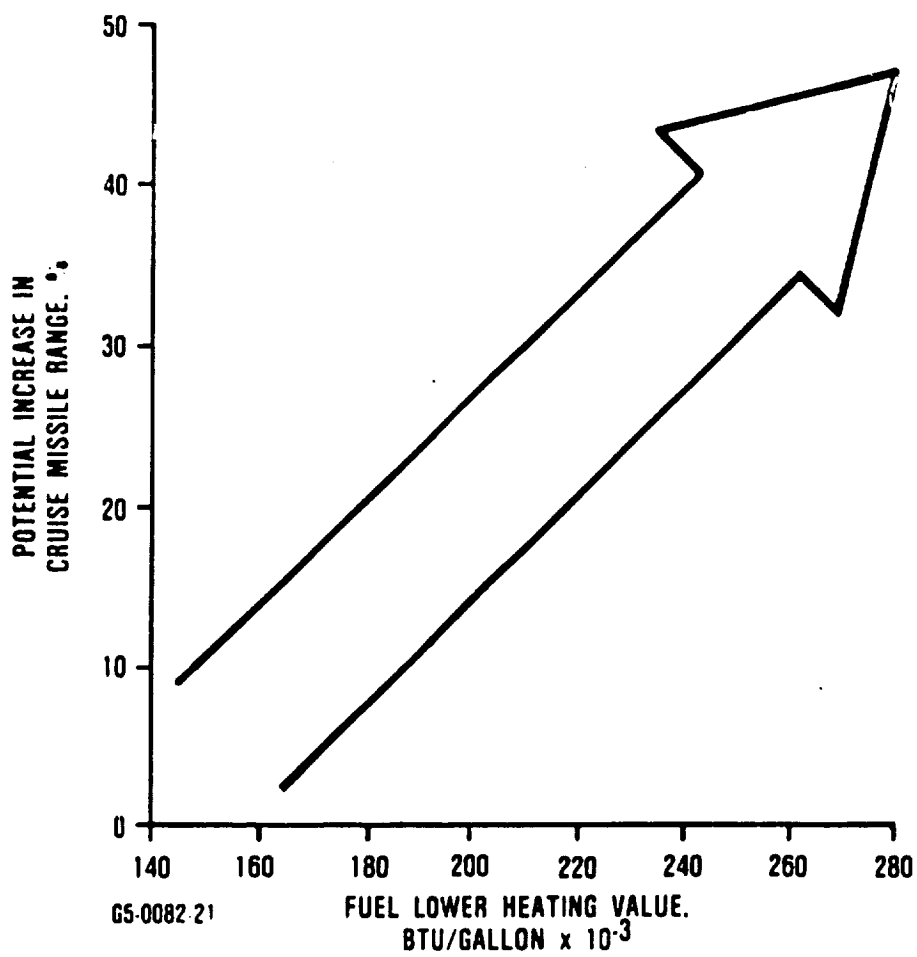


Figure 119. Significant Increases in Cruise Missile Range are Possible with High-Energy Fuels.

characterized for a variety of fuels including the effect of carbon loading and additive packages including catalyst. Following rig test evaluation, the most favorable fuel was successfully burned in an existing low-cost disposable turbojet engine, and combustor efficiencies greater than 95 percent were achieved.

The atomization of slurry fuels requires designs that address the slurry characteristics to centrifuge the solid particles out of solution, and its tendency to plug at much lower skin temperatures than do liquid fuels.

The combustion of slurry fuels requires design methods that address the dual-phase characteristics of the fuel. The air distribution in the combustor must allow a sufficiently rich primary zone to prevent the quenching of the liquid fuel reaction. This reaction provides the heat source for the ignition of the solid particles. The volume and air distribution scheme of the intermediate zone must allow sufficient residence time for the solid particles to complete their reaction.

Knowledge of these phenomena gained during the carbon slurry combustion program enabled GTEC to successfully demonstrate a boron slurry combustion system in 1984.

GTEC is participating in the DARPA ELITE program as a subcontractor to Vought. In this program, fuel ignition tests were performed and a plain jet air blast atomizer design was developed. This injector was used in a test rig to successfully burn boron slurry fuel. A schematic of the rig is shown in Figure 120.

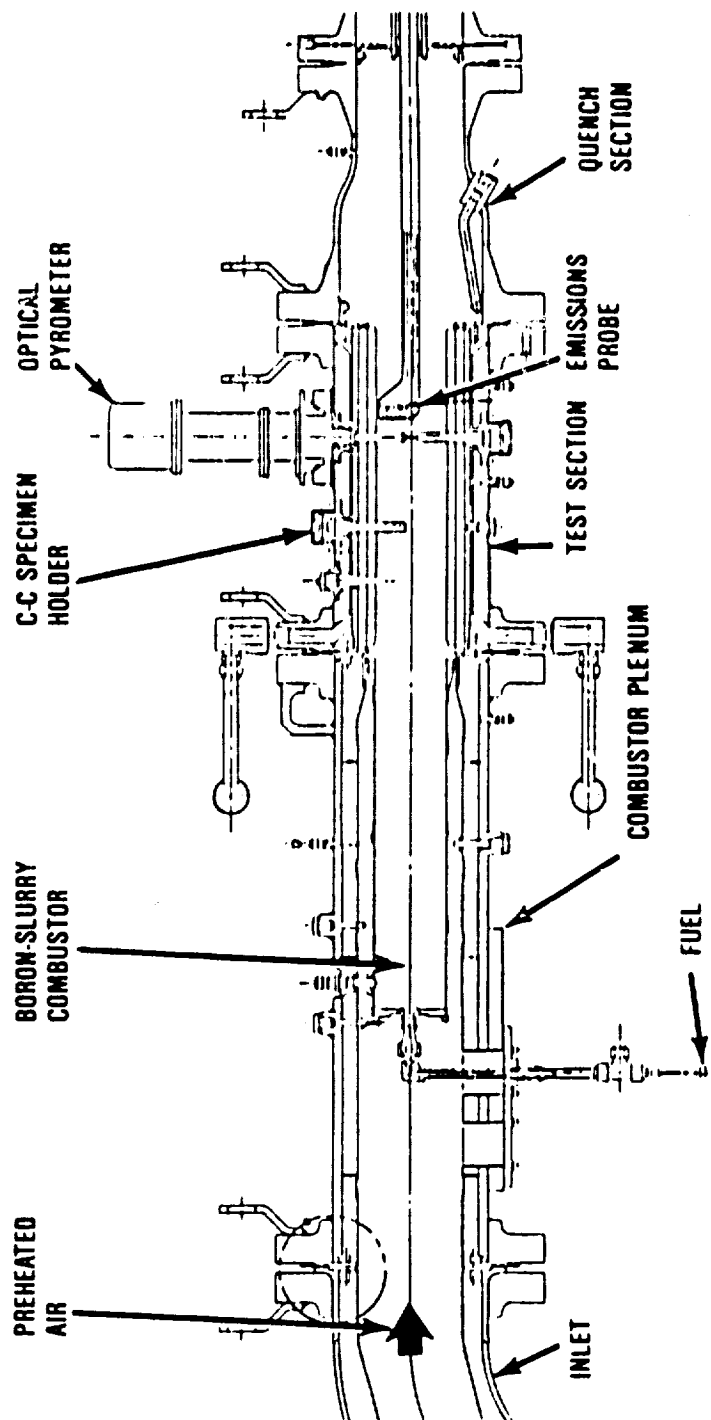


Figure 120. Boron-Slurry Element Combustor Test Rig.

64-0214-46

Spray tests of aluminum slurry supplied by the Signal Research Center were made using the plain jet atomizer developed during the ELITE program as shown in Figure 121. Test results indicated average droplet size to be less than the boron slurry at comparable conditions.

A comparison of the energy-per-unit volume of typical slurry fuels is shown in Figure 122, where the lower heating values are in Btu/gallon. Values for JP-4 and JP-10 are also shown. This figure demonstrates the significant range increase potential for the slurries.

Table 32 presents evaluation results for a specific cruise missile application, showing the significant improvements possible with aluminum- and boron-slurry fuels.

4.4.2.3 Compressor (Axial) Performance

This plan consists of six discrete technology programs, identified as BF through BK in Figure 123. The plan also repeats the schedule for a related technology program entitled "Analytical Modeling and Core Verification for Axial/Centrifugal Compressors" as discussed in paragraph 2.4.2.6, Program Q. The technology addressed by this program is vital to the cruise missile engine as well as to the rotorcraft and commuter engines, and is therefore included in the technology planning for each engine.

BF. Low-Aspect-Ratio Technology for Small Axial Compressors

The objective of this program is to reduce airfoil and end-wall losses in low-aspect-ratio axial stages that are required in

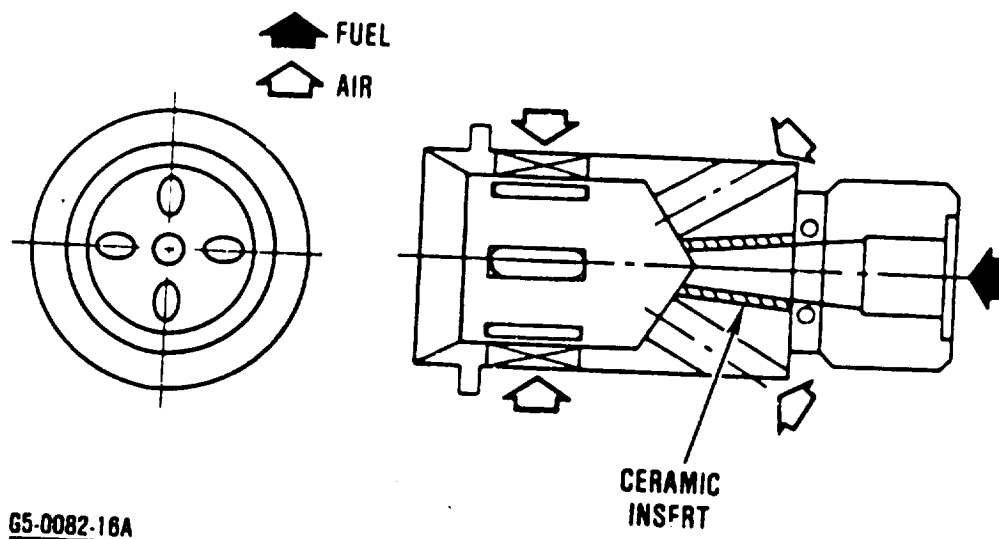


Figure 121. GTEC Pure Airblast Nozzle.

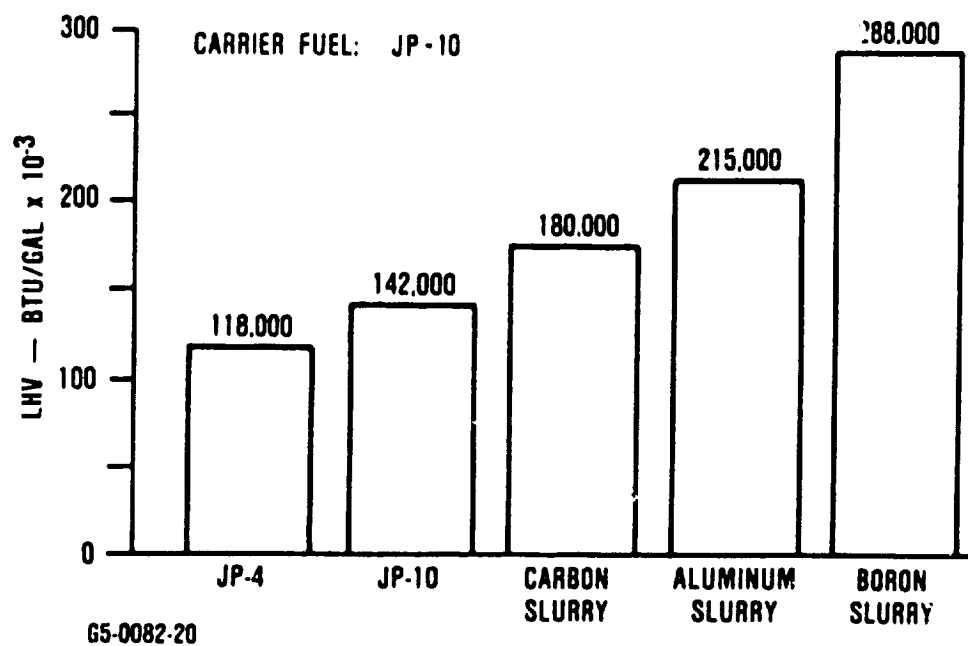
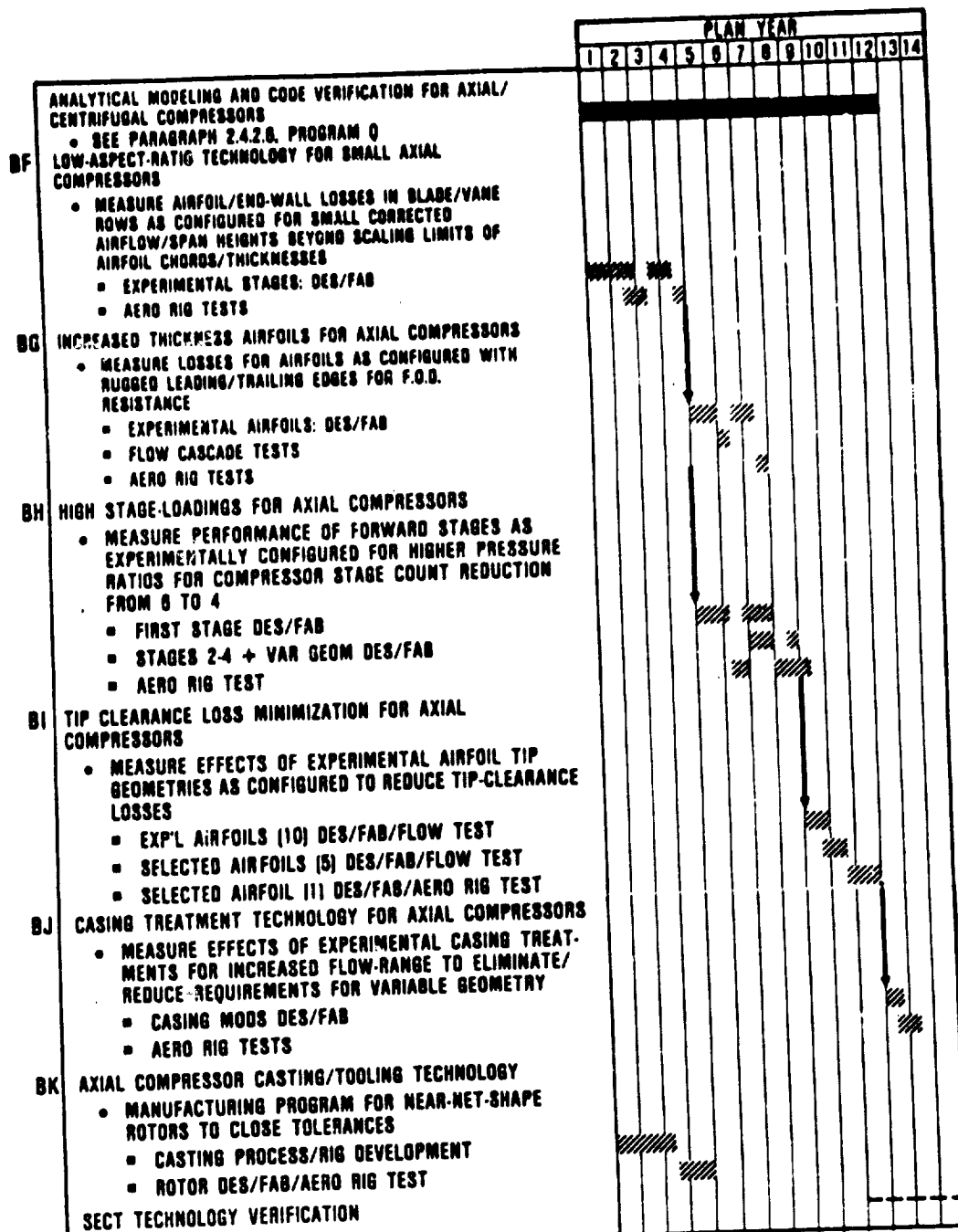


Figure 122. Volumetric LHV Advantage Results in Range Improvement Potential.

ALTITUDE = 24,384M (80,000 FT). MACH = 3.0



06-281-00

Figure 123. Axial Compressor Technology Program Schedules.

the small flow sizes of the SECT year-2000 cruise missile engine. Direct scaling of large axial compressor designs to small size typically leads to practical limits in blade chords, vane chords, and thicknesses. To achieve economical axial compressor designs in small size, the aspect ratio must be lowered. The effects of this are needed before full-stage compressor development in order to thoroughly explore compressor design options and ensure that proper design-parameter selections can be made.

The proposed program is expected to yield a one-point improvement in stage efficiency in the rear stages of axial configurations for the cruise missile engine compressor configuration, and secondarily, to enhance axial compressor alternatives for the rotorcraft and commuter engines.

Program Description

This program consists of two major tasks, from the design of an experimental stage through aerodynamic rig testing, as scheduled in Figure 123. The primary activities of this program consist of the analytical design of a baseline rear stage of the CME compressor configuration and five variations that investigate aerodynamic parameters relevant to low-aspect-ratio stages.

The analytical effort will yield a baseline rear-stage configuration plus five variations for an interior stage. These initial designs will then be fabricated and tested in a full-scale rotating rig simulating at least the rear three stages of the baseline compressor. This rig will be designed to provide for detailed measurements of flow conditions upstream and downstream of the interior (fourth) stage to evaluate the program concepts.

The results of this testing will be reviewed, and modifications to the analytical methods will be made to better predict the test results. Following this examination, four additional design modifications will be analyzed, fabricated, and tested in the three-stage rig. A final report will document the results.

Technical Approach

Axial compressors generally use airfoil blading whose shapes and performance characteristics have been established by cascade testing. Thus, the airfoil shapes and design parameters have been optimized for operation with uniform inlet flow conditions and are free of the effects of endwall boundary layers. For the rear axial stages of small axial and axial/centrifugal compressors, a large percentage of the airfoil (spanwise) operates in the influence of endwall boundary layers.

It is probable that airfoil shapes and design parameters that have been shown to be optimum for large axial compressors may not be so for the rear stages of small axial compressors. Wisler (reference 7) has reported moderate improvements from altered blade shapes with large hub-radius ratios and blading aspect ratio near unity.

Additionally, within the past decade, improvements in analytical methods for compressor design have made it possible to obtain more detailed information, such as pressure loadings and loss distributions for stationary and rotating compressor blade rows. Thus, it is feasible to conduct a systematic design study and experimental verification to determine the best possible concepts for reduced losses in low-aspect-ratio compressor blading.

This program will examine the following concepts for reducing losses in low-aspect-ratio blading:

- o Nonseries airfoils
- o Solidity and reaction
- o Spanwise twist or end bends
- o Spanwise compound leans
- o Endwall contouring

Initial concept testing will be followed by additional analytical design modifications and tests to verify the performance of small low-aspect-ratio stages.

BG. Increased Thickness Airfoils for Axial Compressors

The objective of this program is to determine airfoil design concepts incorporating increased thickness (primarily leading and trailing edges) that reduce manufacturing costs and increase ruggedness and resistance to foreign object damage (FOD), while retaining the performance characteristics of thin, scaled airfoils used in larger axial compressors. Thus, the program is aimed at reducing the initial costs and maintenance costs that have been very high for small axial compressor stages. These results are needed before full-stage compressor development in order to thoroughly explore compressor design options and ensure that proper design-parameter selections can be made.

The benefits from this program are applicable to the cruise missile engine application that uses small axial stages, and secondarily, to enhance axial compressor alternatives for the rotorcraft and commuter engines.

Program Description

This program consists of three major tasks, from the design of experimental airfoils through aerodynamic rig tests, as scheduled in Figure 123.

It is proposed that initial analytical studies be conducted to determine feasible airfoil design concepts employing thick blading. The magnitude of thickness levels will be determined by a manufacturing study that considers production methods, tolerances, and costs. The best concepts resulting from this study will be tested in a cascade rig to determine design and off-design losses and turning.

The cascade rig results will be examined and incorporated into the axial compressor design system. The best design will be applied to one stage of a multistage compressor, and performance will be evaluated in a single-stage test rig for comparison with a baseline thin-blade design.

Technical Approach

The key to this program is to establish methods to retain current compressor performance with increased blade thickness and chord lengths for reduced cost.

A significant body of knowledge exists concerning optimization of propulsion fan blading to cope with the bird-ingestion problem. This information, in conjunction with nonseries airfoil designs, for instance Rechter (reference 8), provides the basis for considering more rugged axial-compressor airfoils for small compressors.

The approach here is to rapidly evaluate a large number of concepts on a cascade rig and choose certain configurations for full-stage test evaluation. A systematic method will be used to screen the candidate configurations, and analytical models will be developed to be included in the future design system.

BH. High Stage Loadings for Axial Compressors

The objective of this program is to determine the effects of increased stage loadings on compressor efficiency in small axial stages. The obvious benefit is reduced stage count and, in the CME application, significant reduction in engine volume.

The initial CME axial compressor configuration is based on a six-stage configuration that incorporates a 1.75-pressure-ratio first stage. This is higher than the corresponding axial configurations in the rotorcraft application, where volume is a lower priority parameter. Further advancement in stage loading capability would reduce the stage count even further and would have a significant impact on missile range. The effects are needed before full-stage compressor development in order to thoroughly explore compressor design options and ensure that proper design-parameter selections can be made.

A program to establish the aerodynamic design technology required to reduce the number of axial stages from six to four, without loss in efficiency potential, would have a significant benefit in terms of life-cycle costs.

Program Description

This program consists of three major tasks, from the stage design through aerodynamic rig test, as scheduled in Figure 123.

The program will be initiated with the design of the first stage of the four-stage axial compressor (including inlet guide vanes). The design would use the latest axial compressor design and analysis methods proven on high-performance fan stages. This design will be tested in a rig capable of running both the first- and four-stage units. Following the test evaluation, the first stage will be redesigned, followed by design of the three aft stages. Fabrication and test of the four-stage compressor would then be conducted, followed by an analysis and a final report.

Technical Approach

The major emphasis of this program is to determine the loading limits for small axial stages. Existing programs are in place to determine loading limits for large 22.7 kg/s (50 lb/sec) compressors, such as the Building Block Compressor for the USAF. As the flow size is reduced to 9 kg (20 lb) and then to less than 2.3 kg (5 lb) per second, it is not clear that the same loading limits can be used. Current estimates suggest that peak efficiency can be achieved with moderately loaded axial stages (first stage $P/P = 1.65$ to 1.75). Two options are available. The first is to retain the same work coefficient and increase the speed to increase the pressure ratio per stage, thus reducing the stage count. The second option is to retain the existing wheel speed and to increase the loading per stage.

This program addresses the latter option and increases stage loading. The risk involves obtaining the same overall efficiency without losing surge margin. This program will examine methods of designing small, highly loaded blade rows and examining changes in aft stages as a result of increased loading in the front stage.

- This program can be accomplished within four years in a multitask effort as shown in Figure 123.

BI. Tip-Clearance Loss Minimization for Axial Compressors

The objective of this program is to establish aerodynamic design methods that desensitize axial compressor blading to tip-clearance leakage. Direct scaling of large axial compressor designs to small sizes typically leads to practical limits in blade running clearance ratios. These effects are needed in advance of full-stage compressor development in order to thoroughly explore compressor design options and ensure that proper design-parameter selections can be made.

The proposed program is expected to yield up to a two-point improvement in efficiency of rear stages where clearance-to-blade height is crucial. These benefits, which are applicable to the CME compressor configurations, secondarily enhance axial compressor alternatives for rotorcraft and commuter engines.

Program Description

This program consists of three major tasks, from the design of experimental airfoils through aerodynamic rig test, as scheduled in Figure 123.

In the past, simple flow-rig tests of turbine airfoil tip geometry, with the tip-leakage effect simulated, have provided information for development of designs that have reduced airfoil sensitivity to tip-clearance effects (i.e., AFAPL LART Program). An initial screening effort of this type to evaluate a large number of concepts will be undertaken, supported by analytical efforts to correlate the results. Following this effort, selection of the best concepts would be made and applied to an interior stage (rotor and/or stator) row of a multistage axial compressor such as the three-stage rig proposed for the low-aspect-ratio compressor program (Program BF). Rig testing at two clearances

will determine the effect of the design modifications on tip-clearance sensitivity relative to the baseline configuration.

Technical Approach

Attempts to determine tip-clearance effects on axial compressors have been more theoretical than experimental. Correlations have been suggested using a number of nondimensional parameters. Clearance/blade height, clearance/tip chord, and clearance/tip exit staggered spacing are the parameters usually mentioned in the literature. Detailed measurements at universities have provided some basic information on tip leakage and corresponding theoretical models.

The proposed approach is to experimentally evaluate a large number of tip configurations in a simplified static flow rig. The above parameters can easily be modified and tested to obtain both overall losses and detailed flow measurements. Then this data would be used to establish empirical correlations and analytical models of the flow in the tip region. The concepts that appear to reduce losses and secondary flow effects would then be incorporated into a multistage test environment.

This technical approach would permit a systematic evaluation of methods to reduce tip-clearance losses.

BJ. Casing Treatment Technology for Axial Compressors for Reduced Variable Geometry

The objectives of this program are to reduce cost and engine complexity for axial compressor configurations that use variable geometry.

• Current compressors require a combination of bleed and variable vane(s) in order to operate in a stable manner over their

range of operation. Configured in a conventional manner, the proposed SECT compressor for the cruise missile engine, with six stages and a pressure ratio of 12, would require a variable inlet guide vane (IGV), Vane 1 (and potentially Vane 2), plus inner stage bleed for stable operation throughout its operating flight envelope. Casing treatment over the front rotors could potentially eliminate the need for variable vanes by substantially increasing the flow range of the front-end rotors, at some penalty in overall efficiency. The elimination of variable vanes would offer substantial benefits in cost, weight, and reliability for future cruise missile engines. The results of this study are needed before full-stage compressor development in order to thoroughly explore compressor design options and ensure that proper design-parameter selections can be made.

The primary activity of this program will be to experimentally determine the effect of various casing treatment configurations on the flow range and stall margin from a fixed operating line, and on efficiency for an existing multistage, variable-vaned compressor. This data, along with analytical modeling, would be used to determine the feasibility and life-cycle-cost advantages of replacing variable vanes with casing treatment on the selected SECT cruise missile engine high-pressure-ratio compressor.

Program Description

This program consists of two major tasks, from the design of casing modifications through aerodynamic rig tests, as scheduled in Figure 123.

A compressor test vehicle will be selected from existing compressors that is similar in overall pressure ratio and front-end stage loading to the SECT high-pressure compressor. After a compressor test vehicle is identified, two or three tip casing

treatment configurations will be designed to fit the front stages of the selected compressor.

Sufficient rig testing of the selected compressor will be conducted to establish the effect of the selected casing treatment configurations on flow range, surge margin, and efficiency for both fixed- and variable-vane operation of the compressor. This will be done over the entire operating range of the compressor, with concentration on the two areas critical to stable transient and steady-state compressor operation, the start region and the midspeed surge knee region.

Using the data from this test and from off-design analytical models for the tested compressor and the SECT cruise missile engine compressor, the feasibility of using casing treatment to replace variable geometry will be evaluated. Estimates will be made for performance, weight, cost, and reliability effects. Analysis will then be performed to establish the payoff for tip casing treatment.

A final report will document the work done, the data taken, the life-cycle-cost results, and the final recommendations relative to the SECT cruise missile engine program.

Technical Approach

Tip casing treatment has been proven to substantially increase the operating range of axial compressor stages. Presently, front-end compressor stages use variable IGV and stator geometry plus bleed between the front and rear stage blocks in order to get sufficient stable operating range in the critical knee and start regions of compressor operation. This is due to the natural flow capacity mismatch that occurs between the front and rear compressor stages of high-overall-pressure-ratio compressors.

If it can be demonstrated that tip casing treatment over the front stages can provide flow range equal to that which results from variable-vane geometry, it would be possible to replace the heavy, complex, expensive, and relatively nonreliable variable-geometry construction with the simple casing treatment construction. The technical approach would be to determine, through experimentation, the flow range of front stages that results from variable vanes and then to determine the flow range for casing treatments with fixed vanes. This could be accomplished in an existing compressor of similar overall pressure ratio and front-end stage characteristics (loading and P/P per stage) as a year-2000 SECT cruise missile engine compressor. An estimated compressor map will be made using the flow range improvements and associated efficiency effects from the rig tests along with the predicted stage characteristics for the tested compressor and the SECT compressor. This map will include the part-speed surge line for the SECT high-pressure compressor with casing treatment and no variable vanes. The map will be compared with predictions for variable vanes in order to establish life-cycle-cost trade factors and part-speed stability comparison. From these results, the payoffs and feasibility of replacing variable geometry with tip casing treatments in the SECT application will be established.

BK. Axial Compressor Casting/Tooling Technology

To use titanium alloys effectively in compressor applications, forging processes (as opposed to castings), are conventionally used. The forging process is used because of the superior fatigue strength of forgings compared to that of castings produced from the same alloy. Design Engineering also requires close tolerance blade profile and blade thicknesses that, to date, have only been achieved through machining.

Compressor performance levels projected for the year 2000 require airfoil tolerances that cannot be obtained by current

titanium casting technology. In an attempt to advance the state-of-the-art pertaining to close tolerance titanium investment casting, GTEC is proposing a three-year research and evaluation program. The advantage of casting titanium compressors is the low cost of subsequent machining. Compressor rotors (integral) would be cast to size or near net shape, requiring only minimal machining operations. This would eliminate many forgings which currently require extensive and costly machining operations to meet design tolerances.

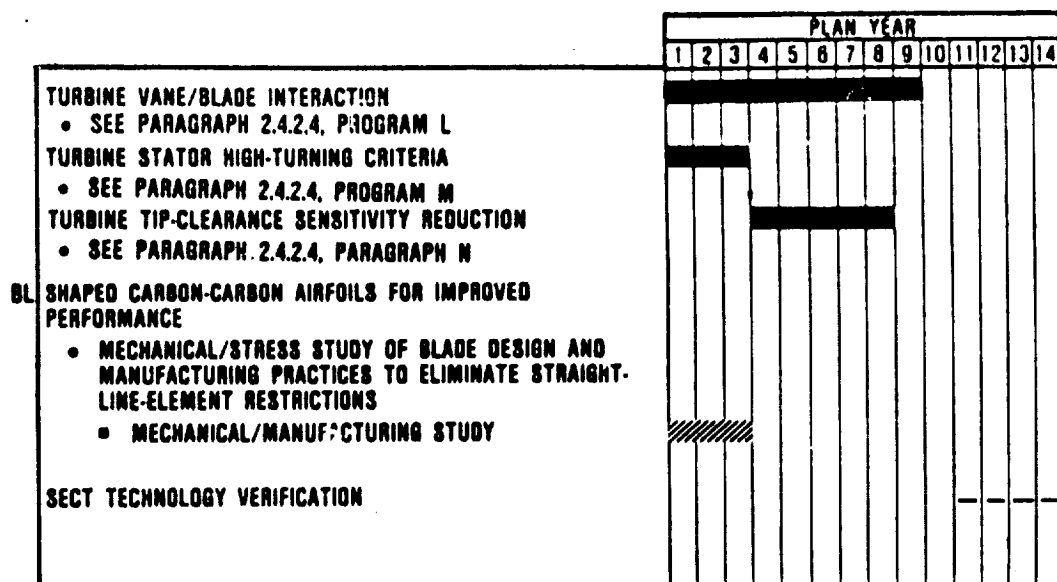
Program Description

This program is scheduled as two major tasks, from the casting process development through aerodynamic rig tests, as referenced in Figure 123.

The program will be based on an existing compressor rotor as redesigned for integral blading. The rotor will be selected to be representative in size and shape of the SECT requirement for year-2000 cruise missile engines. The program will be initiated by selection of a domestic casting vendor. The process development and tooling development will be a dual process; tooling cannot be developed without a process, and the process must be adjustable to the tooling. This research and development program will establish the feasibility of advancing the state-of-the-art in close tolerance integrally cast titanium axial compressor rotors.

4.4.2.4 Turbine Performance

This section presents the plan for turbine performance improvements, as applicable to year-2000 cruise missile engines. The plan consists of four discrete technology programs. Three are shared and one, Program BL in Figure 124 is new.



06-201-120

Figure 124. Turbine Technology Schedules.

The first three shared programs address technologies as discussed for rotorcraft engines in paragraph 2.4.2.4, Technology Programs L, M, and N. These programs are an integral part of this plan as well, since the technologies will apply to the year-2000 cruise missile engines. The remaining Program (BL) is dedicated to year-2000 cruise missile engines.

BL. Shaped Carbon-Carbon Airfoils For Improved Performance

All axial carbon-carbon (C-C) turbine rotors currently under consideration at GTEC are restricted to radial straight line element (SLE) airfoils. In other words, any radial line passing through the airfoil must pass through the blade root and intersect the blade surface only once. This means that the airfoil cannot be twisted, leaned, or dished. This restriction is imposed on the aerodynamic design strictly for mechanical reasons; without it, the airfoil shape can be optimized to improve the turbine efficiency by 1 to 3 points.

The C-C laminates currently planned for use in the ELITE and other advanced missile turbines are quite strong in tension, but weak in shear. To avoid shear stresses, the radial SLE restriction has been imposed on all laminated C-C turbine blades to date.

Program Description

This program is scheduled as a single study task as shown in Figure 124. Several different C-C rotor systems have been identified as possibly meeting the stress requirements of a non-radial SLE airfoil. Of these, two concepts are discussed in the technical section that follows. A primary design for the blade and disk will be selected based on engine application, cost, preliminary stress analysis, and available fabrication capabilities.

GTEC will meet with several vendors to discuss the functional requirements and their available fabrication and coating techniques. Subelement specimens will be fabricated for screening tests.

Subelement tests will then be performed to validate the analytical and conceptual approach of the primary design. Three types of subelements are proposed: specimen, spin disks, and twin-blade rotors. The specimen tests will measure properties for each of the selected C-C architectures. The spin disks will verify the attachment concept, and architecture designs. The twin-blade rotors will verify the manufacturing process and integrity of the twisted airfoil. These subelement tests will be performed at a variety of temperatures using both coated and uncoated C-C.

This experimental verification of the analytical approach and modeling would then allow for future design and testing of full-up rotor concepts.

Technical Discussion

The most promising C-C architectures intended for use in turbine rotors are the polar weaves. They have both hoop and radial filament bundles (tows) of 3000 to 5000 fibers each in the disk and blade. Toward the bore there are more hoop tows than radial, and conversely, more radial tows than hoop in the rim and blade. The radial tows in the blade are needed to take the centrifugal loads while the hoop tows are used only to maintain the radial tow integrity during the fabrication process, and to maintain a more or less uniform ply thickness.

Ideally, the filaments in a fibrous composite should be aligned with the principal stress directions. Unfortunately, this is usually impractical, if not impossible in practice. It

can be impractical from a fabrication standpoint, especially when the geometry or loads are even slightly complicated. If the loading on the part is not proportional, it becomes impractical to keep the filaments lined up with the principal stress directions, because these directions change as the load is applied.

If the radial filaments of the airfoil are undercut, the entire load of the undercut portion of the blade has to be supported by in-plane shear stress. The in-plane shear strength of a 0, 1.57 radian (0, 90 degree) weave is very poor. For the C-C laminate, it is at least a factor of ten less than the tensile strength. A simple radial straight-line-element airfoil will exhibit a simple uniaxial state of stress, and the peak-stress-to-average stress ratio will be close to unity. The shape of an aerodynamic optimized airfoil will be more complex, and likewise it will have a higher peak-to-average stress ratio.

Several possible C-C bladed disk concepts have been briefly investigated for improving the aerodynamic performance of the turbine. Of these, two concepts presently look most promising. One uses an "inserted" blade concept. The other uses an integral bladed disk approach and is therefore more similar to the ELITE turbine rotor. Other concepts include a 3-D weave architecture, and a 2-D weave with an overwrap.

The "inserted" blade concept involves separate blade elements to be fabricated individually, then "inserted" into two disk halves. The blade architecture would be a 2-D laminate molded into the required airfoil shape, then cured and densified to form a net shape or near-net-shape airfoil. This could be achieved by pulling one or more strips of carbon fabric and carbon roving through a pitch bath, then through a die with the approximate cross section of the airfoil. This uncured laminate can then be cut to length and cured between two matched dies to

form the airfoil and blade root. The airfoil would have a uniform cross sectional area, but would otherwise be of arbitrary shape. The blade root would be roughly T shaped, with the arms extending inward (see Figure 125). This near-net-shape blade would then be pyrolyzed and densified in a conventional manner. Several of these blades (airfoil plus root) would be placed in a ring and wound with roving and pitch. This winding would make the hoop load carrying portion of the disk.

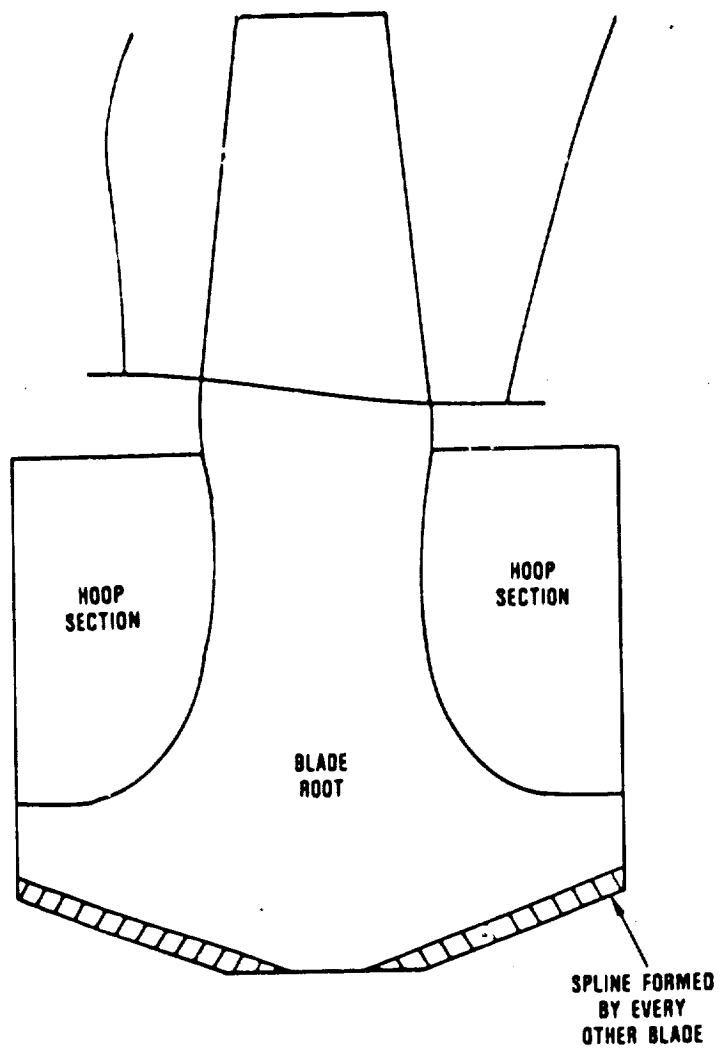
The second design concept would use a more conventional integral bladed disk (blisk) approach. The blisk blank would be fabricated from prepregged fibers then cured, pyrolyzed, and densified. The airfoils would then be machined from the blisk blank. This blank could be a conventional 2-D polar weave laminated composite that has been strengthened in the airfoil region by adding a continuous spiral weave insert (see Figure 126). This spiral weave insert would have fibers in the +45 and -45 degree directions, thus increasing the in-plane shear strength. The number of hoop fibers in the blade could be reduced, thus making room for the spiral weave insert without sacrificing the strength in the radial direction.

4.4.2.5 System Technologies

This plan consists of three distinct technology programs, identified as BM through BO in Figure 127. The plan addresses special technologies that are vital to the engine system as envisioned in this study for year-2000 cruise missile engines.

BM. Advanced Supersonic Nozzles

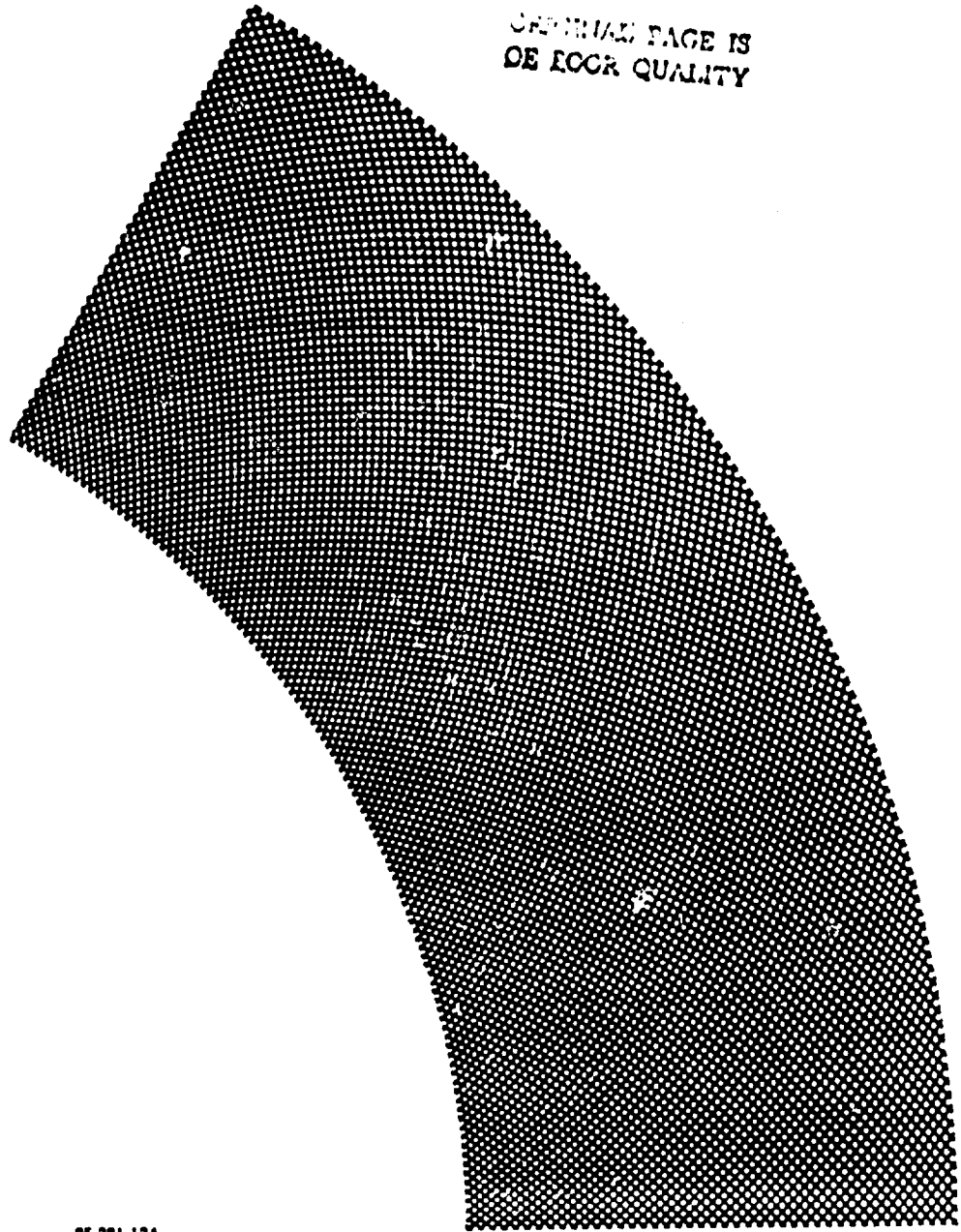
Design requirements and constraints for advanced supersonic cruise missile engine thrust nozzles are functions of the engine and airframe designs, the mission (tactical or strategic),



65-281-137

Figure 125. "Inserted" Blade Concept.

ORIGINAL PAGE IS
OF POOR QUALITY



65-281-134

Figure 126. Proposed "Spiral" Weave.

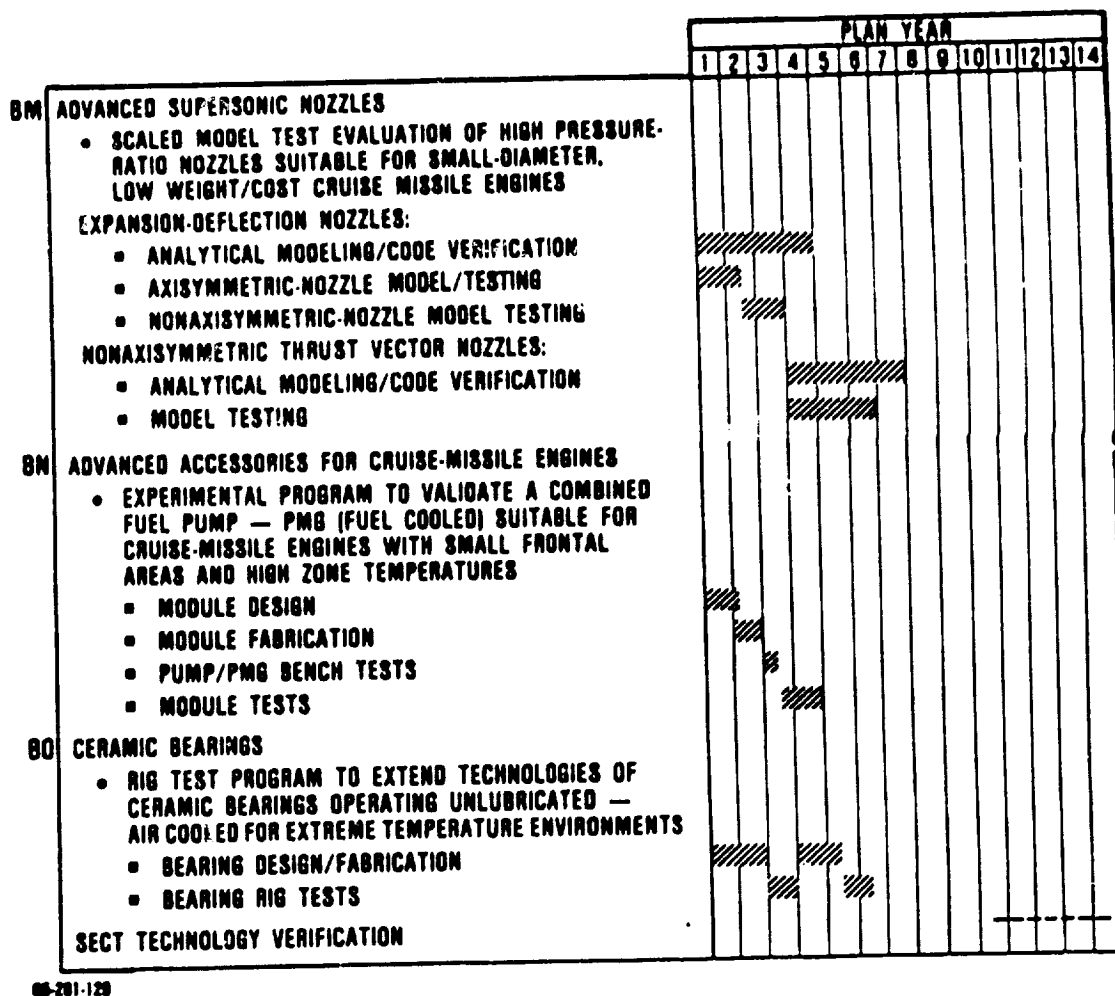


Figure 127. System Technology Schedule.

and the range. In general, however, these requirements and constraints include:

- o Medium to high nozzle pressure ratios (10 to 30 for tactical missions, 40 to 100 for strategic missions)
- o Light weight/small volume requirements
- o Maximum diameter constraints
- o High exhaust gas temperatures/little or no cooling flow available
- o Fairly broad range of operation with high performance requirements
- o Minimized variable geometry for low cost and simplicity
- o Requirements for nonaxisymmetric geometry
- o Low observables requirements

To satisfy these requirements, an advanced supersonic nozzle is required. Studies in this area have shown that the expansion-deflection (E-D) nozzle type would best meet most or all of the above requirements, both for tactical and strategic missions. The objective of the advanced supersonic CME nozzle program is to establish the advanced nozzle technology required for future supersonic cruise missile applications. Each of the two phases of this analytical/model test program will result in expanded analysis/design capabilities.

Program Description

This program consists of five major tasks for E-D and thrust vector nozzles, as shown in Figure 127. The program is planned

for three phases. Phase I consists of analytical modeling, code verification, and model testing of a symmetric E-D nozzle through the first one-and-one-half program years. Phase II consists of a similar program for nonaxisymmetric nozzles, beginning after Phase I and concluding at the end of program year four. Phase III is a similar program for nonaxisymmetric thrust vector nozzles for program years four through seven. Each phase will focus on expanding the experimental data base through model testing and on enhancing current analytical capabilities for advanced supersonic nozzle aerodynamic flow analysis and design.

Under each phase, the initial efforts will define preliminary configurations for parametric model testing. Results of the parametric model testing, which will include full internal wall and base pressure, mass flow, and thrust measurements, will be used to validate and enhance the existing analysis/design system. The final tasks in each phase will include aeromechanical design and model testing for an advanced nozzle for a SECT cruise missile engine application.

Technical Approach

A number of nozzle design studies have been done at GTEC in recent years to support both strategic and tactical supersonic CME studies such as the DARPA-funded ELITE and the USAF-funded ETEC programs, as well as this NASA-funded SECT program. Results of these studies have shown that an E-D nozzle is the best candidate to satisfy vehicle and mission requirements.

Advantages of the E-D nozzle borne out in these studies include:

- o Small volume/light weight.

- o Design performance close to alternative configurations that are larger and heavier.
- o Superior off-design performance due to the aerodynamic adjustment inherent in the E-D nozzle's base region flow field.
- o Nozzle performance is installation-independent.
- o Variable geometry is possible via centerbody translation.

In addition to design studies of axisymmetric E-D nozzles, the ELITE program included studies of nonaxisymmetric (elliptical) E-D nozzles.

Current industry and GTEC aerodynamic analysis/design capability for supersonic nozzles in general, and E-D nozzles in particular, includes the following components:

- o Performance prediction: Theoretical 1-D calculations, supported by experimental data base. For E-D nozzles, the existing data base covers only the high end of the CME pressure ratio range.
- o 2-D flow analysis: The 2-D, finite-element, viscous time-dependent, flow analysis code VNAP2 is used by GTEC for subsonic and supersonic wall contour optimization in axisymmetric E-D nozzle design, as well as for other supersonic nozzle types. Other 2-D methods, such as radial equilibrium analysis for subsonic ducts and the 2-D method of characteristics for supersonic flows, may also be used.

- o 3-D flow analysis: 3-D method of characteristics codes are under development in industry and universities. Application of 3-D inviscid panel analysis codes, such as PANAIR (available at GTEC), may be possible for supersonic nozzles.

Phase I of the CME nozzle technology program will validate and enhance current axisymmetric nozzle design/analysis methods through the combination of parametric model testing and detailed analytical studies. Based on these results, a final E-D nozzle design for the SECT advanced cruise missile engine application will be created and model-tested. The same approach will be followed in Phase II to validate and enhance design/analysis methods for nonaxisymmetric (rectangular or elliptical) E-D nozzles.

Phase III will address variable geometry and thrust vectoring as applied to nonaxisymmetric nozzles for unmanned, nonafterburning cruise missile engine applications, using the same basic approach as in Phases I and II. Significant work has recently been done in government and industry on thrust vectoring, but it has been focused specifically on the manned, afterburning fighter aircraft application. Phase III will build on this experience, as well as on the results from Phases I and II, to focus on the unique requirements and constraints for a thrust-vectoring cruise missile engine nozzle.

BN. Advanced Accessories for Cruise Missile Engines

Advanced supersonic missile engines impose unique requirements on their requisite fuel pumping and electrical power generating systems. These high Mach number applications result in very high engine zone temperature levels that exceed the limits for the wiring insulation and magnet temperatures for permanent magnet generators (PMG).

Fuel pumping systems for these engines must operate at high speeds and must be mounted internally in the engine to reduce frontal area and weight associated with tower shafts and reduction gear boxes.

The objective of this program is to evaluate, through bench testing, a combined fuel pump/PMG module designed for mounting in an expendable supersonic engine.

Program Description

This program consists of four major tasks, from design through module tests, as shown in Figure 127.

Design - Existing and planned GTEC expendable engines will be studied to determine fuel flow and electrical power requirements, operating speed ranges, environmental considerations, and internal physical space allocations. An appropriate existing engine will be selected as a test bed.

Analytical calculations and detailed mechanical design tasks will be undertaken. This will support drawings being made for a prototype combined fuel pump/PMG module and associated rig test hardware. The design will permit both components to be functionally tested as separate units.

Fabrication - Two prototype units and appropriate spare parts will be fabricated. Manufacturing methods for small quantities will be employed, but the design will be compatible with mass production technologies.

Bench Test - Initial tests will be conducted at ambient temperature on the fuel pump and PMG, as separate components, to validate the basic design and to isolate problems unrelated to system experimentation.

Module Tests - The components will be combined and subjected to testing over the expected range of fuel flows and electrical loads. Environmental tests will then be conducted to expose the module to the expected temperature extremes associated with the candidate engine and mission.

Technical Approach

Figure 128 shows the proposed fuel pump/PMG module as conceived for an existing engine. Fuel enters by means of a strut across the aerodynamic flow path. It flows around and through the PMG end turns, slots in the stator, and through the air gap to the pump inlet.

The PMG rotor consists of Samarium cobalt magnets contained by a sleeve that is mounted on an extension of the fuel pump impeller.

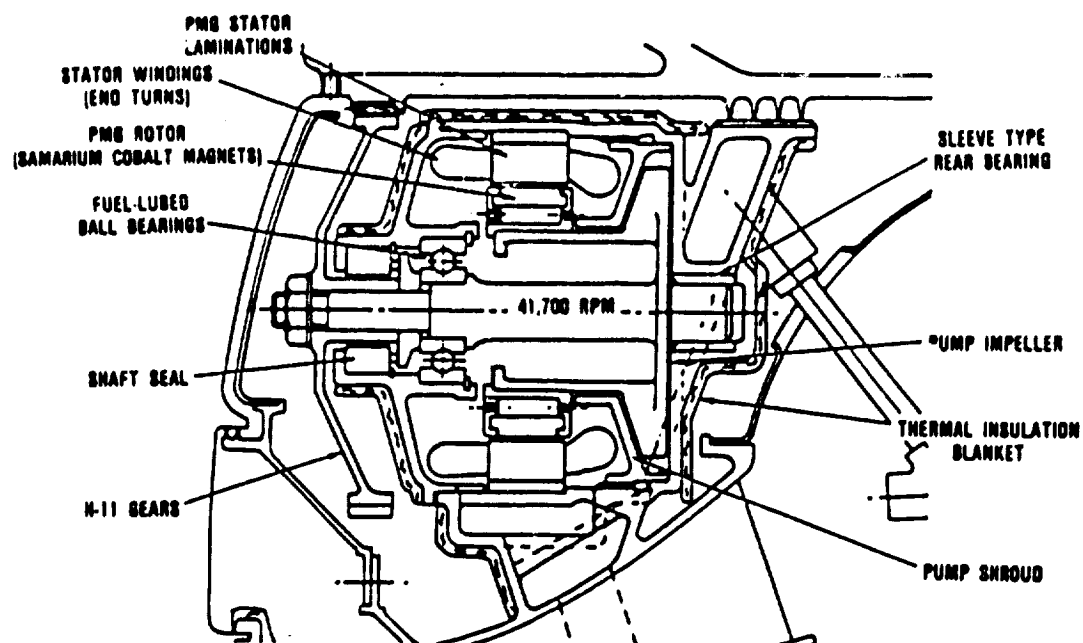
The fuel pump is a simple, low-cost, forced-vortex (Barske) design. The impeller contains five vanes that are equipped with extensions to support the PMG rotor. Discharge of the fuel is through a conical diffuser that is an integral part of the module housing.

The module is driven by an unlubricated gear set directly from the engine shaft. The module is thermally insulated to reduce external heat loads.

The proposed prototype development program will establish the technologies needed for this concept and will validate the design approach for future supersonic expendable engines.

BO. Ceramic Bearings

Advanced supersonic missile engines impose unique requirements on bearing systems, mainly due to the extreme temperature



66-281-128

Figure 128. Proposed Fuel Pump/PMG Module.

environments that exist due to high flight Mach numbers. As a result, conventional liquid lubrication is not feasible in most cases. Depending on the required mission length, various forms of dry lubrication are possible:

- o Unlubricated, air-cooled, all-ceramic bearing
- o Dry-film-lubricated (sacrificial separator), air-cooled, all-ceramic bearing
- o Dry-film-lubricated (external powder supply), air-cooled, all-ceramic bearing

The objective of this program is to investigate the limitations of each configuration, and to further the technology of each. This will be achieved by selecting representative candidate materials and lubricants and evaluating them for advanced missile engine bearing systems.

Program Description

This program consists of two major tasks, bearing design/fabrication and rig tests, as shown in Figure 127. The major activities include preliminary design and materials selection, detail design, fabrication, and rig testing. Two iterations are planned to define the optimum material and lubricant combination.

Design - Existing and planned GTEC expendable engines will be studied for their bearing system and lubrication requirements.

Each bearing configuration selected for evaluation will be the result of design optimizations performed with several analysis techniques available at GTEC, including the dynamic analysis

program developed by Dr. Pradeep K. Gupta. GTEC has been involved in dry-lubricated bearing programs for many years and has developed methods for calculation of heat generation and optimum techniques for bearing cooling.

Fabrication - An appropriate number of bearings from each category will be fabricated for development tests. Although the units will be of a prototype nature, manufacturing technologies employed will be consistent with requirements for large production quantities. Due to the long lead times for bearings, several configurations will be procured simultaneously to enable quick test turnaround time.

Rig Tests - Testing conducted to evaluate the various configurations selected will be performed under simulated engine speeds, loads, and temperatures. Although there are existing bearing test rigs, new bearing rig configurations will be developed to allow testing under the extreme temperature conditions that are representative of supersonic missile engines.

Technical Approach

Unlubricated Bearings - The unlubricated bearing development effort will be specifically devoted to cylindrical roller bearings. The configurations will include ceramic inner and outer rings, ceramic rollers, and a pure carbon separator. Testing will focus on the determination of maximum allowable run times prior to failure.

Unlubricated thrust bearings are not included in this effort since they generate more heat than roller bearings and would not survive even the shortest mission without some form of lubrication.

The ceramic roller bearing will include an attachment scheme to the shaft which consists of two collar-like members that press onto the shaft and over the inner ring guide flanges, thus holding the bearing inner ring concentric to the shaft. The inner ring bore will remain loose on the shaft.

An unlubricated scheme will be considered only for applications where the required mission is in the order of 30 minutes and the bearing DN is less than 1.0×10^6 . Unlubricated all-ceramic roller bearings have been demonstrated successfully in the industry to 0.7×10^6 DN and up to 538C (1000F).

The selection of bearing component materials for use in solid-lubricated bearings will be dictated by several considerations, some of which are currently defined. Others will be experimentally determined. The major factors are expected bearing operating temperature and the minimization of contact frictions.

Based on the expected bearing operating temperatures up to 1500F, known bearing steels are unacceptable due to their loss of strength and hardness at temperatures above 482C (900F). The best developed and most thoroughly tested material that will maintain its strength and wear resistance at temperatures up to and above 816C (1500F) is silicon nitride ceramic. The basic Norton Co. NC-132 material has been well documented in several comparison tests to be superior to competitive silicon nitride materials. There are some questions, however, as to the oxidation resistance of the MgO pressed version versus the Y_2O_3 . Interactions between this oxide layer on NC-132 and certain lubricants could lead to rapid wear at high temperatures. On the other hand, an yttria-containing silicon nitride material that does not oxidize could have a longer wear life even though higher porosity may give it a lower rolling-contact fatigue life.

Perhaps the most important factor in material selection will be the separator. By definition, externally powder-lubricated bearings lend themselves to use of a conventional steel silver-plated separator, but only up to temperatures less than 538C (1000F). A ceramic retainer is not feasible because it lacks strength in the tensile mode and has no ductility. Even a shrouded ceramic separator would probably not withstand the ball pocket collisions, which would lead to web break-up. A more feasible choice for a separator material may be shrouded carbon, although current carbons are limited to approximately 649C (1200F).

The bearing material with the longest rolling contact fatigue life is not necessarily the best candidate because race wear and interaction with the lubricant (to reduce friction and wear) are more important than fatigue life as evaluated under normal high-load, liquid-lubricated conditions. A race candidate with lower fatigue performance might have better wear life because of improved tribochemical interactions. Similarly, the highest strength retainer material at the operating temperature might not be the best candidate if it forms abrasive surface oxides. A lower-strength material that forms lubricious oxides might be a better candidate.

Dry-Lubricated Bearings - The design approach for dry-lubricated thrust bearings is necessarily different from that for conventional liquid-lubricated bearings. Whereas conventional liquid-lubricated bearings are designed and optimized for skidding and fatigue life, solid-lubricated bearings must also concentrate on the separator design to attain maximum reliability. Past experience as well as recent GTEC testing have demonstrated that the bearing separator is the limiting component in unconventionally lubricated bearings. Failures result from the following situations:

- o Unbalance failures (inner land-piloted schemes) due to worsening wear of pilot land
- o Fractures as a result of dynamics created from uneven build-up of solid film lubricant
- o Resonance failures (high ball/race traction transmits ball passing frequency to separator)

The selection of an optimum separator design will rely heavily upon clearance studies and load analyses performed with the latest rolling element bearing dynamic analysis program from Dr. Gupta.

Aside from the separator, the bearing internal geometry will be optimized for considerations of solid film lubrication. Raceway curvatures and contact angles will be selected to produce minimal heat generation, least ball dynamics, and largest internal clearance. Previous efforts at GTEC have demonstrated that solid lubricated bearings may possess extreme temperature gradients, a factor that must be considered in the design.

Since ceramics are being considered for both the rings and rolling elements, a system of shaft attachment must be incorporated to ensure that no tensile stress is transmitted into the ceramic inner ring. The method to be used will be similar to the one previously discussed.

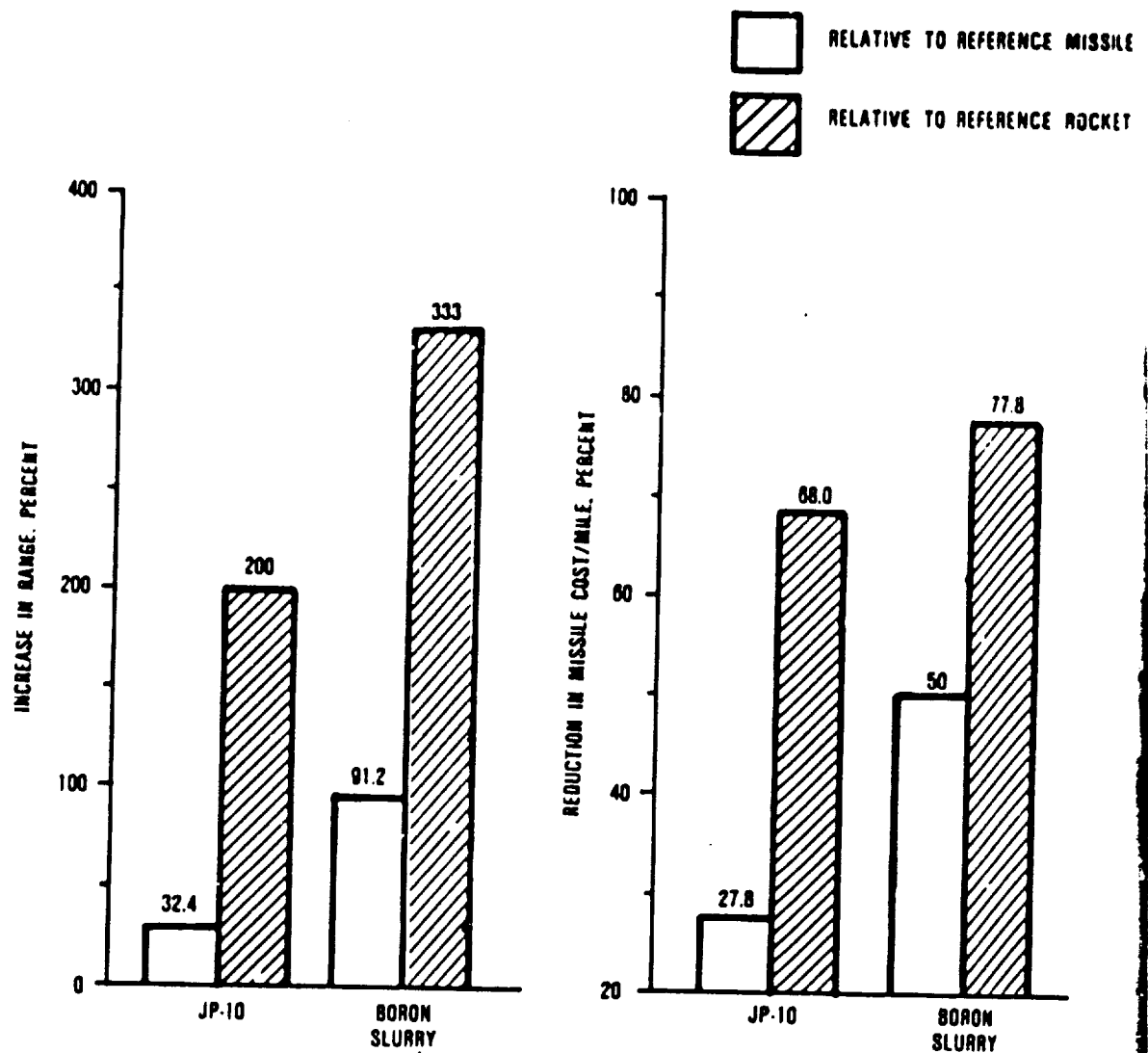
The sacrificial separator material as well as the type of powder lubricant, will be selected based on past GTEC programs that have researched and surveyed the successes and developments in the field. GTEC has accumulated a significant amount of data on the types and methods of introducing dry film lubricants into the bearing.

4.5 Summary

The mission analysis results show a significant improvement in both missile range and missile cost per mile over the reference missile (Figure 129). For comparison purposes, the approximate range and cost improvement relative to a rocket-powered missile also is shown. The advanced missile achieves a 32 percent and 91 percent range increase using JP-10 and boron slurry fuels, respectively, relative to the reference turbojet. When compared to the rocket-powered missile, a 200 and 333 percent range increase is possible with JP-10 and boron slurry, respectively.

Missile cost per mile decreases of 27.8 and 50 percent for JP-10 and boron slurry, respectively, were shown relative to the reference turbojet. A 70 to 80 percent cost per mile reduction is achievable for JP-10 and boron slurry, when compared to the rocket-powered missile.

These significant improvements are dependent on advanced in materials, advanced fuels (boron slurry), and component performance.



KEY TECHNOLOGIES

- ADVANCED MATERIALS (CARBON-CARBON, Ti_3Al)
- ADVANCED FUELS (BORON SLURRY)
- IMPROVED COMPONENT PERFORMANCE

Figure 129. Cruise Missile Mission Analysis Results.

5.0 AUXILIARY POWER UNITS

This section presents Garrett's SECT study approach, methodology, and results as conducted for auxiliary power units (APU) as envisioned for the year 2000. The presentation is organized into four major tasks, as conducted and described in paragraph 1.2 of this report.

5.1 Task I - Selection of Evaluation Procedures and Assumptions

The following paragraphs present the study results for the reference aircraft, duty cycle, APU, projected environmental constraints, economic model, and trade factors (for selected APU changes).

5.1.1 Reference Aircraft

As a typical application of a year-2000 airborne power unit, a commercial aircraft capable of transporting 150 passengers was selected. The application is expected to be in demand throughout the world by the year-2000 by both major and local airline operators. A recent study has been completed for a similar application to be in production in 1990. The requirements and the duty cycle for the SECT study were derived from the 1990 study and from airline and airframe inputs.

The emergency in-flight requirement to start and operate to 15,240m (50,000 ft) altitude is an extension of current capabilities which will require installation design in the airframe to provide proper pressure differentials at the compressor inlet and the turbine discharge areas.

The study assumes an installation weight of two times the APU weight. The aircraft fuel consumption penalty to carry this

installed weight is assumed to be 0.063 liter fuel/hr/kg (0.00755 gal/hr/lb). These factors are based on experience and past studies.

The typical installation is in the extreme aft part of the fuselage. Since it is aft of the pressure bulkhead, and fuel is plumbed to the area, a fireproof enclosure and a fire-suppression system is included. This location has several advantages, such as the following:

- o Noise and turbine exhaust are directed above and away from passengers, crew, and ground personnel.
- o The fairing structure is aerodynamically designed to reduce drag so that volume is not critical.
- o The location is not convenient for other uses because it has limited ground accessibility.
- o It is nonpressurized.

For the purposes of this study, the APU volume was not considered as an evaluation factor.

5.1.2 Reference Duty Cycle

The operational duty cycle for the year-2000 commercial transport is shown in Table 33. The APU is assumed to be operated one hour per aircraft flight/hour. This is typical usage for many local airlines using current 120- to 150-passenger aircraft such as the Boeing 737 and 727, and the McDonnell Douglas DC-9.

TABLE 33. OPERATIONAL APU DUTY CYCLE

Mode	Fuel Consumption Analysis Temp, C (F)	Ambient Temp.** Range, C (F)	Percent of Time	Compressed Airflow Kg/Min (Lb/Min)	Air Pressure kPa (psia)	Electrical KVA
1. Main Engine Starting	†	All	3.3	68 (150)	345 (50)	21
2A. Ramp/Loading	-18 (0)	-40/+4 (-40/+40)	9.9	64 (140)	***	32
2B. Ramp/Loading	-18 (0)	-40/+4 (-40/+40)	1.1	64 (140)	***	67
2C. Ramp/Loading	15 (59)	+4/+27 (+40/+80)	57.6	44.5 (98)	***	32
2D. Ramp/Loading	15 (59)	+10/+27 (+50/+80)	6.4	44.5 (98)	***	67
2E. Ramp/Loading	38 (100)	+27/+50 (+80/+122)	14.8	64 (140)-Max Avail	331 (48)	32
2F. Ramp/Loading	38 (100)	+27/+50 (+80/+122)	1.7	64 (140)-Max Avail	331 (48)	67
3. Service-Checkout	†	All	3.87	32 (70)	***	20
4. 3rd Gen. In Flight*	†	All	1.0	-	-	34
5. Bleed In Flight*	†	All	0.5	Max Avail	-	0

*APU must be able to start and operate up to 15,240m (50,000 ft) altitude (emergency conditions).

**Ambient extremes used as required for APU sizing.

***Airframe regulated.

†One-third time at each of -18, 15, and 38C (0, 59, and 100F).

The APU is normally operated only on the ground. A start is made during taxi, and the unit is run continuously until taxi out for takeoff. However, the APU also serves as a source for redundant electrical and hydraulic power in flight. It becomes flight critical in two-engine aircraft such as the DC-9 when the aircraft has a propulsion engine generator out of service. In this case, the aircraft cannot be dispatched until a backup power source is available.

5.1.3 Reference APU

The reference engine by definition is a unit that has demonstrated the performance specified but is not in production. A cross section of the 1985 technology unit, as selected for this study, is shown in Figure 130.

The gearbox, inlet plenum, and the location of the electronic control unit are subject to installation requirements established during the airframe design period. For the purposes of this study, the installed weight was estimated at twice the engine weight. In commercial usage, these engines include containment features which have the demonstrated capability of containing a maximum energy hub burst at 125 percent of the design maximum rotational speed. These components on the reference engine have added 10 kg (22 lb) to the reference engine weight.

The APU contains an automatic start system and a control system which will limit the applied load to the selected maximum turbine inlet temperature. As an example of the reliability of this system, many airlines allow completely unskilled cleaning crews to operate the on-board APU when the aircraft is located in an airport area which is not convenient to commercially produced electrical power.

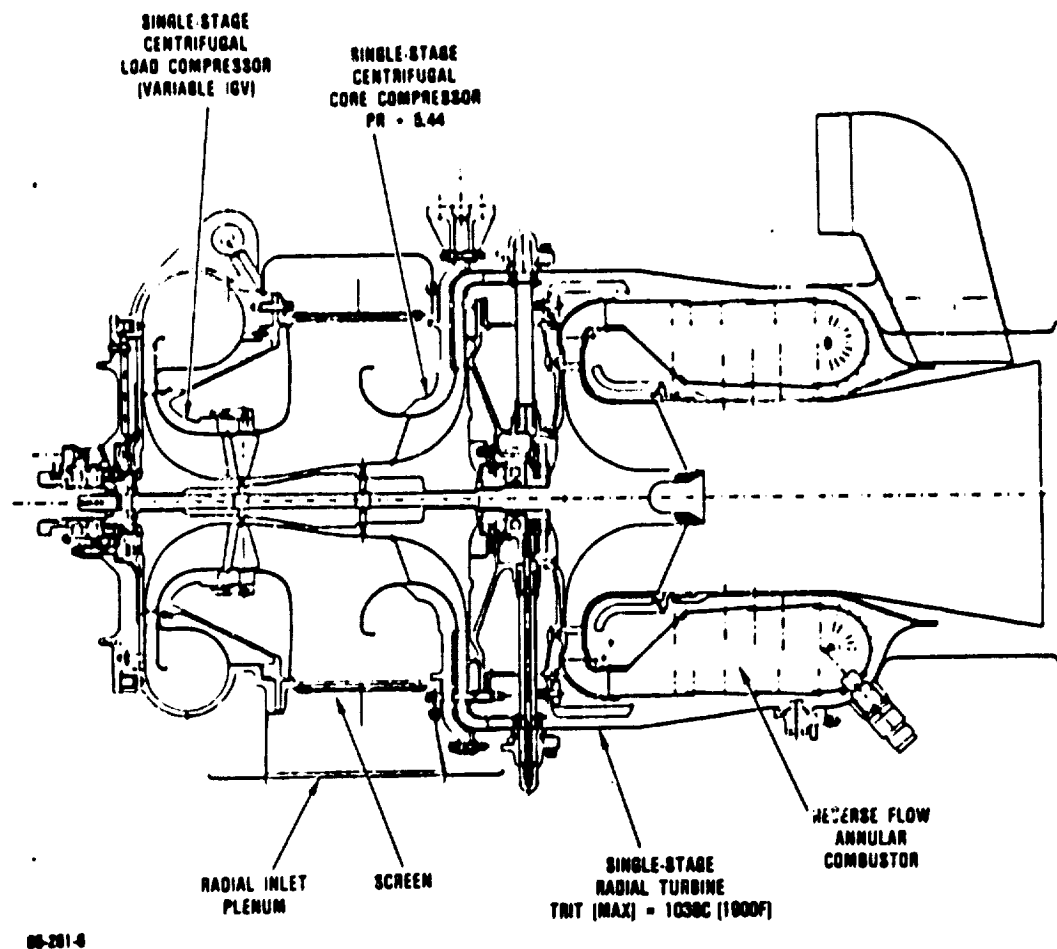


Figure 130. Cross Section of Reference APU Without the Gearbox.

Performance of the reference engine is given in Tables 34 and 35.

The reference turbomachinery estimated weight shown in Figure 130 is 42.0 kg (92.6 lb), including 10.0 kg (22 lb) of containment. The total APU estimated weight is 68.9 kg (152 lb), which includes a gearbox, starter, oil cooler, and five pounds of oil.

The cost of the reference engine in 1985 dollars is estimated at \$120,000 each in production quantities.

5.1.4 Environmental Constraints

APU noise has concerned the airlines, airport authorities, and manufacturers. To address this concern, ICAO has adopted guidelines for the noise certification of APUs installed in aircraft and operating on the ground. These guidelines establish maximum APU noise levels at work stations and at a 20 m (66 ft) perimeter around an aircraft. The airframe manufacturers have been using these ICAO guidelines as a basis for their APU noise level requirements. GTEC uses the guidelines as a goal during the design of every APU installation. The guidelines are stringent and are difficult to meet without adversely affecting aircraft weight, center-of-gravity limits, compartment envelope, APU performance, and system cost.

APU noise reduction technology in the year 2000 will be focused on improved inlet and exhaust duct and muffler designs and on radial turbine and centrifugal compressor aeroacoustic designs. Even with additional research in these areas over the next 15 years, the existing ICAO guidelines for installed APU noise will be difficult to meet. Therefore, the Garrett SECT study has used the ICAO Annex 16 Attachment D APU noise guidelines.

TABLE 34. REFERENCE ENGINE DESIGN-POINT PERFORMANCE*-SEA-LEVEL, STATIC, ISA, MAX, UNINSTALLED

Overall Engine Performance		Component Performance	
		<u>Compressor</u>	
Engine Rating, kW (shp)	267 (358)	o W/θ/δ, kg/s (lb/sec)	1.58 (3.49)
SFC, (kg/hr)/kW, (lb/hr)/hp	0.45 (0.74)	o PR	5.44
Turbine Inlet Temp, C (F)	1038 (1900)	o η _{AD} , %	77.1
Overall Cycle PR	5.44	o η _{poly} , %	81.7
Inlet W/θ/δ, kg/s (lb/sec)	1.56 (3.44)	o Exit corrected flow, kg/s (lb/sec)	0.373 (0.824)
Spool Speed, rad/s (rpm)	6,749 (64,453)	<u>Combustor</u>	
Fuel, LHV, kJ/kg (Btu/lb)	42,798 (18,400)	o η, %	99.5
		o ΔP/P, %	2.8
		<u>Turbine</u>	
		o W/θ/δ, kg/s (lb/sec)	0.64 (1.41)
		o η _{AD} , %	82.9
		o Cooling Flow, %	0
		<u>Load Compressor</u>	
		o W/θ/δ, kg/s (lb/sec)	1.13 (2.50)
		o PR	3.40
		o η _{AD} , %	76.0
		o η _{poly} , %	80.5
		o Exit corrected flow, kg/s (lb/sec)	0.415 (0.915)

*No margins

TABLE 35. REFERENCE ENGINE OFF-DESIGN PERFORMANCE*-SEA-LEVEL, STATIC, ISA, UNINSTALLED (MODE 2C. PER DUTY CYCLE, TABLE 33)

<u>Overall Engine Performance</u>		<u>Component Performance</u>	
		<u>Compressor</u>	
Engine Rating, kW (shp)	180	o W/θ/δ, kg/s	1.58
(equivalent shp)	(242)	(lb/sec)	(3.48)
SFC, (kg/hr)/kW,	0.501	o PR	5.07
(lb/hr)/hp	(0.825)	o η _{AD} , %	74.2
Turbine Inlet Temp, C	859	o η _{poly} , %	79.2
(F)	(1578)	o Exit corrected flow,	
		kg/s (lb/sec)	0.417
			(0.921)
Overall Cycle PR	5.07	<u>Combustor</u>	
Inlet W/θ/δ, kg/s	1.56	o η, %	99.1
(lb/sec)	(3.45)	o ΔP/P, %	3.7
Spool Speed, rad/s (rpm)	6,749	<u>Turbine</u>	
	(64,453)	o W/θ/δ, kg/s	0.64
Fuel, LHV, kJ/kg	42,798	(lb/sec)	(1.40)
(Btu/lb)	(18,400)	o η _{AD} , %	85.9
		o Cooling Flow, %	0
		<u>Load Compressor</u>	
		o W/θ/δ, kg/s	0.74
		(lb/sec)	(1.63)
		o PR	1.97
		o η _{AD} , %	**
		o η _{poly} , %	**
		o Exit corrected flow,	
		kg/s (lb/sec)	**

*No margins

**Compressor at part load using variable IGV.

Materials

The materials for the SECT reference APU reflect those used in current advanced engine demonstrated components. The materials for the major components are:

Compressor

Load Compressor: (Impeller) Ti-6Al-4V Wrought

Core Compressor: (Impeller) Ti-6Al-4V Wrought

Combustor

617 Ni Chrome Alloy

Radial Turbine

Impeller: MAR-M-247 Cast

Diffuser: 738LC Cast

Shaft

718 Nickel Alloy inertia welded to MAR-M-247 wheel

Smoke emissions will be required to be below the level of visibility (SN = 50); as with both the rotorcraft and commuter applications, gaseous emissions will be unregulated.

5.1.5 Economic Model

The economic analysis of APU applications has used life-cycle cost (LCC) analysis for this study in both Task II and Task

III analyses. The primary cost elements are for initial cost, support, and fuel. APU installed weight, which is considered for operational costs (per flight hour), is assumed to be equal to twice the APU weight based on past experience. The APU installation-related costs are calculated based on a representative airframe fuel consumption rate.

Trade-offs were analyzed between the costs of engine acquisition, fuel, direct labor, and material replacement, to ensure the lowest system LCC. Return on investment (ROI) analyses will be made in these tradeoffs.

The analysis used different modeling approaches for Task II and Task III analyses. During Task II, parametric models were primarily used, since results of the evaluations of alternative engine configurations could be obtained much more readily than with a bottoms-up approach.

During Task III, a bottoms-up model, based on individual piece part estimates, was used to more accurately account for major component and line replaceable unit (LRU) costs.

GTEC used the Air Force LSC 1.1 model, which had been used successfully in previous cost analyses of commercial APUs. The LSC 1.1 model allows costs to be evaluated for engine components to the necessary level of indenture as appropriate for the trade studies under investigation. Basic assumptions for these studies are:

- o The aircraft is not all-electric, but may be mostly electric. Advanced system studies indicate that some functions can be performed more efficiently using pneumatics and hydraulics.

- o The installation will allow operation to 15,240 m (50,000 ft) altitude.
- o Initial cost and material are based on a 500-unit production run. APU life is based on 20,000 hours.
- o The installed weight of the APU will be twice that of the APU weight. The penalty of transporting this weight will be a composite of current airframe values; 0.063 liter of fuel per flight hour per kg of equipment weight (0.00755 gal/hr/lb).
- o Spare parts will be procured at a rate of 30 percent of initial parts. Associated labor rates and burden rates will be based on 1985 negotiated rates.
- o Fuel costs will be based on the duty cycle with the assumption that the APU is used one hour per aircraft flight hour (3000 hours/year).

5.1.6 Trade Factors

Engine configurations were evaluated on the basis of the fuel prices selected for this study.*

The investment and maintenance factors are strongly related (inversely) to engine complexity. The influence of engine

*Low Fuel Price: \$0.264/liter (\$1/gal)

High Fuel Price: \$0.528/liter (\$2/gal)

complexity can also be seen in the weight factor (either positive or negative) and typically has only a secondary effect.

The cost of fuel has a strong influence on the overall cost of ownership through both the fuel and weight factors. It dictates emphasis on SFC and on the cost of transporting the weight of the APU.

The trade factor values are given in Table 36 and typify the influence of a 1 percent increase in cost of these factors on the final cost-of-ownership summation.

TABLE 36. APU TRADE FACTORS

	\$0.264/liter (\$1/gal) (Percent)	\$0.528/liter (\$2/gal) (Percent)
Δ DOC/1% Δ Engine Cost	0.135	0.08
Δ DOC/1% Δ Maintenance	0.20	0.13
Δ DOC/1% Δ Fuel Burn	0.55	0.66
Δ DOC/1% Δ Weight	0.10	0.12

As these factors indicate, the fuel and weight factors show a direct relationship to the cost of fuel.

5.2 Engine Configuration and Cycle Evaluation

The cycle/configuration studies for the APU application considered a range of potential combinations of turbine rotor inlet temperatures (TRIT), cycle pressure ratios (CPR), component type,

numbers, and efficiencies, rotor speeds, materials, cooling flows, pressure drops, and leakages as projected for the year 2000. From the engine configurations considered, the two best cycles were selected for evaluation in Task III on the basis of design point specific fuel consumption (SFC) and, subsequently, direct operational cost (DOC). The DOC improvements were estimated through the trade factors established in Task I that relate changes in DOC in terms of changes in fuel consumption, weight, maintenance costs, and initial investment costs. (Parameters are relative to the 1985 reference engine.)

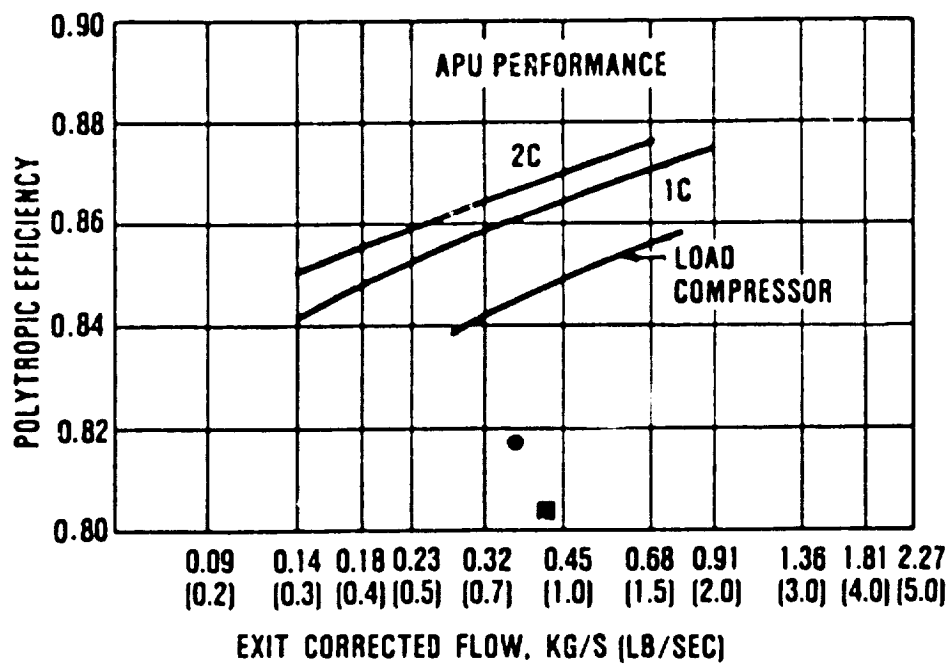
5.2.1 Technology Projections, APU

Technologies have been identified in three major areas: materials, aerodynamics, and mechanical improvements. These technologies impact the cycle study in terms of efficiency levels, turbine inlet temperature limits, and cooling flow requirements, as well as turbine stage count and hub speed limits. Many of the technologies assumed for the APU are the same as previously reported for the rotorcraft in paragraph 2.2.1. Common technologies include materials technologies and resulting mechanical limits.

5.2.1.1 Compressor (Centrifugal) Technology

The projection of efficiency capability of centrifugal compressors in the year 2000 are shown in Figure 131.

The designation 1C refers to a single-stage centrifugal design. Designation 2C refers to a two-stage design. The projection for a load compressor is also shown, but it has been compromised by additional losses in the scroll (1.4 percent) and by the use of variable inlet guide vanes (VIGV) (4 percent).



65-281-75

Figure 131. Projected Centrifugal Compressor Efficiency.

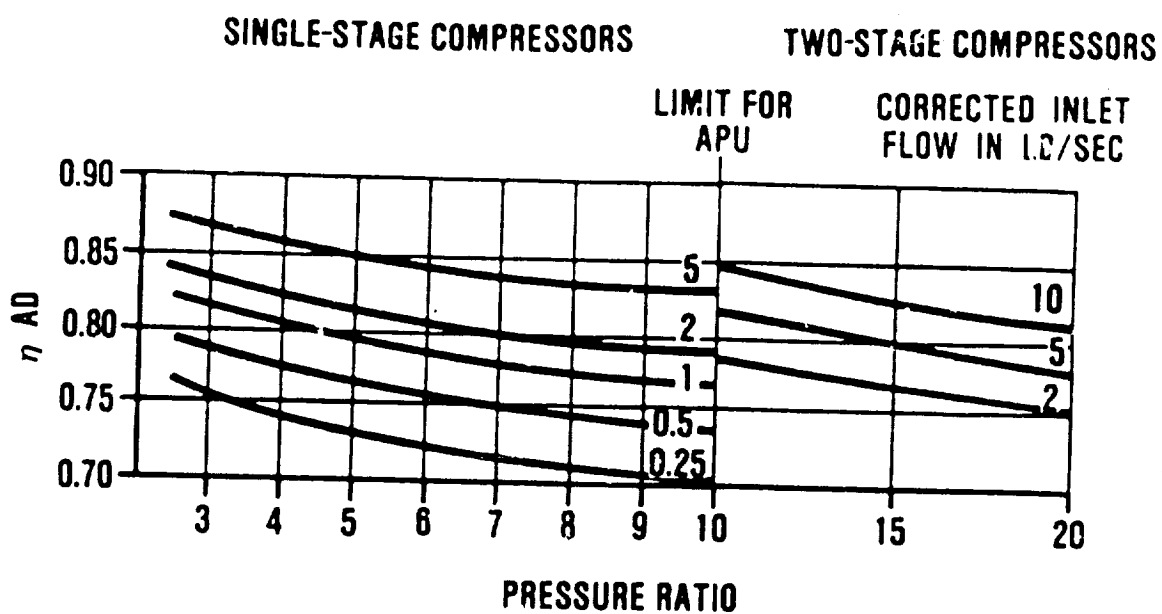
Design criteria used in APU compressors reflect the wide load variability seen in most applications. Therefore, a greater surge margin (over 10 percent) has been assumed. Furthermore, since volume is normally not critical in the selection of an installation, diffusion to an exit Mach number of 0.15 has been used. Similar clearance factors (3 percent of the flow-path width) have been used for APUs, rotorcraft, and commuter engines.

As a further restriction on centrifugal compressor performance, the small through-flow on gas turbines in this power class requires that the pressure rise in a single-stage unit be limited to 10:1 (as shown on Figure 132) to be consistent with efficiencies as shown. The technology projections will be applied to the future designs of this study. However, the projected manufacturing problems associated with producing high-speed rotating components (with acceptable precision and cost) and the operational aspects of maintaining the clearances and surface finishes required to maintain the projected efficiency levels preclude the use of these designs at pressure ratios above 10:1 and at flows below 0.9 kg/s (2 lb/sec).

Turbine Technology

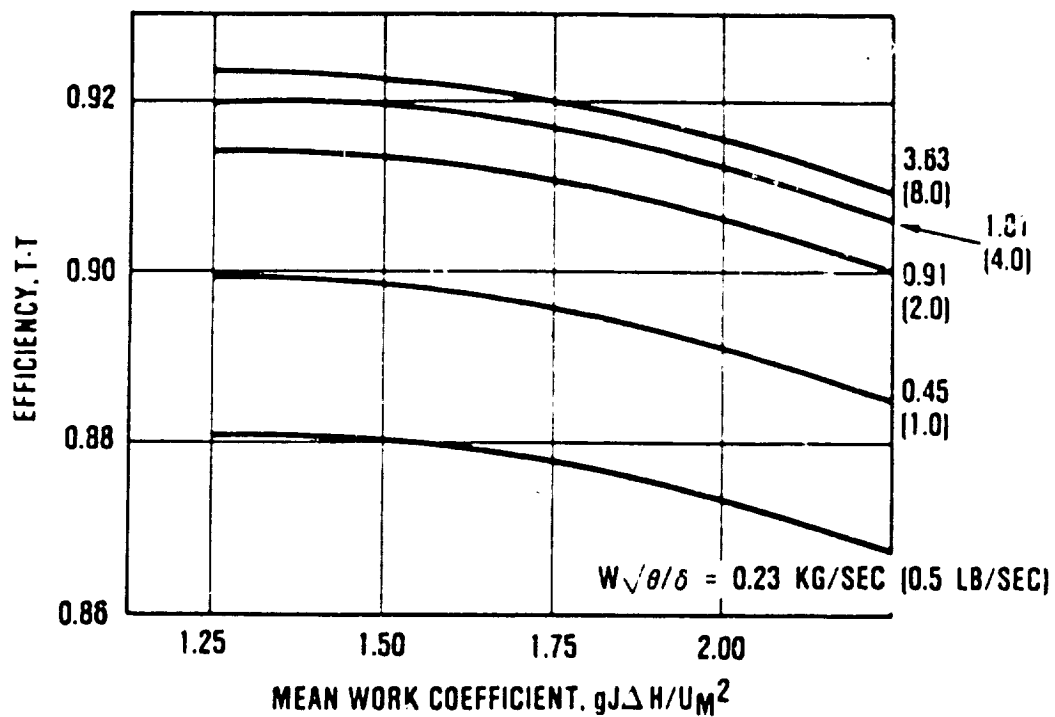
The projection of efficiency in axial turbine stages is shown on Figures 133 and 134.

The metallic "type" geometry assumption is defined as the manufacturing capability of fabricating blades with unrestricted airfoil shapes, similar to current metal airfoils. A minimum blade height of 1 cm (0.4 in.) was set for inserted blades. A 480 m/s (1575 ft/sec) hub speed was also projected as limiting for an inserted blade design turbine wheel.



65-281-17

Figure 132. Projected Centrifugal Compressor Efficiencies.

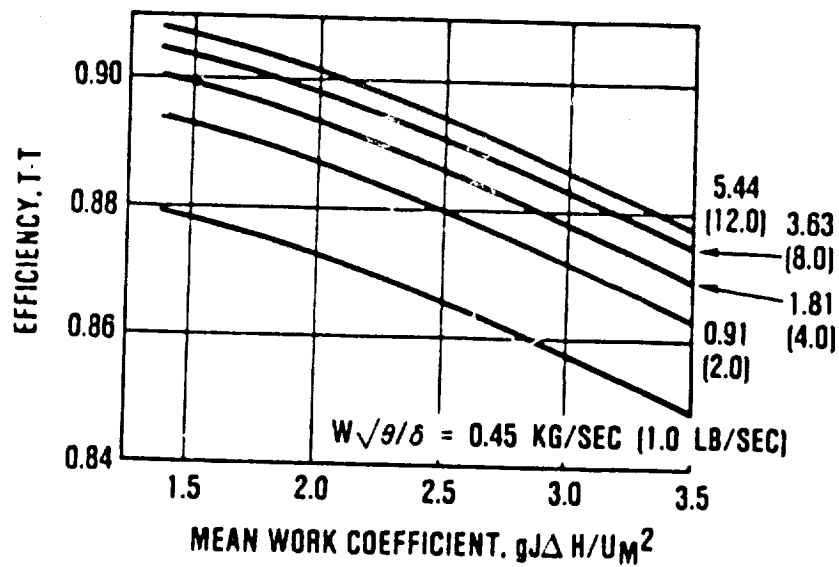


ASSUMPTIONS:

- 1) "METALLIC TYPE" GEOMETRY
- 2) UNSHROUDED BLADE
- 3) 2 PERCENT TIP CLEARANCE
- 4) UNCOOLED

65-281-19

Figure 133. Projected Efficiency for High-Pressure Axial Turbine Stage.



ASSUMPTIONS:

- 1) "METALLIC TYPE" GEOMETRY
- 2) UNSHROUDED BLADE
- 3) 2 PERCENT TIP CLEARANCE
- 4) UNCOOLED

65-281-20

Figure 134. Projected Efficiency for Low-Pressure Axial Turbine Stage.

The projection for efficiency of radial inflow turbine wheels is shown on Figure 135.

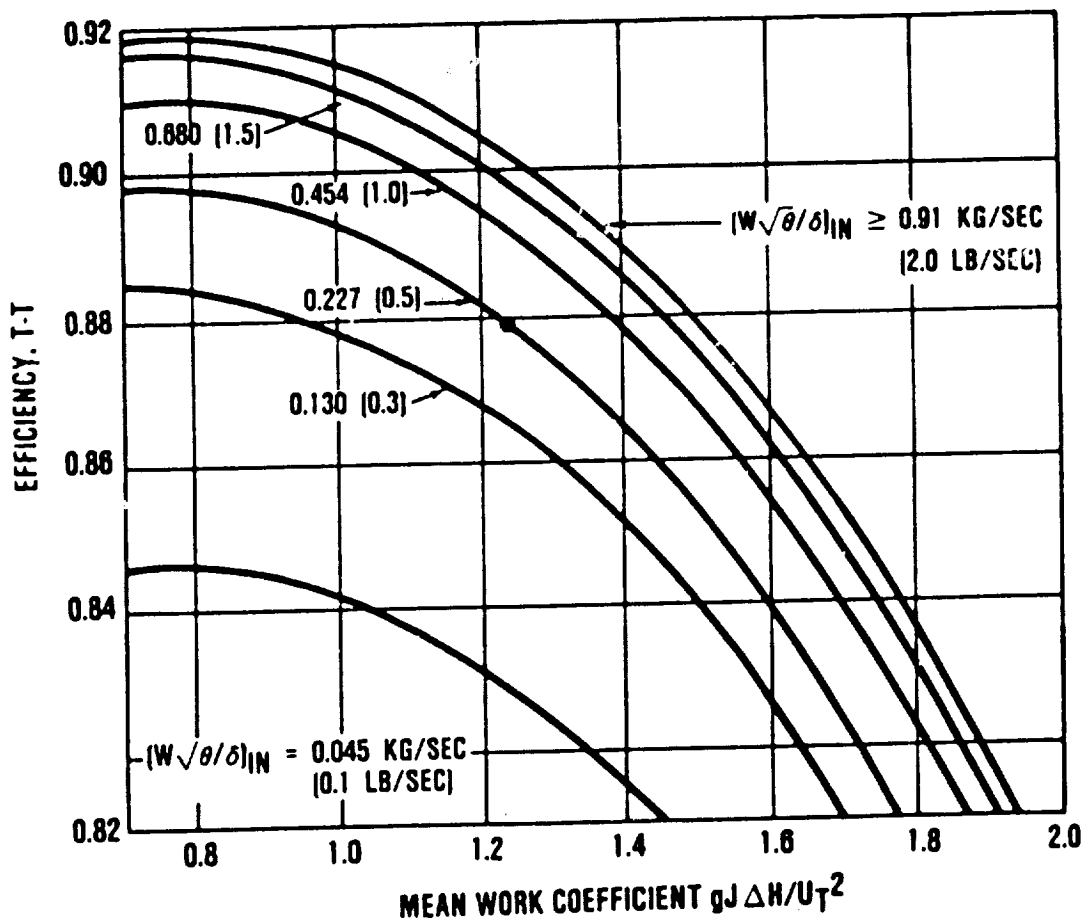
The turbine tip speed on these ceramic radial-inflow turbines was limited to 914.4 m/s (3000 ft/sec). As discussed in the materials projections section (paragraph 2.2.1), the average inlet temperature for uncooled ceramics or ceramic composites was limited to 1371 to 1427C (2500 to 2600F), dependent on combustor pattern factor and application. The usable life of the APU was assumed to be 20,000 hours. The maintenance cost factor included in the study provides for replacement of components that are life-limited short of the APU life. NASA/DOE has sponsored a Ceramic Durability Program (Contract DEN3-27) since 1978 with the objective of determining specimen strength deterioration under thermal cycling conditions that simulate their use in a gas turbine engine. This program has demonstrated that some ceramic materials such as silicon carbide have no significant loss of flexure strength after 3500 hours of thermal cycling (17,500 cycles) between 1371C (2500F) and 204C (400F). Therefore, normal concepts of fatigue life that are typical in metals are not present in these ceramic materials. However, experience with ceramic components is limited.

Combustor Technology

Combustor improvements projected for the year 2000 are shown in Figure 136. Discussion of these technologies is found in paragraph 2.2.1 under the rotorcraft application.

5.2.2 APU Cycle/Configuration Studies

Engine Cycle Studies - The engine cycles shown in Figure 137 were studied as applicable to the duty cycle called out in paragraph 5.1.2.

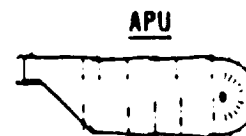


65-281-76

● REFERENCE ENGINE DESIGN POINT EFFICIENCY

Figure 135. Projected Radial Inflow Turbine Efficiency in Year 2000.

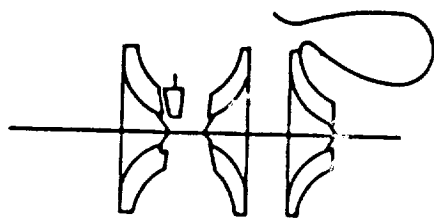
ENGINE PARAMETER	REFERENCE ENGINE APU	YEAR-2000 APU
COMPRESSOR EXIT M_N	0.15	0.15
COMBUSTOR $\Delta P/P$	4.0%	4.0%
COMBUSTOR η	0.998	0.998



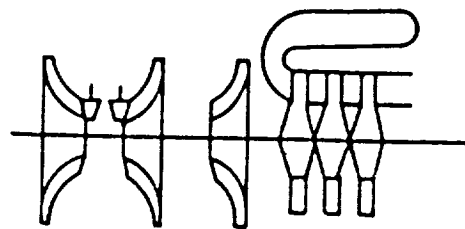
- CYCLE PARAMETERS REMAIN THE SAME
- ADDITIONAL TECHNOLOGY IMPROVEMENTS
 - REDUCED SIZE
 - INCREASED DURABILITY

GS-281-13

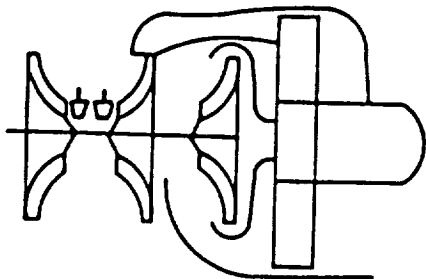
Figure 136. Projected Annular Combustor Performance in Year 2000.



SIMPLE

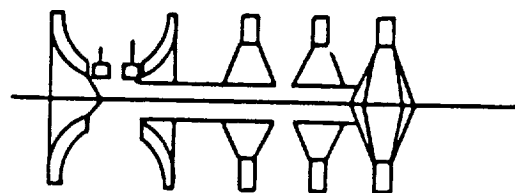


**SIMPLE WITH MULTIPLE-STAGE
COMPONENTS AND VARIABLE GEOMETRY**



REGENERATED

GS-281-26



FREE POWER TURBINE

Figure 137. APU Cycles Investigated in the SECT Study.

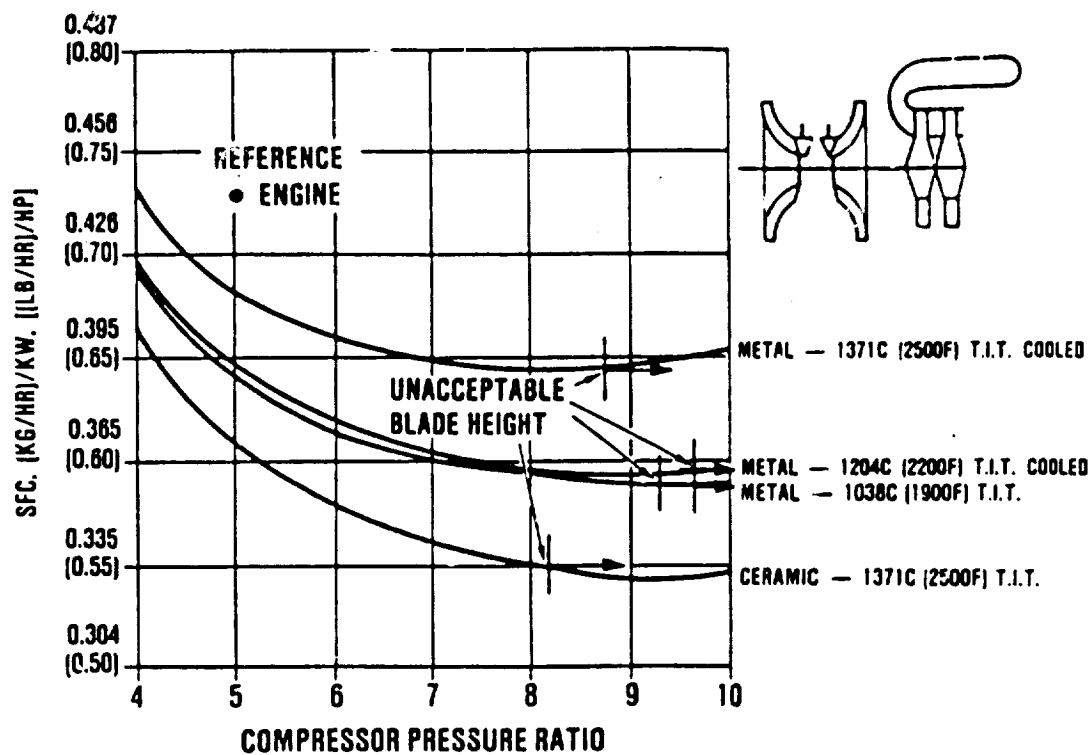
Each engine was evaluated on the basis of the cycle pressure ratio that generated the minimum fuel consumption at the design point (maximum power on a sea-level, 38C [101F] day), using the turbine inlet temperatures as limited by material projections. The cycle analyses of simple-cycle engines using axial turbine wheels are shown on Figure 138. Pertinent points demonstrated by these data include:

- o Optimum pressure ratios occur at less than 10:1; therefore, only one stage of compression is necessary.
- o Uncooled metal turbines at 1038C (1900F) produce SFCs lower than the cooled metallic stages at higher temperatures, due to cooling flow penalties.
- o Best SFC produced by ceramic inserted turbine blade, running at 1371C (2500F) (ceramic limiting temperature).
- o Blade height limitation of 1 cm (0.4 in.) could affect the operation before optimum pressure ratios are reached.

The free power turbine design with axial components was evaluated and the results are shown in Figure 139. Significant factors apparent from this data are as follows:

- o Blade height limit restricts this free turbine design to approximately 6.5:1 pressure ratio.
- o The free turbine cycle SFC is better than any of the single-shaft axial turbine cycles.

Figure 139 also shows a simple-cycle engine with a radial inflow turbine evaluated at three different pressure ratios. The SFC from these units is better than the axial turbine designs.



06-281-05

Figure 138. APU Simple Cycles Using Axial Turbine Wheels.

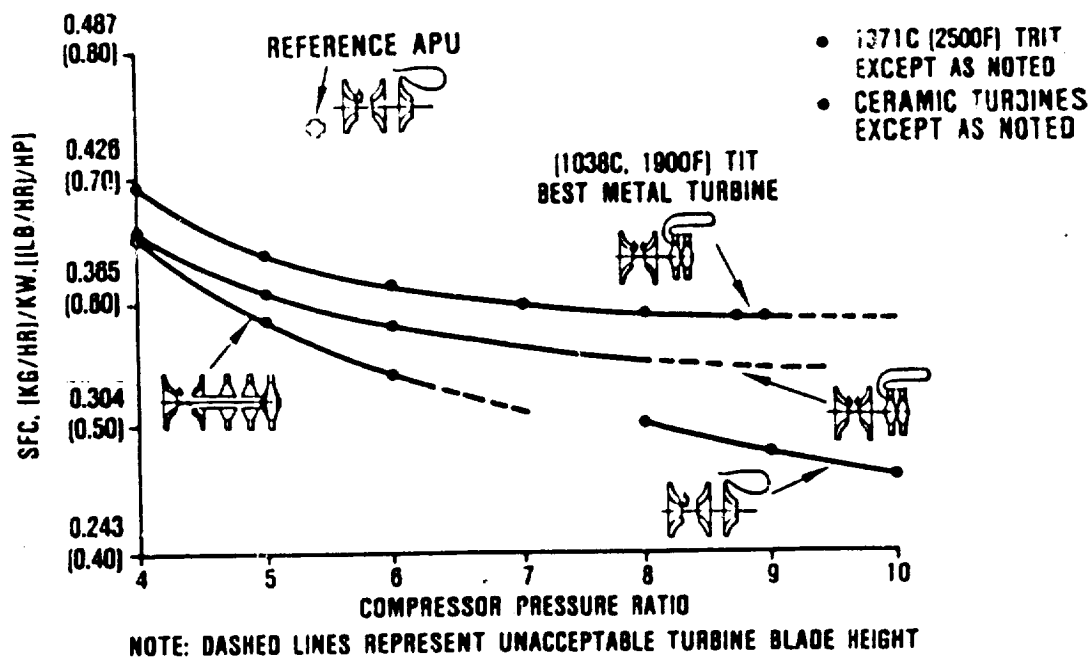


Figure 139. APU Cycle Performance Results.

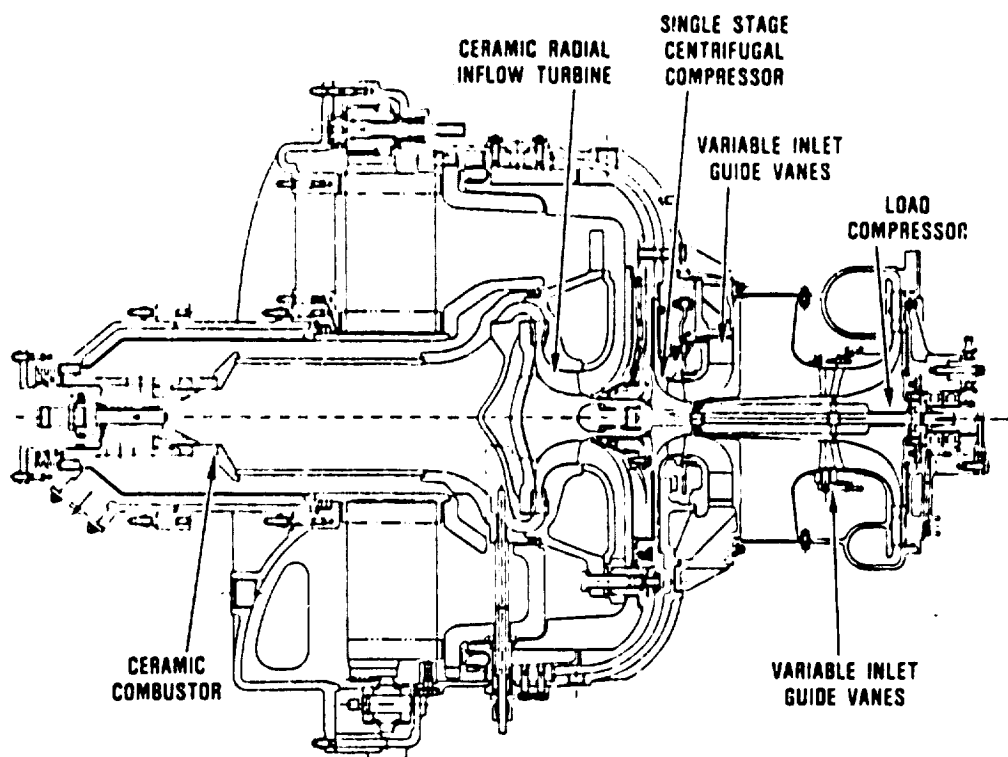
A scaled version of the GTEC AGT101 engine was also evaluated. A schematic of that engine is shown in Figure 140. Figure 141 shows the projected performance of a regenerated engine scaled from the AGT101.

The performance of this engine is shown with two control methods to achieve part power. The variable inlet guide vanes are effective in maintaining part-load SFC by reducing engine through-flow. The loss in aerodynamic efficiency in the compressor and turbine is compensated by the increased effectiveness in the regenerator. The traditional control method of reducing turbine inlet temperature to reduce power output results in a significant increase in SFC. As an example, at the 65 percent power point (point 2C in the duty cycle, Table 33, which is used 57.6 percent of the time), the SFC is 25 percent higher for the reduced temperature point (Figure 141), as compared to the engine with constant TRIT. Based on these results, the regenerated cycle represents a definite advantage in fuel consumption over all other cycles studied.

Engine Cost Studies - Acquisition costs were estimated for the auxiliary power units studied. The basis for these estimates was similarity to existing metallic production components, with factors applied for complexity, machining cost multipliers, number of parts, material costs, and requirements for close tolerances or running clearances. Ceramic component costs were scaled from current experience and projections on the AGT101 engine program. The results of this analysis are shown on Figure 142.

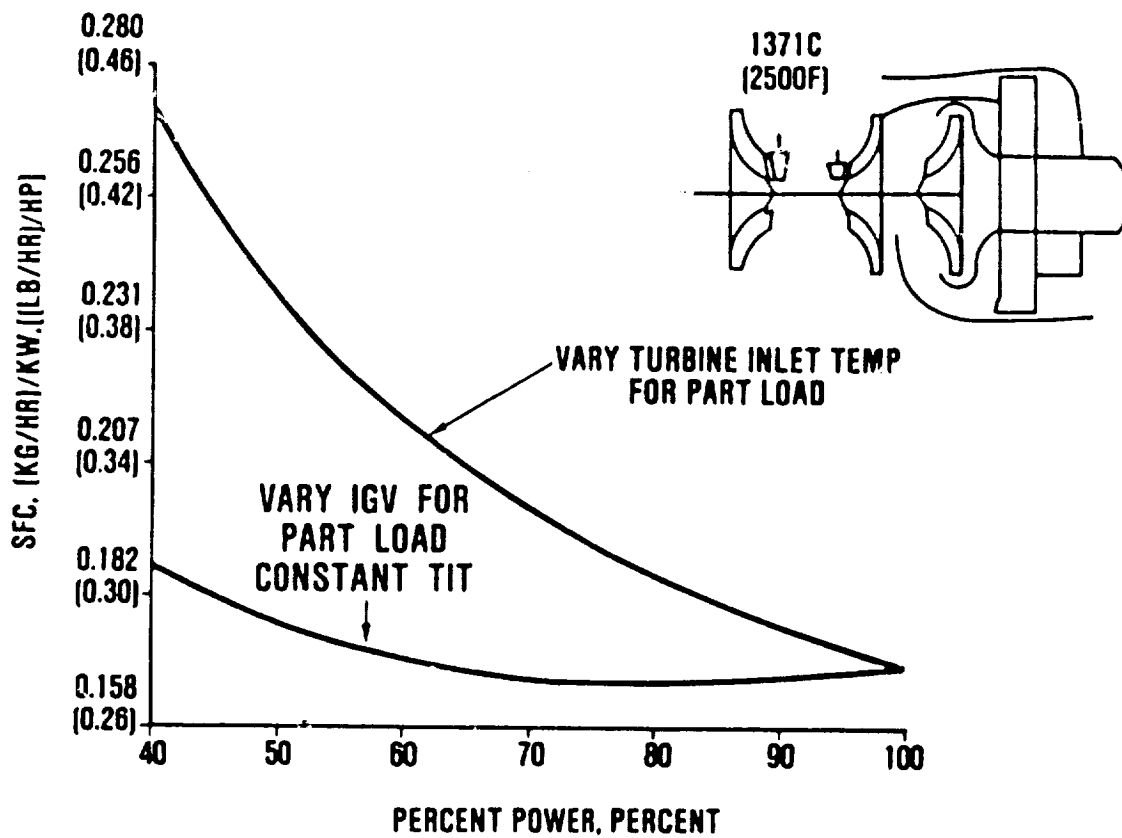
Engine Weight Studies - Weight estimates were completed for all configurations using similar techniques. Scaling of components provided most of the hard data. The ceramic AGT101 components were scaled. The weights used in this study are conservative from the standpoint that projected weight reductions for airborne

ORIGINAL PAGE IS
OF POOR QUALITY



65-281-23

Figure 140. AGT101 Regenerated Engine Cross Section.



85-281-97

Figure 141. Projected Performance for APU Based on Scaled AGT101.

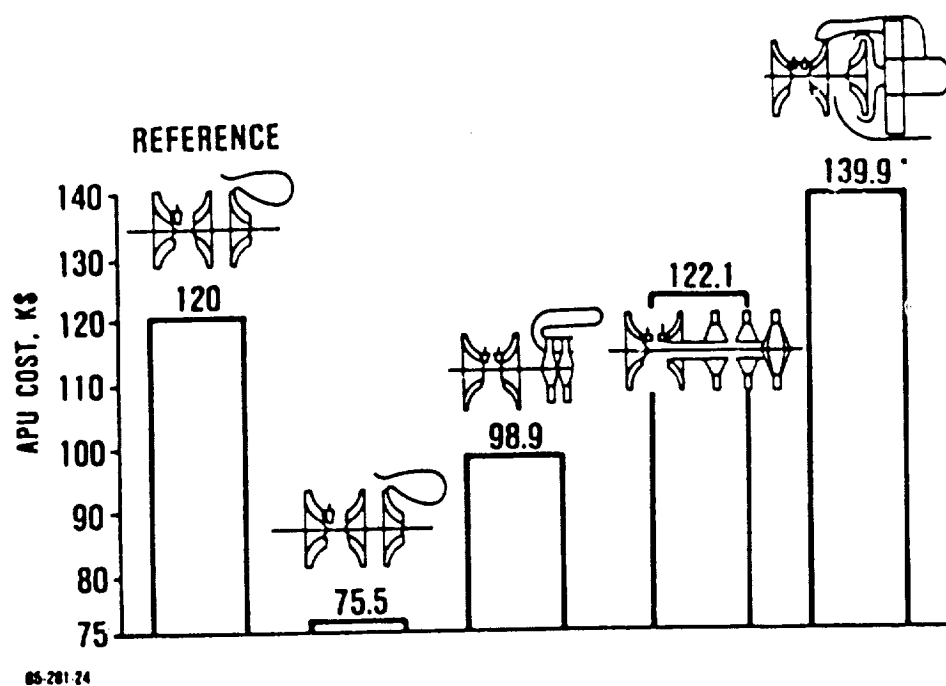


Figure 142. APU Cost Comparison.

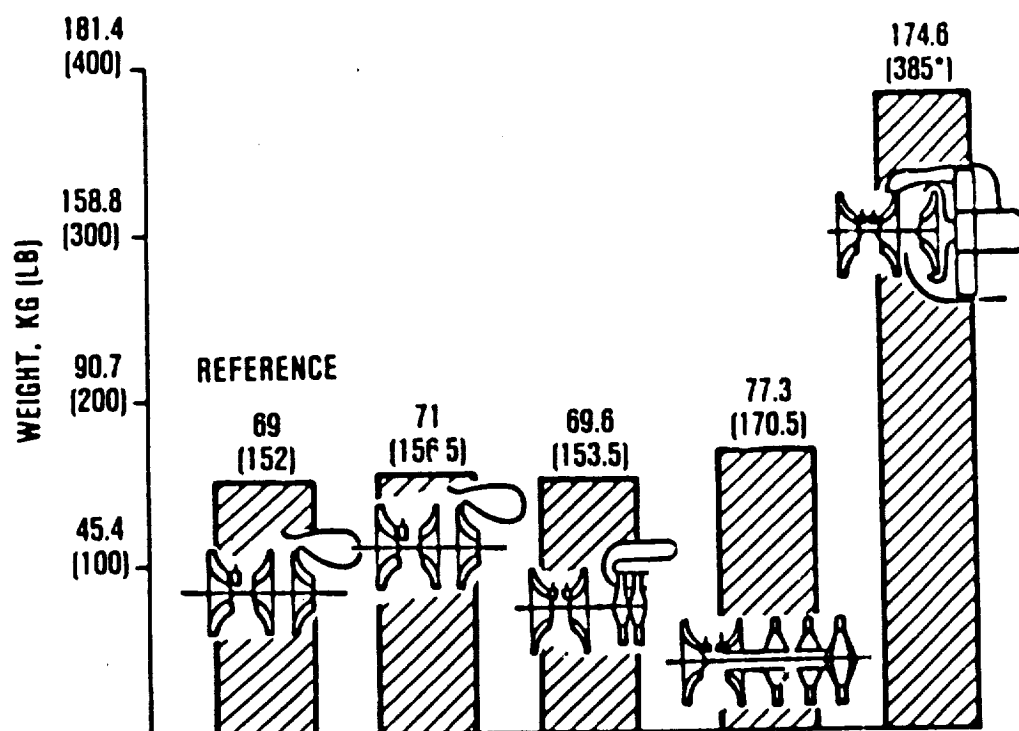
equipment have not been introduced. Moreover, the design concepts for brittle materials are still being developed; thus the actual production weights of a scaled AGT101 or a simple-cycle engine with a ceramic turbine/combustor section may be somewhat lower than those estimated for this study. The estimated APU weights are presented in Figure 143.

5.2.3 Cycle/Engine Selection

Using the previous data in the economic model discussed in paragraph 5.1.5 resulted in the DOC shown in Figure 144. The composite data represents a family of engines on each line that have been optimized at the pressure ratios shown. A simplified engine schematic is assigned to each line to show the cycles studied. All engines, with the exception of the reference (at 1900F) and the metallic turbine (at 2200F) use ceramic turbine stages operating at 2500F TRIT. The direct operating cost, in dollars per hour, is shown with fuel costs of \$1 and \$2 per gallon. The auxiliary power systems shown are restricted by all of the study limitations, such as: blade height, turbine tip speed, turbine inlet temperature, costs, fuel consumption, manufacturing capability, and maximum pressure ratio in a single-stage compressor, etc.

From these analyses, the lowest DOC units were the simple-cycle radial component engine and the regenerated design. Therefore, these two cycles were selected for detailed off-design analyses in the following study tasks.

The simple-cycle engine uses a single-stage centrifugal compressor at a pressure ratio of 8:1, a reverse-flow annular burner, and a radial inflow turbine running at 1371C (2500F). The description of this cycle is found in Table 37. This cycle is selected because it demonstrates the lowest DOC of the simple-



*REGENERATOR CORE WEIGHT = 17.7 KG (39 LB)

85-281-70

NOTE: APU WEIGHTS ESTIMATED AT MINIMUM SFC

Figure 143. APU Weight Comparison.

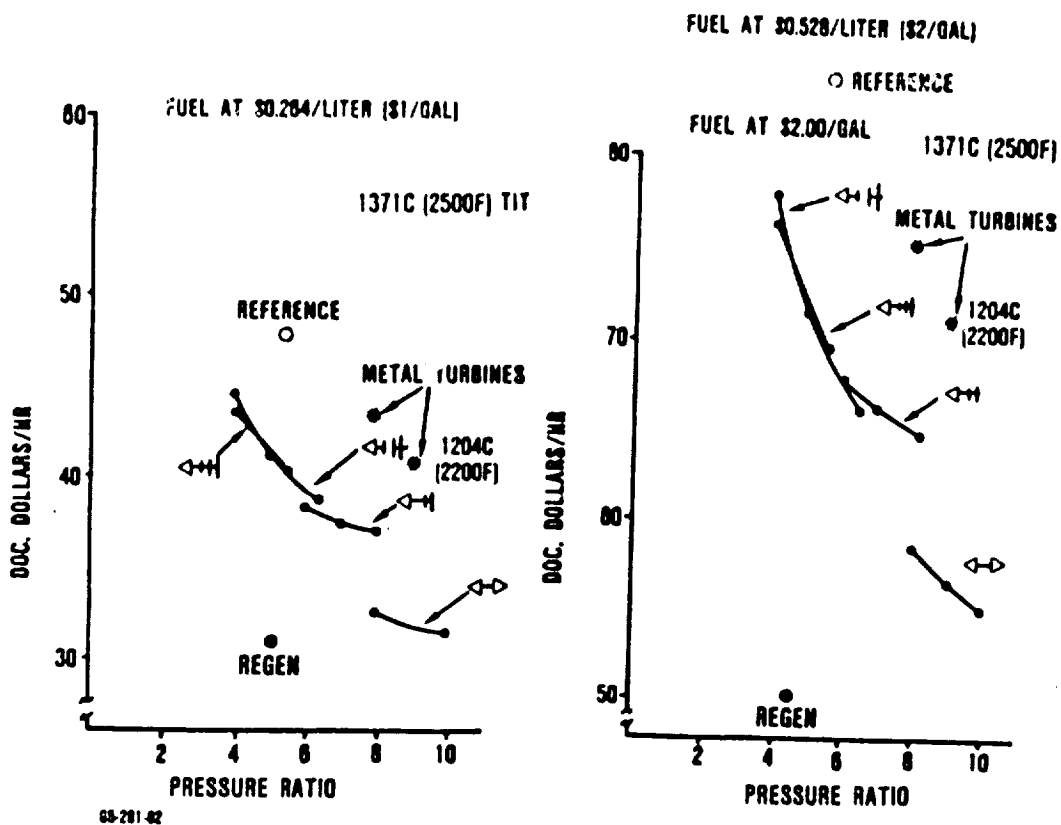


Figure 144. APU DOC Comparison.

TABLE 37. SECT SIMPLE-CYCLE APU DESIGN POINT PERFORMANCE*,
SEA-LEVEL, STATIC, ISA, MAX, UNINSTALLED

Overall Engine Performance		Component Performance	
		<u>Compressor</u>	
Engine Rating, kW (shp)	312 (419)	o W/θ/δ, kg/s (lb/sec)	0.85 (1.87)
SFC, (kg/hr)/kW, (lb/hr)/hp	0.305 (0.502)	o PR	8.03
Turbine Inlet Temp, C (F)	1371 (2500)	o η _{AD} , %	78.5
Overall Cycle PR	7.99	o η _{poly} , %	83.7
Inlet W/θ/δ, kg/s (lb/sec)	0.84 (1.86)	o Exit corrected flow, kg/s (lb/sec)	0.146 (0.322)
Spool Speed, rad/s (rpm)	11,063 (105,642)	<u>Combustor</u>	
Fuel, LHV, kJ/kg (Btu/lb)	42,798 (18,400)	o η, %	99.5
		o ΔP/P, %	4.0
		<u>Turbine</u>	
		o W/θ/δ, kg/s (lb/sec)	0.264 (0.582)
		o η _{AD} , %	87.8
		o $\frac{\Delta H}{U^2}$	1.19
		o Cooling Flow, %	0
		<u>Load Compressor</u>	
		o W/θ/δ, kg/s (lb/sec)	1.13 (2.50)
		o PR	3.40
		o η _{AD} , %	76.9
		o η _{poly} , %	81.4
		o Exit corrected flow, kg/s (lb/sec)	0.415 (0.915)

*No margins

cycle engines, and if fuel costs continue at or below these current levels, the configuration would be chosen for the application. Although an engine at a pressure ratio of 10 shows a lower DOC, further analysis of compressor technology, risks, and costs concluded that a pressure ratio of 10 was not feasible for year 2000 for the efficiency level quoted for the small flows (0.85 kg/s [1.87 lb/sec]). Therefore, the pressure ratio of 8 was selected.

The regenerated engine uses a single-stage centrifugal compressor stage at approximately a 5:1 pressure ratio, a single-can combustor, and a radial inflow turbine with a 1371C (2500F) inlet temperature. The regenerator effectiveness was 94.8 percent; the leakage was 3 percent.

5.3 Task III System Performance Evaluation

5.3.1 Duty Cycle Analysis

Further optimization of the cycle pressure ratio, operational speed, and other cycle parameters to "fine tune" the two engines to function with maximum efficiency during the specified duty cycle was accomplished. The description of the overall engine and component performance is shown in Tables 37 and 38 for the simple cycle and the regenerated cycles.

A preliminary analysis on a large number of engines was completed considering design point fuel consumption as a selection criteria. Since the study had now been reduced to the two cycles, the complete duty cycle fuel consumption was calculated.

As a further investigation, the use of variable geometry on the power section compressor of the simple-cycle configuration was analyzed. The results at part-load indicated that the efficiency penalties in the aerodynamic components (due to the

TABLE 38. SECT REGENERATED APU DESIGN POINT PERFORMANCE*,
SEA-LEVEL, STATIC, ISA, MAX UNINSTALLED

Overall Engine Performance		Component Performance	
		<u>Compressor</u>	
Engine Rating, kW (shp)	315 (423)	o W/θ/δ, kg/s (lb/sec)	1.06 (2.33)
SFC, (kg/hr)/kW, (lb/hr)/hp	0.170 (0.279)	o PR	5.16
		o η_{AD} , %	82.1
		o η_{poly} , %	85.7
Turbine Inlet Temp, C (F)	1371 (2500)	o Exit corrected flow, kg/s (lb/sec)	0.266 (0.587)
Overall Cycle PR	5.12	<u>Combustor</u>	
Inlet W/θ/δ, kg/s (lb/sec)	1.05 (2.31)	o η , %	99.5
		o $\Delta P/P$, %	4.0
Spool Speed, rad/s (rpm)	7,104 (67,836)	<u>Turbine</u>	
Fuel, LHV, kJ/kg (Btu/lb)	42,798 (18,400)	o W/θ/δ, kg/s (lb/sec)	0.498 (1.097)
		o η_{AD} , %	87.4
		o $\frac{\Delta H}{U^2}$	0.94
		o Cooling Flow, %	0
		<u>Load Compressor</u>	
		o W/θ/δ, kg/s (lb/sec)	1.13 (2.50)
		o PR	3.40
		o η_{AD} , %	76.9
		o η_{poly} , %	81.4
		o Exit corrected flow, kg/s (lb/sec)	0.415 (0.915)

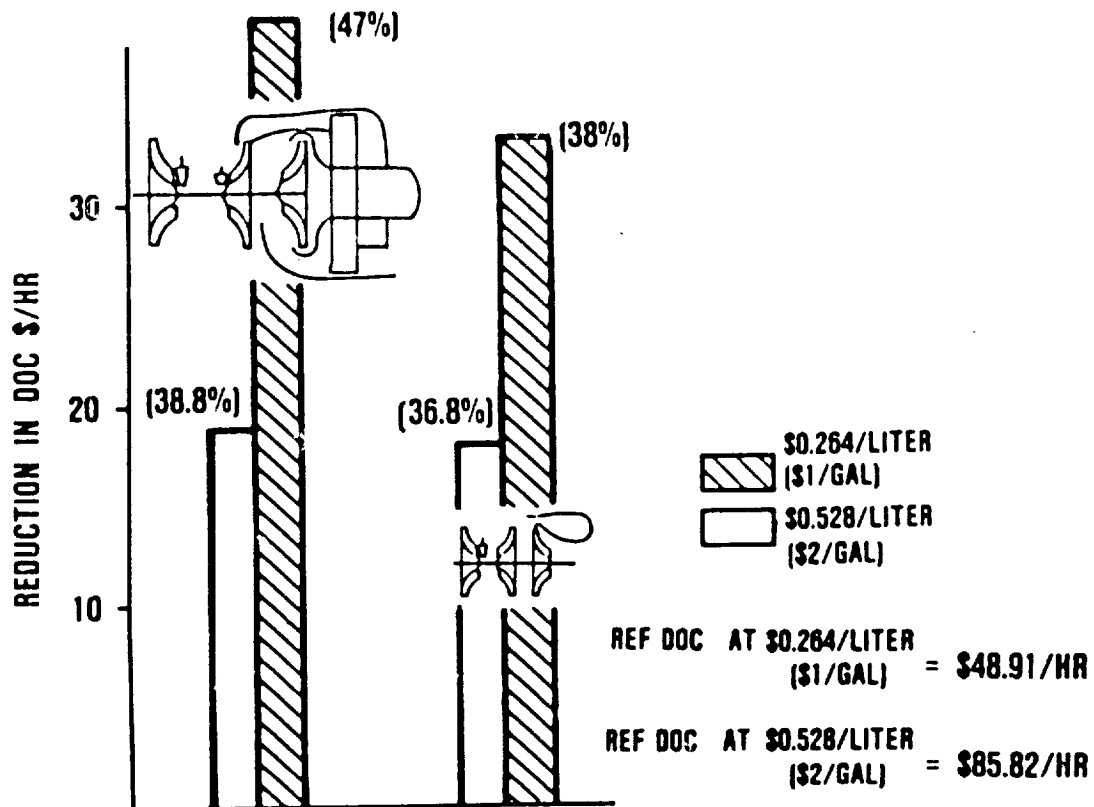
*No margins

reduced flow) produced a fuel consumption that was not significantly improved over the conventional temperature reduction control concept. Therefore, the simple-cycle engine final design did not include variable guide vanes on the compressor.

The regenerated cycle showed definite improved part-load fuel consumption with variable guide vanes, so this cycle was evaluated using this control concept. The load compressor for this system must also include variable guide vanes to shut off bleed flow when it is not required by the duty cycle. Furthermore, a significant reduction in fuel consumption is achieved by aerodynamic improvements in the guide vanes, impeller, and diffuser that will allow complete termination of bleed flow and its shaft power extraction when called for in the duty cycle. (Current systems dump compressed air to avoid surge and stall problems).

The SFC reduction (as shown in Figure 139) can result in significant cost savings for an operator. For example, comparing the reference engine to an advanced simple-cycle (centrifugal compressor and radial inflow turbine with SFC of 0.5 lb/hp/hr average) APU operating 3000 hours per year, results in a fuel savings of more than 44,800 gallons. This is a savings of \$44,800 at \$1 gallon, or \$89,600 at \$2 gallon, per engine per year, or a fleet fuel savings of approximately \$150 to \$300 million over approximately seven years.

A detailed review of initial cost, maintenance cost, and weight was accomplished on both competitive cycles. In addition, the reference engine described in paragraph 5.1.3 was analyzed for fuel consumption for the entire duty cycle. The results of these analyses are presented on Figure 145. The regenerated cycle, when compared to the reference engine, can save the operator over 47 percent (\$40.30 per hour) of the DOC when fuel prices are \$0.528/liter (\$2/gal). The simple cycle can save 38 percent (\$32.60 per hour) under similar conditions.



85-281-27

Figure 145. Reduction in DOC for Selected APU Cycles.

5.4 Small Engine Component Technology Plan

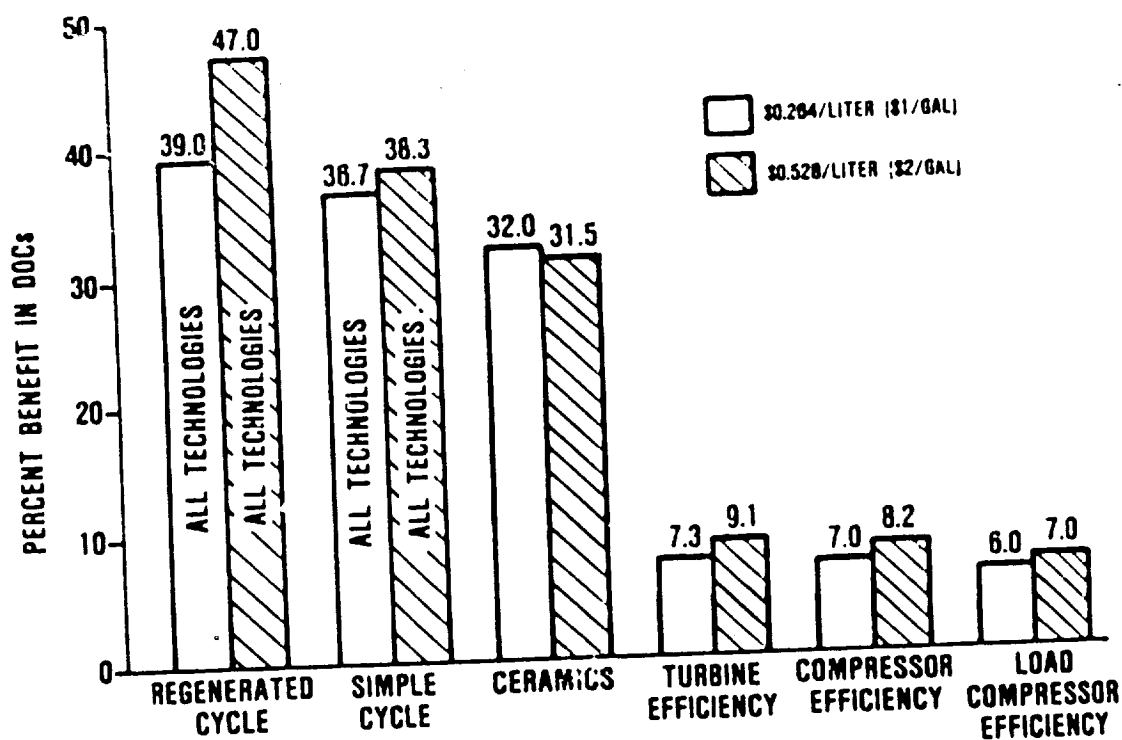
As a result of the analytical effort of this study, it is apparent that in order to provide improved performance from airborne power units, a number of technologies must be addressed, and design data must be generated and verified. For example, several approaches to improved aerodynamic efficiency are worthy of investigation. In addition to the creation of component designs that are less sensitive to rotating clearances, the problem of clearance control for small engines must be investigated through more refined shaft dynamic analyses, thermal analyses, dynamic effects on materials, abradable shrouds, boundary layer control, more precise bearings, and static structural systems.

5.4.1 Advanced Technology Benefits

The benefits to be derived from technology are discussed in the following paragraphs and are shown in Figures 146 and 147. These figures show the relative contribution of each technology to the "all-technology" payoff for the simple-cycle engine.

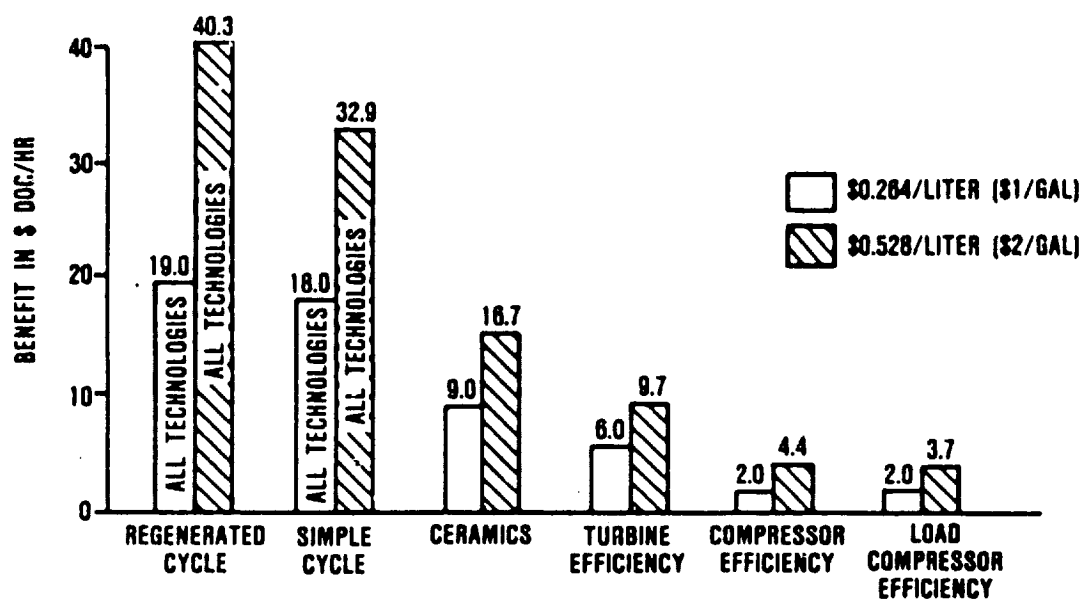
This study for APUs shows that the largest payoffs can be obtained by establishing ceramic materials technologies for inclusion in radial inflow turbine stages (Figures 146 and 147). The capability of these materials to survive exposure to high-temperature gas streams for long durations makes them ideal for use in small radial inflow gas turbines, where conventional cooling techniques are difficult, ineffective, and costly. Silicon nitride and silicon carbide ceramic materials can be used in high-temperature applications at 1371C (2500F). This average temperature can be achieved with a well controlled combustion process with a maximum hot spot of 1538C (2800F).

The ceramic radial inflow turbine wheel represents a major improvement in component performance. The lower density (approximately one-third that of current superalloys) and the strength



65-221-136

Figure 146. DOC Benefits from APU Technologies.



05-281-144

Figure 147. APU Technology Benefit Comparison in DOC Per Hour.

and oxidation resistance demonstrated by the materials at elevated temperatures make them ideal for application in small gas turbine engines.

In order to incorporate the ceramic turbine wheel, the simultaneous verification of ceramic static structures that will experience a similar environment will also be required. Although the mechanical stresses on these parts are minimal, the thermal stresses and metal/ceramic interface must be addressed.

The application of a reverse-flow annular combustor provides a producible envelope for an APU using a radial-inflow turbine design. In order to maintain the required pattern factor, multiple nozzles with closely matched flows will be required. Atomization and good mixing in narrow passages, as well as light-off and stability, must be carefully considered. The requirement for operation to 15,240 m (50,000 ft) altitude will also dictate close installation coordination with the airframe manufacturer to provide in-flight emergency use.

The program to improve turbine efficiency in this small flow class will be directed to allow increased tip speed, lower incidence penalties, and improved stator design to provide more uniform inlet flows.

Significant improvements are also projected for centrifugal compressor stages up to an 8:1 pressure rise. Many of the techniques discussed for the rotorcraft and commuter engines of this study, particularly the designs that will minimize rotating clearance effects, will be applicable to APUs. Improved diffusion and minimized turning losses will also contribute to the projected improvements.

The load compressor technology is also important. A 3.5-point increase in efficiency is projected through the improved impeller performance, use of variable geometry (inlet guide vanes and possibly a variable diffuser), and a design that will allow discharge flow near zero.

The use of gas-lubricated foil bearings capable of operating in the hot environment are not absolutely necessary but will contribute greatly to the reliability, maintainability, and operator's satisfaction in the use of the APU. Problems associated with coking of the oil and bearing cooling requirements can be eliminated by the use of foil bearings.

Technologies such as the cold-end material programs and the high-pressure seals will also contribute to the advantages of the year-2000 APU over current production units.

As shown in the DOC projections (Figure 146), the regenerated cycle for this application has the lowest DOC. As expected, the regenerated cycle demonstrated greater advantages in DOC as fuel price increased.

Since the ceramic materials considered for use in the year 2000 are not subject to normal fatigue-type failures, long lives can be predicted for these components. Therefore, the hot section of the engine (all ceramic) can be run at maximum temperature continuously with the flow varied to match the required power output. Variable inlet guide vanes performance can provide this function. The loss in performance of the aerodynamic components at part speed is compensated for by the increased heat transfer of the regenerator over the part-power range of interest in this application. SFC is reduced dramatically at lower powers, as shown in Figure 141. This results in a regenerator DOC benefit of 2.3 percent at \$1/gal and 8.770 at \$2/gal fuel cost.

5.4.2 Technology Plan

GTEC's recommended plan for small engine component technologies for year-2000 APUs is presented in this section. This plan addresses seven technologies in keeping with the technology benefits presented in paragraph 5.4.1. The technology categories are tabulated below, along with their respective paragraph numbers.

- 5.4.2.1 Ceramics
- 5.4.2.2 Regenerated Engine Technologies
- 5.4.2.3 Radial Turbine Performance
- 5.4.2.4 Combustor Technologies
- 5.4.2.5 Compressor (Centrifugal) Performance
- 5.4.2.6 Materials for "Cold" Parts
- 5.4.2.7 System Technologies

5.4.2.1 Ceramics

This section presents the plan for ceramic technologies as applicable for year-2000 APUs. The plan consists of three discrete technology programs, one as previously discussed for the rotorcraft and commuter engines, and two new programs identified in Figure 148 as Programs CA and CB.

Ceramics for Combustors and Turbine Blades and Vanes - This technology program is discussed and scheduled for rotorcraft engines in paragraph 2.4.2.1, Technology Program B, and is also included in Figure 148 for completeness of APU planning. This program will advance the technologies required for APU ceramic combustors.

CA. Ceramic Radial Turbine Wheel Stator

A ceramic radial turbine wheel and a compatible stator will will result in uncooled operating capability with turbine inlet

temperatures up to 1371C (2500F). By eliminating the wheel and stator cooling requirements and operating at 1371C (2500F), significant improvement in SFC and power density can be achieved over current APUs. Additionally, because the candidate ceramic material, Si_3N_4 , is approximately one-third the density of superalloys typically used for turbines, some weight reduction can be realized. Finally, by eliminating the need for complex cooling schemes and fabrication approaches that would be required for metal turbine components, a potential for cost savings exists with the use of ceramic parts.

To satisfy the high strength requirements, the ceramic turbine wheel will be fabricated from sintered Si_3N_4 . Sintered Si_3N_4 has been developed for radial turbine rotor application at 1371C (2500F) TRIT in the Garrett/Ford AGT101 engine, but fabrication of larger turbine rotors for typical APU applications has not been demonstrated. Although sintered Si_3N_4 has demonstrated high strength (above 689 mPa [100 ksi] at room temperature in flexural testing), its long-life capability at high temperatures has not yet been fully evaluated. Material improvement, fabrication, and characterization are currently being performed under the NASA/DOE AGT101 program and the NASA/DOE Ceramic Initiative programs. Technology developed during those programs will provide the basis for this program.

The ceramic stator will be fabricated from either sintered Si_3N_4 or sintered SiC , both of which provide adequate strength at high temperature. The feasibility of these material systems and the fabrication technology for each were demonstrated during the AGT101 program. The best material for the stator application will be determined during the design phase of the program and will be based on transient stresses and peak steady-state operating temperatures.

Fiber-reinforced and particulate-dispersed ceramic composites are developing material systems that provide the potential for ceramics with improved toughness. These materials, which are being developed in both the Si_3N_4 and the SiC systems under NASA- and ORNL-managed programs, will provide options for rotor and stator material selection as they are developed.

The feasibility of composite ceramic axial rotors with solid hubs of large mass is proposed separately for rotorcraft and commuter engines (paragraph 2.4.2.1, Technology Program B) as a parallel technology program.

Program Description

This program consists of four major tasks, from material development through hot rig testing, as scheduled in Figure 148.

The initial activity will be to configure a turbine wheel and matching stator that are representative in size and shape to the SECT APU engine as conceptualized for the year 2000. These designs will be based on known property values of the candidate ceramic materials. Baseline material testing will also be performed to provide additional design data as required. Design of the adaptive hardware and the rotor attachment scheme will be connected as important facets to assure minimal stressing of ceramic components due to distortion and contact loading.

Ceramic component fabrication process development will emphasize the rotor development, addressing the size and volume influence, dimensional tolerances, and component material properties. Stator fabrication will be performed in parallel, but is anticipated to require significantly less effort due to existing capabilities.

As component fabrication progresses, rotor integrity will be assessed using visual, fluorescent-penetrant and ultrasonic NDE methods, spin testing, and cut-up evaluations. The goal of the fabrication development will be to provide rotors that will sustain spin-proof testing to at least 115 percent of the design speed. Stator screening will be based on thermal cyclic proof-testing to assure their capability of sustaining light-off transients. Rotor attachment testing will also be conducted. Radial rotor to metal shaft attachment methods are being developed in the ACT101 program. This technology will be adapted to the selected configuration as required for this program.

Final parts will be fabricated for aerodynamic rig testing and for follow-on engine environment testing (Program CB). The turbine stator and wheel will be incorporated into a suitable turbine test rig and will undergo cold testing for aerodynamic evaluation.

CB. Engine Environment Test of Ceramic Radial Wheel

The objective of this program is to conduct an engine test evaluation of an integral ceramic radial turbine wheel and matching nozzle. This program assumes the successful progress of a ceramic (monolithic and/or composite) materials/fabrication program as described previously for Program CA. This program will also build on advanced turbine aerodynamic design technologies.

Program Description

This program consists of two major tasks, as scheduled on Figure 148. The major activities of this program consist of the design and fabrication of test-bed engine parts, and engine environment testing at 1371C (2500F).

Design - Specifications for the test rotor will be selected, and aerodynamic and mechanical design analyses will be conducted to configure the rotor and a matching ceramic stator. Design-board layout and detail design will be conducted through preliminary and final design phases. Design activities will include integration of the ceramic stage into a suitable turbine test rig and into a test-bed engine.

Fabrication - Test parts and spares will be fabricated/procured for test-bed engine parts.

Engine Environment Tests

The ceramic turbine stage and adaptive parts will be installed in the selected test-bed engine and will be run at 1371C (2500F) test conditions. Performance and mechanical data will be obtained and compared with design predictions.

Technical Approach

Specifications for a turbine stage will be established that are representative of the SECT APU requirements (simple cycle) as envisioned for the year 2000. The specification will also be compatible with the selection of a suitable engine test bed for engine environment tests.

Analytical design of the integral ceramic radial turbine rotor will draw from the latest technologies available for aerodynamic and mechanical design, materials properties, and fabrication/manufacturing processes. The mechanical design will accept risks commensurate with performance benefits and will be based on the available material properties as established for the pilot rotor.

5.4.2.2 Regenerated Engine Technologies

These technologies will impact APU design options in the year-2000 time frame. For SECT planning purposes, it is envisioned that the regenerator technology will be advanced by separate initiatives such as the NASA/DOE-sponsored programs for the AGT101 and/or related programs.

5.4.2.3 Radial Turbine Performance

This section presents the plan for radial turbine performance technologies as applicable for year-2000 APUs. The plan is made up of two discrete technology programs identified as Programs CC and CD in Figure 149.

CC. Radial Turbine Inlet/Stator Performance Improvement

Current radial turbine design practices concentrate design efforts to optimize the stator and rotor, while less attention is paid to the combustor/turbine transition duct. Historically, an aerodynamically configured scroll has been used upstream of the stator to achieve uniform flow. Future designs will be more size-limited due to the desire to increase APU power density. As the acceptable size of the diameter of the turbine decreases, the transition duct must become more compact. Decreasing duct size implies tighter turning (from axial-to-radial) and, perhaps, higher Mach number levels. Thus, the performance of the transition duct becomes a critical issue, both from a total-pressure loss standpoint and from a stator inlet flow uniformity concern.

Radial turbine performance could be improved from current levels by designing the inlet duct and stator as a system using advanced 3-D, viscous analyses. Moreover, the possibility of reducing envelope size at current performance levels is present.

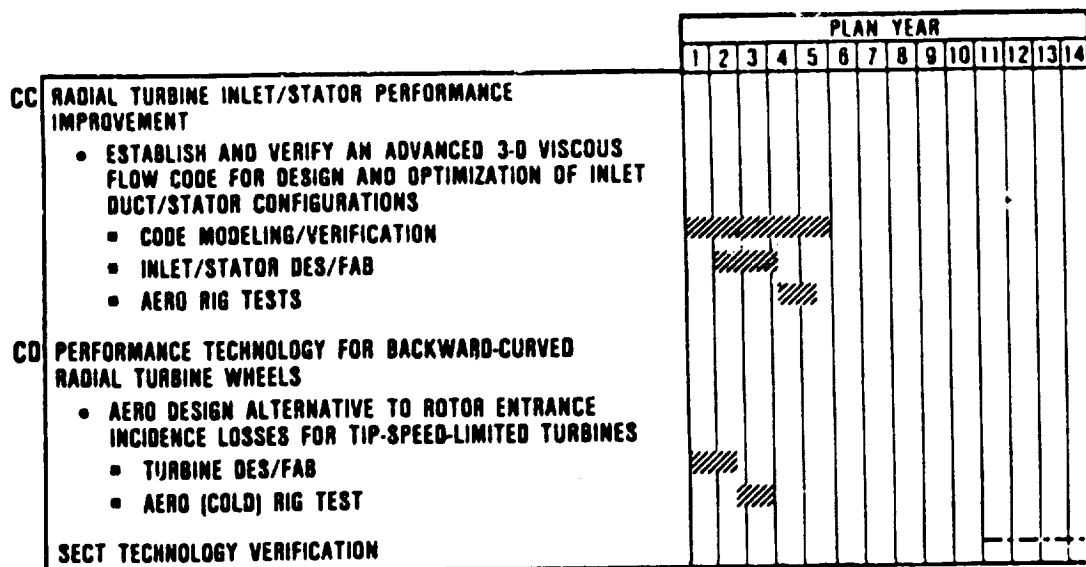


Figure 149. APU Radial Turbine Technology Schedule.

This SECT program will create the tools necessary to design optimized inlet/stator configurations. Actual designs will be generated and tested to calibrate the new codes. The result will be a design system capable of producing radial turbines having enhanced performance levels.

Program Description

This program consists of three major tasks, from code modeling through areodynamic rig tests, as scheduled in Figure 149.

Two computer codes will be generated to analyze the inlet/stator system. Since an iterative process is anticipated, these codes will be written so that file transfers will be easy and thorough.

The first code will be the stator geometry generator. This code must be capable of designing stator sections along streamlines having arbitrary orientation. In addition, the code will have stacking capability to create the full stator 3-D geometry from the several design sections.

The second code will be the 3-D, viscous geometry analyzer. Its input will be a file of geometry from the geometry generator code, plus the applicable flow-field boundary conditions. At this point it is assumed that one or two stator passages, but not all of them, will be analyzed. The code is envisioned as being something like the Denton 3-D code modified to include an appropriate boundary layer analysis.

Analysis and Design - Analysis and design will be conducted to choose a suitable existing system and analyze it with the new codes. This will constitute the baseline configuration, which will then be redesigned to obtain the maximum performance

possible. The only constraint will be that it does not violate the maximum diameter of the baseline design.

A second redesign will be accomplished to minimize the system maximum diameter. A judgment will be made as to defining this diameter; for example, whether it is minimized when the system losses are equal to the baseline system losses. It could also be based on equivalent engine power densities.

The choice of these two redesigns is due to the desire to bracket a reasonable range of design constraints and parameters.

Fabrication - To validate/calibrate the design codes, testing of the system redesigns is essential. The test vehicle will be the baseline system cold air test rig modified to accept the redesigned systems. Adequate instrumentation will be included for obtaining detailed flow-field characteristics. The required new rig hardware will be procured.

Rig Tests - Two types of activities are performed in this task: rig testing, followed by data reduction and analysis. Testing of the redesigned systems will begin with construction of a full performance map that will cover a wide range of pressure ratios and corrected speeds. This will allow off-design characteristics to be compared to the baseline turbine map. It would be desirable to flow the system without the rotor to obtain measurements downstream of the stator. This possibility will be investigated.

Data reduction/analysis will follow each test. The accuracy of the design codes will be assessed and calibrated if required. The change in system performance will be deduced from the stage data. If system-only tests are run, the effects of the different flow fields on the rotor will also be determined by comparing the predicted system losses to measured system losses.

Technical Discussion

Current radial inflow stator designs use an axially constant cross-section vane shape placed into a meridionally converging (endwall contouring) passage. The vanes are designed along a mean streamline using streamtube widths consistent with the meridional flow path. Average inlet/exit flow conditions are used in the analyses. This procedure accounts for the unloading of the front portion of the vane (on the average) but does not consider the actual gradients in flow properties present at the stator leading edge.

The stator inlet flow conditions are a result of the combustor exit conditions plus the combustor/turbine transition duct geometry. Typically, this duct design is accomplished by fairing in a reasonable flow path followed by analyses to ensure against endwall flow separation.

The advanced design concept will consider the transition duct and stator as a system. Flow property gradients present at the duct exit will inherently be a part of the stator design. Optimum systems will then be designed as a result of trading duct performance and stator performance. Actual stator loadings at the endwalls will allow optimum endwall contouring. The vanes will be three-dimensional. It is likely that, for axial flow at the duct inlet, the stator meridional flow path will no longer be purely radial. It may be beneficial to do some of the meridional turning, presently done in the duct, in the accelerating flow field of the stator. This would lead to a "mixed flow" type of stator design.

CD. Performance Technology for Backward-Curved Radial Turbine Wheels

As the work requirement of a radial turbine increases, so does the inducer tip speed. When the tip speed requirement

surpasses the wheel material capabilities, the designer is faced with trading high Mach number and exit swirl (downstream losses) for flow entering the rotor at positive relative angles (incidence losses). Typically, the lesser penalty is due to incidence, so the design becomes a tip-speed-limited configuration. These incidence losses, however, can be two points (or higher) for high-work turbines.

The SECT APUs of this study did not suffer from this trait because of the projected (year 2000) ceramic capability of tip speeds of up to 9144 m/s (3000 ft/sec). This tip speed is adequate for turbines having pressure ratios up to 10:1. An approach to improve turbine performance prior to that time, which could also be applied to the SECT ceramic turbine, is presented here.

This program will advance the concept of the backward-curved "radial" turbine blade, a concept that relaxes the radial constraint and allows the inlet portion of the blade to have backward curvature (this is routinely done in compressor impellers). The nonradial inlet alleviates the incidence problem but creates higher stress levels. Considering the progress being made in dual-alloy wheels and the improvements in ceramic materials, these higher stress levels may soon be tolerable. This means higher performance for the majority of recent radial turbine designs.

Program Description

This program consists of two major tasks, as scheduled in Figure 149.

- Design - GTEC has designed and mechanically tested a nonradial bladed turbine wheel. The data will be reviewed and applied

to a dual-alloy configuration where higher blade stress levels are attainable. This will give guidance to the new mechanical constraints. A candidate production turbine that is tip-speed limited will be selected, along with a suitable turbine test rig.

The candidate wheel will be redesigned to dual-alloy, non-radial blade mechanical limits. Investigation of several angles of backward curvature are anticipated in the iterative mechanical/aerodynamic design. The intent is to incorporate as much backward curvature as possible for performance purposes while maintaining mechanical integrity.

Fabrication - This task begins with the procurement of actual wheels for cold-test purposes. Testing planned includes both strain-gaged specimen and whirlpit tests to ensure the mechanical acceptability of the design. To expedite the schedule, a rig wheel will be machined from aluminum or another suitable material for cold aerodynamic tests.

Rig Tests - The test, which will take place in an existing rig, will include a stator for which data is readily available. A full-performance map will be generated for comparison with the initial data. Shifts in the efficiency characteristics will be compared to design predictions. Data reduction and analysis will follow the test to obtain insight into the basic aerodynamics of the new design.

Technical Discussion

The concept of the nonradial "radial" turbine blade is not new. GTEC designed and whirlpit-tested one several years ago. The estimated performance gain was substantial, although the configuration was never tested aerodynamically. At the time of this design, the dual-alloy concept had not been formulated, so the

nonradial bladed wheel was designed to be cast in a single material. This constraint compromises the blade material selection since it also has to have properties appropriate for a good hub design. The result of the previous program showed higher than acceptable bending stresses in the curved portion of the blade.

With dual-alloy wheel properties, the cast blading material can be selected, based strictly on blade stress requirements. Likewise, the disk material is chosen independently of blading requirements. The combination of discrete material selection, along with improved material properties (since the earlier design), makes the nonradial "radial" turbine blade concept a potential advancement for improved performance.

Looking farther ahead, this concept is also a possibility with ceramic radial turbine wheels. An important parameter that allows the use of backward-curved blades is the material strength-to-weight ratio. Advanced ceramic material property projections imply higher ratios than current metallic properties. Thus, the concept could be proven and used for immediate performance improvements and be applied in future ceramic designs as well.

5.4.2.4 Combustor Technologies

These technologies must be advanced for year-2000 APUs. GTEC envisions a requirement for ceramic reverse-flow combustor technologies as discussed for the rotorcraft engines in paragraph 2.4.2.5, Technology Programs O and P.

5.4.2.5 Compressor (Centrifugal) Performance

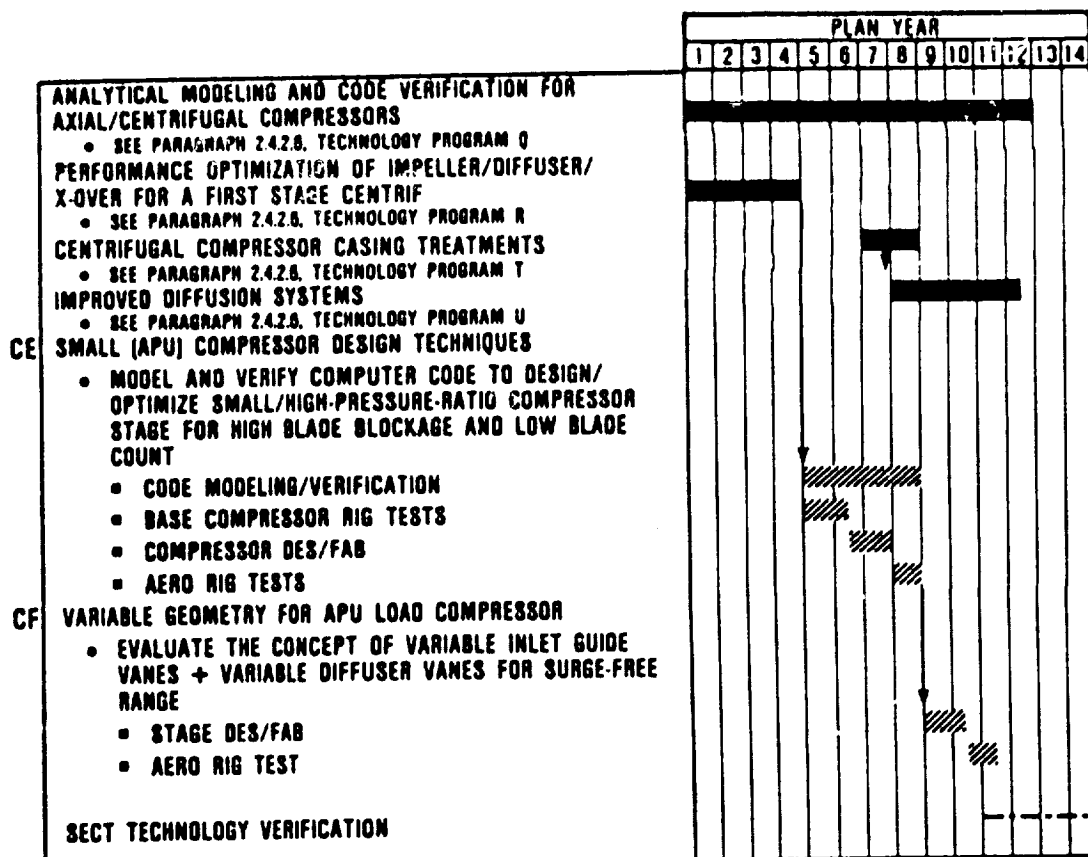
- This section presents the plan for performance improvements to centrifugal compressors as applicable for year-2000 APUs. The

plan consists of six discrete technology programs, four as previously discussed for the rotorcraft and commuter engines, and two new programs identified as CE and CF in Figure 150. The first four technology programs are discussed in paragraph 2.4.2.6, Programs Q, R, T, and U.

Program CE, which addresses design techniques for small APU compressors, is planned to follow the first-stage Performance Optimization Program (R) to maximize the benefits for this plan. Similarly, the load compressor program (CF) is scheduled to take full advantage of the basic compressor programs and Program CE for best plan results.

CE. Small (APU) Compressor Design Techniques

The one-stage centrifugal compressors proposed for the SECT APUs are characterized by high-pressure ratios (8 to 10:1) and low flow rates (0.45 to 0.91 kg/s) (1 to 2 lb/sec). A major challenge in meeting the performance goals of these compressors is overcoming the restrictions that current materials and manufacturing techniques impose on the aerodynamic design of compressors of this size. GTEC experience with scaling an 8:1 pressure ratio from 11.34 to 0.91 kg/s (25 to 2 lb/sec) produced greater performance decrement than could be accounted for by Reynold's number effects and increased parasitic losses. This shortfall is apparently because minimum blade thicknesses do not scale, which causes increased blade blockage. This is a critical performance parameter with the high Mach numbers that high-pressure-ratio machines require. Also, current manufacturing techniques dictate that blade count be lower than that for a full-sized compressor. This SECT program will examine the design tools and techniques used for centrifugal compressors, and will modify or develop new ones for use in small, high-pressure-ratio compressors.



00-281-141

Figure 150. APU Compressor Technology Schedule.

Program Description

This program consists of four major tasks, from code modeling through aerodynamic rig tests, as scheduled in Figure 150.

Code Modeling/Verification - This task will consist of three main activities. First, a feasibility study, including a review of the latest modeling techniques to determine whether an entirely new model should be developed or if an existing one should be modified. The second activity involves software development where the proposed analytical modeling will be turned into a workable computer code. The third activity is a proof-of-concept stage where the model will be tested against the aerodynamic rig data and modifications will be made until satisfactory agreement is obtained.

Base Compressor Rig Tests - An existing test rig will be modified for extensive flow-field measurements. L2F and high-response transducer measurements will be major additions to current test data. Since the NASA scaled version of the AFAPL 8:1 compressor experienced many of the problems that this technology program will address, it is an excellent candidate.

Compressor Design/Fabrication - An improved compressor, based on the new model and baseline compressor data, will be designed.

Aero Rig Tests - A test similar to that run on the baseline compressor will be conducted with the redesigned compressor. Extensive flow-field measurements using the LDV will be obtained. These will also be compared to the model results as a proof-of-concept.

Technical Approach

Although centrifugal compressor flow fields have been measured before, they have usually been for large lower-speed impellers where the viscous and Mach number effects that will be prevalent in the SECT APU compressor are minimal. The data obtained in Task I will be important to the development of the new model. This model must be able to account for the 3-D compressible viscous flow. Since the thick vanes and high Mach numbers of small high-pressure-ratio compressors are conducive to shock loss, attempts will be made to apply some of the shock-free design techniques for axial-flow compressors to centrifugal.

CF. Variable Geometry for APU Load Compressor

One reason that SFC is compromised in gas turbine APUs is that typical load compressors do not possess sufficient range to allow low-load operation without employing an inefficient surge valve. To circumvent this problem, the load compressor proposed for the SECT APU will employ variable geometry in the form of variable inlet guide vanes and variable radial diffuser vanes in order to provide additional compressor range and eliminate the need for a surge valve.

This technology program covers the design and evaluation of the variable geometry centrifugal compressor stage to be used as the load compressor for the SECT APU.

Program Description

This program is scheduled as two major tasks, as shown in Figure 150.

Various variable diffuser concepts will be evaluated and a final concept will be detailed. Compressor performance and range estimates, including the effects of variable geometry, will be made. The compressor will be mapped at various IGV and radial diffuser vane angles to measure the variable geometry concept.

Technical Approach

In order to obtain the gains in SFC that are available from a variable-geometry load compressor, two goals must be accomplished. First, the compressor must have considerable range and high efficiency at its nominal setting. This will allow the compressor to be matched at peak efficiency at full load and will minimize the efficiency loss that will occur at part-load and at no-load conditions. Even though the load compressor will produce considerably lower pressure ratios than the engine compressor (4 to 5:1, as opposed to 8 to 10:1), design tools based on engine compressors should assure that this goal is met.

The second goal is that a reliable, practical, producible mechanical actuation system must be developed to vary the radial diffuser vane angle through sufficient range with a minimum end-wall leakage. R&D efforts are currently under way at GTEC to evaluate and optimize several candidate concepts.

Load compressors have unique complexities that engine compressors do not have. This includes the requirement for some sort of scroll to transfer bleed air to its intended area of use. Also, load compressor power absorption must be reduced to as low a level as possible for quick starting of the power section of the gas turbine with the smallest, lightest starting system possible. Because of the requirement to operate over such a wide range of conditions, load compressors also challenge the

mechanical design to provide for vibration resistance under situations where significant rotating stall can be present. The technology program that addresses the problems of high-performance centrifugal load compressors with variable geometry must address all of these operating characteristics.

5.4.2.6 Materials for "Cold" Parts

These technologies can benefit APUs in much the same manner as discussed for the rotorcraft engines in paragraph 2.4.2.7, Programs V, W, X, and Y.

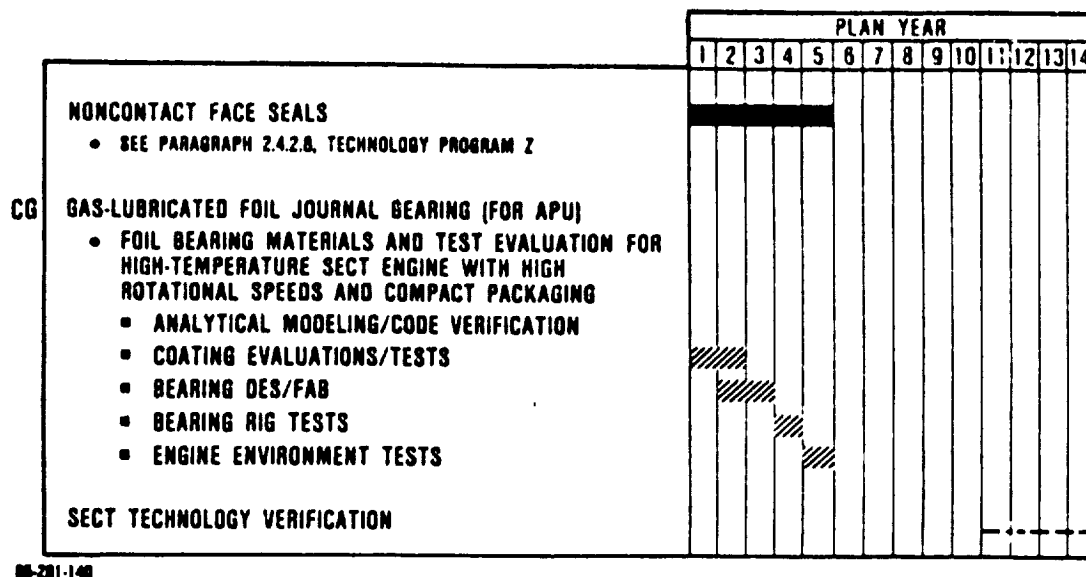
5.4.2.7 System Technologies

This section presents the plan for system technologies as applicable to year-2000 APUs. The plan consists of two discrete technology programs, one as previously discussed for the rotorcraft engines, and one new program identified as CG on Figure 151.

The first program addresses the requirement for noncontact face seals as discussed for rotorcraft engines in paragraph 2.4.2.8, Technology Program Z. This program is an integral part of this plan as well, since the requirement is projected for year-2000 APUs. The second Program (CG) is dedicated to future APUs.

CG. Gas Lubricated Foil Journal Bearing (for APU)

Future trends for high-performance and high-power-density APUs will impose severe requirements on the turbine end bearing. Projected APU engine cycles will feature 1371C (2500F) turbine inlet temperatures through extensive use of ceramic components. High rotational speeds and compact packaging are also envisioned for these units. The gas-lubricated foil journal bearing offers the potential to meet these future gas turbine requirements.



06-281-148

Figure 151. Systems Technology Scheme for APU.

The anticipated extended operating conditions, under high distortion and misalignment, are:

- o 816C (1500F) foil temperature
- o 10,470 rad/s (100,000) rpm speed
- o 34.3 N/cm² (50 psi) unit load capacity

These requirements can be compared to current foil journal bearing load capacity limits under ideal rig test conditions of 20.7 N/cm² (30 psi) unit load capacity for temperatures up to 649C (1200F) and 34.3 N/cm² (50 psi) for temperatures up to 371C (700F). Rotor speeds for these tests were less than 5235 rad/s (50,000 rpm).

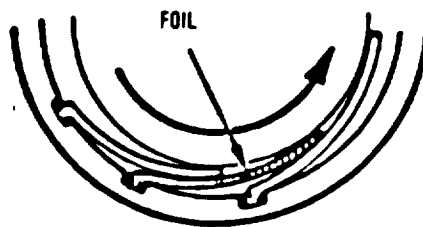
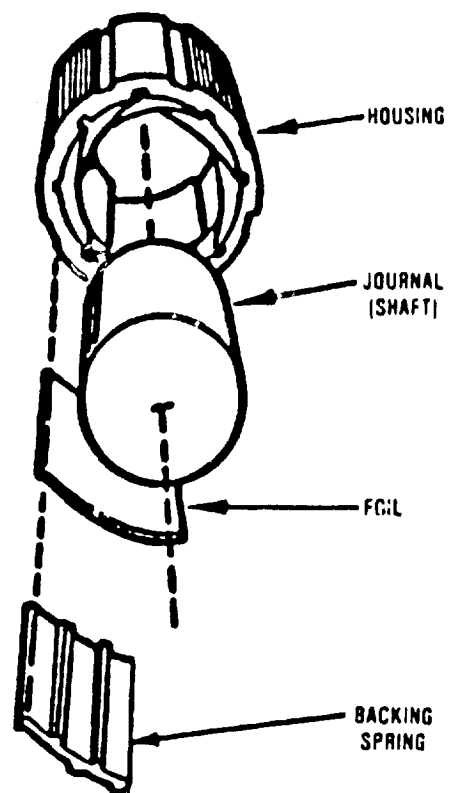
A schematic of the current GTEC foil journal bearing design is shown in Figure 152. The design features overlapping foil leaves supported by flexible backing springs. A thin antifric-tion coating on the foils allows self-starting capability. While this basic design provides a baseline configuration from which design iterations can proceed, it is subject to modification.

Program Description

This program consists of four major tasks, from analytical modeling through engine environment tests, as scheduled in Figure 151.

The requirement for high load capacity at high temperatures will require a fully coordinated effort between bearing and coat-ing development. The foil bearing materials and coatings will also require development to withstand the higher operating tem-peratures achievable with ceramics.

The requirement to define alternate materials may necessi-tate changes to the basic geometry of the bearing. While a



GS-281-133

Figure 152. GTEC Self-Acting Foil Journal Bearing Concept With Backing Spring.

coupled elastohydrodynamic analysis is still expected to be valid, program modifications will be required to reflect the new geometry of the bearing.

Corresponding to the trend for higher power density engines, rotor speeds and temperatures will increase. While the high surface speed of the bearing journal must be taken into account in the bearing design, the tendency of rotor configurations toward supercritical operation and overhung bearing supports is of more concern. The support characteristics of the foil bearing will be evaluated to ensure proper bearing operation under these extreme dynamic operating conditions.

Due to the complexity of the foil bearing configuration, these dynamic performance parameters can best be obtained by rig testing. A foil bearing test rig specifically designed to evaluate bearing dynamic parameters will be used to assess the following quantities:

- o Cross-coupling stiffness coefficients
- o Bearing damping characteristics
- o Power dissipation
- o Dynamic orthogonal stiffness coefficients

The bearing design will consider the load degradation influence of thermal and mechanical distortion and bearing misalignment. An integrated design analysis will be conducted to supplement the bearing design and optimization procedures. The analysis will consist of:

- o Bearing elastohydrodynamic analysis
- o Rotor dynamics analysis
- o Secondary flow analysis
- o Thermal analysis
- o Structural analysis

These individual analyses will be fully iterated with comprehensive rig testing to evolve a viable foil bearing design.

Technical Approach

To achieve high load capacity at elevated temperatures, the appropriate foil/journal coating combination must be identified. A dedicated coating evaluation program will be initiated at the outset of the program to enhance the possibility of defining an acceptable coating pair. It is expected that, by the start of this program, a considerable body of knowledge regarding previously tested coatings will exist. This program will not be limited to screening existing coatings, but will include the development of new coatings.

As coatings and materials for this application are selected, bearing design activities will begin. In concurrence with these materials, compatible foil bearing designs will be synthesized. This will require modifications to the elastohydrodynamic analysis to treat these new bearing geometries. Bearing design activity will continue to be iterated with bearing performance test results.

Test rigs will be required to evaluate the various parameters required for complete evaluation of the foil bearing. Due to the complexity of attaining some of the dynamic bearing characteristics, more than one test rig may be required. The design of these test rigs constitutes an important step in ensuring the proper evaluation of the iterated bearing designs. The test rigs will evaluate the following bearing characteristics:

- o Static load-deflection curve
- o Static breakaway torque
- o Actual sway space

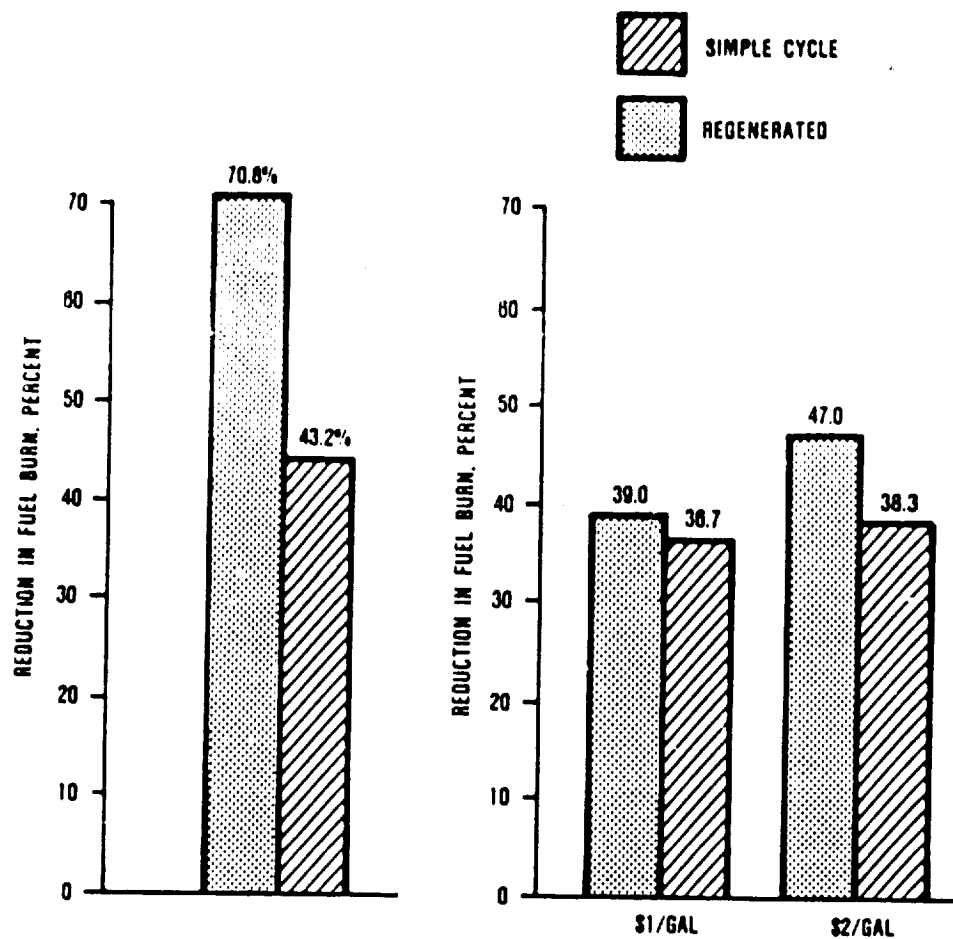
- o Bearing bottoming load
- o Bearing hysteresis
- o Dynamic orthogonal stiffness
- o Dynamic cross-coupling stiffness
- o Rotor bearing dynamic response
- o Load capacity
- o Power dissipation

Many of the preceding characteristics are routinely evaluated on existing foil journal bearing test rigs. The complete itemization of desired bearing characteristics are the result of extensive testing and evaluation of bearing/rotor system dynamics.

The foil journal bearing application to the hostile turbine-end environment of the advanced APU will be a success-oriented program based on extensive GTEC experience. The first demonstrator JFS100 jet fuel starter was successfully operated in 1973. That unit used both foil journal and thrust bearings to completely eliminate the oil lubrication system. Since then, turbine-end foil bearings have been successfully operated in the JFS190 jet fuel starter, the GTCPl65 APU, and are incorporated in the AGT101 advanced gas turbine.

5.5 Summary

As determined by the mission analysis, the advanced engines achieve fuel burn reductions of 43.2 and 70.8 percent, respectively, for the simple and regenerated cycles (Figure 153). Despite the fuel burn advantage of the regenerated engine, however, the corresponding size, weight, and cost advantage of the simple cycle result in nearly equal DOCs at the low fuel price. At the high fuel price, however, the lower mission fuel requirements of the regenerated engine translate into a significant DOC



KEY TECHNOLOGIES

- ADVANCED MATERIALS
(CERAMICS, CERAMIC REGENERATOR)
- IMPROVED COMPONENT PERFORMANCE
(TURBINE, COMBUSTOR, COMPRESSOR AERO)
- SYSTEM TECHNOLOGIES
(METAL MATRIX SHAFTS, SEALS)

Figure 153. APU Mission Analysis Results.

advantage. Specifically, the regeneratd cycle reduces engine DOC by 47 percent relative to the reference engine, compared to 38.3 percent for the simple cycle.

These significant improvements depend on advanced materials, component performance, and system technologies.

6.0 CONCLUSIONS

This section presents the conclusions of Garrett's SECT study as conducted to identify high payoff technologies for year-2000 engines and to formulate technology plans. These conclusions apply to small gas turbine engines in the 186 to 746 kW (250 to 1000 shp) or equivalent thrust range. The engine applications studied are for rotorcraft, commuter, cruise missile, and APU.

6.1 Technology Benefits

The results of this study show that the high payoff technologies can produce important benefits (i.e., SFC, weight, and cost) for year-2000 engines. Moreover, these engine benefits can translate into significant savings in aircraft direct operating costs (DOC) and dramatic improvements in cruise missile range. The study results further show that evaluation of technology benefits is dependent on the fuel price projected for the year 2000. A fuel price range* was assumed for the rotorcraft, commuter, and APU engines in this study. A single value fuel price,** based on JP-10, was assumed for the cruise missile engines.

Rotorcraft, Commuter, and APU Engines

1. Selection of either a simple or a heat-recovery cycle will be fuel-price dependent.

*Low fuel price = \$0.264/liter (\$1/gal)

High fuel price = \$0.528/liter (\$2/gal)

**JP-10 fuel price = \$2.64/liter (\$10/gal)

- o At low fuel prices (\$1/gal), both simple and heat-recovery cycles will be competitive in terms of DOC.
 - o At high fuel prices (\$2/gal), heat-recovery cycles will have a definite DOC advantage over simple cycles.
2. Significant DOC reductions are possible from the projected year-200 engine technologies.
- o Rotorcraft - Fuel burn reductions of 22 and 42 percent are projected for simple and recuperated engines, respectively. This translates to system DOC reductions of 7.0 and 7.4 percent at \$1/gal. At \$2/gal, DOC reductions of 8.7 and 11.4 percent are predicted for the simple and recuperated engines respectively.
 - o Commuter - Projected commuter benefits will be similar to those for the rotorcraft.
 - o APU - Simple and regenerated engines are projected to achieve fuel burn reductions of 43 and 71 percent, respectively. At \$1/gal this translates to DOC reductions of 37 and 39 percent. At \$2/gal, simple and regenerated engines are projected to reduce DOC by 38 and 47 percent, respectively.

Cruise Missile Engines

3. Limited-diameter, low-volume engines are required for this application to achieve interface compatibility

with launchers and to facilitate increased missile fuel fraction for increased mission range. There are no known gas turbine engines of current technology that are suitable for the cruise missile of this study.

- o A year-2000 missile-turbojet system is projected to increase the mission range, compared to current rocket-powered systems, by approximately 200 percent (315 percent with slurry fuels). This system is projected to increase the missile range by 32 percent, compared to a near-term (1989) reference turbojet-powered missile.

6.2 High Payoff Technologies

The results of this study show that technology planning for year-2000 engines should support both simple-cycle and heat-recovery-cycle engines for the rotorcraft, commuter, and APU applications. Technology planning for cruise missile engines should address extremely compact, high-temperature turbojets.

Rotorcraft, Commuter, and APU Engines

1. Ceramics for high-temperature combustors, turbine blading, and/or rotors will dominate engine cycles and configurations.
2. Ceramic heat recovery devices will be needed to meet the probability of rising fuel costs.
 - o Ceramic recuperators are envisioned for rotorcraft and commuter engines.

- o Ceramic regenerators, similar to the disk type incorporated in the NASA/DOE-sponsored AGT101 vehicular engine, are envisioned for APUs.
- 3. Metallic technology advances will be required for turbine disks and blades and shafting to facilitate increased blade speeds, rotational speeds, and engine weight and cost reductions.
- 4. Combustor technologies will be required for high temperatures (1427C [2600F]) and heat release rates, with emphasis on pattern factors ≤ 0.12 .
- 5. Advanced turbomachinery components are vital to these high cycle-pressure-ratio (simple cycle) and temperature-ratio engines.
- 6. System technologies will be required to meet the mechanical and packaging challenges of these compact engines with high rotational speeds. Advanced seals and lubricants will be required. Foil journal bearings will be beneficial for small, compact APUs.

Cruise Missile Engines

- 7. Coated carbon-carbon materials for hot-section parts show the most promise.
- 8. Advanced metallics for high-temperature, axial-compressor stages will be required to meet the requirements of high flight Mach number and high cycle-pressure-ratio.
- 9. Combustor technologies will be needed for extremely high temperatures (1927C [3500F]) and heat-

release-rates, with emphasis on improved pattern factors.

10. Advanced turbine and compressors will be required. Multistage axial compressor technologies for low weight/cost, with minimum variable geometry, will be important. Non-straight-line-element turbine blading (coated carbon-carbon) will be important for acceptable turbine performance levels.
11. System technologies will be required for compact thrust nozzle systems. High-temperature accessories of low cost/weight will require new/advanced technologies.

REFERENCES

1. "User's Manual for HESCOMP - Helicopter Sizing and Computer Program," Boeing Vertol, NASA CR-152018, September 1973, Revised 1979.
2. "Weight Analysis of Turbine Engine - Small," GTEC, NASA CR-165049.
3. "Parametric Study of Helicopter Aircraft Systems Costs and Weights," NASA Report No. O-22305.
4. "Application of Advanced Technologies to Small, Short Haul Transport Aircraft" (STAT), NASA CR-165610.
5. "Advanced Material Technology Candidates for the 1980s," NASA CR-165176, August 1980.
6. Humphreys, J.R., "Why So Few All-New General Aviation Aircraft," Society of Experimental Test Pilots Technical Review, Vol. 12, No. 3, Spring 1975, pp 43-50.
7. Wisler, D.C., "Core Compressor Exit Stage Study," Volume II, NASA CR-159498, November 1980.
8. Rechter, M., P. Schimming, M. Starcken, "Design and Testing of Two Supercritical Compressor Cascades," ASME Paper 79-GT-11, March 1979.

PRECEDING PAGE BLANK NOT FILMED

APPENDIX A

LIST OF SYMBOLS

PRECEDING PAGE BLANK NOT FILMED

LIST OF SYMBOLS

Symbol

AN ²	Turbine Annulus Area (in ²) Multiplied by Rotor RPM Squared
C-C	Carbon-Carbon
CDI	Combustor Diffuser Interaction
CMD	Constant Mean Diameter
CME	Cruise Missile Engine
COD	Constant Outside Diameter
CPR	Compressor Pressure Ratio
CST	Constitutional Solution Treatment
Ct/Sigma	Rotor Corrected Thrust Coefficient
DN	Bearing Mean Diameter Times RPM
DOC	Direct Operating Cost
DS	Directionally Solidified
E/ ρ	Elastic Modulus to Density
FOD	Foreign Object Damage
gJAH/U _M ²	Turbine Stage Mean Work Coefficient
HESCOMP	Helicopter Sizing and Performance Computer Program
HHR	High Heat Release
HIP	Hot Isostatic Pressing
HOGE	Hover Out of Ground Effect
IGV	Inlet Guide Vanes
IPS	Inlet Particle Separator
IRP	Intermediate Rated Power

LIST OF SYMBOLS (Contd)

Symbol

ISA	International Standard Atmosphere
K	Constant
LART	Low Aspect Ratio Turbine
LDV	Laser Doppler Velocimeter
L/D	Lift/Drag Ratio
L2F	Laser Two Focus
LHV	Lower Heating Value
LPT-NOZ $\Delta P/P$	Low-Pressure Turbine Percent Pressure Drop
MMC	Metal Matrix Composite
M _N	Mach Number
MPa	MegaPascals - $N/m^2 \times 10^6$
NDE	Nondestructive Evaluation
NHP	High-Pressure Spool Physical RPM
N _{LP}	Low-Pressure Spool Physical RPM
N _{RAM}	Inlet Recovery
PF	Pattern Factor
PFC	Planar Flow Casting
P _H	High Pressure
P _L	Low Pressure
PM	Powder Metal
PMG	Permanent Magnet Generator
P/P	Pressure Ratio Across the Axial Compressor Stage

LIST OF SYMBOLS (Contd)

Symbol

PR	Pressure Ratio
RCS	Radar Cross Section
RSP	Rapid Solidification Process
SFC	Specific Fuel Consumption
SLE	Straight Line Element
SLS	Sea Level, Static
Solidity	Rotor Blade Area/Disc Area
TOGW	Takeoff Gross Weight
T/J	Turbojet
TRIT	Turbine Rotor Inlet Temperature
TSFC	Thrust Specific Fuel Consumption
T-T	Total to Total
V _{Best Range}	Velocity at Which the Aircraft's Range is at a Maximum
V _{REF}	Reference Velocity
W/θ/δ	Corrected Airflow
WATE-S	Weight Analysis of Turbine Engine - Small
W _{cool}	Turbine Cooling Flow (Percent of Core Flow)
η _T	Turbine Efficiency
ΔDOC	Change in Direct Operating Cost
ε	Heat Exchanger Effectiveness
ΔH/θ	Turbine Corrected Work
δ	P/14.696 psi

LIST OF SYMBOLS (Contd)

Symbol

$\Delta P/P$	Percentage Pressure Drop
η_{AD}	Adiabatic Efficiency
η_{poly}	Polytropic Efficiency
η	Efficiency

ORIGINAL PAGE IS 443
OF POOR QUALITY